The Dissertation Committee for Nico Mark Hauwert certifies that this is the approved version of the following dissertation:

GROUNDWATER FLOW AND RECHARGE WITHIN THE BARTON SPRINGS SEGMENT OF THE EDWARDS AQUIFER, SOUTHERN TRAVIS AND NORTHERN HAYS COUNTIES, TEXAS

Committee:

John Sharp, Jr., Supervisor

Jay Banner

Philip Bennett

Marcy Litvak

Barbara Mahler

GROUNDWATER FLOW AND RECHARGE WITHIN THE BARTON SPRINGS SEGMENT OF THE EDWARDS AQUIFER, SOUTHERN TRAVIS AND NORTHERN HAYS COUNTIES, TEXAS

by

Nico Mark Hauwert, B.S.; M.S.

Dissertation

Presented to the Faculty of the Graduate School of

The University of Texas at Austin

in Partial Fulfillment

of the Requirements

for the Degree of

Doctor of Philosophy

The University of Texas at Austin

May 2009

Acknowledgements

Like converging flow paths in a karst aquifer, this study came from many contributions. From the start of the dissertation, my wife Susan M. Wall, M.S. and Austin's premier environmental educator, managed my graduation requirements, supported me and raised my beloved daughter Tara while I was taking classes, hiking in the rain on the research site, or in other ways obsessing on my study. My graduate supervisor, Dr. Jack Sharp, gave me important feedback and insight on this dissertation and emphasized the quantification of hydrogeologic parameters, the role of fractures and fissures in groundwater flow, and urban changes to groundwater flow and recharge. Dr. Sharp led me to many important literature sources, constructively challenged my findings, considerably helped me convey the results, and expanded my horizons through a class trip abroad to England. I had many other mentors who taught and inspired me, including Dr. Marcy Litvak on evapotranspiration measurement; Bill Russell, my main guide in the late 1970s through 1990s to the underground frontier; Raymond Slade for his advice and insight on the Edwards Aquifer and hydrology; Dr. Jay Banner, for his insightful observations on vadose zone processes and the Edwards Aquifer and for his frequent support on various Edwards Aquifer studies; Dr. Phil Bennett, who introduced a world of geochemical tools; Dr. Stuart Dean, formerly of University of Toledo Dept. of Geology, who inspired me with his observation skills and knowledge of fracture genesis; and Dr. David Maidment, who introduced me to ArcGIS. Ted Small and John Hanson, formerly of the USGS, helped train and calibrate me in the characteristics of the hydrostratigraphic members of the Edwards Aquifer and critically verified my early mapping. Sadly, Ted Small passed away in 2007. The scope of this study was a huge

undertaking requiring the support of many colleagues. Joe Beery, forever with the BS/EACD, has provided amazing assistance on the field work. David Johns, Beckie Morris, Marcy Litvak, Brian Hunt, Scott Hiers, Sylvia Pope, Mark Sanders, Stephanie Helcamp, Sandy Kelso, and Robbie Botto have all worked with me closely and frequently on many aspects of this study. Hydrogeologists, in particular Joe Beery and Brian Hunt of BS/EACD and Scott Hiers of COA, assisted in the refinement of the map interpretation, as well as investigation of discrepancies or new discoveries reported by other local geologists that could be field checked. Shu Liang, formerly of BSEACD, is the most loyal, committed, and knowledgeable GIS support I have known, was instrumental in developing the surface geology working maps into a geodatabase coverage. My City of Austin Watershed Protection and Development Review Department supervisors David Johns, Ed Peacock, Nancy McClintock, and Tom Ennis have been incredibly supportive managers for the research and funded many aspects of this ongoing research. The Austin Water Utility Water-Quality Protection Lands (WQPL) program, particularly Kevin Thuesen, Willy Conrad, and Johnny Ross, as well as Mark Sanders from the Balcones Canyonland Preserve program permitted my research access, assisted in the monitoring and security, and purchased over $5,000 in equipment used in the study including the ET Tower frame and flumes. The WQPL program also contracted for a survey of a large portion of the Flint Ridge catchment area. The Hill Country Conservancy, through George Cofer and Fred Ellis, gave the evapotranspiration tower a boost with a $10,000 grant for field laptop, datalogger, radiation, and soil moisture sensors. Austin Energy provided a boom truck and crew to help raise the climate tower. The Board of Directors of the BS/EACD, and supported my early work including geological mapping, aquifer testing, and groundwater tracing later funded a portion of my field work and analysis associated with aquifer testing and groundwater tracing analysis.

The University of Texas Department of Geological Sciences funded a portion of my travel expenses and lab analysis. I am very grateful to the citizens of Austin who purchased the lands so that thereby allowing much of this research to take place and northern Hays County well users who gave me access to many, many sites. I incorporated comments from City of Austin hydrogeologist David Johns, technical editor Mary-Love Bigony, Texas Speleological Survey Travis County project manager William Russell, COA WQPL manager Kevin Thuesen, and BS/EACD hydrogeologist Joe Beery in the dissertation. The scope of this research was so broad that I found it challenging to organize, so I was very grateful that committee members, particularly Dr. Jack Sharp and Dr. Barbara Mahler, gave extensive and critical review of the drafts and suggested reorganization that greatly enhanced this dissertation. Kristie Laughlin of LB Guyton and Associates illustrated the geological cross sections presented here.

Groundwater Flow and Recharge within the Barton Springs Segment of the Edwards Aquifer, Southern Travis and Northern Hays Counties, Texas

Publication No._____

Nico Mark Hauwert, Ph.D.

The University of Texas at Austin, 2009

Supervisor: John M. Sharp, Jr.

The Barton Springs Segment, part of the karstic Edwards aquifer in Central Texas, is a Sole Source aquifer, is habitat to rare karst species, and provides water to a well-loved municipal swimming pool, yet its hydrogeologic properties remain insufficiently understood. For this study, the hydrogeologic characteristics of the Barton Springs Segment were investigated using several approaches, including mapping of hydrostratigraphic units and faults, measurement of upland infiltration, groundwater traces, and aquifer tests. The depositional environment, diagenesis, fracturing, down-dropped and dipping faulted blocks, and subsequent dissolution were determined to play important roles in controlling groundwater flow-path development within the Barton Springs Segment. In particular, downdropped fault blocks create groundwater gradients to the southeast that influence flow in the Edwards outcrop area. Upland internal drainage basins were found to be extremely efficient at conveying recharge to the underlying aquifer. The maturity of natural internal drainage sinkholes can be measured by its bowl

volume, which grows in proportion to the catchment area it captures. A 19-hectare internal drainage basin, HQ Flat sinkhole, was monitored for rainfall, evapotranspiration, soil moisture, and discrete runoff to the cave drain. During a 505-day period, 5.5% of measured rainfall entered the cave drain as discrete recharge, 26% of measured rainfall infiltrated through soils on the slopes, and the remaining 68% was lost through evapotranspiration. This amount of upland infiltration is consistent with infiltration measurements in other karst areas and is much larger than the 1% upland recharge of rainfall that was previously estimated. A chloride mass balance indicates that at the adjacent Tabor research site, about 50% of rainfall infiltrates to a 6-meter depth. Dye-tracing and pump tests demonstrated that primary and secondary groundwater flow paths are the major influence on transmissivity within the Barton Springs Segment. Groundwater tracing breakthroughs reveal very high advection and relatively low dispersion. Drawdown response to pump tests indicates a very high degree of anisotropy, controlled by location of groundwater flow paths. Overall the Barton Springs Segment is a mature karst aquifer with highly developed rapid, discrete network for both recharge and groundwater-flow.

Table of Contents

Appendices

List of Tables

List of Figures

Chapter 1. Introduction

It is a difficult task to characterize the properties of a karst aquifer such as the Barton Springs Segment of the Edwards Aquifer (Barton Springs Segment), in Travis and Hays Counties, Texas (Figure 1.1). Groundwater studies frequently rely on limited observations and the assumption that subsurface properties are similar throughout (homogeneous) in order to characterize the aquifer. Limestone aquifers are even more challenging in that uneven distribution of solution-enlarged conduits creates exaggerated heterogeneity of aquifer properties. The Barton Springs Segment is intensely fractured and faulted compared to areas immediately to its east and west. This fracturing imparts a high degree of anisotropy to the aquifer. Not only is the aquifer complex compared to other aquifers not fractured or composed of soluble rock (karst), but the Barton Springs Segment is cryptic (Appendix A). Urban expansion, ranch and agricultural practices, and dam construction on local creeks and rivers have obscured observations and added complexity to an already complicated system.

The Barton Springs Segment is an important water supply, and is a federally-designated as a Sole-Source Aquifer south of the Williamson Creek watershed (Federal Register, 1988). The cities of Buda, Mountain City, Hays, Manchaca, and Sunset Valley depend on it for their water supply. The Barton Springs Segment is part of the larger Balcones Fault Zone portion of the Edwards Aquifer that include the Northern and San Antonio Segments (Figure 1.2). The aquifer provides economical water sources for local industries in the sole source area. Preservation of the Barton Springs Segment insures future generations have clean water supplies and are not left with expensive mitigation resulting from poor or short-term planning (Ernst et al., 2007; Freeman, 2008). Most of the water flowing through the Barton Springs Segment discharges at Barton Springs that is the sole home for the endangered aquatic Barton Springs salamander (*Eurycea sosorum;* Federal Register, 1997) and a recently distinguished blind aquatic salamander (*Eurycea waterlooensis*). Barton Springs pool also provides a source of funding for the City of Austin through paid admission, although there is a larger underlying critical

importance of local natural resources that is easily overlooked. The natural resources of the Central Texas area attracts populations just as the springs along the edge of the Edwards Aquifer attracted earlier settlers that were originally sustained by their flows. Local character and economy may depend on the sustenance of natural resources like Barton Springs and natural areas of the Edwards Aquifer (Lerner and Poole, 1999; Sherer, 2006; Crompton, 2007a; Crompton, 2007b; Ernst et al., 2007; Lynch, 2007; Nowak et al., 2007).

This chapter examines heterogeneity and anisotropy as they relate to karst aquifers and the Barton Springs Segment of the Edwards Aquifer (Barton Springs Segment). Spring discharge from the Barton Springs Segment is introduced in this chapter. Appendix A examines how conceptual models of the Barton Springs Segment and Edwards Aquifer have changed over time and what factors may influence how we view the aquifer. The scope of this study is introduced in this chapter.

1.1. ANISOTROPY AND HETEROGENEITY

Anisotropy and heterogeneity in groundwater systems have often been discussed primarily to evaluate if there is a scale at which the system can be modeled using a more simplified and less data-intensive equivalent porous media approach. In karst terranes, which produce about 25% of the world's potable water, understanding anisotropy and heterogeneity is particularly challenging. Frequently models fail to adequately characterize karst aquifers that are far more complex than the simplifying models allow. However, such understanding is important in order to protect these sensitive resources from surface impacts (Pairise and Gunn, 2007). Groundwater flow has been related to fracture trends in consolidated carbonate rocks (Mayer and Sharp, 1995; Sharp, 1998). Some findings suggest that as the system size increases in fractured karst aquifers, more larger conduits dominate the flow system (Zahm, 1998; Sharp et al., 2000; Halihan et al., 2000). In this view, as the system size increases one may expect a greater discrete component of flow. In karst systems, dissolution is six orders of magnitude greater in fractured rock (Kiraly, 2002).

One approach for addressing heterogeneity is to find a suitable scale or Representative Elemental Volume (REV) that is relatively homogenous. Domenico and Schwartz (1998) noted the following for defining a REV:

1) The tests for a REV should be at the same scale as the area of interest;
2) Some models can be utilized for specific purposes without demonstrating a REV or quantifying the size limit of the REV;
3) Some systems may not have an REV at any scale; and
4) If the continuity condition does not apply at the scale of the problem, then:
   (a) discrete characterization is necessary,
   (b) turbulent rather than Darcy's Law flow conditions may predominate if the apertures are large, and
   (c) hydraulic conductivity may vary with changes in hydraulic head.

Parameters or properties may show different patterns over time and space such that the REV may differ within a system for each parameter.

The heterogeneity of karst aquifers has been examined by comparing large-scale numerical simulations with field data. Worthington (2003) created a groundwater MODFLOW model of the Mammoth Cave area and compared the results with extensive groundwater tracing and water-level data. He found a mean absolute potentiometric head error of 12 m, an under-measurement of Turnhole Spring discharge of 94%, and simulated groundwater velocities two to three orders of magnitude lower than measured velocities.

Attempts to simplify complex recharge and flow conditions in models can result in highly inaccurate or subjective results (Kiraly, 2002). One limitation of testing for REV by model comparison is that many different combinations of input parameters can be used to achieve similar groundwater heads and discharge. Several examples follow.

A groundwater model was used to establish time-of-travel protection zones in the limestone Biscayne Aquifer of Miami-Dade County. Later tracing from injection wells 100 m away from the wellfield measured mean groundwater flow rates to be one to two orders of magnitude faster than those derived from the simulation (Renken et al., 2005).

To delineate the wellhead protection zone for three production wells near Walkersville, Maryland, the Maryland Dept. of the Environment identified 5-year and 10-year time-of-travel radii around the well field using a numerical model. However, groundwater tracers injected by Aley and Field (1993) from the "5-year time of travel" contour arrived at the three production wells 17.5 hours after injection. Several years later about 900,000 gallons of raw sewage of spilled in the "8-year time of travel zone", as originally delineated by the wellhead protection numerical model (Aley, 2007, personal communication). Dye introduced at the spill site first arrived at the production wells in 11 to 13 days. A similar travel time was shown for fecal coliform from the spill, which peaked at about 20,000 colonies per 100 ml. *Cryptosporidium* was detected in the raw sewage that discharged into the karst aquifer (Aley, 2007, personal communication). The delineation of the wellhead protection zone using dye tracing helped prevent a major health problem as city, county, and state officials took prompt action to develop alternate water supplies. This case also demonstrates how modeled groundwater travel times based on limited data differ from directly traced travel times.

The groundwater basin for Dewitt Spring, a Paleozoic carbonate spring near Logan, Utah, was delineated based on the mapped geological framework (Eckoff, Watson, and Preator Engineering, 1996). Darcian calculations, based on the groundwater gradient, delineated a time-of-travel zone of up to a 15-year time maximum for travel 8 km across the groundwater basin (State of Utah, 1995). Five traces injected beyond the calculated 3-year time-of-travel arrived within 8 to 31 days (Spangler, 2002). Three of the five tracers arriving at Dewitt Springs were injected beyond the originally delineated groundwater basin (Spangler, 2002).

Smith et al. (2005) compared a MODFLOW model of the Barton Springs Segment of the Edwards Aquifer (or Barton Springs Segment) to discrete flow data from groundwater tracing. The model was useful for estimating spring flows and potentiometric heads, but it failed to show convergent and divergent flow routes observed through groundwater tracing. The model underestimated tracer arrival times by three to five orders of magnitude. However, these same modeling results led some researchers to

conclude that the Barton Springs Segment can be adequately simulated as a porous media system (Scanlon et al., 2003).

For the purposes of water protection, a carbonate aquifer should be characterized using: (1) groundwater tracer tests; (2) mapping of the geological framework; and (3) estimating source area size using discharge magnitudes, water balances, potentiometric-surface maps, aquifer tests, and other methods (Schindel et. al., 1996; Gunn, 2007).

1.2. THE BARTON SPRINGS SEGMENT AND ITS DISCHARGE SITES

The Barton Springs Segment extends from the City of Austin and the Colorado River southward to the cities of Buda, Kyle, and Mountain City near the Blanco River (Figures 1.1 and 1.2). A Saline-Water Zone or "Bad-Water Zone" is defined by groundwater with greater than 1,000 mg/l dissolved solids and bounds the Barton Springs Segment to the east, approximately along Interstate 35 and South Congress Avenue (Flores, 1990).

The main discharge site for the Barton Springs Segment is Barton Springs, which discharges into Barton Creek in Zilker Park about 1 km from the Colorado River (Figure 1.3). Barton Springs has four orifices: Main Barton, Eliza, Old Mill, and Upper Barton Springs. William Barton lived at Barton Springs in 1837 and originally named Main Barton, Eliza, and Old Mill Springs after his daughters Parthenia, Eliza, and Zenobia, respectively (Brune, 1981). Old Mill Springs was also called Walsh Springs after a mill was erected there by W. C. Walsh. Old Mill Springs is also known as Sunken Gardens springs because of its sunken walls that were built by the National Youth Administration from 1935 to 1937.

The U.S. Geological Survey (USGS) reports flow from Barton Springs as the combined flow from Main Barton, Eliza, and Old Mill Springs. The mean flow of Barton Springs from 1917 to 1981 was calculated as 1.4 m^3/s (50 ft^3/s; Slade et al., 1986; Baker et al., 1986). Average daily discharge is available for 1917 to 1918 and from 1978 to present. For other periods since 1898, flow measurement was infrequent. Simple time-weighting of the infrequent flow measurements may not adequately capture the variation between measurements. Very severe historical droughts, such as those occurring in the

late 1910s and 1950s when measured Barton Springs flows declined as low as 0.34 and 0.28 m^3/s (12.1 and 9.7 ft^3/s), respectively, are not repeated in the relatively short record of 1978 to present. In August 1996 and October 2000, the USGS reported a daily average flow of 0.48 and 0.45 m^3/s (17 and 16 ft^3/s), respectively, the lowest flow reported since the 1950s. Monthly averaged flow values have been computed from 1917 to 2006 from graphical extrapolation of measured values that considers typical flow recession and precipitation events and magnitude (Slade, et al., 1986; Slade, 2008, personal communication). In this dissertation, "Barton Springs flow" refers to USGS-reported Barton Springs flow unless otherwise specified.

The discharge of spring outlets associated with Barton Springs and lower Barton Creek varies. Taylor and Schoch (1922) noted that "Barton Springs issue at many different points, and some of these points even change occasionally. One of the springs issues at the mouth of Barton Creek, in the middle of the bed." It is possible that Taylor and Schoch are describing a spring orifice that is now under Town Lake of the Colorado River. They observed that the Barton Springs orifices were sensitive to blocking by obstructions, and noted that Old Mill Spring had become covered with mud and ceased flowing for several years prior to 1922. As a severe drought preceded 1922, it is possible that flow conditions influenced this drying of Old Mill Spring as well.

The flows of the individual Barton Springs outlets vary depending on whether Barton Springs pool is full or drained (Slade et al., 1986). The flow diversion suggests hydraulic connection between Old Mill, Eliza, and Upper Barton with the Main Barton Spring in Barton Springs pool. After the transient storage in the pool and local aquifer associated with pool drawdowns have stabilized, the combined flows represent total flows, even though flows of specific outlets may have shifted. As springflow rates and groundwater levels increase, springs appear farther upstream but downstream of the Loop 360 bridge.

In this study, "low-flow conditions" refer to conditions when the combined flow of Main Barton, Eliza, and Old Mill outlets of Barton Springs are less than 1.1 m^3/s (40 ft^3/s). Under low-flow conditions, the total dissolved solids of Barton Springs increases and discharge of overflow springs becomes very small or ceases. Below a flow rate of

1.1 m^3/s (40 ft^3/s), Upper Barton Springs ceases to flow. In the early 1920s, before the pool dam was built from 1929 to 1930, Old Mill Spring historically ceased flowing when combined Barton Springs flows were between 0.8 and 1.1 m^3/s (30-40 ft^3/s), although in 1925 Old Mill Spring continued to flow even as combined Barton Springs flow declined below 0.44 m^3/s (16 ft^3/s). Palmer (1986) and Schindel et al. (1986) suggest that in karst areas where spring clusters existed, some of the springs that dry during low-flow conditions that may be overflow springs. Overflow springs are created by excessive flow in a normal flow conduit, causing some flow to backup into a higher, normally dry conduit. Old Mill, Upper Barton Springs, and other small springs discharging upstream of Barton Springs pool and downstream of Loop 360 appear to serve as overflow springs.

Differences between moderate- and high-flow conditions are less distinct than the shift to low-flow conditions. Moderate-flow conditions are defined as Barton Springs flows between 1.1 and 2 m^3/s (40 and 70 ft^3/s). High-flow conditions are defined to be above 2 m^3/s (70 ft^3/s).

Within the aquifer, excessive recharge can also create a fourth flow condition: overflow conditions. This condition was observed during tracer tests in 2005 during which eastern aquifer flow routes were backed up and diverted flow to western flow routes and/or to San Marcos Springs. The overflow condition is described below in section 4.3 and may not coincide with any specific discharge rate of Barton Springs, although it appears to be limited to infrequent excessive recharge conditions.

Cold Springs are a group of springs discharging from the south bank of the Colorado River about midway between the Loop 1 MoPac bridge and the upstream Red Bud Trail crossing of the Colorado River (Figure 1.4). Some of these springs discharge at the current Town Lake water level, but additional discharge through Colorado River bottom sediments can be detected by temperature contrast. Total Cold Springs flow could be measured by traditional methods of flow measurement under drought conditions before Town Lake was constructed. Under most flow conditions the flow of Cold Springs is too small in comparison with much larger Colorado River flows to accurately resolve Cold Springs flows. Consequently, most flow measurements of Cold Springs were collected either during drought conditions before Town Lake was constructed or

constituted only the part of Cold Springs discharged above the Colorado River, and thus underestimate average flow.

Hill (1892) described "several unnamed springs breaking out at the river level beneath Deep Eddy Bluff, west of the river." He described "almost due north of Barton Springs, beneath the highest bluff of the river at Deep Eddy, along other fracture lines, there is another group of fissure springs but, owing to the fact that they are at the base of a high bluff and accessible only by boat and at the low-level of the Colorado, few people have seen them. They discharge at a large volume, but as they break out in the river's edge it is impossible to gage them." Hill also mentions a "principal spring" as "Sand Springs," that is located "between the dam and the city," that appears to be Cold Springs which lies about halfway between the old dam site (near Tom Miller Dam) and Barton Creek. The location described by Hill for Sand Springs does not precisely match that of Cold Springs because Cold Springs is nearly due west of Barton Springs, not due north, and is on the south bank of the Colorado River not the west bank. However, Hill's map shows a fissure spring at the site of Cold Springs (Figure 1.4), and he maps no other spring between the dam and city other than Barton Springs. According to Reddell and Russell (1961), many people reported a spring-fed cave under the bluff opposite Deep Eddy swimming pool that could be entered during low flow before Tom Miller dam was constructed, although no such cave reported below the lake level has been observed in recent times. Cold Springs is further examined in Chapter 4. Other minor springs identified include Powerhouse, Bee Creek, and Rollingwood Springs (Figure 1.4).

Created by an upstream rock scarp, Deep Eddy was a popular swimming hole in the Colorado River that became a resort site in 1902. This rock scarp is now submerged beneath Town Lake (Figure 1.4). The current Deep Eddy pool is a manmade pool on the north bank of the Colorado River that is fed by wells constructed in alluvial deposits, and is downstream of Deep Eddy bluff.

The fact that discharge from the Barton Springs Segment is limited to two general sites, Barton and Cold Springs, indicate a large degree of anisotropy and heterogeneity of groundwater flow within the aquifer system. Abbott (1973) stated that the Edwards Aquifer discharged from a few large springs, which was evidence that a few "master

conduits" had pirated flows from other conduits. Within a homogeneous aquifer, discharge would be expected to be distributed evenly at elevations below the water table along the 4 km of aquifer outcrop along the Colorado River and Barton Creek. The focusing of discharge at two principal locations reflects the convergence of flowpaths within the aquifer.

The volume of groundwater-saturated rock present in the Barton Springs Segment is about 2.1 $x10^{10}$ m^3 (Slade et al., 1986) to 2.6 $x10^{10}$ m^3 (Hauwert, 1997) during low-flow conditions at Barton Springs flow of 0.5 to 0.7 m^3/s. The volume of transient groundwater discharged during recession of Barton Springs flow of 0.3 to 3 m^3/s is 3.8 x 10^7 m^3 (Slade et al., 1986). The total groundwater volume is about 3.7 x 10^8 m^3 (Slade et al., 1986) during low-flow conditions based on an average specific yield of 0.17.

Another source of discharge from the aquifer is pumpage. Permitted well pumpage currently is about 0.3 m^3/s (10 ft^3/s; Smith and Hunt, 2004). The majority of pumping volume is focused within the Buda area. The Hays County portion of the Barton Springs Segment relies solely on the Edwards Aquifer for water supply, although some water supply systems supplement with water from the City of Austin (the Colorado River), the underlying Trinity Aquifer, the Saline-Water Zone, and the Guadalupe River basin. The City of Austin used water-supply service from the Colorado River to replace well pumpage for many portions of the Travis County over the Barton Springs Segment. In some areas of Travis County, the use of alternative sources may have been necessary as urbanization reduced the usable quality of the aquifer locally (Hauwert and Vickers, 1994). Pumping wells are not uniformly distributed across the aquifer, in part because well yields vary spatially.

1.3. SCOPE OF THIS STUDY

This study investigates the heterogeneity and anisotropy of the karstic Barton Springs Segment in southern Travis and northern Hays counties, Texas, by field examination of its geological framework, recharge, and flow systems. It summarizes investigations since the late 1800s for an overall understanding of the Barton Springs Segment. This dissertation first examines the geological framework, then examines

recharge and discharge processes, and finally characterizes groundwater flow. Chapter 2 describes the characteristics of the hydrostratigraphic units and correlate solution cavities and springs observed with each unit. Chapter 3 examines recharge through soils and sinkholes. At a site scale, field measurements quantify the diffuse and discrete recharge through an upland sinkhole basin. Chapter 4 recapitulates dye tracing, water-level data, geochemical studies, and aquifer testing to quantify the degree of anisotropy and heterogeneity in the aquifer.

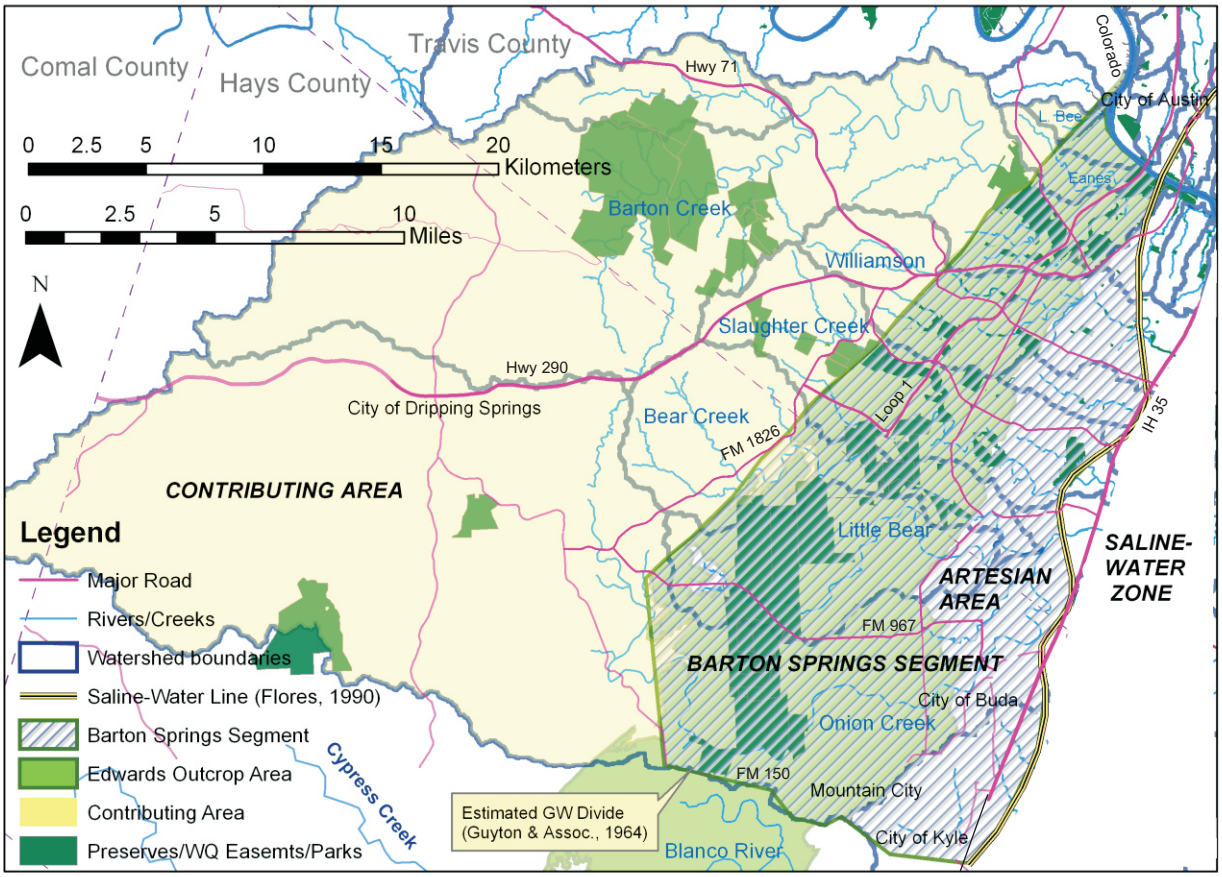

Figure 1.1. Study area: Barton Springs Segment of the Edwards Aquifer. The Barton Springs Segment is bounded to the north by the Colorado River, to the east by the Saline-Water Line that approximately follows IH 35 and Congress Avenue, to the west by the edge of Edwards outcrop area, and to the south between the Blanco River and Onion Creek.

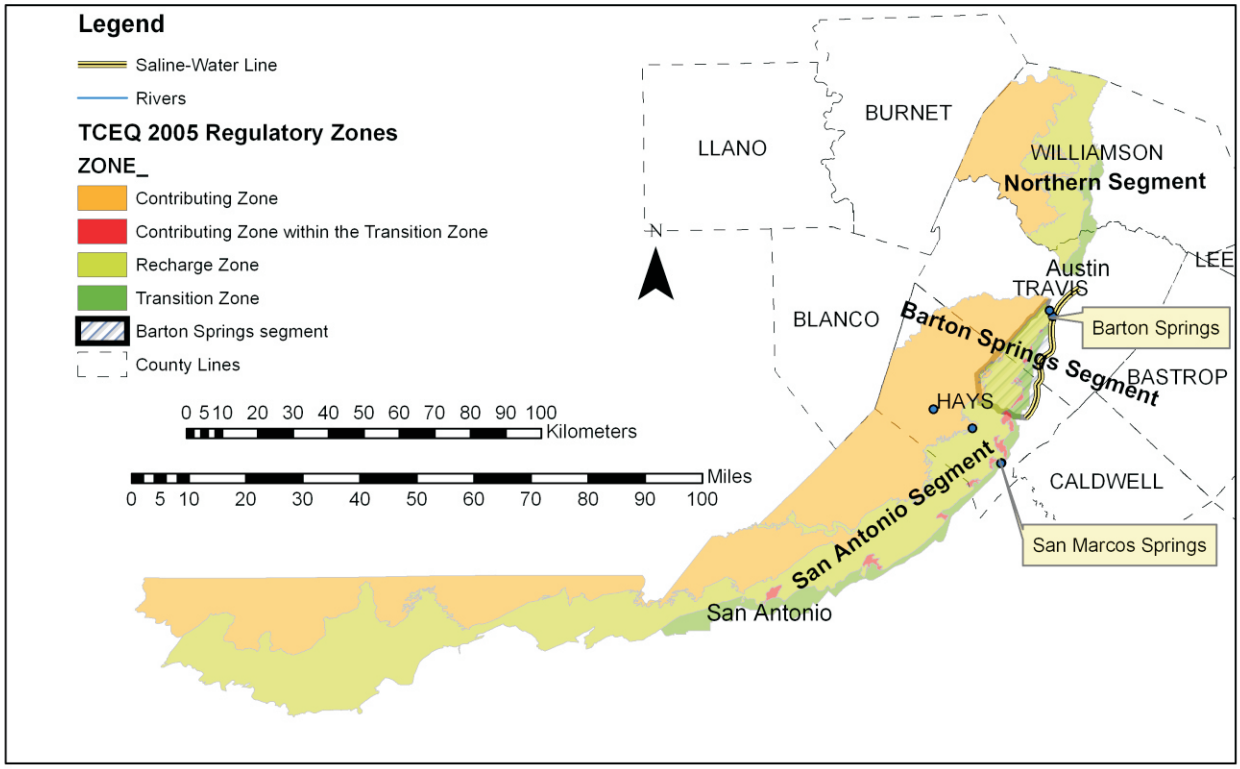

Figure 1.2. Balcones Fault Zone portion of the Edwards Aquifer.

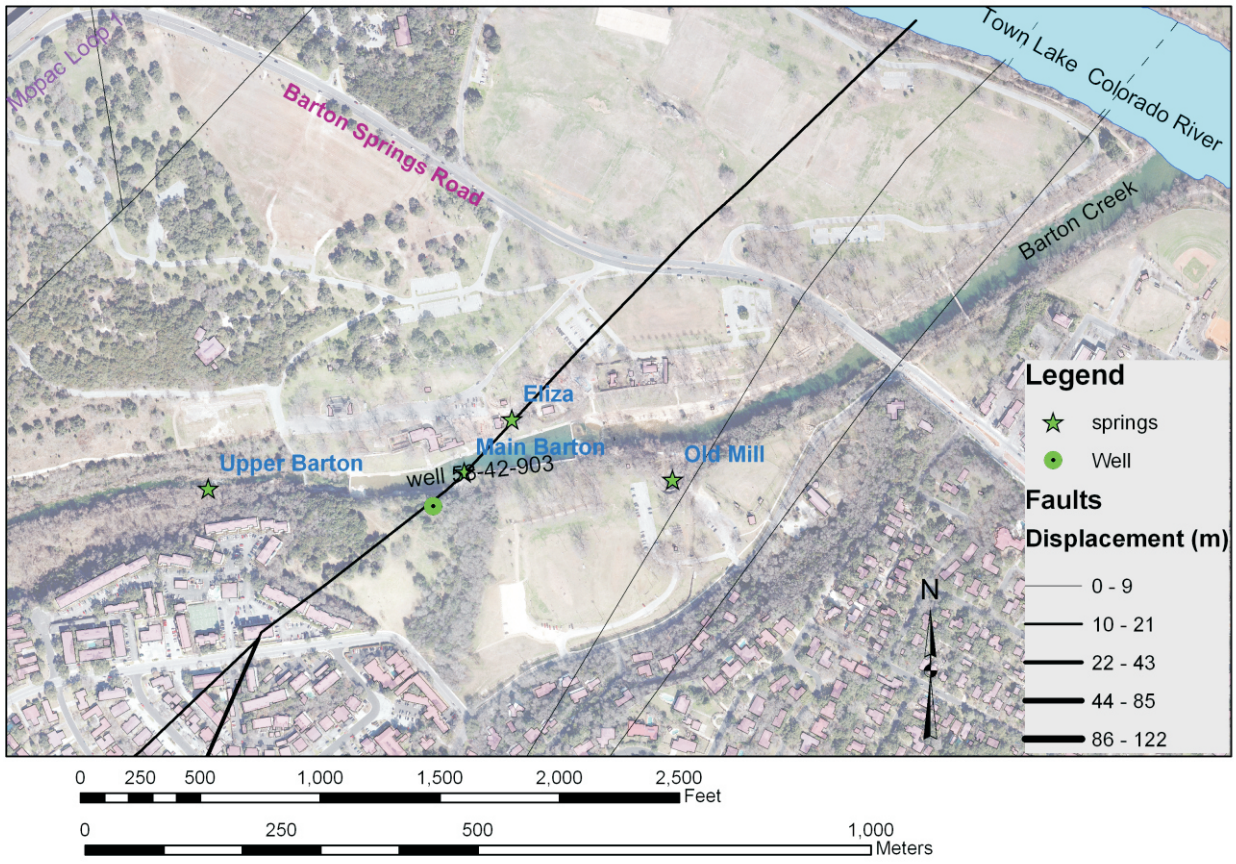

Figure 1.3. Barton Springs. Located in Zilker Park, Barton Springs consists of four known spring orifices, Main, Eliza, Old Mill, and Upper Barton Springs. Most of these springs are associated with fault exposures. The USGS reports Barton Springs flow from Main, Eliza, and Old Mill based on Barton Creek flow measurements above and below Barton Springs pool, in addition to measured Old Mill Spring tributary flow. A rating curve relation from well 58-42-903 is used to estimate Barton Springs flow between individual flow measurements of Barton Creek.

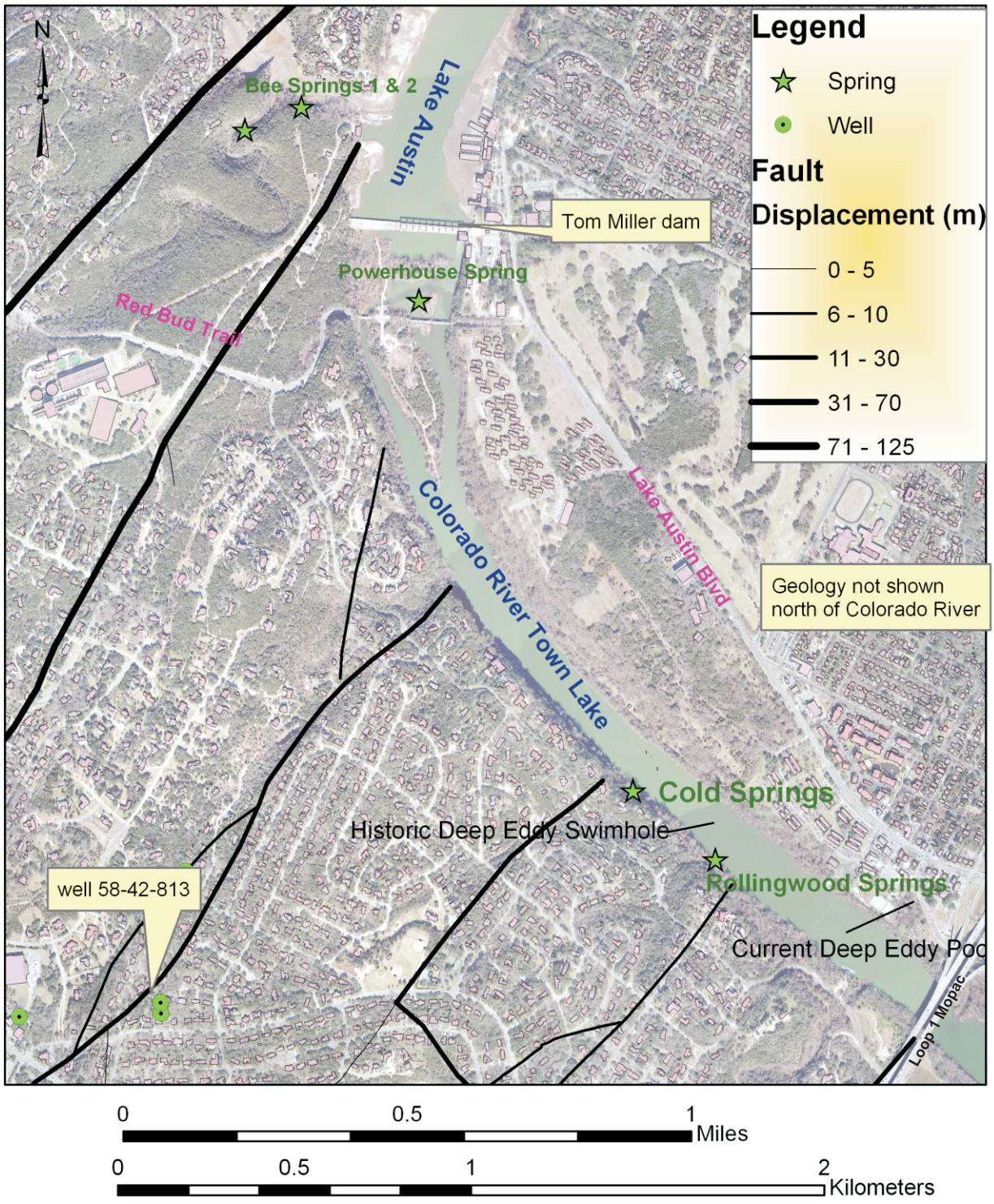

Figure 1.4. Cold and other springs along the Colorado River.

Chapter 2. Geological Framework

This chapter describes the influence of the geological framework on anisotropy and heterogeneity of the Barton Springs Segment. The geological framework includes the depositional and solutional characteristics of hydrostratigraphic units, diagenesis, stratigraphic dip, and fractures. The geological framework is inferred from field mapping of hydrostratigraphic units on the surface, in caves, and in logged wells.

2.1 INTRODUCTION

The rocks of the Barton Springs Segment vary in composition, structure, and hydraulic properties both laterally (localization of conduits, fissures, and fractures) and vertically (differences between individual beds and members). Geologic mapping of portions of the Barton Springs Segment were conducted by Hill and Vaughan (1898), DeCook (1963), the Bureau of Economic Geology (Rodda, et al., 1970 and unpublished quadrangle maps), Moon (1942), Strong (1957), McReynolds (1958), Smith (1978), Kolb (1981), Proctor et al. (1981), Young (1982), and the City of Austin (Snyder, 1985),. Previous mapping of portions of the study area by Young et al. (1975, 1977, 1982) distinguished formations of the Austin Group in greater detail than were incorporated for the recent Barton Springs Segment mapping. South of the Colorado River, the Edwards Group was proposed to include informal rock units of similar hydraulic properties (hydrostratigraphic units) by Rose (1972). These hydrostratigraphic rock units were refined and, through field mapping, correlated across the San Marcos Platform of the Balcones Fault Zone (Maclay and Small, 1984). Within the Barton Springs Segment, the Edwards Aquifer consists of the Edwards Group and overlying Georgetown Formation (Table 2.1). Mapping of the Barton Springs Segment using hydrostratigraphic units began in 1994 as a cooperative project of the US Geological Survey (USGS), the Barton Springs/Edwards Aquifer Conservation District (BS/EACD), and the Texas Water Development Board (TWDB, Small et al., 1996). The purpose of the mapping was to gather detailed data on the geological framework and to determine how the framework influenced groundwater recharge and flow. Hydrostratigraphic mapping assists in the

delineation of recharge areas by identifying the outcrop of the Edwards Aquifer. The mapped faults then can be compared to observable solution development in the vadose zone and traced groundwater pathways in the phreatic zone to examine the influence of geologic structure on groundwater flow.

2.2 METHODOLOGY OF HYDROSTRATIGRAPHIC MAPPING

The methodology for the cooperative mapping completed in 1996 is described briefly in Small et al. (1996). The mapping of the Barton Springs Segment continues to be refined with improved methods and documentation (Hauwert et al., 1997b; Hauwert et al., 2003). The outcropping rock units of the Barton Springs Segment of the Edwards Aquifer are mapped using hydrogeologic subdivisions modified from Maclay and Small (1984) and follow the stratigraphic nomenclature of Rose (1972) for the Kainer and Person Formations of the Edwards Group on the San Marcos platform (Table 2.1). The carbonate-rock classification system of Dunham (1962) is used for the lithologic descriptions. The hydrostratigraphic members are best distinguished using sequences of beds, as in places individual beds may superficially resemble beds in other units. Measured sections are described in order to distinguish the units, to distinguish marker beds and patterns within the hydrostratigraphic units, and to note lateral variations.

Unconsolidated materials, such as alluvial material, terrace deposits, fill materials, and spoil types were not mapped, but can exceed 7 m (20 ft) thickness, based on geotechnical borings and backhoe trenches. These unconsolidated units can be important sources for small springs in the artesian area of the Barton Springs Segment and Saline-Water Zone. If shown on the same map, the unconsolidated units obscure the complicated underlying geological framework. Additionally, the terrace and alluvial deposits require a different methodology, including borings, to map their thickness and extent. The alluvial and terrace deposits have been mapped previously (McReynolds, 1958; Proctor et al., 1981), along with the springs discharging from them.

In 1994 and 1995, John Hanson, then of the USGS, and I conducted field mapping of the entire Barton Springs Segment. Hanson initially focused his mapping efforts on refining the Kainer Formation of the Edwards Group by constructing measured

sections along portions of Barton Creek upstream of Mopac (Figure 2.1; Hanson, 1995; Appendix B). Field verification and rock unit identification training was conducted by Ted Small on previously mapped outcrops in the San Antonio area. Measured sections were created by John Hanson and me from rock exposures across the study area (Appendix B). From 1994 to 2002, Shu Liang, formerly of BS/EACD, developed and updated a Geographic Information System (GIS) from our field maps. The geologic coverage has been periodically updated based on new field discoveries and refinements and was reported by BS/EACD in a wall map format in 1997 and 2003. I have continued to update this geodatabase since 2004.

Since 1999, many rock outcrops with hydrostratigraphic units, marker beds, lithologic contacts, and faults were located within 1-m horizontal and vertical accuracy as control points using a Trimble XRS or Trimble XH Global Positioning System (GPS). The Trimble XRS postprocessed locations of a benchmark were compared to known coordinates and elevations to verify accuracy on numerous occasions. This geological control point documentation was critical for documenting the degree of field verification in specific areas. Valuable feedback was obtained from other geologists who examined portions of the study area.

Well data, geotechnical borings, and trenches also were mapped as control points, within 1-m accuracy. Geophysical logs from the TWDB, Texas Commission of Environmental Quality (TCEQ), and the Texas Railroad Commission (TRRC) were compiled as subsurface control points to verify surface mapping and create geologic cross sections (Hauwert et al. 2004a). A number of wells were logged by the Edwards Aquifer Authority (EAA), GeoCam, and Collier Consulting at the request of BS/EACD.

Faults were mapped in the field based upon the following criteria (Billings, 1947, p.155-171): (1) fault features such as slickensides, mullion structures, fault drag, fine-grained gouge, mineralization, and breccia; (2) offset in strata or structures; and (3) abrupt changes in lithology. Linear ridges, scarps and valleys; angular stream deflections or offset drainages; and sag ponds are commonly observed along faulted and fractures zones (Wesson et al., 1975; Woodruff, 1977). Although physiographic criteria alone were not used to define faults, they were used to extrapolate faults between exposures.

Faults and fractures with minor offsets of less than 2 m (5 ft) are not always included on the mapping. Fault orientation was measured using a Brunton compass or GPS line feature. Because faults are poorly exposed in the study area, most faults were identified and mapped based on abrupt changes in surface lithology. Where abrupt changes in surface lithology could not be directly observed or precisely delineated, faults were inferred (dashed) to account for the discontinuity. Future re-examination might reveal that estimated cross faults are actually dipping fault blocks or relay ramp structures.

Caves were entered to record subsurface hydrostratigraphic units on cave maps. While a few caves were mapped by me, most were mapped by volunteers of the Texas Speleological Survey (TSS). Once the hydrostratigraphic members were distinguished for Travis County caves, William Russell of TSS calculated the cave volume of each unit (Russell, 2007). I digitized the vertical profiles of a representative number of Travis County caves to illustrate their characteristics across hydrostratigraphic units. The original cave maps and my hydrostratigraphic unit interpretations are presented in Appendix C. The longest known Travis County caves were digitized from caves maps and their morphology was compared to recharge and aquifer characterizations derived by Palmer (1991).

2.3 RESULTS

The surface geology of the Barton Springs Segment is shown in Figure 2.2. Geologic cross sections across Barton, Slaughter and Bear Creeks are shown as Figures 2.3, 2.4, and 2.5.

2.3.1 DEFINITION OF SURFACE HYDROLOGIC AREAS

From the hydrostratigraphic mapping shown, it is possible to delineate outcrop areas of the Edwards Aquifer where runoff can directly recharge the Barton Springs Segment (Edwards outcrop area), areas to the west of the Barton Springs Segment underlain by the upper member of the Glen Rose Formation (contributing area), areas within the Edwards outcrop area or on the eastern edge where overlying confining units drain toward the Edwards outcrop area (eastern drainage area), and exposure of overlying confining units that are not known to contribute to the Edwards Aquifer, but generate

runoff downstream of the Edwards outcrop area (artesian area, Figure 2.6). For practical purposes, exposures of overlying confining and underlying units entirely surrounded by areas of Edwards outcrop are considered Edwards outcrop areas. Earlier mapping of the contributing, Edwards outcrop, eastern drainage, and artesian areas were conducted by Slagle et al. (1986) and formed the base of the original TCEQ official Recharge Map. The hydrologic areas used here are similar to those of Slagle et al. (1986), and are distinguished from the commonly used regulatory zones to avoid confusion.

As shown on Figure 2.6, the combined Edwards outcrop and eastern drainage areas are 241 km^2 (94 mi^2) in surface area. Because of a lack of access or insufficient outcrop, a few areas mapped as potential recharge areas have not been sufficiently examined to establish if Edwards outcrop is indeed present. The delineation of these areas generally agrees with but may not always correspond to the Contributing, Recharge, and Transition Zones adopted by the Texas Commission on Environmental Quality (TCEQ) official Edwards Rules maps.

In addition, regulatory zones used by TCEQ (and municipalities such as the City of Buda (2005) that rely entirely on TCEQ zones) are not sufficiently flexible to adapt to new geologic map revisions. In November 2002, the BS/EACD petitioned TCEQ for revision of the Recharge Zone definition based on the most recent mapping, and although some of its interpretations were eventually adopted in September 2005, some were not (Smith and Hunt, 2002). Even though TCEQ defines all associated Edwards Aquifer units as being those above the Glen Rose Formation south of the Colorado River (as did Rose, 1972, and Small et al., 1996), TCEQ (2005) decided that exposures of the Basal Nodular Member serve as an aquiclude north of the Comal County line (TCEQ, 2005, see section 2.4 and glossary for "Recharge Zone"). Some small areas west of the City of Buda where the Georgetown Formation is observed at the surface and in shallow trenches were not included within the Recharge Zone in the official TCEQ Recharge Zone maps. Despite some differences, the hydrologic areas are the same as corresponding zones on state and municipal regulatory maps in most areas of the Barton Springs Segment. The City of Austin relies on a site-by-site determination of the Recharge Zone boundaries for

regulation of proposed development within 457 m (1,500 ft) of the TCEQ Recharge Zone boundary (COA, 2006).

The infiltration properties of a hydrostratigraphic unit can vary considerably across the Edwards outcrop area. In the bed of Onion Creek in Hays County, water can pond up to a meter or more deep for weeks over the Kirschberg Member, one of the most permeable unit of the Edwards Aquifer. About 70 m (200 ft) downstream of this "pond" is Crippled Crawfish Cave (see Figure 2.1 and Appendix G). This swallet has been measured to drain (whirlpool) at a rate of about 0.27 m^3/s (13 ft^3/s) into the subsurface on several occasions.

The eastern drainage area consists of overlying units such as the Del Rio Clay and the Buda Limestone and contributes runoff to the Edwards outcrop area from the eastern edge. Most of the eastern drainage area has a relatively short drainage to the eastern side of the Edwards outcrop area. The Manchaca Flow Route flows along the eastern edge of the Edwards outcrop area and rapidly carries groundwater across the Barton Springs Segment (Chapter 4). For these reasons, the hydraulic connection of the eastern drainage area with the underlying Edwards Aquifer may be indistinguishable from the Edwards outcrop area (Smith and Hunt, 2002). Where the Del Rio Clay is thin and overlying the Georgetown Formation, soil-piping sinkholes are observed that could recharge the Edwards Aquifer. Observations of flow loss, gains, and caves in the overlying confining units are described in section 2.3.6. Some parts of the eastern Edwards outcrop and eastern drainage areas may frequently or invariably run off downstream of the Edwards outcrop area without significant recharge to the aquifer. Consequently, the hydraulic connections from the artesian area to the Edwards Aquifer require examination using excavations, flow measurements, groundwater tracing, and other tests to more precisely establish recharge potential.

2.3.2 DEPOSITIONAL CHARACTERISTICS OF THE HYDROSTRATIGRAPHIC UNITS

The Cretaceous depositional environment in the study area is summarized by Rose (1972) and Lundquist (2000). Relatively rapid rates of sea floor spreading and volcanic activity released carbon dioxide gases to the atmosphere and corresponded to an

increase in annual temperatures of 10 to 15º C relative to recent temperatures. This caused relatively high sea levels during the Cretaceous (Savin, 1977; Berner et al., 1983). The rising water levels covered considerable land surface and decreased the albedo, increasing heat absorption and water vapor in the atmosphere (Barron et al., 1981; Barron et al., 1995). Relatively shallow marine waters covered the study area during much of the Cretaceous.

The hydrostratigraphic units are grouped into overlying confining units, Edwards Aquifer, and underlying units (Table 2.1). The overlying confining units include, in descending stratigraphic order, rocks of the Taylor Group, Austin Group (Austin Chalk), Eagle Ford Group (Eagle Ford Shale), Buda Formation (Buda Limestone), and Del Rio Formation (Del Rio Clay). The Edwards Aquifer incorporates the Georgetown Formation of the Washita Group, and the Person and Kainer Formations of the Edwards Group. The underlying units are rocks of the Trinity Group, in particular the Glen Rose Formation.

2.3.2.1. Overlying Confining Units

The Taylor Group consists of a dark calcareous clay. Only the lower Sprinkle Formation of the Taylor Group is exposed over the Barton Springs Segment. Surface erosion limits the Sprinkle Formation to a maximum thickness of about 120 m (400 ft) within the Barton Springs Segment (Young, 1977; Lundquist, 2000).

The Upper Cretaceous Austin Group overlies the Eagle Ford Group and is a chalky, variably marly, fossiliferous limestone, and in places includes igneous deposits, with a thickness of about 119 m (360 ft; Lundquist, 2000). The lower Austin Chalk contains *Inoceramus subquadratus*, which was noted by Young and Marks (1952) to be restricted to the lower 30 m (100 ft) of the Austin Group in Williamson County. The upper Austin Chalk contains a marine reptile, *Mosasaurus maximus,* that was recovered from the base of the Austin Group along Onion Creek (Shumard, 1860; Texas Memorial Museum, 2008). The oysters, *Inoceramus undulatoplic atus, Exogyra ponderosa,* and *Phyrygia a ucella* are present in the upper half of the Austin Group (Young, 1977; Lundquist, 2000).

Igneous deposits of the Austin Group may influence groundwater flow, as described in section 2.5, so particular attention was paid to mapping their outcrop. Most exposures of igneous deposits in the Barton Springs Segment weather easily and are poorly exposed except in creekbeds and excavations. Igneous deposits include a volcanic plug at St. Edwards University, exposures along Ben White Boulevard construction, at Blunn Creek preserve, along railroad tracks north of St. Elmo Road, in the Williamson Creek bed east of Emerald Forest Drive, in a tributary of Slaughter Creek about 500 m south of Slaughter Lane and about midway between Manchaca Road and Brodie Lanes, and north of Bear Creek east of FM 1826 (Figure 2.7). Igneous deposits also were reported in excavations along Queenswood Drive within the neighborhood northwest of Slaughter Lane and Manchaca Road (Sansom, personal communication, 1997).

Igneous deposits are described in greater detail by Moon (1942), Kolb (1981), Young (1982), and Caran et al. (2006). Hill and Vaughn (1898) observed that the igneous deposits were interbedded and extruded through the Austin Chalk and that "intrusive sheets and dikes of soft, much decomposed material of a basaltic nature occur within 10 miles" (18 km) of the Cretaceous Pilot Knob volcano, located east of the Barton Springs Segment. Collingwood and Reggter (1926) found that the Cretaceous "serpentine" deposits were a complex series of volcanic breccias, tuff, sill, and dikes that followed pre-existing faults and were both intrusive and extrusive from place to place. It is possible that molten materials followed existing fractures, minor faults, and heterogeneities in the consolidated Cretaceous stratum and that the fractures were reactivated by Miocene tectonics (Strong, 1957; Woodruff, 1985).

Young (1982) mapped igneous deposits in South Austin, where subdivision construction created fresh exposures, although Young's maps exclude large adjacent faults. He found fragments of Austin Chalk within the igneous deposits that would normally be found higher in the stratigraphic section. Young also inferred that the igneous exposures were discontinuous. Based on these two observations, he reasoned that the nepheline-type igneous deposits in South Austin were explosion craters rather than linearly continuous dikes. In addition to the sites north of St. Elmo Rd and railroad tracks and Williamson Creek east of Emerald Forest Drive examined by Young (1982) and

Housch (2006), other fault-bounded nepheline-type deposits were observed in the Slaughter Creek tributary (Small et al., 1996). The line of nepheline-type exposures trended approximately between the St. Edward's University paleovolcano and another basalt volcano south of Bear Creek mapped by Moon (1942) and Kolb (1981). I had difficulty reconciling the exposures mapped by Young (1982) with what I could see in outcrop, particularly as new exposures were discovered. The igneous deposits were interpreted in Small et al. (1996) and in the current map as a fault-bounded linear feature, similar to the dikes described by Hill and Vaughn (1898) and Collingwood and Reggter (1926), that is poorly exposed except at creek crossings and excavations that lie in a relatively straight line from the St. Edwards University paleovolcano to the basaltic paleovolcano north of Bear Creek. Alternately, it is possible, although unlikely, that Miocene faulting placed the discontinuous volcanoclastic deposits adjacent to lower-lying limestones of the Austin Group as narrow downdropped grabens.

The Eagle Ford Group underlies the Austin Group and is a calcareous, sandy shale, with a thickness of about 12 to 14 m (40 to 47 ft) in south Travis County and thinning southwest on the San Marcos arch (Adkins, 1932, p. 430; Lundquist, 2000). The source of the Eagle Ford sediments is erosion of the paleo Ouachita Mountains to the northeast across the current Red River (Lundquist, 2000). The flaggy, sandy shale erodes easily and is poorly exposed except within a few creeks. The Eagle Ford Group upward sequence includes the black, wavy, and "soapy" Pepper Shale; the light-colored and silty, iron-bearing Cloice Shale; the fissile shales and white crystalline biomicrite or biosparite limestones of the Bouldin Flags; and is superimposed by the gray calcareous South Bosque Shale (Lundquist, 2000). The uppermost Eagle Ford Group contains phosphatic pebbles up to 8 cm (3 in) in diameter (Adkins, 1932, p. 431). Some of the rock fragments emit a petroliferous odor when fractured. Fossil fish remains and ascending zones of *Acanthoceras sp* ., *Eucalycoceras bentonianum* , *Neocardioceras*, *Romaniceras*, *Coilopoceras*, *Prionotropia*, and *Alectryonia lugubris* also are found in the Eagle Ford Shale (Adkins, 1932, P. 435). The contact of the Eagle Ford Group and underlying Buda Formation is separated by an unconformity in the Barton Springs Segment (Adkins, 1932, p. 431).

The Buda Limestone is a dense, variably nodular, sublithographic or "porcelaneous" (Sellards et al., 1933, p. 397), light gray mudstone, commonly containing orange calcispheres or pelloids and tiny calcite-filled fractures. Its characteristic fossils include *Budaiceras*, ammonites, *Exogyra clarki* , *Pecten roemeri* , *Codiopsis texana* Whitney, and several species of *Mantelliceras* (Adkins, 1932, p. 399-400). The Buda Formation has a thickness of 11 to 18 m (35 to 50 ft) in the Barton Springs Segment. It thickens to the southwest across the San Marcos Platform (Lundquist, 2000).

The Del Rio Clay is a 15 to 18 m (50 to 60 ft) thick, dark blue-green to yellow-brown, variably gypsiferous clay commonly containing pecten-type fossil clams and an abundance of the fossil oyster *Ilymatogyra arietina*, formerly *Exogyra arietina* (Roemer, 1949b). These fossil oysters are commonly referred to as "ram's horns" or "devil's toenail." The upper Del Rio Clay contains *Gryphaea mucronata* in Travis County (Adkins, 1932). The Del Rio may contain thick horizontal or vertical selenite seams and filled fissures, particularly in faulted areas. A very hard, *Ilymatogyra*-laden bed can be observed near the base of the Del Rio Clay in south Travis and north Hays County. Adkins (1932, p. 390-394) observed a full section of Del Rio Clay near the mouth of Barton Creek at the Barton Springs Road crossing shortly after construction and believed it to be 24 to 30 m (80 to 100 ft) thick. This Barton Creek exposure is now weathered and poor; better exposure of the Del Rio Clay exists east of Barton Creek and north of Loop 360 on City of Austin greenbelt parkland. Pyrite is common within the Del Rio Clay, suggesting its deposition under reducing conditions.

2.3.2.2. Edwards Aquifer

The Edwards Aquifer consists of the Georgetown Formation of the Washita Group and the underlying Edwards Group that consists of the Person and Kainer Formations.

The Georgetown Formation, which overlies the Edwards Group, was deposited on the eroded surface of the Person Formation in deeper water than was characteristic for most of the Edwards Group (Rose, 1972, p. 71). The Georgetown Formation is a marly, nodular packestone and grainstone limestone and contains the characteristic brachiopod

Waconella wacoensis, formerly *Kingena wacoensis* (Roemer, 1849b). The Georgetown Formation contains a number of other characteristic fossils, including *Rastellum carinatum* (Lamarck, 1806), formerly known as *Ostrea (Alectryonia) carinata*, *Texigryphaea washitaensis*, various echinoids and ammonites, and various types of pectin including *Neithea texana*. The University of Texas recovered the remains of a marine reptile *Ichthyosaur* from the contact of the Georgetown Limestone and Del Rio Clay at Marbridge along Bear Creek (Figure 2.1). The thickness of the Georgetown increases from south to north across the Barton Springs Segment, ranging from 12 to 18 m (40 to 60 ft) in the study area. The contact of the Georgetown Formation and the underlying Person Formation is a reddish to orange oxidized, bored, and pitted horizon that is evidence of a disconformity where the underlying Edwards Group was lithified and exposed prior to Georgetown Formation deposition (Adkins, 1932; Abbott, 1977).

The Edwards Group was previously named "the Barton Creek limestone" by Hill and Vaughan (1898) with its excellent exposure in its type locality along Barton Creek in South Austin (Adkins, 1932). In general, the Edwards Group as a whole is distinguished from overling and underlying units by the presence of chert; massive, regular limestone bedding; rudists such as *Caprinuloidea* and *Toucasia*; and pulverulites (Adkins, 1932). Hill's original measured sections are reproduced and reinterpreted in Appendix B. Within the study area, the thickness of the Edwards Group, consisting of the Person and Kainer formations, is about 140 m (450 ft) within the City of Buda area and diminishes to a thickness of about 105 m (350 ft) in the northwest corner near Red Bud Trail bridge (Figure 1.4) over the Colorado River.

The Person Formation of the Edwards Group consists of the Marine, Leached, Collapsed, and Regional Dense Members of the Edwards Group. The overlying Cyclic Member of the Edwards Group may also be present, although it has not been identified in measured sections within the Barton Springs Segment and so is not considered here.

The undivided Cyclic and Marine Members consist of a chert-bearing wackestone containing abundant *Caprinuloidea* (caprinid) fossils. Erosion prior to Georgetown Formation deposition limits exposure of the Marine Member within the study area. In the Hays County portion of the study area, the Cyclic and Marine Members, if present, have

a maximum thickness of less than 21 m (70 ft). On Bear Creek near the Hays and Travis county line, the Marine Member may only be about 1.5 m thick (5 ft), based on the presence of caprinid-bearing beds directly below the Georgetown Limestone (see Marbridge measured section in Appendix B). The lower portion of the Marine Member is difficult to distinguish from the upper part of the undifferentiated Leached and Collapsed Members because of their similar lithology and lack of measured section exposure in northern Hays County.

The undivided Leached and Collapsed Members underlie the Marine Member in Hays County and the Georgetown Formation in Travis County. The combined thickness of the two members ranges from about 21 m (70 ft) near the Blanco River to less than 7 m (25 ft) near the Colorado River. These members consist of a light-colored, relatively clean wackestone, although burrowed mudstones, grainstones, and intervals of crystalline limestone also can be found. In portions of south Travis County, the Leached and Collapsed Members may have a light pastel-pink tint, possibly from oxidation during Cretaceous exposure. Chert lenses also are common. A wide variety of fossils can be found in these members, particularly *Toucasia*, *Chondrodonta*, and miliolid foraminifera. The base of the Leached and Collapsed Members is particularly fossiliferous, containing packestones or grainstones of *Toucasia, Chondrodonta,* miliolid foraminifera*, Caprinuloidea*, and in at least one location *Cladophyllia*. Remnant siliceous petrified wood was encountered overlying exposures of the Leached and Collapsed Members in portions of the Hays County, west of FM 2770 and south of FM 967 in the study area (Figure 2.1). Cronin (1932) and Abbott (1977) noted the presence of petrified wood within the Person Formation of Comal and Hays Counties. Young (1986) associated the petrified wood found by Cronin (1932) with Pleistocene terra rossa deposition rather than Cretaceous deposition. The hypothesis of fossilized Pleistocene plants fails to explain why these siliceous fossil remnants are strongly associated with exposures of specific beds in the Edwards Group and are not otherwise widely distributed. The hypothesis offered by Quinlan (1978, p. 66) that some terra rossa are remnants from extensive dissolution of certain soluble beds agrees overall with the correlation of terra rosa with those soluble beds. The collapsed zones common in the Leached and Collapsed Members

probably were caused by the fall of overlying limestone into the voids created by early dissolution of thin evaporate layers and lenses (Rose, 1972, p. 55). The lower 5 m (15 ft) of the undifferentiated Leached and Collapsed Members commonly contain a large collapsed zone (Rodda et al., 1970) that Rose (1972) distinguished as the Collapsed Member.

The Regional Dense Member (RDM) is the lowermost member of the Person Formation. It is a dense, argillaceous mudstone. The RDM has a characteristically light tan color, nodular surface weathering, fissile-bedding and wispy iron-oxide stains. This member has a thickness of 4.5 to 10 m (15 to 32 ft) in the Barton Springs Segment, and thins toward the Colorado River. Fossils are not abundant within the RDM, and many of the fossils common in other members of the Edwards Group, particularly miliolid foraminifera, are characteristically lacking within the RDM. The fossil *Pleuromya knowltoni* is unique to this member. *Ceratostreon texanum* has been observed: (1) in a resistant bed within the lower half of the RDM in Bowie High School Cave, (2) in Hays County southwest of FM 1626 and FM 967, and (3) by Abbott (1973) on a Colorado River bluff near Red Bud Trail. On downhole survey logs, the natural gamma increases significantly through the RDM, reflecting its greater clay content. On aerial photographs, the RDM has a much lighter tone than adjacent unit exposures. The depositional environment of the RDM was low energy (Rose, 1972), and as expected for flat-lying, low energy beds, the RDM is laterally extensive. Small quarries mined for road base were commonly excavated in this member. An abandoned quarry exposing the top of the RDM in Zilker Park near the Colorado River contained the footprints of dinosaur theropods, plant fossils, and the shell of a Cretaceous turtle, *Osteopygis* (Texas Memorial Museum, 2008). Polygonal mud cracks occur at or near the top of the RDM in exposures of Zilker Park and along Barton Creek. The shallowing of the Cretaceous sea toward the end of RDM deposition may have been caused by a gentle rise of the San Marcos Platform (Rose, 1972).

The Kainer Formation includes the Grainstone, Kirschberg, Dolomitic, and Basal Nodular Members. The combined thickness of the Kainer Formation generally is about

100 m (300 ft) thick within the Barton Springs Segment, but may be less on some portions of the western edge of the study area.

The Grainstone Member is the uppermost member of the Kainer Formation. It is 14 to 18 m (45 to 60 ft) thick and consists of a dense, tightly cemented, miliolid grainstone. The Grainstone Member typically has a very light gray, almost white or light yellow color on fresh surfaces and contains intervals of mudstone to wackestone limestone. The Grainstone Member was deposited under high energy conditions (Rose, 1972) and commonly shows cross-bedding. Within the study area, *Chondrodonta, Caprinuloidea,* and less commonly *Toucasia* are commonly found in the uppermost massive miliolid grainstone bed of the Grainstone Member. Layered chert nodules, mudcracks, and pulverulite are present in the lower half of the member. A distinctive *Turitella* packestone is commonly found near the base of the Grainstone Member. *Eoradiolites* also are found in the Grainstone Member.

The Kirschberg Member is a 12 to 23 m (40 to 75 ft) thick evaporitic limestone consisting of crystalline rock and chalky pulverulite with chert nodules and lenses. The name "Kirschberg" was derived from the original German name for "Cherry Mountain" near Fredericksburg, Texas in north Gillespie County, where gypsum and alabaster horizons are still present (Barnes, 1944). Evaporite deposits are present within the Edwards Group outcrop in Maverick County, including an anhydrite seam; a 7 m- (20 ft-) thick rock salt deposit stratigraphically positioned near the top of the Edwards Group; and a gypsum or alabaster seam are reported (Adkins, 1932). Gypsum seams are also reported in Menard County, Kinney County, and Gillespie County (Adkins, 1932). The Kirschberg Member probably was formed in highly saline, sabkha tidal flats (Rose, 1972). Finely laminated crusts or algal laminations, mudcracks, *Cladophyllia* coral, rudists such as *Caprinuloidea*, *Toucasia*, and chert layers are common in the Kirschberg Member. Eroded Kirschberg hills often contain terra rossa soils and reddish, siliceous, erosional remnants bearing *Cladophyllia*, *Caprinuloidea*, and *Toucasia* . Quartz megacrystals commonly fill voids inside rudist fossils of these siliceous remnants. The pulverulite layers are composed of euhedral dolomite crystals loosely cemented with calcite (Hill et al., 1898; Mahler, 1997; Lynch et al., 2004). The Kirschberg Member is a

highly-recrystallized sparite such that original matrix and fossils are not commonly observed, except those fossils replaced by silica.

The Dolomitic Member consists of resistant, highly-bedded wackestone. The upper half typically contains a poorly-sorted matrix that distinguishes it from the Leached and Collapsed Members, which it can superficially resemble. A tan-gray 1-m (three-ft) thick marker bed near the top of the Dolomitic Member contains *Dictyoconus walnutensis.* Chert in the Dolomitic Member commonly appears as isolated nodules rather than the continuous bedded chert characteristic of the Kirschberg and Grainstone Members. A miliolid grainstone, very similar to beds of the Grainstone Member, can be found below the *Dictyoconus* marker bed in some areas. A 1.2-m (4-ft) thick series of thin "rhythmic" beds that macroscopically resemble the RDM of the Person Formation is positioned near the middle of this unit. Like the RDM, the rhythmic beds show an increase in natural gamma radiation on geophysical logs across the Barton Springs Segment. The rhythmic beds also contain an uppermost mud-cracked interval, as observed in the City of Austin-owned Stoneledge (quarry) Water Quality Protection Land in Hays County (Figure 2.1). Below the rhythmic beds, a massive *Caprinuloidea* bed can be found in upper Barton Creek. The Dolomitic Member has a thickness of about 43 m (140 ft) in much of the Barton Springs Segment. In Hays County, the lowermost bed of the Dolomitic Member is a distinctive, massive 2-m thick *Toucasia* wackestone that is honeycombed from selective weathering of its fossils.

The Basal Nodular Member is the lowermost member of the Kainer Formation and Edwards Group within the Barton Springs Segment. Its depositional environment was marked by a slight regional deepening of the inland sea following prior exposure of the lithified Glen Rose Formation tidal flat deposits (Ellis, 1985). The Basal Nodular Member appears to be indistinguishable from the Walnut Formation, which is present north of the Colorado River where it consists of the Bull Creek and Bee Caves Members described by Moore (1961) and Rodda et al. (1970). The Basal Nodular Member is highly fossiliferous and nodular, containing an upper *Texigryphaea* packestone intermediate miliolid grainstones and burrowed mudstone, and a lower *Ceratostreon texanum* packestone (Moore, 1961; Moore, 1964; Rodda et al., 1970; Small et al., 1996).

In some exposures, burrows are differentially dissolved to produce honeycombed texture and the matrix is highly recrystallized and oxidized such that the Basal Nodular Member superficially resembles the Kirschberg Member. Natural gamma downhole logs show a distinct gamma increase within the Basal Nodular Member. The Basal Nodular Member is 14- to 20-m (45- to 65-ft) thick in the Barton Springs Segment (Small et al., 1996).

2.3.2.3. Underlying Units

The contact of the Basal Nodular Member and Glen Rose Formation is marked by a discolored hardground surface. The upper Glen Rose Formation of the Trinity Group is exposed west of the Barton Springs Segment. It is strongly bedded with alternating marly and massive beds that weather into a stair-step topography (Stricklin et al., 1971). One of the uppermost beds of the Glen Rose Formation is a *Caprinuloidea* packestone. Celestite nodules also are abundant near the top of the Glen Rose Formation (Hill and Vaughan, 1898; Adkins, 1932). Gypsum outcrops were described by Adkins (1932) within the Glen Rose Formation near the mouth of Bull Creek north of the study area in northwestern Travis County. Large theropod footprints, possibly of *Acrocanthosaurus*, are found within the upper Glen Rose Formation west of FM 1826 in Hays County. Shallow water deposition of the Glen Rose Formation is consistently indicated by these dinosaur tracks, as well as ripple marks, plant fossils of *Chara* algae and cycads, gypsum seams, and its overall lithology (Adkins, 1932). Characteristic Glen Rose Formation fossils include *Trigonia*, *Pecten*, *Alectryonia carinata* , *Orbitolina texana* foraminifera, and various echinoids (Adkins, 1932). The Glen Rose Formation is up to 270 m (825 ft) in thickness (Stacy Park well in South Austin, Figure 2.1), but thins to 18 m (55 ft) near Kerrville (Adkins, 1932).

2.3.3 DIAGENESIS AND MATRIX POROSITY

The matrix is described as the "solid framework of a porous system" (Field, 2002b). In this study, the matrix is considered to be the phreatic groundwater-bearing rock between fissures, conduits, caves, bedding plane partings. Within the unsaturated zone, where specified, matrix may refer to portions of soil between macropores and rocks of the unsaturated vadose zone between fissures, conduits, caves, and bedding plane

partings. In this subsection, the diagenesis of the rock matrix of the Barton Springs Segment is examined. Ellis (1985) described the diagenesis of the Edwards Aquifer as consisting of:

i) Cretaceous diagenesis
    1) Deposition of marine and fresh-water calcic and magnesium calcite cements.
    2) Two types of dolomitization:
        - Fine-grained anhedral dolomite formation in a sabkha depositional environment
        - Silt-sized euhedral dolomite crystal formation in a schizohaline environment, where fresh water mixes with restricted saline waters. These are the pulverulitic layers.
    3) Replacement of some calcic shells and evaporates with silica. Chert nodules probably formed early after deposition, but after at least some of the dolomitization took place.
    4) Deposition of evaporates (such as halite and gypsum) in a sabkha environment.

ii) Post-Miocene development of fresh-water aquifer system:
    5) Incongruent dissolution of magnesium, neomorphism of some micrite to microspar, and an influx of clays that preferentially sorb magnesium.
    6) Dedolomitization by removal of magnesium-rich brines by fresh water with higher calcium to magnesium ratio.
    7) Deposition of spar cements filling some voids.

Porosities typically of 25 to 35% but as high as 43% were measured in dolomites of the Edwards Group where incomplete dolomitization resulted in the fresh-water dissolution of undolomitized micrite (Ellis, 1985).

An important element of diagenesis is the dissolution of the matrix framework by meteoric or mixing groundwaters undersaturated with respect to calcite. Within the Barton Springs Segment, prominent matrix dissolution processes include:

8) Dissolution of soluble evaporitic deposits, including halite and gypsum, resulting in large voids and collapse of overlying beds (Rodda, 1970; Rose, 1972; Hovorka et al., 1993, p. 39-42).
9) Dissolution of calcite cement in pulverulites. The loose euhedral dolomitic crystals are easily eroded by fast-flowing groundwater along focused groundwater flow paths (Mahler, 1997). The pulverulitic beds within the Kirschberg Member are visible in the walls of numerous caves and in downhole videos of wells. This process could be the most significant for the development of groundwater flow routes.
10) Dissolution of rudists and burrows to create honeycombed porosity. In packestones and wackestones containing rudists such as *Caprinuloidea*, *Toucasia*, and *Requienia*, the fossils frequently are preferentially dissolved. This preferential dissolution results in a "honeycombed" texture of well-connected voids. The preferential dissolution of burrows also creates honeycombed texture, particularly within the Basal Nodular Member of the Edwards Group. Although honeycombed texture commonly is associated with the Edwards Group, it also is common within beds of the upper Glen Rose Formation on the contributing area.
11) Dissolution of limestone, particularly along fractures, by water undersaturated with respect to calcite.

2.3.4 Influences of Igneous Deposits

Igneous deposits can serve as barriers to groundwater flow (Hill and Vaughan, 1898; Meinzer, 1923; Brune, 1981; Kuniansky et al., 2001) or provide mixing fluids and carbon dioxide that potentially can enhance limestone dissolution (Gary and Sharp, 2006). Lava flows are likely to contain voids in the form of vesicles, lava tubes, and fractures from rapid cooling and shrinking (Meinzer, 1923, p. 104, 100-111) and tuffs can be very porous (Meinzer, 1923). Smyth and Sharp (2006) summarize processes that increase the hydraulic conductivity of tuff including trapping of gases by subsequent flows, postdepositional mineralization such as devitrification, and fracturing. The

porosity of the igneous deposits in the Austin area is greatest in the brittle center where voids are most encountered, and least within soft, very fine-grained clay interbeds and edges (Collinwood and Reggter, 1926). Gary and Sharp (2006) hypothesize that volcanism enhanced karst development within the Cretaceous carbonates of Sistema Zacatón of northeast Mexico by elevating CO_2 and H_2S. It is not known whether these igneous processes influenced the aquifer development of the Barton Springs Segment. Igneous sills and dikes can create groundwater barriers (Meinzer, 1923, p. 190). However, within the Barton Springs Segment, there is little evidence that these igneous rocks are significant in terms of regional flow. This is consistent with Oetting (1995), who observed no geochemical evidence of igneous interaction with groundwater in the Barton Springs Segment.

2.3.5 Effect of Stratigraphic Dip

The gradient created by stratigraphic dip strongly influences groundwater flow in limestone aquifers. Palmer (1986), White (1999b), and Ginsberg and Palmer (2002) noted that groundwater in vadose conduits flow generally along the down dip direction, with possible slight deviation from the influence of fractures, whereas phreatic conduits tend to be oriented perpendicular to dip. Early geologists observed that the edges of the Balcones Fault Zone marked a deflection in dip east of the fault zone to relatively flat-lying strata to the west. Hill and Vaughan (1898) noted "south of the Colorado River…the rocks of the Edwards Plateau are more nearly horizontal than those of the Rio Grande plain; their average dip is less than ten feet to the mile, while in the plain the dip averages between 50 and 100 feet to the mile." Baker et al. (1986) reported an east-southeast dip averaging 21 to 23 m (70 to 75 ft) per mile across the Barton Springs Segment. Distinction of actual bedding dip from offsets resulting from faulting and localized fault drag requires relatively detailed mapping that had not been conducted before the mid 1990s (Small et al., 1996). Consequently, earlier reports of eastward dip across the Barton Springs Segment likely combined fault displacements and stratigraphic dips. Eastward dipping beds are visible along Bear Creek for about 2 kilometers upstream of Marbridge (Figures 2.1 and 2.5). In some areas of the Barton Springs Segment,

northeastern dipping bedding planes were mapped in Figure 2.2 in association with scissor faults and ramps. The geologic map and cross sections reveal that although a few specific blocks do have dips to the east, northeast, or southeast, most of the bedding dip within fault blocks across the Barton Springs Segment is essentially flat. It is possible that regional eastward dips as slight as 3 m (10 ft) per mile are present but were not detected.

Local groundwater within the Edwards outcrop area tends to flow southeast, east or northeast even though the stratigraphy is flat. In the study area, very few instances of southeastern dipping bedding planes are indicated by field mapping, although fault blocks are commonly downdropped in this direction. Consequently, it is actually the stair-stepped fault blocks and not dip in the stratigraphic units that creates eastward or southeastward hydraulic gradients, as illustrated in Figures 2.3, 2.4, and 2.5.

Downdropped fault blocks create great disparities in saturated thickness and transmissivity across the Barton Springs Segment. The saturated thickness diminishes to zero along the far western side of the outcrop area and increases to the maximum aquifer thickness of about 150 m (500 ft) in the artesian area (Baker et. al., 1986; Hauwert, 1997; Smith and Hunt, 2004). The saturated thickness diminishes during low-flow periods such that portions of the western side of the outcrop area become essentially dry (Slade et al., 1986; Hauwert, 1997; Smith and Hunt, 2004). The decrease in transmissivity from the artesian area to the Edwards outcrop area can be directly attributed to decreasing saturated thickness from east to west across the Barton Springs Segment.

2.3.6. FAULTS AND FRACTURES

One of the most striking features of the surface hydrostratigraphic map is the high degree of faulting, which resembles a broken sheet of glass (Figure 2.2). Faults in the Barton Springs Segment are part of the Balcones Fault Zone. This fault zone developed above an ancient Ouachita mountain range and structural belt (Flawn et al., 1961; Woodruff and Foley, 1985). Some faulting and fracturing probably has occurred following consolidation of the Cretaceous sediments (Sellards and Baker, 1934; Bryan, 1936; Maclay and Small, 1984), possibly associated with uplift on the San Marcos Arch

(Kastning, 1986). The most significant faulting occurred in the Miocene (Maclay and Small, 1984).

The faults are normal faults and many formed en-echelon to the northeast to southwest trend of the Balcones Fault Zone. Oblique en-echelon faulting typically forms as a result of uneven displacement or strike-slip faulting (Wilcox et al., 1973). However, strike-slip faulting is discounted for the Balcones Fault Zone because of the lack of evidence for horizontal movement (Strong, 1957). The lack of surface expression of strike-slip faulting is insufficient to eliminate its possibility since in other areas where deep-seated basement strike-slip faulting has occurred, such as the San Andreas fault in California and Bowling Green Fault Zone in northwest Ohio, the primary surface expression are en echelon normal faults rather than strike-slip faults (Wilcox et al, 1973; Hauwert, 1991). In the case of the Barton Springs Segment, post-depositional rise in the San Marcos Platform most likely created a series of ramp and scissor faults (Collins, 1993, Collins 1995.) These faults vary in displacement along their extent. In some areas of the Barton Springs Segment, particularly where inferred cross faults are mapped, more detailed mapping is required to distinguish whether the abrupt changes observed in surface lithology are created by cross faulting or ramp structures.

Fault offsets are highly variable across the Barton Springs Segment, even along the same fault. Faults with major offset in the Barton Springs Segment include the Mount Bonnell fault, which has a maximum displacement of 90 to 120 m (300 to 400 ft) in the northeastern corner of the Barton Springs Segment and in most places serves as the eastern edge of the Edwards outcrop area, and the Mustang Branch and Mountain City faults, each with a maximum displacement of about 30 m (100 ft, Figure 2.2). The fault displacement rarely remains consistent across the Barton Springs Segment. North of the Colorado River, the offset of the Mount Bonnell fault was measured as 200 m (670 ft, Damon, 1924) and its offset decreases to the south (Senger and Kreitler, 1984). The Mount Bonnell Fault is known as the Tom Creek Fault in Hays County (DeCook, 1963). An offset in bedding exposed as a fault in some localities may be expressed as dipping strata or as a monocline in other areas. In some instances, single faults separate into a number of smaller faults. In many instances, the displacement may change along the

length of the fault as rotational faults, as described by Billings (1947) and Donath (1962). Cross sections west to east across the Barton Springs Segment show a net vertical offset of 326 m (1,070 ft) along Bear Creek and 384 m (1,260 ft) along Barton Creek that results almost entirely to fault offsets (Figures 2.3 and 2.5; Hauwert et al., 2004b).

Fracturing and faulting play an important role in the karst maturity of the Barton Springs Segment. In fractured limestone aquifers, a single fracture or small numbers of fractures can dominate the flow system (Paillet et al., 1987, Marrett, 1996; Marrett et al., 1999; Halihan et al., 2000; Sharp et al., 2000). Halihan (2000) inferred that the permeability contributing to well yields of the Edwards Aquifer was influenced by fractures and not significantly by matrix or conduits. The rational for the importance of fractures relative to conduits is that conduits rarely intercept wells whereas fractures observed in typical outcrops can account for the highest permeability found in wells. Because faults are associated with crushed material, voids, and fractures, they represent planes of weakness along which groundwater flow is focused, facilitating the dissolution and erosion of the host carbonate rock into more integrated conduits frequently parallel to the general direction of faulting. Faults initially can have open apertures from tensional stresses or poorly matching sides (Meinzer, 1923, p. 185; Lowe, 2000).

The disparity of well and spring yields between the relatively unfractured and low-yielding Edwards Plateau Segment of the Edwards Aquifer and the highly productive Balcones Fault Zone portion indicate that faulting plays an important role on transmissivity (Abbott, 1977). Fractures aligned parallel to the predominant flow gradient are favored for aperture development (Mandel, 1966; Hushey et al., 1967; Kiraly, 2002). Conduit development is particularly favored in down-dropped graben blocks (Kuniansky et al., 2001). The fact that faults and fractures exist throughout an aquifer, yet the conduits are focused on selected faults and fractures, suggests that the fractures do not necessarily control the location of conduits (Huntoon, 1992). Groundwater tracing indicates that across much of the Edwards outcrop area of the Barton Springs Segment, groundwater flow is influenced by gradients formed by down-dropped fault blocks and flows perpendicular to general northeast-fault trends (Hauwert et al., 2004a). Studies in the San Antonio Segment comparing aquifer-test transmissivities to mapped faults have

not shown strong correlations (Hovorka et al., 1995, p. 107). There are limits in assessing the importance of fractures versus conduits on groundwater flow based on observations from wells and outcrops in that: (1) the distinction between fractures, fissures, and conduits may be inconsistent in the literature, and (2) fracture apertures in outcrop are unrepresentatively large compared to those present within the deeper phreatic zone (Walsh et al., 1973; Mace and Hovorka, 2000; Klimchouk, 2004).

The definition of apertures as fractures or conduits is inconsistent in the literature. Bear (1993) defines a fracture as "a part of the void space of a porous medium domain that has a special configuration: one of its dimensions, the aperture, is much smaller than the other two ones." White (1999) used a 10-millimeter aperture size to distinguish between fractures and conduits. Such definitions do not specify whether a fracture is a product of tectonics, solution enlargement, or both, and may inadvertently imply that fractures and conduits are distinguished by aperture size. Many cave passages within the Barton Springs Segment occur along solution enlarged bedding planes or solution-enlarged fissures and would be considered fractures under this definition. A solution-enlarged fissure may be categorized as a fracture by some investigators and as a conduit by others. Halihan (2000) shows fracture apertures exceeding tens of centimeters in width. The largest fracture apertures measured in Zahm's (1998) study of the Barton Springs Segment "exhibited significant solution enhancement." According to Kulander et al. (1979), fractures are formed nearly instantaneously from stress failure. Extensional fractures are formed with maximum tensional stresses that are perpendicular to the fracture plane and maximum compressional stresses that are parallel to the fracture plane, and extensional displacement occurs perpendicular to the fracture plane, creating an aperture. Change in the stress field or solution development can subsequently modify a fracture. Kulander's definition of fractures is used in this report because it distinguishes apertures created by tectonic and solutional causes. Portions of these tectonic features become enlarged through dissolution, stress release through overburden removal, erosion, and other later processes to become planar, solution-enlarged, or otherwise widened planar apertures called fissures (Meinzer, 1923).

Most fracture observed at the surface result from stress release and do not remain open far into the subsurface. Stress release causes fissure apertures parallel to the erosional surface and fracture frequencies to increase exponentially toward the surface (Meinzer, 1923, p. 114; Ford and Ewers, 1978, p. 1792; Chernyshev, 1983; Klimchouk, 2000). Vertical fracture spacing in a glacial till in Sweden increased from 5 cm wide at 2 m depth to 20 cm wide at 6 m depth (Hinsby et al., 1996). Hydraulic conductivity in gneissic and granitic rocks tested in Sweden correlates inversely to depth (Neretnieks, 1993), reflecting overburden release or surface weathering. Rock failure curves by Donath (1970) found brittle failure of the Crown Point limestone of Vermont to occur at 4000 bars of differential stress at 1400 bars of confining pressure, but only 2000 bars of differential stress resulted in failure at about 400 bars of confining pressure. In order to view fractures minimally affected by near-surface pressure release, Ford and Ewers (1978) recommended fracture mapping in deep caves. In addition to pressure-release fractures created by surface denudation, other fractures created by post-tectonic processes include those created by quarry blasting, removal of adjacent rock parallel to quarry or bluff walls, underlying voids (e,g. collapse caves), etc., although these late-origin but otherwise "pure" fractures are not considered significant to groundwater flow in the Barton Springs Segment. Therefore, extensional fractures are not expected to be open at depths of 70 m depths where the water table and phreatic zone are generally present unless the fractures are solutionally enlarged into fissures or conduits.

In order to examine the effects of extensional fractures without the effects of solution and pressure release, fracture apertures and connectivity in less soluble rocks of deep mines can be observed (Meinzer, 1923). Fractures in the granitic Stripa mine of Sweden were closed or mostly very tight with few open apertures at fracture intersections (Abelin, et al., 1985; Neretnieks, 1993). Even in crystalline rocks however, preferential pathways or "channeling" can be created by dissolution, erosion, variations in apertures width, and fracture intersections (Paillet, 1988; Tsang and Hale, 1988; Neretnieks, 1993). Fractured dolomites, alluvium, and sandstones can display solution features such as caves, sinkholes, sinking water bodies, and localized spring discharge (Meinzer, 1923, p. 136; Huntoon, 1981; Hauwert, 1991; Worthington, 1999; Shade et al., 2001). Solution

and pressure release may account for borehole tracer breakthroughs that are different than those predicted by examining fracture apertures in crystalline rocks in Sweden (Moreno, et al., 1983). The contrast between spring discharge, transmissivity, and cave development of the Edwards Aquifer in comparison to the equally faulted and fractured but less soluble overlying confining units, such as the Buda Limestone, Austin Chalk or Eagle Ford Shale, reflects the importance of fracture enlargement by solubility in the development of permeability within the study area (Brune and Duffin, 1983).

In soluble fractured rocks, the effects of dissolution and fracturing are so inter-related that it difficult to separate the significance of each factor individually in the development of preferential pathways. Extensional fracture features, such as hackles, plumes and other fracture features described by Hodgson (1961) and Kulander et al. (1979), can be used to distinguish fractures unmodified by solution. Fault planes unmodified by solution are distinguished by slickenlines on both faces and are expected to have large apertures following the removal of gouge, breccia, and mineral fill that are proportional to the amount of displacement. Solution features such as rills and scallops on fracture faces indicate solutional enhancement. The solutional development of most apertures encountered within the study area lie along a spectrum of karst maturity and overburden release, from a fresh tight fracture to a pressure-release or solution-enlarged, planar fissure and eventually to a rounded conduit or sinkhole.

Fracture traces are natural lines visible on aerial photographs and less than 1.6 km (1 mi) in length (Lattman, 1958). Lineaments are fracture traces greater than 1.6 km (1 mi) in length. They are distinguished by linear alignments of features such as topography, vegetation type and density, soil tone, stream segments, bedrock scarps and prominent bedrock fractures. Like fractures, fracture traces and lineaments are thought to be influenced by geologic structure, lithology, and rock solubility (Trainer, 1967). Fracture traces and lineaments may be related to fractures (Lattman and Nickelsen, 1958; Lattman and Matzke, 1961; Hough, 1960; Krothe and Bergeron, 1981), although the terms are not interchangeable. Lineaments were mapped across the Barton Springs Segment in De La Garza and Slade (1986). Fracture traces serve in early mapping to delineate possible faults, and as discontinuities extending to the water table level to reflect possible

influences on groundwater flow. Fracture trace and lineament densities and shifts in their prominent orientation have been used to delineate the extent of major fault zones, even when covered with more than 35 m of loosely consolidated overburden (Hauwert, 1991).

Fracture skins increase the heterogeneity of the rock because of differences in porosity, diffusivity, permeability, and sorption, and because of their large surface area relative to the total rock volume (Robinson et al., 1998). Sorption on the fracture skin can reduce concentrations of soluble constituents. Mineral deposition, clay filling, and organic growths on a fracture skin can inhibit flow and transport from the aperture into the rock matrix (Moench, 1984; Fu et al., 1993; Sharp, 1993; Sharp et al., 1995; Zimmerman et al., 2002).

2.3.7. SOLUTIONAL CHARACTERISTICS OF THE HYDROSTRATIGRAPHIC UNITS

Solution cavities also develop preferentially along more soluble or softer bedding planes as a result of chemically undersaturated or rapidly moving groundwater flow. Through the processes of dissolution, erosion, and/or collapse, specific water pathways tend to become larger and better integrated over time. The presence and form of caves reflects properties of the hydrostratigraphic units they develop within.

The hydraulic properties of individual hydrostratigraphic units are examined using a variety of techniques. Some studies have examined variations in hydraulic properties of individual stratigraphic units using packers in a few pumping wells of the Barton Springs Segment (Flores, 1990). In general, well bores are very small in relation to the scale of the aquifer-wide heterogeneities, such as solution-enlarged conduits, expected in karst areas (White, 1988). On a larger scale, the solutional properties of the hydrostratigraphic units can be examined in outcrops and caves. Caves within the Barton Springs Segment can extend vertically across hydrostratigraphic units and allow a larger area of observation for a feature than a well bore.

Cave morphology typically expresses the permeability of the rock unit. Vertical shafts typically develop in association with fractures penetrating relatively low permeability units: horizontal passages develop in relatively high permeable units (White, 1988). Palmer (1991; 2003) describes the significance of lateral cave passage

morphology worldwide (Figure 2.8). Cave morphology reflects the aquifer pre-solutional porosity as a function of recharge type: discrete, diffuse, or hypogenic (Palmer, 1991). Discrete flow is reflected by branchwork patterns resembling those of dendritic streams in morphology and are formed as a result of discrete recharge and discrete, converging groundwater flow. Branchwork cave patterns by far represent the most common morphology worldwide (Palmer, 1991). Where fractures have a predominant influence on groundwater flow, cave passages tend to have an angular network pattern, although this cave morphology is observed in only 10% of known caves and typically only where overlying confining rocks inhibit surface karst topography (Palmer, 1975). Maze passages reflect conditions where flow is evenly distributed, such as seepage through insoluble but permeable beds, mixing zones, and flooding of conduit systems or other sustained high gradients, such as around dams. Anastomotic maze passages predominate under phreatic conditions where the hydraulic gradient and bedding dip are relatively flat (Palmer, 1991) or where hypogenic flow seeps evenly across lower underlying and originally less-permeable beds (Klimchouk, 2000b). Diffuse infiltration through porous, soluble rock or diffuse flow through a rock matrix with high intergranular porosity results in spongework morphology, although this pattern also can be created along mixing zones. In some cases, probably restricted to mixing zones, diffuse flow through permeable but insoluble rock matrix can create network maze type caves (Palmer, 1991). Calcite-undersaturated recharge water infiltrating rocks with high interparticle porosity become calcite-saturated within a few meters of the surface and consequently rarely form caves except along mixing zones (Palmer, 1991).

Physical and analog models have been created using electrical analogs, sand flow analogs, and plaster of paris dissolutional simulations to examine cave development (Ewers, 1982). The simulated caves resemble dendritic systems that grew from the simulated discharge point out to the recharge areas. The cave growth was not gradual, but showed rapid increases at points where the developing conduit connected with a pre-existing conduit.

The hydrogeologic characteristics of the Barton Springs Segment are expressed in the patterns of its cave passages. The caves of the Barton Springs Segment follow a

branchwork pattern, where smaller tributaries and conduits join larger conduits (Figure 2.9). This cave pattern reflects the dominance of discrete recharge and advective groundwater flow overall (Palmer, 1991; Palmer, 2003). One example of maze morphology is found in Bandit Cave, which lies in the Cold Springs groundwater basin, about 0.5 km south of the Colorado River. The most obvious reason for the maze morphology of Bandit Cave is historic flooding along the entrenched paleo-Colorado River with temporary storage in the adjacent aquifer. No examples of spongework have been documented in caves within the Barton Springs Segment.

All of the hydrostratigraphic units of the Edwards Aquifer are relatively permeable and none are true aquitards (Rose, 1972; Maclay and Small, 1984). However, the hydrogeologic properties of each unit vary such that each has characteristic solutional properties. In this dissertation, the solutional properties of the hydrostratigraphic units are presumed in part on the presence or absence of known enterable passages and springs. Cave sites are named in this report for reference, although their locations are for the most part intentionally not mapped here in order to preserve the safety of untrained curiosity-seekers, the caves themselves, and their fauna (BCCP Karst Subcommittee, 2007).

In general, members containing permeable beds, such as (in decreasing tendency) the Kirschberg, Marine/Leached/Collapsed, and Dolomitic Members, typically have horizontal caves associated with them. These are located immediately above and below less-permeable members and beds (e.g., the Georgetown Formation, the RDM, and rhythmic beds of the Dolomitic Member). Less soluble, more competent units, such as the Grainstone Member, retain openings from collapse. Internal collapse of large blocks is commonly observed in thick, soluble units of the Kirschberg and Collapsed Members. Vertical pits are formed by a cave passage breaching through the less-soluble units such as the Georgetown Formation, the RDM, the Grainstone, and Basal Nodular Members, as predicted by White (1988).

The overlying Taylor Group, Austin Group, Eagle Ford Shale, Buda Limestone, and Del Rio Clay are generalized as “overlying confining units” in this study, although their aquitard properties have not been critically examined and may not be as uniform as commonly assumed. Hill and Vaughan (1898) accepted that springs discharging along

the east side of the Edwards Aquifer originated as artesian flow from the underlying Edwards Aquifer. In Uvalde County, Leona River Springs discharges from the San Antonio Segment under artesian pressure through the Austin Group (Garza, 1962). Along the eastern edge of the Barton Springs Segment, potentiometric-surface elevations of the Edwards Aquifer approach or exceed the elevation of some of these springs discharging from overlying confining units even during drought conditions (Hauwert, 1997). These springs commonly discharge from surface terrace, alluvial deposits, or conduits in the Buda Limestone and Austin Chalk. During a 2001 aquifer test for the Buda Water Supply System, a well completed in the Austin Chalk declined in response to pumping of the Edwards Aquifer test well (Mikels, 2001). Because the artesian area springs discharge from the overlying confining units at relatively low rates (less than 6 l/s) and have as much as 50 m or more of less permeable clays, shales, chalk, and limestone, it is commonly assumed that most of these springs are derived from local sources and that the Barton Springs Segment is hydraulically separate from the overlying confining units.

Only a few minor caves and sinkholes are documented in the Austin Chalk and Buda Limestone, although extensive caves in the Austin Chalk (such as Robber Baron's Cave in San Antonio) and Buda Limestone (such as Academy Cave under Texas State University in San Marcos) occur farther south. Shade and Krejca (2007) observed a few creek swallets and one cave that developed within the Austin Chalk across Hays County, and that six caves (including Academy Cave) developed within the Buda Formation. Springs commonly drain from the Buda Limestone in the Austin area, especially its basal section directly above the Del Rio Clay contact. I observed a partially water-filled 0.7 m diameter cave conduit within the Buda Formation by descending 20 feet into a hand-dug well prior to its plugging just south of Slaughter Creek and west of Manchaca Road. COA staff have reported observing unquantified flows of Williamson Creek completely cease along a fault between the Austin Chalk and Buda Limestone, a short distance downstream of Manchaca Road and 4 km downstream of the Edwards outcrop area.

The Del Rio Clay is a low-permeability overlying confining layer over the Edwards Aquifer, although localized breaching by macropores could occur. Selenite

seams, commonly observed in the Del Rio Clay in faulted areas, that suggest mixing of calcium-bearing waters with sulfur derived from pyrite. Hill (1901) suggested that the calcium originated from shells of *Illymatogyra arien tina* but did not rule out possible fracture-focused flow from the overlying Buda Formation. Active water-producing fissures in the Del Rio Clay are rare but have been reported by construction workers at the intersection of Ben White Boulevard and Highway 290 (Hauwert and Vickers, 1994; Figure 2.1). On December 12, 2002, I measured between 0.06 to 1.6 m^3/s (2.1 to 5.6 ft^3/s) of flow loss on Slaughter Creek across "Elm Waterhole" which is underlain by Del Rio Clay downstream of the Edwards outcrop area (Figure 2.1). Soil-piping features are commonly observed on Del Rio Clay exposures overlying the Georgetown Formation. Dye tracing of these soil piping features have not yet been conducted to establish whether or not hydraulic connections with the Edwards Aquifer are present. Overall, the solutional development and the degree of cross-formational flow of the overlying confining units have not been sufficiently examined to assess, if any, that occurs.

The Georgetown Formation has relatively low permeability in many areas (Land and Dorsey, 1988; Small et al., 1996). However, localized solution development creates hydraulic connection with the underlying Edwards Group. The Georgetown Formation also contains the entrance shaft to Antioch Cave, the most significant recharge swallet documented within the Barton Springs Segment. Antioch Cave is developed along a fracture in Onion Creek, and can recharge as much as 2.5 m^3/s (90 ft^3/s) through 6 m (20 ft) of the Georgetown Formation into the underlying Edwards Group (Hauwert and Rauschuber, 1994; Fieseler, 1998; Smith et al., 2001). Another 0.7-m wide fissure at the top of the Georgetown section southwest of the intersection of FM 1626 and FM 967 appears to completely drain a tributary of Onion Creek under most runoff conditions. These examples demonstrate the difficulty of applying randomly located aquifer testing to karst when the predominant flow is localized along specific conduits. There are no known horizontally-extensive caves mapped within the Georgetown Formation of the Barton Springs Segment. However, swallets like Antioch Cave that developed within the Georgetown Formation are extremely important for recharge to the Barton Springs Segment.

The Marine, Leached and Collapsed Members as a group are second to the Kirschberg Member in susceptibility for solutional development (Small et al., 1996). Large sinkhole basins develop within these units. Numerous caves with extensive horizontal passages have formed in these permeable Person Formation units, including Antioch Cave, Airman's Cave, and Barton Skyway Cave (Appendix C; Russell, 2007). Shafts extend 7 to 10 m through the Leached and Collapsed Members in Sunset Valley Cave and Driskill Cave and continue through smaller conduits into the RDM. Hill and Vaughan (1898) stated that the uppermost water-bearing strata in the Austin area is about 15 m (50 ft) below the top of the Edwards Group, which is likely in the lower portion of the Leached and Collapsed Members.

Of the caves that originate within the RDM or penetrate into the RDM, very few show any indication of horizontal development within this unit. Oetting (1995) reports geochemical differences above and below the RDM in some wells along the Saline-Water Line of Bexar County, but not in wells of Comal and Bexar Counties. He inferred that the RDM serves as a local, limited aquitard. The permeability contrast between the RDM and the more permeable overlying Leached and Collapsed Members is demonstrated by the development of the 2-mile long Airman's Cave above the RDM (Hauwert and Russell, 1996.) That hydraulic breaches exist through the RDM beneath Airman's Cave is shown by the roughly 0.23 m^3/s (1 ft^3/s) of water that discharged from the cave entrance under high-water table conditions in 1992. This high-water table flow most likely rose via conduits penetrating through the RDM. Many caves (such as Maple Run, Sunset Valley Cave, Driskill Cave, Sendero Sink, and the Breached Birth passage in Blowing Sink) extend into or through the RDM, and nearly always undergo a reduction in passage size in that section. In most cases, passages draining from the Leached and Collapsed Members are too small for human exploration where the passage descends into the RDM. In a few cases, extensive collapse within the underlying Grainstone and Kirschberg Members has resulted in impartial or complete collapse through the RDM. Abbott (1984) presented observations from a quarry in the San Antonio Segment where vertical conduits are well developed through the RDM. In 2006, small flows were followed along nearly every tributary to Barton Creek downstream of Loop 360. No losses were detected in

tributary stretches underlain by RDM. From these observations, it is inferred that within the Barton Springs Segment the RDM locally perches vadose flows, although vertical conduits can allow hydraulic connection between the Person and Kainer Formations.

The Grainstone Member beds tend to be massive and resistant in outcrops. These control creek levels and cave ceilings. Solution runnels observed along Barton Creek at Campbell's Hole and at Twin Falls are naturally sculpted within the Grainstone Member (Figure 2.1). The tightly-packed miliolid fossils make the Grainstone Member more massive and competent and less soluble and erodable than the underlying Kirschberg Member. The contrasts in characteristics between the Grainstone and Kirschberg Members create conditions that develop more open caves than are found in any other stratigraphic interval of the Edwards Aquifer. The Kirschberg Member has collapsed in many locations from loss of soluble materials, but the Grainstone creates a relatively competent "roof" that keeps the dissolved and collapsed interval at the top of the Kirschberg Member open. Collapsed-entrance caves are common in the Grainstone Member near the contact with the Kirschberg Member, although lateral caves extend along the immediately underlying pulverulite bed (such as Whirlpool (Appendix C), Get Down and Djerido Caves (Appendix C). Many more caves extend through the Grainstone than through the superimposed RDM. Most cave passages through the Grainstone are tight and circular descending, resembling a corkscrew.

Most of the known cave development in the study area occurs within the Kirschberg Member. The largest sinkholes and many broad, shallow karst depressions have formed within the Kirschberg Member. Overall, the Kirschberg Member is the most permeable unit within the Barton Springs Segment and commonly shows cave development focused along pulverulitic beds that are composed of euhedral dolomite grains weakly cemented with calcite. A 1-m (3-ft) thick pulverulitic bed at the top of the Kirschberg Member is be the most significant bed within the Edwards Aquifer for cave development. The Kirschberg Member also is highly permeable and collapsed as a result of ancient leaching of evaporitic materials by groundwater (Rodda, et al., 1970; Rose, 1972). Hill and Vaughan (1898) probably were referring to the pulverulitic beds when describing water-bearing "arenaceous beds … composed of very fine particles of sand

embedded in a white or limy matrix." The instability of the breakdown materials within the Kirschberg Member limits direct observation in numerous caves, including Djerido (Appendix C), Bliss Spillar, Equinox, and Dunvegan Caves. Where the Kirschberg is exposed on the surface, abrupt changes in dip commonly reflect the collapse of underlying beds. Because of the high strata-influenced permeability of this member, caves developed within the Kirschberg Member in the Edwards outcrop area typically do not show particular influence from faulting and fracturing, but instead trend parallel to local dip or down-dropped fault blocks (e.g., Flint Ridge Cave; Figure 2.9). In the artesian area or closer to discharge springs, groundwater flow through the Kirschberg Member becomes more focused along faults, fractures, and regional gradients. Along the portions of the Sunset Valley Groundwater Flow Route, the groundwater flow is localized through the Kirschberg Member along the trend of the Barton Springs Fault (See Chapter 4). It is also likely that groundwater flow is localized through the Kirschberg Member along the Manchaca Flow Route, which follows major fault trends to Barton Springs.

Caves developed within the Dolomitic Member are strongly influenced by faults and fractures. Cave passages such as the lower portions of Flint Ridge Cave and Blowing Sink trend northeastward along prominent fractures. Strong stratigraphic control is observed in caves above the rhythmic beds, such as Bee Creek Cave. Perched water is commonly observed in wells, caves (Cave X, Flint Ridge, upper level flow in Midnight Cave), and springs (Bee Creek Springs, Backdoor Springs) in the upper Dolomitic Member, particularly immediately above the rhythmic beds. Some caves penetrate vertically through the less-permeable rhythmic beds (e.g., Midnight Cave).

Although the Basal Nodular Member has a relatively lower permeability than its overlying units, the hypothesis (Rodda et. al., 1970; Brune, 1981; Texas Commission on Environmental Quality, 2005) that the Basal Nodular Member forms an impermeable base below the Edwards Aquifer is not supported with field observations in the Barton Springs Segment. Examination demonstrates that the Basal Nodular has high localized permeability and this unit has been included within the Edwards Aquifer as the Basal Nodular Member (Rose, 1972; Maclay and Small, 1984; Small et al., 1996) as far north

as the Colorado River. Many caves found in the lowermost portion of the Dolomitic Member (e.g., Walton/Walsh Well, El Sotanito, and Toucasia Cave) typically are expressed as vertical pits draining into the Basal Nodular Member but becoming impassable within about five m (15 ft). The total mapped cave volume for the Basal Nodular Member is relatively low because its type of cave development is limited to tight vertical pits or fissures entering from the overlying Dolomitic Member (Russell, 2007). Because dissolution can be focused along tight fissures and bedding-plane conduits, the lack of cave volume does not necessarily show the Basal Nodular Member is impermeable.

Horizontal cave development overlying the Basal Nodular Member suggests some permeability contrast is present with the overlying Dolomitic Member, similar to the way Airman's Cave perches within the Leached Collapsed Member over the Regional Dense Member. One of the longest caves within the Barton Springs Segment, Ireland's Cave, has a massive *Toucasia* packestone at its entrance, similar to the bed perching over the lowermost Dolomitic Member overlying the Basal Nodular Member, although its stratigraphic relation has not been critically examined because of heavy debris filling of the entrance, high carbon dioxide gas levels, and other access problems.

A surprising find is that perched springs on the western side of the Barton Springs Segment discharge from within the Basal Nodular Member itself. In fact, the more abundant vegetation associated with the Basal Nodular member outcrop distinguishes it on aerial photographs (Kolb, 1981). The Buttercup Creek area of the Northern Segment (Figure 1.2) contains a surprising high density of caves localized within the Walnut Formation (Russell, 1993). Groundwater tracing in the Buttercup Creek area reveals that shallow groundwater flow is constrained to cave streams within the Walnut Formation that discharge from a major spring developed in the uppermost beds of the Glen Rose Formation: a clear example of cross-formational flow (Hauwert and Warton, 1997). The extensive cave development in Natural Bridge Caverns of the San Antonio Segment occurs solely within the Basal Nodular Member and uppermost Glen Rose Formation (Abbott, 1973; Kastning, 1986). Kastning (1986) mapped the cave development west of New Braunfels as being much greater within the Basal Nodular Member and upper Glen

Rose Formation than in superimposed members of the Edwards Group. He attributed this to late Cretaceous uplift of the San Marcos Arch that produced stratigraphic dip parallel to prominent fracture trends where dissolution focused. The San Marcos Arch may also create a barrier responsible for the groundwater divide between the Barton Springs and San Antonio Segments of the Edwards Aquifer (Klempt et al., 1979).

Solution cavity and cave development within the Basal Nodular Member is strongly associated with fractures and preferential dissolution of burrows creating some honeycomb cavities. Cuttings from wells (Stoneledge WQPL, well 58-50-1C1, see Figure 2.1) drilled into the Basal Nodular Member and some outcrops often show a characteristic dark discoloration that may imply local lack of oxygenated groundwater flow. The dichotomy of solution development within the Basal Nodular Member can be explained by relatively late cave development within the Basal Nodular Member because groundwater perched above the Basal Nodular Member requires sufficient stream incision to promote sufficient hydraulic gradient for dissolution (Hauwert and Warton, 1997). If the Basal Nodular Member matrix has low permeability, then dissolution can focused in relatively small fractured areas with steep hydraulic gradient allowing small conduits to form relatively quickly. Within the artesian area and eastern edge of the Edwards outcrop area where the Edwards Aquifer is relatively thick and local creek base levels are above the elevation of the Basal Nodular Member, rock dissolution and groundwater flow occur more easily within the Dolomitic Member above the Basal Nodular than downward through the Basal Nodular and upper Glen Rose Formation. Hauwert (1997) excluded the Basal Nodular Member for the purposes of calculating the volume of groundwater present in the Edwards Aquifer. Hypogenic conceptual models of karst maturation proposed by Klimchouk (2004) suggests that vertical conduits eventually develop and transmit flow through the Basal Nodular Member between the Trinity and Edwards Aquifers as a result of chemical and or thermal gradients. A more detailed characterization of the Basal Nodular Member is warranted.

Geologic structure and its influence on conduit development can be observed in the subsurface. The trend of Airman's Cave is strongly related to a series of subparallel faults (Appendix C; Hauwert and Russell, 1996). Flint Ridge Cave trends southeastward

or perpendicular to fault trends within the Kirschberg Member section, but deflects 90 degrees to follow ceiling fractures within the Dolomitic Member sections. Small-scale structures, including localized folding and solution-collapse karst features, frequently are observable in the subsurface. Fault drag and collapse above solution-enlarged cavities creates localized folding. Localized folding and collapse features typically are found within the soluble Collapsed and Kirschberg Members. Infrequently folding and collapse is found within the RDM and Grainstone Members in association with larger underlying collapses within the Kirschberg Member.

To date, the total mapped cave volume of the Travis County portion of the Barton Springs Segment is 20,500 m^3 (725,000 ft^3; Russell, 2007). Although not yet tabulated, it is assumed that the mapped caves in the Hays County portion of the Barton Springs Segment have a similar volume, because the aerial extent of Travis and Hays Counties on the Edwards outcrop area is roughly the same. The mapped cave volume of the Barton Springs Segment constitutes about $3.4x10^{-5}$ % of the 6×10^{10} m^3 ($2.11x10^{12}$ ft^3) total estimated aquifer volume estimated by Smith (2006, personal communication). This percent of known cave volume is 3 orders of magnitude lower than the 0.017 specific yield estimated by Slade et al., 1986. This calculated volume of caves is a minimum estimate because there are likely many more caves and smaller voids that are undiscovered, insufficiently examined, undocumented, or yet unknown (Appendix B). Hydrostratigraphic units such as the Georgetown, RDM, and Basal Nodular Members are breached by fissures and shafts that are not reflected by cave volume estimates. Some units or portions of units have limited surface exposure within the Barton Springs Segment, in particular the Marine/Cyclic Members and portions of the Dolomitic and Basal Nodular Members.

2.4 CONCLUSION

Revised surface geological mapping defines the surface exposure of hydrostratigraphic units of the Edwards Group and Georgetown Formation, as well as the underlying units, and overlying confining units. Based on the surface mapping, the boundaries of the Edwards outcrop, eastern drainage, artesian, and eastern edge of the contributing areas were distinguished. The combined Edwards outcrop and eastern drainage areas are 241 km^2 in size.

The hydrologic properties of the Edwards Aquifer are geologically controlled. The branchwork morphology of caves in the Barton Springs Segment reflects a predominantly discrete recharge and discrete groundwater flow system. The depositional environment, diagenesis, fracturing, down-dropped and dipping faulted blocks, and subsequent dissolution play an important role in the evolution of the Barton Springs Segment. Conduit development is localized along the intersection of specific relatively soluble beds with specific extensional fractures and faults. Solutional development is localized particularly along the intersection of fractures and specific soluble beds within the Marine, Leached, and Collapsed Members and Dolomitic Member. Permeability within the Kirschberg Member is localized within highly solutionally-evolved layers and is little affected by fractures. The intervals of greatest cave development are the uppermost pulverulitic bed on the Kirschberg, immediately underlying the Grainstone Member, other pulverulitic beds deeper within the Kirschberg Member, the Leached and Collapsed Members immediately above the RDM, other specific beds within the Marine/Leached Members, the beds within the Dolomitic Member immediately above the rhythmic beds, and other specific beds within the Dolomitic Member. The association of cave development above and below less-soluble beds (Georgetown Formation, RDM, rhythmic beds of the Dolomitic Member, Grainstone Member, Basal Nodular Member) suggests that contrasts in permeability play an important role in conduit development.

Faults and extensional fractures play a prominent role as discontinuities where selective fractures are solutionally enhanced. Solution development localized along faults and extensional fractures is particularly important for the development of fissures, vertical pits, and caves within the Georgetown Formation, Regional Dense, Basal Nodular, Grainstone, and Dolomitic Members of the Edwards Group. Extensional fractures that are unmodified by solution into planar fissures or rounded conduits are expected to be effectively closed at the water table depth and, therefore, relatively insignificant for groundwater flow or storage within the phreatic zone of the Barton Springs Segment.

Table 2.1. Hydrostratigraphic units of the Barton Springs Segment. Modified from Small et al., 1996.

Hydrogeologic subdivision		Group	Formation	Member	Full Thickness (m)	Lithology	Field Identification	General Hydrogeologic Properties
Quaternary		Alluvium			<10	gravel	loosely or unconsolidated limestone or shale	high permeability
		Colorado River Terrace Deposits			<10	gravel	loosely or poorly consolidated with quartz cobbles	high permeability
Upper Cretaceous	Overlying Confining Units	Taylor	Sprinkle		120	calcareous clay	dark clay	low permeability
		Austin			119	chalk	*Inoceramus subquadratus*, *Inoceramus undulatoplicatus, Exogyra ponderosa, Phyrygia aucella* and occasional igneous deposits	gen. low permeability, conduits possible where faulted or weathered on surface
		Eagle Ford		South Bosque Shale Bouldin Flags Cloice Shale Pepper Shale	12 - 14	calcareous sandy shale	*Fish fossils, Acanthoceras sp.*, *Eucalycoceras bentonianum*, *Neocardioceras*, *Romaniceras*, *Coilopoceras*, *Prionotropia*, *Alectryonia lugubris*	general low permeability
		Washita	Buda		11 - 18	nodular to massive porcelaneous limestone	Orange pelloids in massive beds, *Budaiceras*, ammonites, *Exogyra clarki*, *Pecten roemeri*, *Codiopsis texana* Whitney, and *Mantelliceras*	commonly feeds shallow wells and small springs
			Del Rio		15 - 18	clay	*Ilymatogyra arietina,* pyrite, gypsum seams	low permeability clay
Lower Cretaceous	Edwards Aquifer		Georgetown		12 - 18	nodular to massive fossilferous limestone	*Waconella wacoensis, Arctostrea carinata*, *Texigryphaea washitaensis*, *Neithea texana*, echinoids, and ammonites.	vertical fissure development
		Edwards	Person	Cyclic and Marine undiv.	0 - 21	massive limestone	chert and caprinids	cavernous
				Leached and Collapsed undivided	21 - < 7	wackestone, mudstone, and grainstone with well-sorted matrix	*Toucasia*, *Chondrodonta*, and sparse miliolid foraminifera	horizontal and vertical extensive cave deveopment
				Regional Dense	4.5 - 10	well-sorted lt tan fissile mudstone	*Pleuromya knowltoni*, rarely *Ceratostreon texanum,* iron-oxide stains	local aquitard frequently breached with vertical fissures
			Kainer	Grainstone	14 - 18	lt gray-white massive grainstone	Miliolid foramnifera, *Chondrodonta*, caprinids, turitella, mudcracks, and bedded chert	small corkscrew passages and rooms. Serves as competent roof over Kirschberg Mbr
				Kirschberg	12 - 23	crystalline limestone and dolomite pulverulite	Terra rosa. *Cladophyllia, toucasia, caprinid-bearing siliceous remnants*	extensive cave development esp. in pulverulitic beds
				Dolomitic	~ 43	Highly bedded gen. with poorly-sorted matrix	*Toucasia, Caprinid, Dictyoconus walnutensis.* Nodular chert	significant cave development primarily along fissures
				Basal Nodular	16 - 18	fossilferous, nodular limestone	*Texigryphaea* packestone intermediate miliolid grainstones and burrowed mudstone, echinoids, lower *Ceratostreon Texanum* packstone	vertical pits and fissures. Produces many minor springs.
	Underlying units	Trinity	Glen Rose		150 - 250	Alternating massive limestone/dolomite and marl layers	dinosaur tracks, plant fossils, celestite nodules, *Trigonia*, *Pecten*, *Alectryonia carinata*, *Orbitolina texana* foraminifera, various echinoids	little cave development documented here although supports abundant springs/wells.

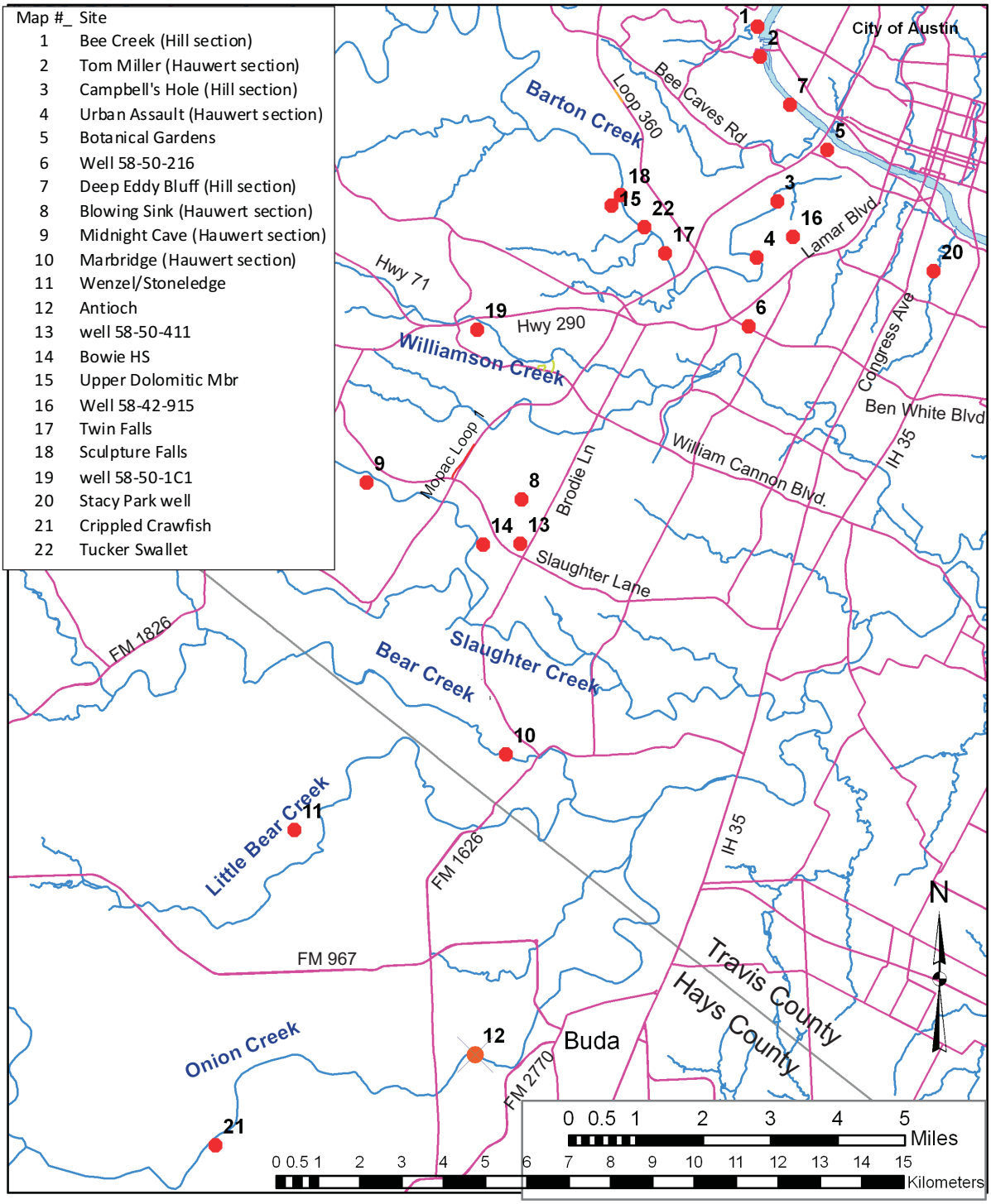

Figure 2.1 Selected sites of geologic discussion. Measured sections, specific well control points, and other geologic points of interest discussed in the text. The Edwards Group was originally known as the Barton Creek limestone because of the excellent exposure in the deeply incised creek. Note: most of the sites mapped here are not publicly accessible without permission by the property owner.

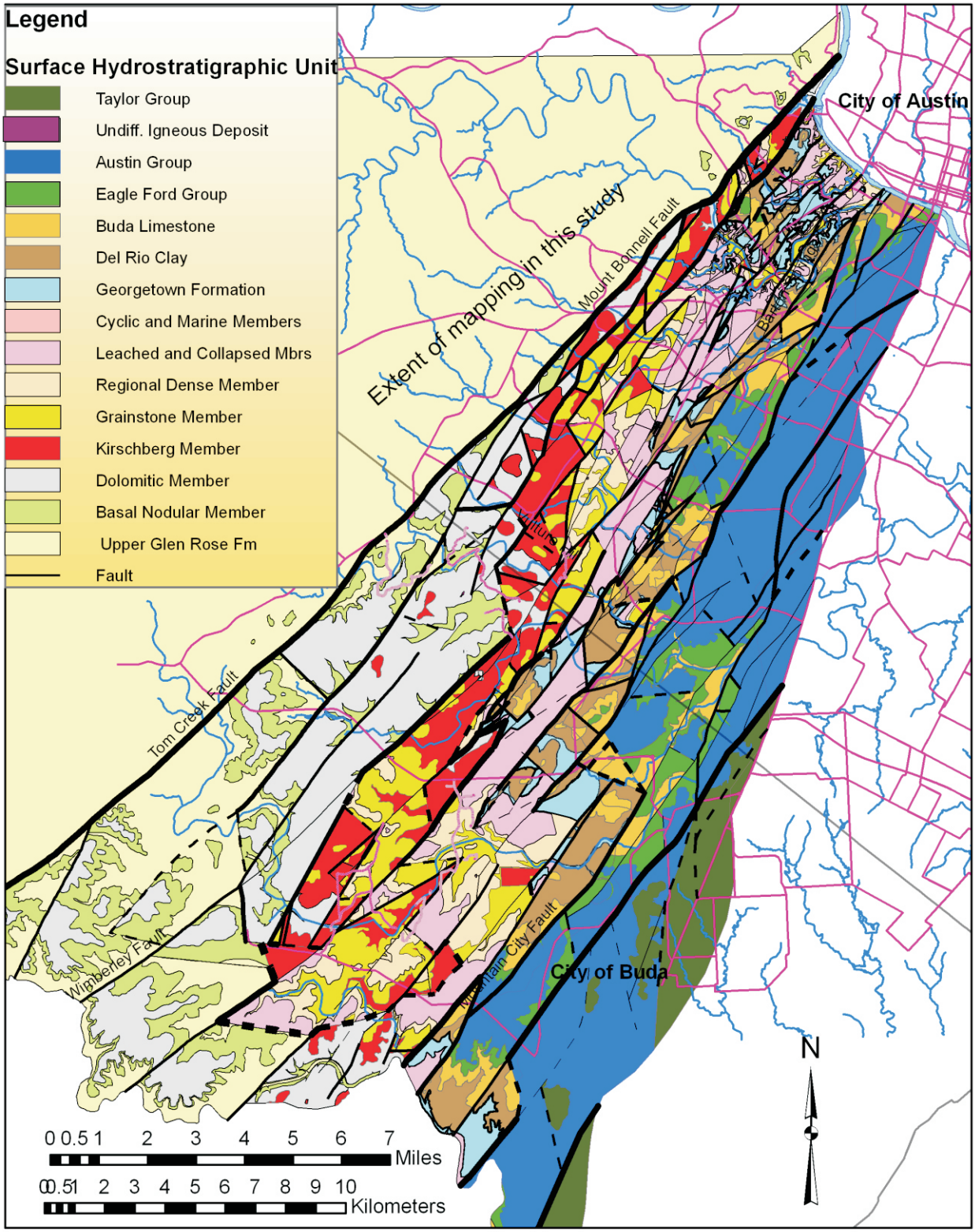

Fig. 2.2. Surface hydrostratigraphic map of the Barton Springs Segment. Surface exposure of hydrostratigraphic units mapped in Small et al., 1996, and revised by Nico Hauwert (Jan. 2009 update).

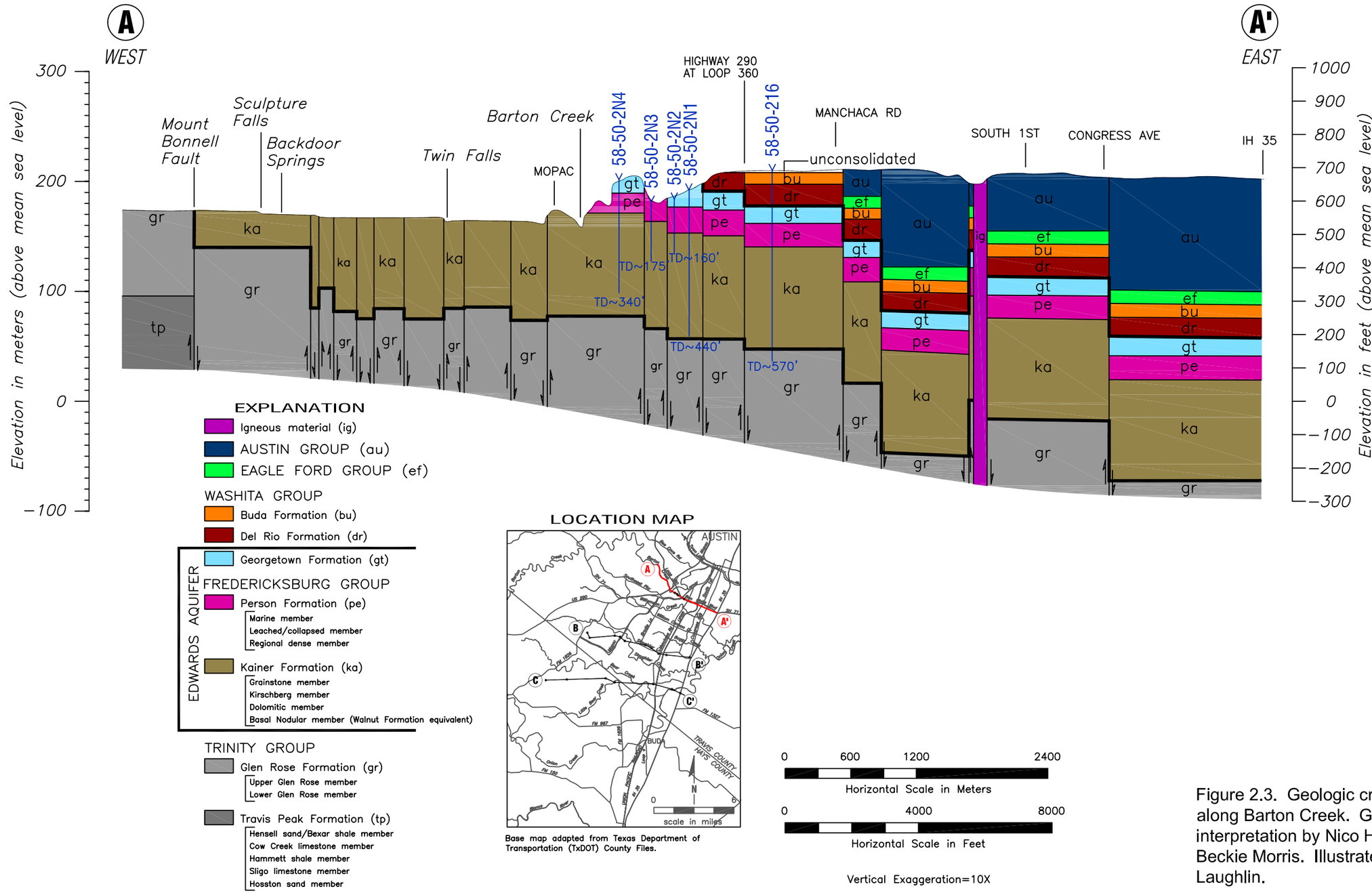

Figure 2.3. Geologic cross section along Barton Creek. Geology interpretation by Nico Hauwert and Beckie Morris. Illustrated by Kristie Laughlin.

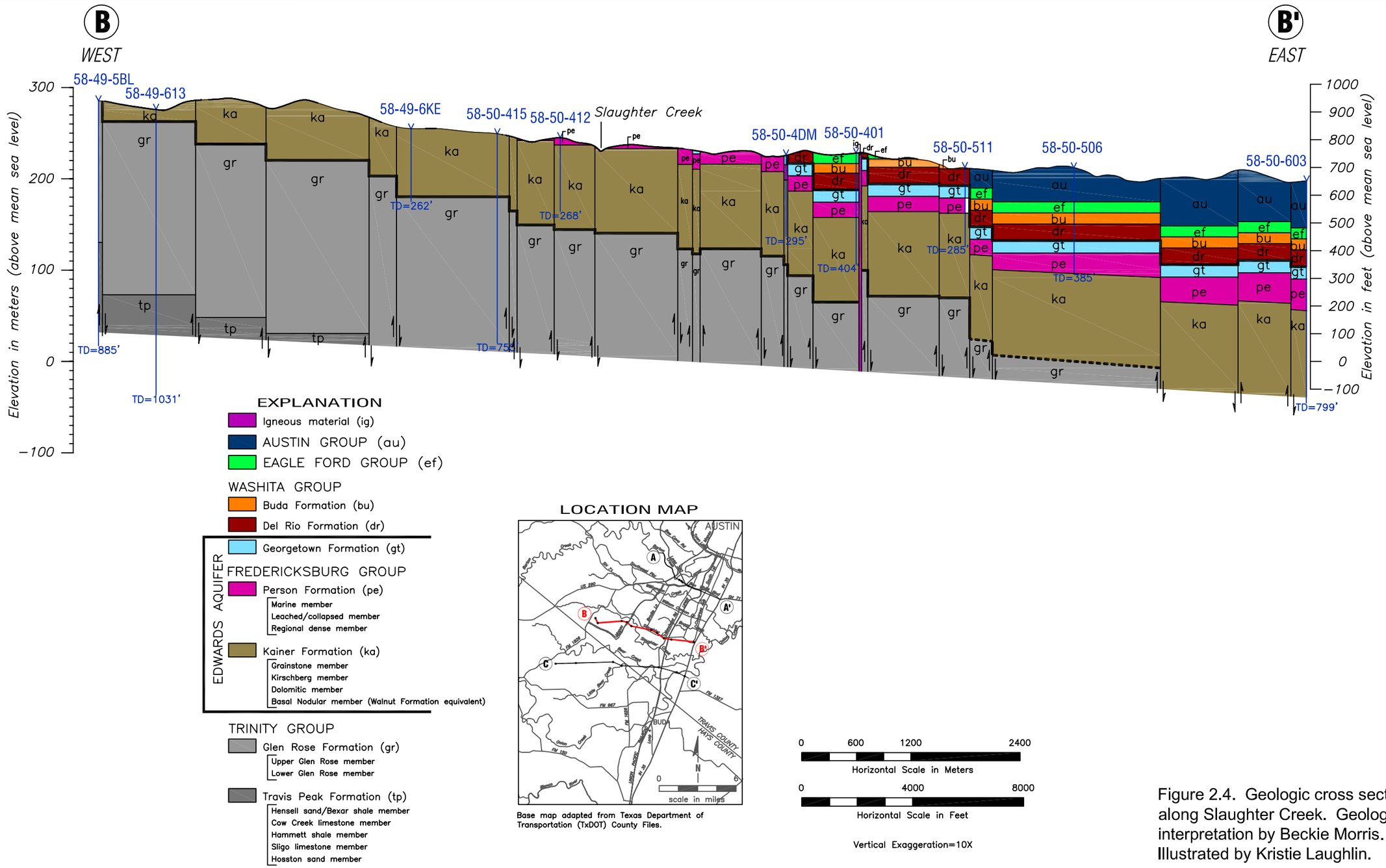

Figure 2.4. Geologic cross section along Slaughter Creek. Geology interpretation by Beckie Morris. Illustrated by Kristie Laughlin.

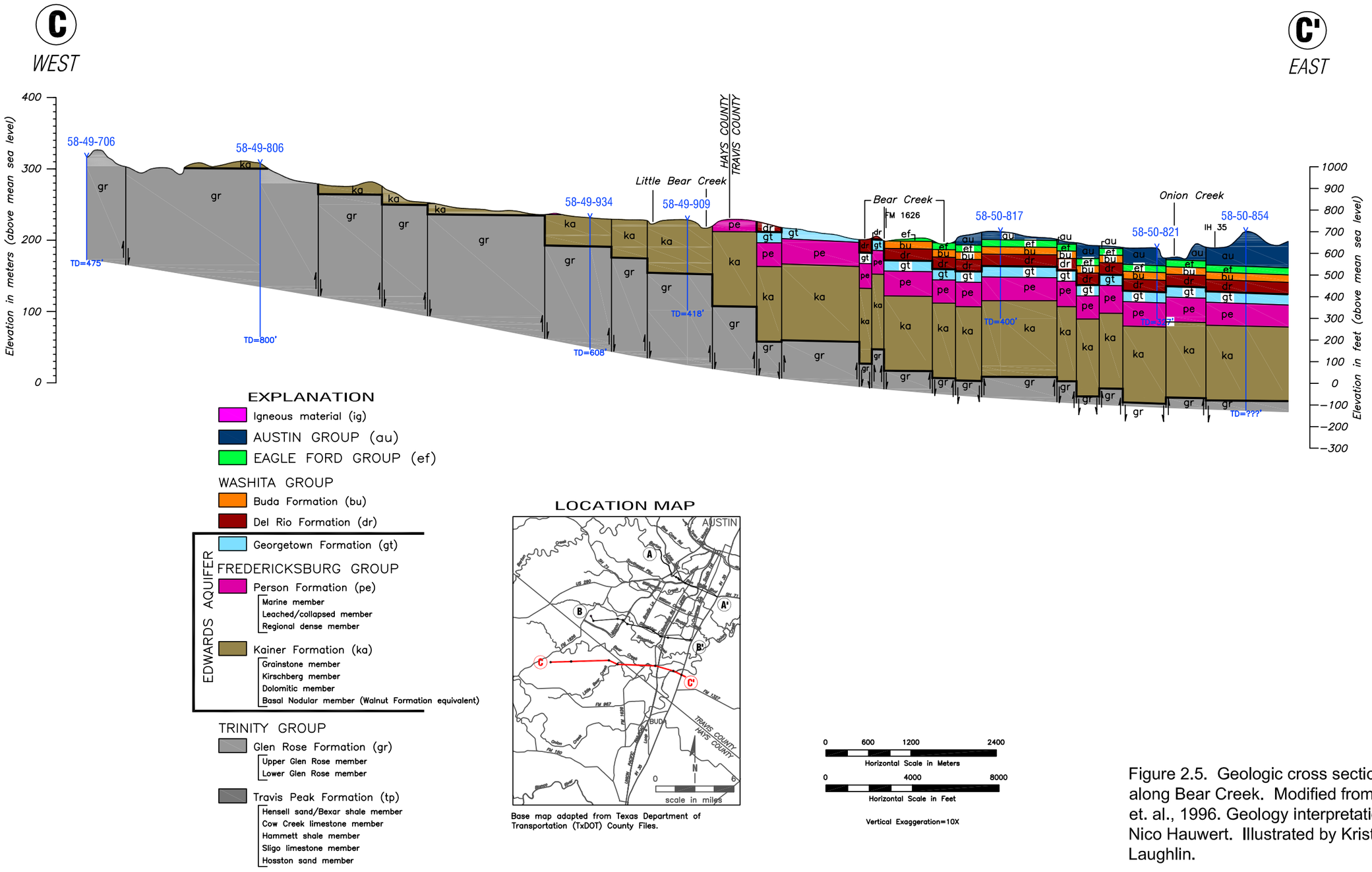

EXPLANATION

- Igneous material (ig)
- AUSTIN GROUP (au)
- EAGLE FORD GROUP (ef)

WASHITA GROUP

- Buda Formation (bu)
- Del Rio Formation (dr)
- Georgetown Formation (gt)

EDWARDS AQUIFER

FREDERICKSBURG GROUP

- Person Formation (pe)
  - Marine member
  - Leached/collapsed member
  - Regional dense member
- Kainer Formation (ka)
  - Grainstone member
  - Kirschberg member
  - Dolomitic member
  - Basal Nodular member (Walnut Formation equivalent)

TRINITY GROUP

- Glen Rose Formation (gr)
  - Upper Glen Rose member
  - Lower Glen Rose member
- Travis Peak Formation (tp)
  - Hensell sand/Bexar shale member
  - Cow Creek limestone member
  - Hammett shale member
  - Sligo limestone member
  - Hosston sand member

LOCATION MAP

Base map adapted from Texas Department of Transportation (TxDOT) County Files.

0 600 1200 2400
Horizontal Scale in Meters

0 4000 8000
Horizontal Scale in Feet

Vertical Exaggeration=10X

Figure 2.5. Geologic cross section along Bear Creek. Modified from Small, et. al., 1996. Geology interpretation by Nico Hauwert. Illustrated by Kristie Laughlin.

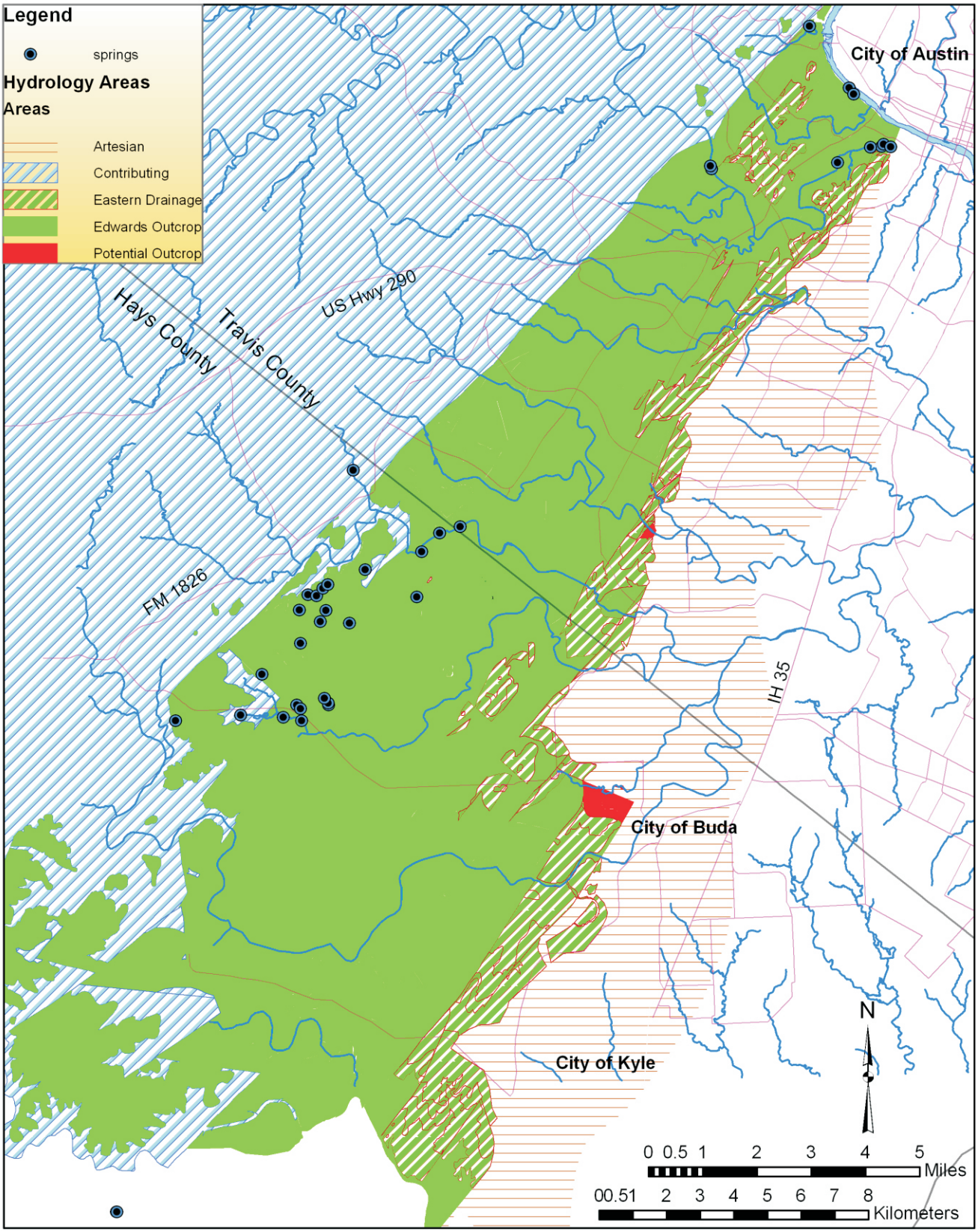

Figure 2.6. Surface hydrology areas. Based on surface mapping of hydrostratigraphic units in Small et al., 1996 as revised by Hauwert in January 2009.

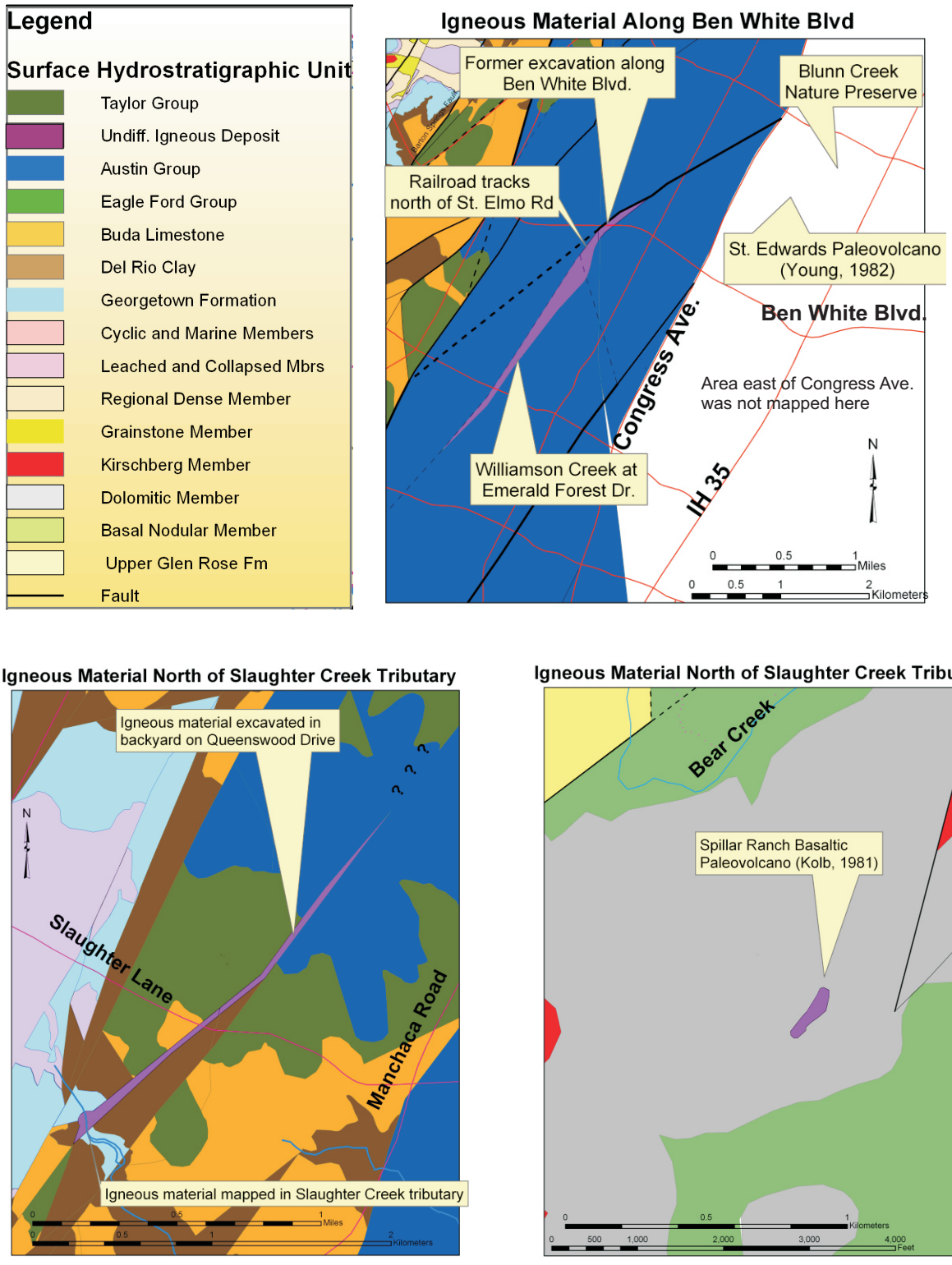

Figure 2.7. Observations of igneous deposits. Exposures of igneous deposits were mapped across the Barton Springs Segment.

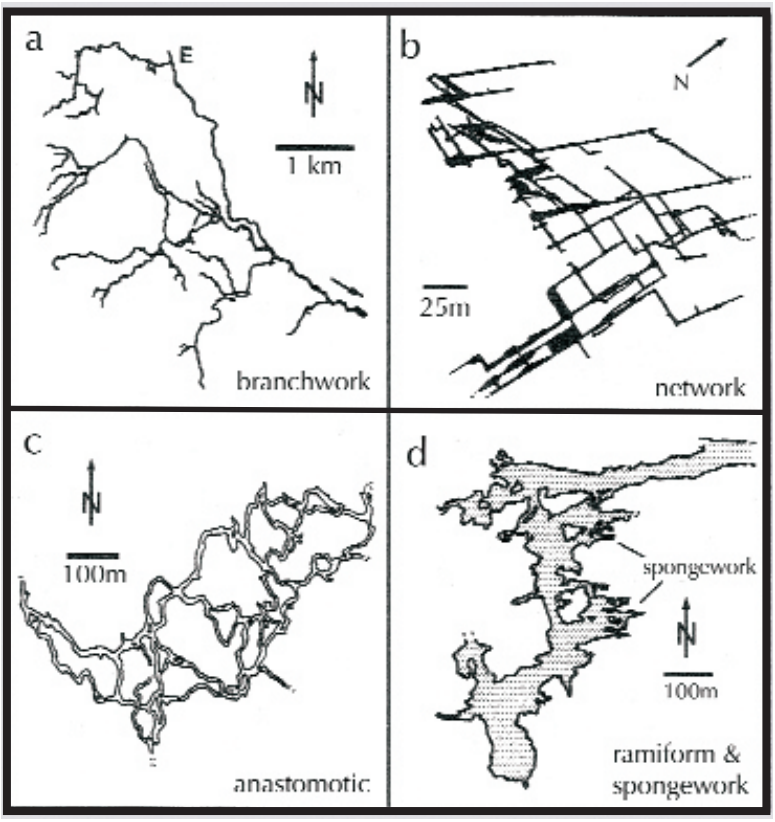

CAVE PATTERN		curvilinear branchwork	rectilinear branchwork	anastomotic maze	network maze	spongework maze	ramiform pattern
SOURCE OF AGGRESSIVE WATER	dolines	●	●	●	•		
	sinking streams	●	●	●	●	•	
	uniform seepage				●	●	
	mixing of 2 sources				●	●	●
	hypogenic			•	●	●	●
DOMINANT STRUCTURES	bedding-plane partings	●		●		●	●
	fractures		●		●		●
	matrix porosity					●	●

Figure 2.8 Ideal cave passage patterns. Worldwide cave passages are diagnostic of the recharge and groundwater flow processes that create them. Dot size indicates relative importance of recharge or flow process in developing specific cave passage patterns. Branchwork morphology is the most common and is characteristic of discrete recharge and flow. From Palmer, 1991 and Palmer, 2003.

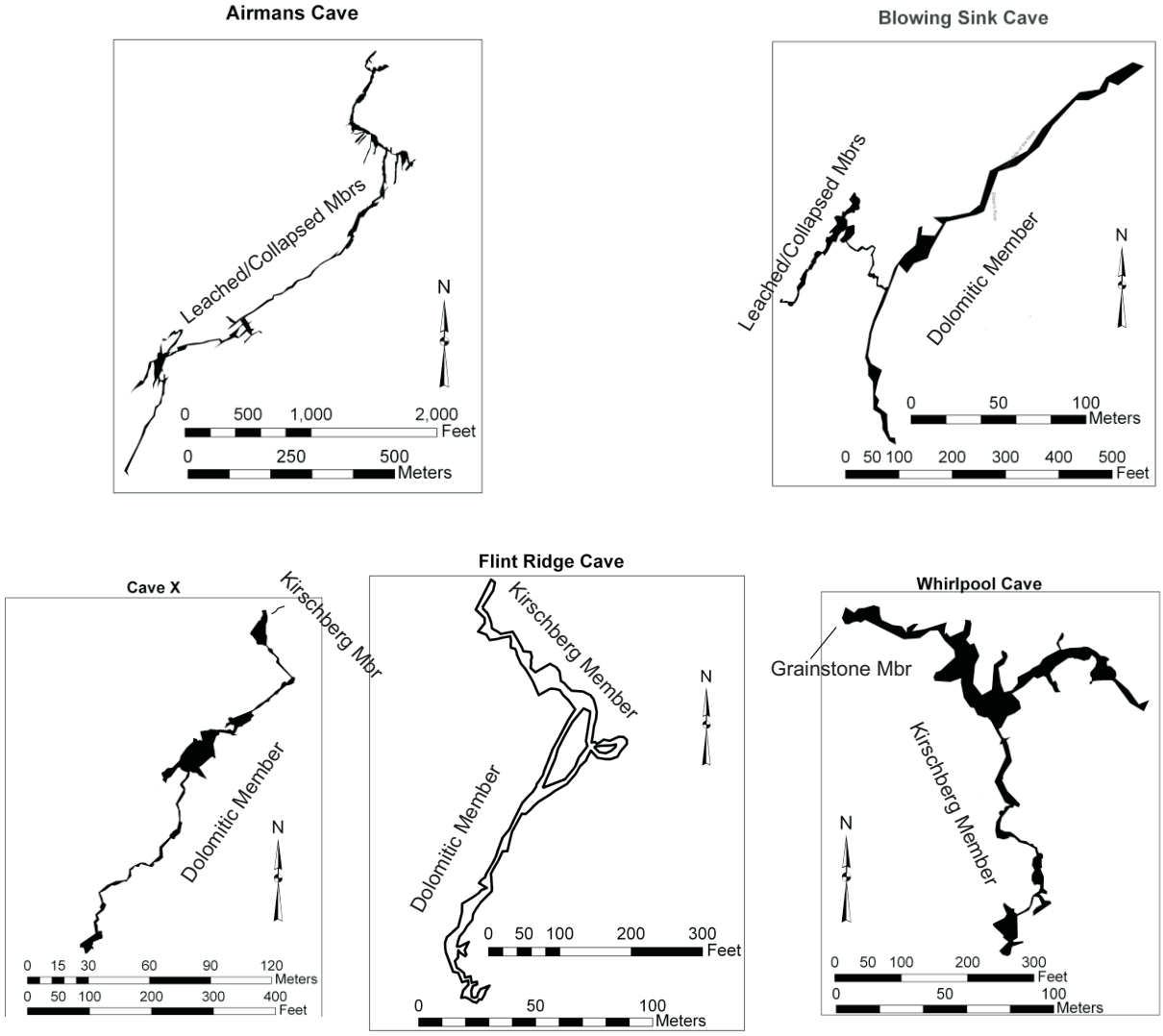

Figure 2.9. Cave morphology of the Barton Springs Segment. The plan view of 5 of the longer caves in the Barton Springs Segment show curvilinear and rectilinear branchwork morphology, that reflect discrete recharge through sinkholes and creek swallets and advective groundwater flow, according to Palmer's (1991; 2003) classification (see Figure 2.8). No caves in the Barton Springs Segment are known to have ramiform morphology that are characteristic of diffuse flow. Cave maps are from various authors are compliled by Texas Speleological Survey and Elliott (1997). Hydrostratigraphic units shown at cave passage level interpreted by Hauwert. Note that cave passages developed within the Kirschberg Member are highly influenced by bedding and commonly trend southeast, while passages developed within the Leached/Collapsed and Dolomitic Members tend to develop along fractures that most commonly trend northeast.

Chapter 3. Surface Recharge to the Barton Springs Segment

3.1 INTRODUCTION

In order to insure the Barton Springs Segment will remain a potable and highly productive water supply, an accurate understanding of recharge sources is critical for management practices, water-protection regulations, and preserve acquisition. Since 1997, citizens of Austin approved over $100 million investment in water-quality protection lands within the Barton Springs Segment and since have protected 17% of the Edwards outcrop area with land purchases and conservation agreements. The Barton Springs Segment also houses rare and listed-endangered karst species, required for protection by federal permit (Federal Register, 1997). Complex interactions between people and aquifer ecosystems may not be sufficiently understood now to fully evaluate their importance. Hays County, US Fish and Wildlife and conservation groups such as the Hill Country Conservancy and Nature Conservancy are also participating in land acquisition and landowner conservation agreements. Knowledge of recharge sources is critical to most efficiently protect the most important lands with limited acquisition resources. Through the combination of research, public education, and regulation practices such as disposing wastes and urban runoff into sinkholes are no longer commonplace (Appendix A).

This chapter examines how surface recharge contributes to the Barton Springs Segment, including:

(1) recharge infiltration through the soil,

(2) development of karst structures that convey recharge from the surface and through the epikarst and vadose zones to the water table, and

(3) recharge in large sinkhole basins.

This study uses a number of methods to examine recharge. Recharge estimates from other limestone areas of the world are compiled to estimate ranges of expected recharge. This study focuses on large upland sinkhole basins in the Barton Springs Segment that are commonly hypothesized to be the most significant upland recharge structures. Relations between geomorphological features (bowl morphology, bowl depth, and sinkhole catchment area of upland sinkholes) to recharge significance are examined. A representative number of combined catchments of sinkholes are mapped across the Barton Springs Segment. Site-scaled recharge is measured on two upland research sites. Recharge calculations from site climatic and hydrologic data are compared to calculations using chloride concentrations in rainfall, runoff, cave drips and Barton Springs.

3.1.1. Recharge in Karst

The amount of recharge to an aquifer depends "largely upon the nature of the soil and rocks," particularly in basins underlain by limestone (Maxey, 1964). Even in non-karstic watershed basins, differences in runoff may depend more on type of bedrock than on soils, morphology, or annual precipitation patterns (Weyer, 1971). Limestone aquifers, even in cases where little primary porosity is present, are commonly permeable because of fracturing (Jakucs, 1977, p. 69) and dissolution. Karst landscapes have efficiently-developed internal drainage and precipitation can infiltrate rapidly beyond the depth of transpiration and atmospheric evaporation (Jennings, 1985). The maturity of a karst area can be quantified by a pitting index, which is a comparison of internal drainage areas to the entire outcrop area (Williams, 1972). White and White (1979) found a ratio of internal drainage area to be 0.25 over the Mississippian limestones of the Appalachian Plateau and 0.06 over the Ordovician carbonates of the Valley and Ridge province. The difference was attributed in part to the greater dolomite content of the Ordovician carbonates.

The natural surface recharge of a karst area can be classified as:

(1) allogenic recharge, where flow from an upstream source area (such as the contributing area) infiltrates through recharge features (swallets) in the major creek channels.

(2) authogenic recharge where rain falls directly onto the karst aquifer (such as the Edwards outcrop area).

(2a) diffuse infiltration, and enters the aquifer through the soil and fractured rock matrix (Burdon and Papakis, 1963).

(2b) internal drainage (also called internal runoff), where rainfall or runoff recharges the aquifer through sinkhole drains.

(3) overflow caprock or perched aquifers (such from overlying confining units), where overflow water enters the aquifer through vertical shafts, soil pipes, and widened fractures overlying less-permeable material (White, 1999a).

Karstification within the Edwards Group began in the Cretaceous Period during a long period of exposure, prior to deposition of the overlying Georgetown Formation (Abbott, 1977; Sharp, 1990). Cretaceous fracturing associated with the rise of the San Marcos Arch may have influenced the development of groundwater flow paths parallel to the Miocene Balcones Fault Zone (Kastning, 1986).

Karst aquifers develop in soluble rock where groundwater flows through the dissolved openings (Aley, 2000b). Karst areas are characterized by sinkholes, losing streams, caves, and large springs. Mature karst terrains develop conduits that enlarge and connect recharge areas with discharge areas. Where favorable pathways exist between recharge and discharge areas, surface recharge points in creek bottoms can accept large volumes of creekflow and become swallets. For example, Barton Creek is hypothesized to have originally been a tributary to Williamson Creek, but was pirated by subsurface flow toward an early Barton Springs (Woodruff, 1984b). The subsurface flow route eventually dissolved and eroded into the steep-walled stream channel it is today. Incision and lowering of the base level of the Colorado River led to the lowering of active spring locations as well as the active conduits that feed them (Veni, 1992). It is the localization of flow that creates preferential groundwater-flow paths that are single, well-connected conduits or a series of subparallel conduits that rapidly convey groundwater from

recharge to discharge areas. Studies of karstic flow systems developed in Kentucky suggest that the flow paths resemble branching networks, where smaller branches connect to larger trunk conduits (Thrailkill, 1985; Quinlan, 1989). In karst areas in general, most cave development probably focused near the water table, although some development occurs in the vadose zone and below the water table (Ford and Ewers, 1978). Caves, conduits, and fissures originally developed deeper in the vadose zone or phreatic zone form important elements or surface recharge after surface denudation.

Hypogenic processes are subsurface rather than surface recharge that can eventually support or even surpass epigenic karst development from shallow surface sources to discharge sites (Klimchouk, 2000). Hypogenic groundwater flows are thought to be driven by chemical or thermal gradients. The possible role of hypogenic karst development within the Barton Springs Segment from the Saline-Water Zone or underlying Trinity Aquifer has not been critically examined by any study. These sources are discussed in Chapter 4.

The epikarst (or subcutaneous zone, White 1999a) is the "uppermost zone of exposed karstified rocks, in which permeability due to fissuring and diffuse karstification is substantially greater and more uniformly distributed in area, as compared to the bulk rock mass below" (Klimchouk, 2000a). Within the shallow epikarst, the enlargement of fractures by stress release and surface weathering typically play important roles in flowpath evolution (Klimchouk, 2004a).The epikarst is believed to be significantly higher in permeability than the deeper vadose zone (if present) as a result of stress release and weathering of rocks in contact with calcite-undersaturated surface waters and soils with relatively high carbon dioxide content (Klimchouk, 2000a). Flow through the deeper vadose zone is anticipated to be more discrete than in the epikarst zone, with flow focused through horizontal perched conduits connected with vertical shafts (White, 1988; Klimchouk, 2000a).

In karst areas, much surface runoff flows a short distance before recharging into sinkholes (dolines) or infiltrating into highly permeable karst soils (Meinzer, 1923, p. 133; White, 1977; Jennings, 1985). Recharge to karst aquifers can be discrete, such as flow entering a creek swallet, or diffuse, such as infiltration through soils (Aley 1975;

Jones et al., 2000). In a mature karst area of New Zealand, Gunn (1983) observed that more infiltration occurred through soils and macropores than through large sinkhole drains. Clay and iron-rich soils, such as terra rossa, may block the bottoms of some recharge features and create temporary ponds and swamps over karst areas (Sawicki, 1909; Lindley, 2005).

As karst features mature, dissolving macropores or fractures can develop into solution-enlarged fissures, and eventually into nearly circular bowls (Jennings, 1985, p. 114). Solution sinkholes have a direct relation between their diameter and depth (Coleman and Balchin, 1959; Ford, 1964; Jennings, 1975). In Canterbury, New Zealand, Jennings (1975) found the following relation ($r^2 = 0.87$) between the depth and diameter of 90 sinkholes:

Sinkhole depth (m) = 0.16 * sinkhole diameter (m) + 0.79 m (1)

Joints and faults influence sinkhole morphology, create elongation along the fracture trend, and enhance sinkhole size, depth, and steepness (Lavalle, 1968; Kemmerly, 1976). Troester et al. (1984) observed that at the highest stage of maturity, a sinkhole develops a "star" pattern in aerial view as it pirates well-defined channels. Similarly, sinkhole catchment basins progress in maturity from linear to hexagon shaped, although this ideal morphology is modified by topographical slope (Williams, 1972). Kastning and Kastning (2003) described common karst geomorphic features, including spillways and recharge area for sinkholes. Characteristics and terminology for solution sinks are illustrated in Figure 3.1.

Sinkholes that are created primarily as a result of collapse rather than recent surface solution are known as collapsed sinkholes and pitted dolines (Roglic, 1972). Collapsed sinkhole entrances are not created primarily by shallow surface dissolution. Therefore, they commonly have different recharge behavior and geomorphology than solution sinkholes. Collapsed sinkhole entrances are created by erosion of the land surface over pre-existing caves. The presence of vertebrate remains in many Central Texas collapsed sinkholes indicates that much collapse occurred in the Late Pleistocene (Abbott, 1973). As the stress fields generated from an open cavity below reach the surface eventually collapse occurs (Aley et al., 1972). Collapsed sinkhole development is

enhanced by other factors, such as loss of buoyant support of unstable materials from changes in the water table, enhancement of dissolution of supporting materials by surface flow diversion, placement of structures over underlying cavities, and other causes (Aley et al., 1972; Newton, 1984). A detailed karst assessment of Camp Bullis north of San Antonio found that only 6.9% of the karst features were collapsed sinkholes (Veni, 1999). Jennings (1985) noted that collapsed sinkholes could be distinguished from solution sinkholes by their vertical walls and irregular diameter-to-depth ratios. Because collapsed sinkholes open through thin roofs over pre-existing cave rooms, they commonly can be distinguished by underhanging or convex cross section (Hauwert et al., 2005; White and White, 2006; Figure 3.1). Although collapsed sinkhole morphology is not specifically described by Milanović, an illustrative example (1981, p. 61) of a collapsed sinkhole is shown with an underhanging cross section.

Shafts are vertical pipes inferred to be exposed conduits originally carrying flow from the vadose to the phreatic zone. Shafts commonly develop along fractures and faults through less-permeable units (White, 1988; Veni, 1999). Shafts may be part of a "stair-stepped" cave system, which originated by carrying surface flows from a catchment area downward to the water table (White, 1988). Shafts also have been associated with deeper hypogenic flows across underlying units that formerly were confining layers (Klimchouk, 2000b).

The term "karst depression" is used to describe soil-filled, immature sinkholes less than 0.3 m (1 ft) deep. These are solutionally developed and contain subsurface drains. The infiltration of karst depressions was the subject of a study by Lindley (2005, see also section 3.1.4.1). Karst depressions are very common across the Barton Springs segment and individually are limited in recharge significance both by their small catchments and the nature of fill material covering and filling their drains. The term "closed depression" is locally by others to denote a similar, sometimes nonkarstic feature, although this term is not used here since karst literature uses this term with wider definition to include all sinkholes (White, 1988).

3.1.2 Soil Properties

Soil properties greatly influence the soil's ability to transmit recharge and associated contaminants. Soils can be classified simply by horizons: 0 (plant residues), A (leaching zone), B (accumulation zone), and C (unconsolidated parent material from surface weathering) to recognize their origin and characteristics. These horizons reflect pedogenesis and layers may possess similar hydraulic properties. Contrasts in hydraulic properties within horizons, subhorizons, and the bedrock can create hydraulic heterogeneity within the unsaturated zone.

The capacity of water to infiltrate soils depends on: 1) soil and underlying rock hydraulic conductivity; 2) soil thickness and structures, such as clay layers, surface compaction, roots, and piping; 3) initial water content from previous precipitation; and 4) time from beginning of precipitation, as infiltration rate tends to decrease over a rain event (Hillel, 1998). In soils, water infiltrates as capillary suction, which directs water laterally, and gravity, which directs water downward. Laterally focused suction becomes less dominant as the infiltration rate increases (Hillel, 1998; Li et al., 2008; Sheng et al., 2009). Where continuous layers are present, low permeability layers limit infiltration. If moisture flows through the entire soil matrix (distributed flow conditions), then soil moisture gradients can be used to distinguish net upward or downward movement and to interpret the depth to the transient boundary where evapotranspiration or recharge dominates (Delin and Herkelrath, 2005). The infiltration capacity of the soil varies with soil permeability and once this capacity is exceeded by precipitation, surface runoff flows are generated (infiltration excess runoff, Horton, 1940). Highly structured clay soils and limited macropore development serves to locally reduce infiltration to the underlying bedrock (saturation excess runoff; Calvo-Cases et al., 2003). Rainfall interception, uptake, and transpiration by plants within the soil reduce the amount of water available for recharge.

The degree of heterogeneity in soils can be complex, and it is difficult to gather sufficient data to fully characterize them. Grego et al. (2006) found that in an untilled agricultural field, even 102 test holes, spaced 10 by 20 m across a 3.4 hectare area were insufficient to characterize the soil moisture. Comparing chloride concentrations in the

soil and rainfall, De Silva (2004) found high variability of recharge across small areas in non-karstic test sites of Sri Lanka, Australia, Senegal, and the United Kingdom, where the coefficient of variation exceeded 0.4 for 12 out of 18 sites.

Soil infiltration also varies with topography. Delin et al. (2000) measured recharge through the soils of a 2.7-hectare cornfield in Central Minnesota using well-hydrograph analysis, chloroflorcarbon dating, and a soil water balance. The lowland portion of the site recharged at a rate of 29 cm/year and the upland portion recharged at a rate of 18 cm/year. The difference between upland and lowland recharge was primarily attributed to focusing of runoff at lower elevations, soil lamination of the upland site, and a coarser texture soil composition in the lowland portion. Li et al. (2008) found lower soil hydraulic conductivity with lower elevation in large sinkhole basins because of the accumulation of fine-grained sediment. The combination of focused runoff and diminished soil hydraulic conductivity in the lower elevations of a large sinkhole basin increases the amount of recharge through the main sinkhole drain.

Preferential flow occurs through only a fraction of the total soil volume (Hillel, 1998). These preferential flow paths include dessication cracks, roots, wormholes, and unstable wetting fronts (Hill and Parlange, 1972; Bevin and Germann, 1982; Dekker et al., 2001). Rapid recovery of tracers through soils and shallow Glen Rose limestone bedrock to a trench was attributed to roots associated with dense juniper thickets and bedrock conduits (Taucer et al., 2005). The presence of vegetation significantly enhanced the infiltration through soils covering sinkholes in Spain, although the presence of rock fragments had no effect on infiltration (Li et al., 2008). A recharge study in a non-karstic area of western Australia found that half of the recharge was through macropores (Sharma and Hughes, 1985). A common limitation of unsaturated zone models is that they tend to poorly estimate fracture and matrix interactions, and the models can simulate superficial observations without capturing small-scale processes that may overshadow soil-water flow (Fairley et al., 2004).

With increasing karst maturity, the spatial heterogeneity of infiltration through soils increases (Kiraly, 2002). In soils overlying karst areas, macropores such as soil pipes and sinkholes can direct infiltration rapidly into the underlying bedrock (Jennings,

1985). Soil is commonly thin on karst landscapes and may be completely absent at sinkhole openings where drainage is focused. The National Research Council (2001) concluded that "there exists a body of field evidence indicating that infiltration through fractured rocks and structured soils does not always occur as a wetting front advancing at a uniform rate."

Tracing has been used to study transport through soil; tracer transport has typically been found to be faster than expected (Quisenberry and Phillips, 1976, Kung et al., 2000; Helmke et al., 2005). In fact, even in apparently homogeneous, structured, and clay-rich soils, preferential flow is more the rule than the exception (Dekker and Ritsema, 1994; Flury et al., 1994; Kelly and Pomes, 1998). Jarvis et al. (1987) found that 70% of the rainfall infiltrated dry clay soils through desiccation cracks. Transport of wastewater effluent constituents was observed through 30 m of unsaturated, structured sand, silt, and clays, resulting in water-quality changes in the underlying water table (Vengosh and Keren, 1996). The transport times for chloride, sodium, and boron were 0.5 years, 2 years, and 2 years, respectively, indicating that clays have limited capacity to retain metals and organic constituents. In this case, saturation of available sites limited cation exchange and absorption.

3.1.3 Sources of Surface Recharge to the Barton Springs Segment

Sources of surface recharge include recharge derived from rainfall over the Barton Springs Segment and its contributing area, as well as urban leakage from surface land use. Existing measurement of recharge sources of the Barton Springs Segment has been sparse. Water balances from other karst areas worldwide are examined for ranges of recharge rates on carbonate rocks.

3.1.3.1. Water Balances in other Karst Areas

Water balance studies require accurate measurement of rainfall, evapotranspiration, runoff, and recharge. The measurement of spatially distributed rainfall is frequently a limiting factor in the accuracy of water balance and rainfall/runoff models (Dawdy and Bergmann, 1969; Wilson et al., 1979; Amorocho, 1982; Nicks, 1982; Beven and Hornberger, 1982; Hamlin, 1983; Shah et al., 1996). Potential

evapotranspiration has been used to estimate actual evapotranspiration (evaporation and transpiration or ET). The Thornwaite and Mather (1955) method has commonly been used to estimate potential evapotranspiration in the past. However, calculation of evapotranspiration using this method overestimates actual values because it does not account for water deficits that may reduce evapotranspiration (Alley, 1984). Hess and White (1974) found that 19% less evapotranspiration occurred in the karst areas of the Mammoth Cave area than in nonkarst areas of the same river basin. The difference in evapotranspiration was attributed to the rapid internal drainage system and quick infiltration of surface runoff. This suggests that in water balances where evapotranspiration and recharge are not directly measured, the contribution of karst recharge is often underestimated.

The creek characteristics can influence how much recharge occurs in an aquifer. Where catchment areas extent upstream of the karst aquifer, allogenic sources can increase recharge to the karst aquifer. The limits of allogenic sources will be governed both by catchment size as well as the recharge capacity of the creek channels. The amount of allogenic recharge may vary between different karst aquifers depending on the amount of contributing area catchment. The relative proportion of upland recharge can be greater than expected because within creek valleys there are more recharge rejected from the aquifer because of shallower water tables and higher amounts of evapotranspiration (Karrenberg and Weyer, 1970; Weyer, 1972).

Dublyanskii et al. (1984) evaluated the water balance of a 150-km^2 upland sinkhole basin over 18 years in Crimea, Ukraine, with precipitation gauges, soil and evaporation pans, condensation chambers, and 13 weir flow gauging stations. They found the amount of precipitation becoming evapotranspiration, runoff, and recharge amounted to 33%, 33%, and 34% of the input water, respectively.

A 1-year long water balance of the karstic Carboniferous limestone of Mendip Hills, England, was conducted from 1969 to 1970 (Atkinson, 1977). Of the measured precipitation averaged from 10 rain gauges within the spring catchment, 45% left as evapotranspiration estimated by Pennman-Monteith, 1% was added to soil moisture and water-table storage, and 54% recharged. The dry valleys of the limestone plateau are

sufficiently mature to the point that all runoff enters sinkholes except during extreme flooding conditions. Less than 20% of the spring discharge was attributed to leakage from underlying aquifers. Discrete ("quickflow") and diffuse ("baseflow") recharge were each estimated to compose about half of Cheddar Springs flow, based from springflow recession of one of the largest of the 15 major discharge springs. Atkinson (1977, p. 100) interpreted the diffuse infiltration to be composed of epikarst drainage from areas between the sinkholes and underlying leakage.

New technology allowed more precise measurement of evapotranspiration of natural landscapes. Eddy correlation is the most direct measurement of evapotranspiration on vegetated landscapes (Ham and Heilman, 2003). Eddy correlation relies on turbulent transfer of heat and water vapor to measure both sensible and latent heat flux directly above the canopy. Beginning in the 1990s, evapotranspiration was measured at Central Texas sites using Bowen-ratio energy balance and eddy-covariance direct measurement towers. Dugas et al. (1998) estimated that 65% of rainfall was recycled to the atmosphere as evapotranspiration, 30% infiltrated, and 5% ran off over a 5-year water balance over the Trinity Aquifer in Uvalde County. An analysis of available Bowen ratio-derived evapotranspiration, rainfall, and streamflow led Huang and Wilcox (2005) to surmise that upland recharge over the San Antonio Segment was more than 10% greater than previous estimates. Similarly, early studies of the adjacent Trinity Aquifer to the west (Muller and Price, 1979) estimated only 1.5% of rainfall recharged that aquifer, while more current estimates cluster around 7% (Mace et al., 2000b). Ockerman (2002) estimated that 44% of the recharge to the Edwards Aquifer in Bexar County originated from stream channel losses, and the remaining 56% originated as direct infiltration on upland areas.

A compilation of recharge estimates from karst aquifers worldwide is presented in Table 3.1. The percent of recharge from rainfall on the outcrop areas vary from current values for the Trinity Aquifer at 7% up to nearly 100% in Hungary and Tunisia, except for 1986 estimates for the Barton Springs Segment which are 0.9%. A range of 30 to 60% of recharge from rainfall is included in the range of 14 of studies referenced in Table 3.1,

while 6 studies outside the Central Texas area include values lower than 30% in their range.

3.1.3.2. Rainfall and Climate

Surface recharge to the study area is affected by its climate. The climate of the study area is a transition between subtropical subhumid and subtropical humid (Larkin and Bomar, 1983). The climate is strongly influenced by the flow of tropical marine air from the Gulf of Mexico. Air moisture content overall decreases from east to west. The southern and eastern portions of the Edwards Plateau receive short-term heavy precipitation from orographic rise of air masses across the Balcones Escarpment. Orographic precipitation in central Texas results primarily from: (1) a relatively steep rise of about 500 m (1,500 feet) over 40 to 80 km (25 to 50 miles) from the coast and (2) warm air masses from the coast that can be extremely unstable (Petersen, 2005). The average annual rainfall in Austin from 1856 to 2002 is 85 cm (33.4 in), based on a monthly compilation of measured rainfall by David Johns of City of Austin Watershed Protection and Development Review Department.

3.1.3.3. Water Balance of the Barton Springs Segment

In the Barton Springs Segment, the need to distinguish between recharge from upland areas and creek beds became evident in the 1970s and 1980s, when rapid population growth required both more water supply and greater urbanization. A water balance for the Barton Springs Segment was based on data from continuous flow or water-level stations upstream and downstream of or across the Edwards outcrop area on Barton and Onion Creeks collected over a 42-month period between July 1979 and December 1982 (Woodruff, 1984a; Slade et al., 1986). Continuous flow data was collected upstream of the Edwards outcrop area on Williamson, Slaughter, and Bear Creeks while partial flow records were reported to have been collected downstream of the Edwards outcrop area for the study. Flow in Little Bear Creek downstream of the Edwards outcrop area was reported for three days in 1980 and for three days in 1983. Flow loss data, supplemented with estimated runoff coefficients for the intervening Edwards outcrop area between the five main creek channels, estimated the proportion of

recharge contributed by major creeks and intervening areas (Table 3.2). Intervening areas are the Edwards outcrop areas outside the five main creek channels includes upland and prominent stream channels. Upland areas, by contrast, are areas of the Edwards outcrop area above the major creeks and their major tributaries. Fifteen percent of the recharge was estimated to occur in the intervening areas between the major creek channels, and the remaining 85% to recharge through the beds of six major creeks. The estimated 3-year recharge volume was found to be within 10% of Barton Springs discharge volume over that period. Only about 0.9% of the mean rainfall was estimated to recharge the aquifer directly through intervening areas of the Edwards outcrop area, as 85% of the rainfall was estimated to be lost to evapotranspiration, 9% left as surface runoff, and 5% recharged the Edwards Aquifer through the major creeks that drained the contributing area (Woodruff, 1984a). Over this 42-month water balance, evapotranspiration was not directly measured; instead, typical evapotranspiration values from a constantly watered evapotranspiration sewage lysimeter were reported as support of the values used in the water balance.

In Slade et al. (1986), the amount of rainfall that was assumed to recharge over the intervening areas between the main channels of some major creeks over the Edwards outcrop area (0.9%) was significantly smaller than values measured in other karst areas over the world or over the adjacent Trinity Aquifer (see Table 3.1). The Edwards Aquifer has relatively well-developed karst compared to the Trinity (Elliott and Veni, 1994) and 250 times greater average yield (Mace et al., 2000b). Consequently, the Edwards Aquifer must have a more efficient recharge structure and higher recharge to rainfall ratio than less karstic limestones, sandstones, and shales. In fact the 0.9% of rainfall allocated to recharge of the intervening areas by Woodruff (1984a) was less than the 1.0% of recharge from rainfall estimated for the Eagle Ford Shale outcrop, based on a one-year water balance in Bell County (Harrison, 1996). The assumption that the recharge of the intervening Edwards outcrop area is 0.9% (Woodruff, 1984a) is contrary to observations by early investigators (Hill and Vaughan, 1898; DeCook, 1957; Appendix A) that the Edwards Aquifer has a well developed recharge structure. The underestimation of upland recharge may have significantly affected the results of the 1980s water balance study for

the Barton Springs Segment. The relatively small proportion of total recharge attributed to upland areas by Woodruff (1984a) has been used as the rationale for lower levels of protection for upland recharge areas (TxDOT, 1989; URM, 1983; Woodruff, 2001). Thus, it is important to understand the role of upland recharge in the water budget of the Barton Springs Segment.

3.1.3.4. Urban Leakage

Urban leakage is one source of leakage to the Barton Springs Segment. Utility trenches, utility lines, and wells create enhanced pathways for recharge to enter the aquifer (Sharp et al., 2001). Urban leakage originates from irrigation, infrastructure leakage through water lines, wastewater lines, septic tanks, and lift station releases (Garcia-Fresca, 2004; Garcia-Fresca and Sharp, 2005). For the entire City of Austin service area, Garcia-Fresca (2004) estimated that surface recharge decreased from 53 mm/yr to 31 mm/yr because of increased impervious cover from urbanization, but that urban leakage of water, wastewater, and irrigation of 94 mm/yr essentially doubled natural recharge in the Austin area. Less than half of the Barton Springs Segment lies within the City of Austin service area. The urban leakage contribution specific to the Barton Springs Segment has not been quantified.

3.1.4 Upland Recharge Study

Several hypotheses were developed for this study. The first is that the Barton Springs Segment is a mature karst aquifer and is expected to have recharge rates comparable to other karst areas of the world. The previously estimated value of less than 1% average recharge from rainfall on the Edwards outcrop area is probably too small. Second, upland sinkholes are relatively efficient for infiltrating rainwater and runoff compared to other Edwards outcrop areas. Third, the sinkhole bowl enlarges in response to greater calcite-undersaturated flows that reflect the size of the catchment area.

Two research sites were selected to examine upland recharge. These are centered on two large sinkhole basins because these have measurable discrete and diffuse infiltration components. Large catchments, the lack of human disturbance, the limited number of channels entering these two sinkholes, and assured access to the sites through

the City of Austin made them ideal study sites. This study was initiated in 2002, and preliminary results were reported in Hauwert et al. (2005). The methodology of this study is introduced in section 3.2.

3.1.4.1 Description of the Research Sites

The two sites are the J17 and the Tabor water-quality protection land (WQPL) sites (Figures 3.2, 3.3, and 3.4). Both lie on the Edwards outcrop area of the Barton Springs Segment and are bisected by major creeks or their tributaries. Away from the creeks, both sites are relatively flat (<3% slopes), and contain large, broad internal drainage basins terminating in sinkholes. A number of well-developed drainages on both sites lose their definition or never carry flow to the nearby creeks. Runoff as sheet flow tends to converge within gentle to well-defined channels that convey flow across much of the sites. Soil covers the surfaces of both sites, although bedrock exposure is common. The soils are mapped on both sites as Speck Stony Clay Loam (Werchan et al., 1974). Werchan et al. (1974) described this soil as being slowly permeable with low water capacity, containing up to 80% chert and other rock fragments on soils with slopes of 1.5% to 3.5%, and having soil depths of 0.36 to 0.46 m (14 to 18 in). Both sites contain predominantly juniper (*Juniperus ashei*) and Escarpment live oak (*Quercus fusiformis*) thickets with intermittent grasslands. The types of vegetation found on the sites are provided by personal communication from Sanders (2007) and Windhager (2007). They are listed in Appendix H.

3.1.4.1.1 Headquarter Flat Sink (J17 Tract)

Headquarter Flat sinkhole and cave (HQ Flat) is located on the COA J17 Water-Quality Protection Land tract in South Austin (Figures 3.2 and 3.3). A detailed description of HQ Flat is provided by Russell (2004). In 1984, the former landowner, Ira Yates, reported that the cave "takes considerable water after rains." Russell suggested the cave was a significant recharge feature and he cleared rocks and debris around the entrance to enhance recharge. He described an estimated 1,600-m^2 (0.4 acre) depressed area in the drainage leading to the sinkhole that had to fill before surface flow could

continue to the cave. Russell estimated that the catchment area drained "an extensive area to the south and west" of about 0.065 km^2 (16 acres). Much of the known extent of the cave had been investigated by cave explorer Mike Warton in the 1980s, when the cave was mapped to a depth of 10 m (32 ft).

A second hydrogeologic study (Ford, 2000) describes surface drainage and karst development on the J17 tract. This report described surface flow on the J17 tract to be primarily sheet flow toward the Danz Creek tributary of Slaughter Creek (Figure 3.3). It described HQ Flat as a "small sink" and noted "the recharge potential to the aquifer from the sink is probably small to medium since the surface opening is moderate in size but the drainage area affected by the sink is relatively small." From the surface entrance the report believed the cave "appears to pinch close at about 5 feet (1.5 m)."

These two reports offer divergent descriptions and evaluations of the same karst feature. Such contradictory views of the same feature or site are common in recharge feature assessments and point to the need for a quantitative examination of the recharge.

An infiltration study on the J17 site compared karst depressions (small upland, soil-filled, immature sinkholes) to background soil infiltration (Lindley, 2005). Lindley measured an average infiltration for soil-filled karst depressions of 0.16 cm/hr that ranged from 0.06 to 0.3 cm/hr. Infiltration on background soil plots, where karst features were not observed, averaged 0.25 cm/hr and ranged from 0.06 to 0.4 cm/hr. However, once excavated the infiltration rates of the karst depressions exceeded those of background soil plots by 15 to 30 times. From dye tracing, it was observed that water infiltrated into 10- to 20-cm diameter conduit drains in the base of the soil-filled karst depressions, following plant roots and rock fragment/soil interfaces through the soil. Two karst depressions, only one of which was on J17, had open apertures prior to excavation for Lindley's study and measured infiltration rates of 3.45 to 5.7 cm/hr. Even though clay accumulations lowered the relative infiltration rate of small upland sinkholes or karst depressions, the small karst depressions infiltrated a higher portion of runoff than the local background soil plots because runoff was focused to lower elevations (Scanlon et al., 1999; Lindley, 2005).

The Kirschberg bedrock underlying the shallow subsurface of J17 and Tabor has characteristics of a soil. The pulverulitic layers are weakly cemented and appear soft and

sandy, even when examined in caves (such as Whirlpool, Get Down, and Flint Ridge caves) more than 13 m (40 ft) below the ground. Intensive dissolution focused within the Kirschberg Member have made collapsed bedrock blocks a common subsurface feature. Terra rossa commonly is encountered within the bedding planes and other cavities. Terra rossa (a reddish, clay rich soil with siliceous remnants) also overlies the Kirschberg bedrock as a true soil. The Kirschberg Member characteristically is highly recrystallized and broken into small and large blocks. Roots penetrate below the bedrock surface and can be observed in Kirschberg Member caves. Some of these same characteristics, including an apparently thick, clay-rich soil, root penetration, loose bedrocks blocks, and soft bedrock, can give the false impression that the Kirschberg Member, which is actually the most permeable bedrock unit of the Edwards Aquifer, is a soil of low permeability.

3.1.4.1.2. Flint Ridge Cave (Tabor Tract)

Flint Ridge Sinkhole and Cave (Flint Ridge) are located on the COA Tabor Water Quality Protection Land tract in South Austin (Figure 3.4). The geology, hydrology, biology, speleological features, and the history of exploration in Flint Ridge are described by Elliott (1997), Veni (2000), and Russell (2004), The cave is listed in a joint US Fish and Wildlife permit by the COA and Travis County as a preserve for karst invertebrate species of concern. Texas Department of Transportation (TxDOT, 1989) concluded that Flint Ridge was not a major recharge feature: that its catchment area was limited to 0.003 km^2 (0.75 acres) and that water entering the cave likely fed “seeps or ephemeral springs” along Bear Creek rather than supply direct recharge to the Edwards Aquifer water table. Because of its assumed limited catchment area, TxDOT estimated that a water volume of 2,500 m^3 (2 acre-feet) would exceed the actual average annual recharge to the cave. Veni (2000) estimated the surface catchment of the cave to be 0.16 km^2 (40 acres) in area, that within the catchment of Flint Ridge, an average of 3.6% of rainfall would recharge, and that typical intense storms would yield an average of 415 to 593 m^3 of runoff to the cave entrance. From high water marks inside the cave after a 20-cm storm in October 1998, Veni estimated about 1,000 m^3 of flow had passed through the cave, but believed some of the recharge must have entered through other features rather than via the cave entrance of

Flint Ridge. Veni (2000) acknowledged the difficulty in estimating recharge from Flint Ridge and the need for installation of gauges to measure flow directly.

3.2. METHODOLOGY

A methodology was developed to assess upland internal drainages across the Barton Springs Segment based on geomorphology. HQ Flat and Flint Ridge sinkhole basins were monitored to measure their recharge contribution.

3.2.1. Locate and Map Recharge Features and Areas Using GPS and GIS

First, the common geomorphological characteristics of internal drainage basins were examined. Then the extent of these features were identified and mapped across the Edwards outcrop area of the Barton Springs Segment. A methodology and classification for quantifying the most recent surface dissolution associated with a recharge feature (as opposed to subsurface dissolution caused by paleo groundwater flow processes or post-depositional dissolution that occurred during the Cretaceous Period) was developed for use in the Barton Springs Segment, including catchment area (also called drainage or recharge area), rim (characterized by a sharp break in slope around the entrance), and aperture (conduit; Figure 3.1). Each feature was examined to determine whether solution or collapse processes were the primary agent in its development at the surface. For this study, sinkholes where solution was the primary agent in development of the surface opening were recognized by concave, "bowl-shaped" cross sections, while collapsed sinkholes were recognized by a convex cross section (Figure 3.1, Hauwert, et al., 2005).

This study characterizes "internal drainage basins", defined here as natural areas where at least 90% of the runoff generated within a given catchment area does not discharge from the basin on the surface under natural conditions. This condition is attributed to the combination of a solution-enlarged sinkhole bowl that is capable of temporarily storing surface runoff and the permeable drain present at the base of sinkholes that transmit runoff into the subsurface. As defined here, internal drainage features and catchment areas are not necessarily large; a small karst feature can capture more than 90% of the runoff from a relatively small catchment area. However, this study examined only large internal drainage basins and did not include areas where many small

sinkholes or karst depressions may serve a similar function of intercepting runoff, except where those smaller karst features lie within mapped internal drainage basins for larger sinkholes.

"Open internal drainage basins" are the most common type consisting of a sinkhole basin capable of capturing more than 90% of the runoff generated within its catchment. Open internal drainage basins are naturally formed and have open apertures such that runoff readily enters the cave. Open internal drainage basins are the subject of this study.

"Ponded internal drainage basins" are similar in origin and recharge characteristics, but they differ in that sediment and other debris have obstructed the drain. Greater evaporative losses can be expected from ponded internal drainage basins.

An "artificial internal drainage basin" is similar to a natural internal drainage basin, but has its entire drainage diverted to a manmade depression, such as a rock quarry. Where the artificial internal drainage basin extends to the water table, the recharge contributed by these features may be diminished by greater evaporative losses compared to open internal drainage basins.

Open internal drainage basin, ponded internal drainage basin, and artificial internal drainage basins and catchment areas were identified and mapped across the entire Barton Springs Segment using a combination of tools including:

(1) interviews with local cave explorers, speleologists and property owners,

(2) discovery by COA or BS/EACD staff,

(3) closed contours indicated on 1 and 3 m (2 and10 ft) contour topographic maps and supporting catchments,

(4) dark-toned circular features on aerial photos,

(5) field Global Positioning System (GPS) delineation of rims and surface divides around sinkholes,

(6) flood debris and incised discrete channels to sinkholes may also indicate the presence of a large catchment area,

(7) well-defined channels or flow that abruptly terminate,

(8) runoff trailed to sinkhole during or shortly after a sufficient rain event.

Assessment of sinkholes included recognizing the recharge feature, categorizing its recharge, locating the feature, measuring its bowl volume, mapping its catchment area, and excavating features to assess subsurface extent. A Trimble XRS GPS (acquired by BS/EACD in 1999 through an Environmental Protection Agency 319h grant administered by the Texas Commission on Environmental Quality) and a Trimble Pathfinder GPS (acquired by the City of Austin) were used to locate known recharge feature openings, measure larger sinkhole rim dimensions, and delineate catchment areas for sinkholes. Because of historical practices described in Appendix A, all rockpiles are customarily examined for airflow, voids from washed-in fill, internal drainage conditions, fill extending below the surface, and historical aerial and topographic maps in order to discover filled sinkholes and caves. The karst features were mapped in ArcGIS version 9.1 software, produced by Environmental Systems Research Institute (ESRI). Sinkhole bowl volumes were calculated either by (1) simple application of an ideal cone formula using the field measurement of the rim area and bowl depth ("C" in Figure 3.1 and glossary) or (2) site survey of larger sinkhole bowls. The northern half of the Flint Ridge catchment area was surveyed professionally for the City of Austin WQPL (Figure 3.4). Historical cave and sinkhole information is available primarily through the Texas Speleological Survey (TSS), which compiles reports from its volunteers who map and investigate caves.

3.2.2. Water Balance of Sinkhole Basins

HQ Flat and Flint Ridge have been monitored continuously for flow to the cave entrances since July 2002 and March 2003, respectively. In both basins nearly all surface runoff flows to the cave through a limited number of discrete drainages. The catchment area of each sinkhole was estimated by field inspection with a GPS, as well as 2-foot contour interval map coverages derived from 2000 aerial surveys (COA). Flow from 94% of the catchment area for both features converges though drainages that were

monitored during the study. The remaining areas drain around the measurement structures or directly to the sinkhole drains.

Within a closed sinkhole basin of known area over a selected time interval, the amount of rainfall can be proportioned as follows:

$$P = ET + I + DR + S \quad (2)$$

where:

P= Precipitation volume (m^3)

ET = evapotranspiration flux volume (m^3)

I = infiltration from soil and lesser karst features into the underlying bedrock (diffuse infiltration, m^3)

DR = internal runoff that enters the cave drain (discrete recharge, m^3)

S = change in water storage in soil during the reference period (m^3)

A 505-day period, from April 2, 2004, to August 20, 2005, was selected for measuring water balance. The starting day represented the first time synchronized monitoring instruments were operational, produced the highest quality data, and avoided data gaps affected by power problems experienced early in the monitoring.

3.2.2.1 Precipitation Measurement

Precipitation was measured primarily from readings from visual plastic All-Weather rain gauges at HQ Flat and Flint Ridge sites. The gauge orifice was placed 700-1,000 millimeters above the ground to meet World Meteorological Services and United States standards (Shaw, 1994). The gauges were placed in relatively open areas with no trees or other obstructions present in a 45-degree vertical plane measured from the ground horizon. The visual rain gauges are accurate to within 0.0254 cm (0.01 inch) from June 2004 to present and 0.254 cm (0.1 inch) from 2002 to May 2004. These visual rain gauges are designed with a funnel cap that reduces evaporative loss compared to an open vessel. One of the visual rain gauges was checked daily for 3 weeks from November 23, 2006, to December 14, 2006, and was found to have no measurable (<0.025 cm) evaporative losses. The gauge test does not rule out that greater evaporative losses occur

in the summer months, but their long-term readings did not under-report, on the basis of comparison to calibrated tipping-bucket totals. Even though the gauge at Flint Ridge site was read less frequently than the gauge at HQ Flat, roughly at 2 to 4 week intervals, its station had a slightly higher precipitation total suggesting that evaporative losses were insignificant.

Additional automated precipitation measurements were taken primarily using three 0.0254 cm (0.01-inch) Rainwise tipping bucket rain gauges with HOBO dataloggers owned by City of Austin and stationed at J17 HQ Flat, at Tabor tract Flint Ridge, and farther west on the Tabor tract near Bear Creek (Figures 3.3 and 3.4). Tipping-bucket rain gauges are prone to plugging from bird droppings and require careful maintenance. The Rainwise tipping buckets require a small calibration shift, based on verification with a graduated cylinder as well as correlations among other stations and visual rain gauges. Monthly correlations from the visual rain gauges and tipping buckets, as well as comparison of expected versus measured tip counts with a graduated cylinder, were used to develop a calibration shift for the tipping buckets, which otherwise under-reported precipitation. Supplemental rain gauge information was collected periodically by additional ISCO rain gauges using an ISCO 3230 logger, but because of greater power needs and complexity, these gathered only periodic data. Each tipping-bucket rain gauge was calibrated using a 500-ml graduated cylinder. Monthly totals of rainfall were compared at all gauges to find potential data gaps. Missing daily data were replaced with data from the closest rain gauge.

3.2.2.2. Measurement of Discrete Recharge into Caves

Recharge to the underlying aquifer consist of: (1) discrete recharge, where internal runoff enters the opening at the lowest point of the sinkhole and (2) diffuse infiltration, where surface runoff passes through the soil, epikarst, or smaller recharge features and percolates to the water table. The flow entering the cave drain at the lowest elevation of HQ Flat and Flint Ridge sinkholes was measured as discrete recharge. The measurement of runoff at these sites also estimates runoff generated outside of internal drainage basins from upland areas to creeks in the Edwards outcrop area.

3.2.2.2.1 HQ Flat

Discrete recharge was measured using a ISCO 3230 flow meter installed at a weir (June 30, 2002, until April 1, 2003) or flume (April 15, 2003 to present) on the drainage channel flowing to HQ Flat (Appendix G). The flume was an aluminum 0.6 m (2 ft) H-flume. Using ArcGIS and site observations, 94% of the runoff to HQ Flat flows through this single channel from the west, which makes the site ideal for runoff monitoring. A 0.3 m-high dirt berm was placed south and west of HQ Flat to divert overland flow within the natural basin from the south to the channel entering the west side of the sink. The design of weirs and flumes used in this monitoring was adapted from Shaw (1994) and Kilpatrick and Schneider (1983).

The possible error from the flow structure, with periodic independent flow meter checks, in a stable channel when the structure is not exceeded is about $\pm$5 to 8% (Slade, 2004; Harmel et al, 2006). The ISCO 3230 flow meter has level accuracy of 0.003-0.01 m that varies with magnitude of water-level change and typical long-term calibration change accuracy of 0.5% (Teledyne ISCO, 1999). Additional error in level measurements occurs when temperature deviates from 22^{o}C.

Other possible errors associated with flow measurements are biased toward underestimation of the flow. The flow entering HQ Flat from local runoff generated off a 0.01-km^2 (2.7-acre, or 6% of entire HQ Flat catchment) area immediately east of the sinkhole was not measured. Flumes and weirs can leak, the channels monitored do not include all of the flow to the sinkholes, equipment problems can lead to data gaps, and occasionally flow is below or exceeds the sensitivity of the measurement structure. Leakage was measured using a Marsh McBirney flow meter flow downstream of the structure, and corrected in the data analysis for one period where the leakage was found significant. The measurement range of the 0.62-m (2-ft) H flumes and compound wiers are 0.04 to 300 l/s (0.0014 to 11 ft^3/s) and 0.01 to 140 l/s (0.005 to 5 ft^3/s), respectively. Flows below or above these structure designs are omitted. Flow exceeded the flumes capacity on several occasions at both HQ Flat and Flint Ridge sinkholes.

3.2.2.2.2. Flint Ridge

In order to evaluate whether or not other open internal drainage basins had discrete recharge in proportion to their catchment areas, flow monitoring was conducted at Flint Ridge. Three defined drainages entering the sinkhole rim were monitored. Flow to the two largest drainages was metered using a 0.6 m (2-ft) aluminum H flume in each. The smallest of the three drainages was metered using a compound weir cut from unpreserved 2-cm (0.75-in) plywood and edged with aluminum angle iron. Each drainage was monitored by an ISCO 3230 bubbler flow meter. Local runoff generated within a 0.017-km^2 (4.1-acre) area immediately south of the sinkhole is not measured by the flow meters.

3.2.2.3. Measurement of Evaporation and Transpiration

Evaporation and transpiration (evapotranspiration or ET) were measured nearly continuously using eddy covariance. Ten-hertz measurements of wind speed and acoustic temperature were made with a three-dimensional sonic anemometer (CSAT-3, Campbell Scientific), and 10-Hertz measurements of water vapor concentration were made with an open path infra-red gas analyzer (LI-7500, LI-COR). The anemometer and gas analyzer were controlled by a micrologger (CR23X for the first 10 months, then a CR5000, Campbell Scientific), and driven by solar power. The instruments were placed 15-m high and above the canopy on a Rohn tower.

Eddy covariance requires measurement of the vertical component of airspeed and variations in absolute humidity from mean humidity:

$$\text{Evapotranspiration} = \frac{\underline{w'\rho_v'}}{\rho_w} \qquad (3)$$

where:

w' = vertical component of airspeed (time average in m/s)

ρ_v' = variations in absolute humidity about the mean value (time average)

ρ_w = mean value of absolute humidity (converted from watts/m^2 to mmoles/m^2s to cm/30 min interval)

Thirty-minute fluxes of latent heat and sensible heat for a 505-day test period are calculated on 10-hertz datasets following procedures outlined by Litvak et al. (2003). Initial data gaps were caused by power outages, lowering of the instrument for annual calibrations, and particulates (including raindrops) obscuring the glass lens of the gas analyzer. The readings represent average evapotranspiration for the fetch area, which varies with wind direction and sensor height. As a general guideline, the fetch ranges from 20 to 200 times the instrument height, with the farther fetch extending in the direction of prevailing winds (Monteith and Unsworth, 1990), although the actual fetch will vary with wind speed and other factors. The ET flux tower lies near the center of the Headquarter Flat sinkhole catchment, which has a 1-degree slope to the north, southeast, and southwest. The ground slope increases in elevation from the ET tower to the south at a maximum slope of 3 degrees. Because of the minimal slope in the direction of prevailing winds, the flux field was not rotated to account for slope.

The ET data were filtered to remove poor-quality data, including readings taken when the wind approached the flux sensors from the north, where the tower distorts wind velocities, and during rain intervals. Of 24,285 30-minute intervals comprising the 505-day test period, 5,585 data gaps were present after this quality filtering. At this stage the filtered values are corrected for energy balance, based on the Bowen ratio of sensible heat to latent heat. To fill in the gaps remaining after filtering and energy balance, monthly correlations of postprocessed and filtered ET data were related to net radiation readings. On a monthly basis, the ET to net radiometer correlations had R^2 correlations greater than 0.7 and averaging 0.83. Where gaps existed in the J17 tower net radiation record, readings from an ET tower located 21 km south on the Texas State University Freeman Ranch were used. Measured nighttime ET values are relatively very small so that data gaps of nighttime intervals are assumed to be zero. Following net radiation gap filling, 813 daytime 30-minute gaps remained. Where up to three consecutive data gaps remained, the gaps were filled by averaging adjacent ET values. Where larger data gaps remained, such as an entire day, the daily total was calculated as 0.75 of the potential

evapotranspiration values reported by Texas A&M University from a weather station at the City of Austin Davis Water Treatment Plant, based on an R^2 correlation of 0.56. Most of these gaps occurred during the 4 months of the test period because of insufficient power, a condition that was later corrected. The accuracy of measuring an average evapotranspiration across the fetch area using eddy covariance with energy balance corrections is about $\pm$ 5% (Ham and Heilman, 2003).

Additional instruments used for meteorological and energy balance measurements include air temperature and humidity (HMP45C, Vaisala), net radiation (Radiation and Energy Balance Systems Q7.1), incoming and upwelling solar radiation (LI-190 SB, Kipp and Zonen), and photosynthetic photon flux density (PPFD, LI-190SA, Licor).

Conservative water-quality constituents, such as chloride and isotopes (oxygen and deuterium) are used to estimate recharge to aquifers (Vacher et al., 1980; Jones, 2000; Scanlon et al., 2002). In order to use chloride to estimate recharge accurately, several conditions must apply: (1) downward "piston" flow is occurring through the phreatic zone to the water table; (2) rainfall is the only significant source of chloride; (3) the lithology is well drained; (4) the land surface is relatively flat and runoff is minimal; (5) no chloride sinks are present; and (6) no significant change in land use occurs (Sukhija et al., 1996; Hendrickx and Walker, 1997; Scanlon, 2000.) A potential source of chloride is the dissolution of limestone rock (White, 1965; Moller et al., 2007). Gee et al. (2005) found that chloride estimations of recharge from soil water underestimated recharge measured by lysimeters by 2 to 8 times and warned that mineral dissolution could contribute to such errors. As discussed in section 2.3, the Edwards Group was deposited in a marine setting and evaporites occur within some of its members. The Saline-Water Zone is enriched in chloride and sulfate and leakage from this source is observed in some wells and Barton Springs. Chloride levels can be elevated in groundwater from various anthropogenic sources (COA, 1997, Panno, et al., 2002).

The accuracy of the chloride mass balance method may be compromised in fractured or soluble rocks where preferential flow focuses flow through the unsaturated zone (Scanlon, 2000). The application of chloride concentrations for estimating recharge is more accurate at lower recharge rates, and an approximate maximum resolution limit

of 300 mm/year is suggested (Scanlon, et al., 2002). Given local average annual rainfall of 850 mm per year, any recharge above 35% of rainfall exceeds this resolution limit. Consequently, because of sources of chloride in the rock and low resolution of the test, factors that can potentially underestimate recharge using chloride in the Edwards Aquifer and should be carefully considered.

Evaporation was estimated independently by comparing water quality of rainfall, runoff, cave drips, and Barton Springs. Chloride and sulfate concentrations were measured in surface runoff and cave drips from the Tabor research site by UT graduate student Brian Cowan and me as part of his master's thesis project (Cowan et al., 2007). Perennial cave drips in Barker Ranch Cave, about 5 m below the surface, were sampled during baseflow, during rain events, and after at least three rain events in 2007. Barker Ranch Cave has an internal drainage basin adjacent to the Flint Ridge catchment. Drip samples from the Flint Ridge Drip Room, which is about 47-m deep, also were sampled. Runoff quality samples were collected during and shortly after rain events with autosamples and grab samples at Flint Ridge and on the surface near Barker Ranch Cave. Because the runoff was sampled within internal drainage basins within the Tabor tract this runoff enters Flint Ridge and Barker Ranch Caves as discrete recharge. A composite rain sample was collected over May 2008 on the roof of University of Texas Geology Building using a rainwater collector under a rainfall quality program led by Dr. Jay Banner. A rain sample was collected in October 2000 using a rain water collector by City of Austin Watershed Protection and Development Review Department Water-Quality Management staff. Barton Springs samples were collected by City of Austin Watershed Protection Department and USGS staff. The samples were analyzed at the Lower Colorado River Authority Laboratory using EPA 300.0 method although some samples were analyzed with City of Austin Water Utility laboratory and USGS laboratory. Rainfall collected locally were compared to annually averaged values from rainfall water quality reported for National Atmospheric Deposition Program stations in Attwater Prarie Chicken National Wildlife Refuge (Attwater) and Sonora.

In this study, we can reduce the potential problems of aquifer mixing of chloride-rich groundwaters and chloride enrichment by rock dissolution by comparing chloride

concentrations in cave drips that are expected to be beyond the effects of evaporation. Evaporation is not expected below the 5-m cave drip depth (Scanlon et al., 2002). Because both chloride and sulfate should increase in concentration directly proportional to evapotranspiration, the ratio of sulfate to chloride is used to determine when other processes, such as aquifer mixing or rock-water interaction, account for increasing concentrations. Sulfate to chloride ratio trends are used to distinguish which phase (cave drip or aquifer spring) is most representative for deriving evapotranspiration rates. Both sulfate and chloride should be enriched at the same rate by simple evaporation, and any change in their ratio is assumed to result from other processes. The cave drips lie in internal drainage basins where no runoff leaves the catchment.

The water lost through evapotranspiration is calculated by comparing the chloride concentration in rainfall with subsurface chloride concentrations using the following relation:

$$ET_{wq} = C_{rw}/C_{gw} \quad (4)$$

where:

C_{rw} = concentration in rainwater (mg/l)

C_{gw} = concentration in subsurface groundwaters (mg/l)

3.2.2.4. Measurement of Soil Moisture and Diffuse Infiltration

Available soil-moisture storage is the amount of releasable water held in the soil, and varies at any given time between the field capacity and permanent wilting point (Ferguson, 1994). Soil moisture was monitored for the purposes of selecting a water balance interval over which no net change in soil moisture storage occurred. By selecting intervals with no net change in soil moisture storage, the amount of water in the soil can be neglected for the purposes of the gross water balance. Alternatively, the data could estimate changes in soil moisture storage, such as for short-term water balances, although larger errors may result because of the heterogeneity of the soil and soil moisture. As the water balance time interval increases, the maximum average soil moisture change becomes less significant in comparison to the net precipitation accumulated over that interval. Soil moisture data were also utilized in the calculation of the energy flux

balance. A third purpose for soil moisture data is to examine heterogeneity in the soils across the research sites and to characterize infiltration through the soils to the bedrock.

Soil thickness was estimated by hand-dug test holes, soil trenches dug with a backhoe, and outcrop observations to determine the volume of soils across the internal drainage basin sites (Figure 3.3). Gravimetric analysis was used to determine the water content. Soil trenches allowed examination of the soil to bedrock transition and distinguished the bedrock from weathered rock. The trenches and hand-dug holes are useful for examining the distribution of soil thickness and soil moisture at the time of excavation as a reflection of soil heterogeneity. Seven trenches were excavated on the J17 tract by TxDOT staff using a backhoe as part of a separate study by soil scientist Larry Wilding on local soils. Backhoe soil trenches are relatively disruptive to the natural landscape systems, so relatively few trenches were excavated. Soil moisture samples were not collected within several hours of precipitation events so that surface moisture was not directly transmitted to excavated sampling depths.

Gravimetric soil moistures were calculated as described by Black (1965). Samples were collected from a small excavated pit or backhoe-dug trench. Samples from representative depths were taken from the wall of the excavation and collected in sealed plastic bags. Three representative portions were taken from each bag, weighed on a weighed sheet of filter paper, and oven dried for at least 24 hours. After drying, the mass of the soil portions were remeasured. Soil volume was measured after drying by water displacement in a graduated cylinder. Additional tests were conducted to examine the potential for undermeasurement of soil moisture from moisture loss from the sealed bags prior to oven drying; and condensation of moisture lost from the soil within the bags. A number of plastic bags containing soil samples were sealed, weighed, oven-dried for at least 24 hours to measure how much moisture could be expected to be lost through leakage and condensation. The method selected to estimate the possible significance of moisture loss overestimated the possible leakage because samples were not subjected to that high a temperature for so long between collection and processing. Of 14 leakage measurements, the leaked moisture mass averaged 3.5% and ranged from zero to 6.1% of the total soil moisture. Fourteen bag condensation measurements were made, which

averaged 0.3% of total sample moisture mass and ranged from 0.016% to 1.6%. Based on these possible error estimates, the leakage and condensation are relatively small compared with the precision of the test.

Soil-moisture sensors measured soil moisture continuously at a test site near the ET tower. Continuous measurements of water content at 2.5 cm, 5 cm, and 9 cm depth were made using Campbell Scientific water content reflectometer probes (CS615) installed horizontally. Soil temperature and heat flux were measured continuously at depths of 2.5 and 10 cm using thermocouple probes and heat flux plates. Heat flux plates were installed at a depth of 5 cm, and storage heat flux in the zero to 5 cm layer was calculated from both soil temperature measurements at 2.5 cm depth and estimates of heat capacity (Kimball and Jackson, 1979). The depth to bedrock and change in soil moisture from the start to the end of a reference period were used when it was necessary to estimate the gross change in water storage within the soils.

Over long periods of time, the change in storage within the soil and epikarst becomes less significant in comparison with cumulative volumes of rainfall or recharge. Consequently, although there can be significant error associated with estimating the total soil water storage of a site over short intervals, but over long periods the effect of these errors are negligible. Over the scale of an individual rain event, soil moisture content is very important in determining whether the field capacity is exceeded and runoff will occur. In this study, once water descended below the soil it was assumed to recharge the underlying aquifer. Some water storage is expected in the epikarst and vadose zones. By selecting soil moisture cycles for start and stop intervals, similar epikarst and vadose conditions are expected such that no significant change in storage has occurred. The estimation of no change in soil-moisture storage is not intended to imply that the water flow from the soil, epikarst, or vadose is not significant over a water balance cycle, only that the amount of storage was approximately the same at the beginning and end of a cycle.

Diffuse infiltration through soil and minor recharge features likely is highly variable across both basins (Dingman, 1994, p. 247-249). Diffuse infiltration through soils is determined in a relative sense in this dissertation since the methodology used does

not distinguish how much diffuse flow through small pores versus, rapid flow through macropores in the soil, and direct infiltration into bedrock where soil is absent. Diffuse infiltration is the only component of the water balance that is not directly measured, but is estimated as the remainder of the water balance. The diffuse infiltration (I) for the water balance is calculated by:

$$I = P – DR – ET \quad (5)$$

3.2.2.5. Measurement of Runoff Into or Out of Basins

No runoff leaves either sinkhole basin under any flood conditions because of the bowl configurations of the basin and the capacity of the basin to absorb runoff generated within the basin. Following major flood events, high water marks along adjacent Danz Creek, a tributary to Slaughter Creek on the J17 tract, were walked to ensure no floodwaters from the creek entered the HQ Flat basin. Even after the largest rain event observed in November 2004, high water marks indicated that Danz Creek would have to rise an additional 0.6 to 1 m (2 to 3 ft) and fill a wide area before it could flow into the HQ Flat basin. A flood retention dam built on Danz Creek upstream of HQ Flat also serves to stabilize the downstream flood flows such that they are not likely to cross the topographic divide and enter HQ Flat.

3.3. RESULTS

The upland recharge types were characterized by sinkhole morphology. The recharge of an internal drainage basin was measured using a water balance approach, which was verified using chloride concentrations in rainfall, runoff, and cave drips.

3. 3.1. Sinkhole Hydrology and Geomorphology Characterization

One hundred fifteen internal drainage basin sinkholes were identified within the portion of the Barton Springs Segment recharging to Barton Springs, with a combined catchment area of 21.5 km^2 (8.3 mi^2). Ninety-five open internal drainage basins were mapped across the Edwards outcrop area contributing to Barton Springs with a combined catchment area of 16.7 km^2 (6.5 mi^2). Thirteen open internal drainage basins, with a net catchment area of 0.9 km^2 (0.3 mi^2), were identified within the portion of the Barton Springs Segment over the Cold Springs groundwater basin. The catchment area for HQ Flat was determined to be 0.19 km^2 (46 acres) in size. This is larger than the 0.065-km^2 (16-acre) area estimated by Russell and Jenkins (2002) and the "moderately small" catchment area described by Ford (2000). The catchment area for Flint Ridge is 0.28 km^2 (69 acres) in size, which also was larger than the previous estimate of 0.003 km^2 (0.75 acres) by TxDOT (1989) and 0.16 km^2 (40 acres) by Veni (2000). Twenty-two ponded internal drainage basins were identified across the Barton Springs Segment, with a combined catchment area of 4.0 km^2 (1.5 mi^2). The one artificial internal drainage basin identified was an abandoned quarry with an estimated catchment area of 0.9 km^2 (0.3mi^2). The percentage of the Edwards outcrop area feeding Barton Springs (212 km^2 or 82 mi^2) that was mapped to comprised open internal drainage basins, ponded internal drainage basins, and artificial (quarry) internal drainage basins is 8%, 2%, and 0.4%, respectively.

The bowl volume of 33 solution features was compared to its associated catchment area (Figure 3.5). The unfiltered plot of bowl volume versus catchment area has a no significant correlation, perhaps suggesting that the relationship may be affected by complex factors other than sinkhole maturity, such as the solubility of different rock types or anthropogenic modifications to the sinkholes.

The relation between bowl volume and catchment area appears to be influenced by variations between the hydrostratigraphic units. The largest bowl volumes and catchments are developed in the Kirschberg or Leached and Collapsed Members (Figure 3.5). The Grainstone Member, Regional Dense Member, and Basal Nodular Member are less soluble than other members of the Edwards Group, and, therefore, have subdued bowl development. There is considerable scatter in the relation between bowl volume and catchment for smaller sinks developed within the less soluble units. This may be explained that the same amount of runoff generated from a given catchment area develops a smaller bowl in less soluble rock types.

Some of the largest internal drainage basins, such as the catchment to Blowing Sink, may contain multiple large bowls. The bowl volumes and catchment area for complex internal drainages, where multiple solution sinks exist within a single internal drainage basin, can be combined to reflect the net surface dissolution of the basin.

Anthropogenic factors strongly influence sinkhole bowl volumes and catchments. Of 33 sinkholes examined for bowl volumes and catchment areas in this study, six were obviously filled, six had catchment areas dissected, and three were both filled and dissected. However, the 33 sinkholes were selected purposely as being relatively unimpacted internal drainage basins; hence the overall proportion of anthropogenically-affected sinkholes across the Barton Springs Segment is much higher. By filtering out the 15 obviously impacted sinkholes, the relation between bowl volume and catchment improves the relation between natural sinkhole bowl volumes and their catchment area to an R^2 of 0.52 (Figure 3.6).

By filtering out sinkholes developed within the less soluble RDM, Grainstone, and Basal Nodular Members and the anthropogenically filled and dissected caves, and summing those catchments with multiple large solution sinkholes, 15 upland internal drainage basins remain of the 33 sinkholes examined (Figure 3.7). The best fit is a linear relationship where the catchment area in square meters is 300 times the bowl volume in cubic meters. This relation has a high R^2 of 0.9. The relation between sinkhole bowl volume and catchment area in their natural form provides a useful tool for assessing sinkholes within the Edwards Aquifer. Large shifts below the general trend in bowl

volume to catchment area may suggest a feature that originally had a larger catchment area that was affected by anthropogenic drainage diversions (Figure 3.6).

On the J17 and Tabor research sites, the caves found followed the general morphological influence predicted based on underlying hydrostratigraphic units. Large solution bowl sinkhole basins, such as HQ Flat and Flint Ridge, were limited to exposures of the Kirschberg, Leached and Collapsed Members. Where the contact of the Grainstone and Kirschberg Members was exposed on the sites, a line of at least four large collapsed sinkholes caves are present within the HQ Flat catchment area (Figure 3.3). The Grainstone Member was acting as a competent roof while the immediately underling pulverulitic bed of the Kirschberg dissolved or was eroded within the paleophreatic zone. The three collapsed sinkholes within the HQ Flat Sink basin serve as visible examples of macropores where sheet flow from the hillside could enter the bedrock without passing through any soil cover.

3.3.2. Water Balance Results

The water balance for HQ Flat sink shows recharge and evapotranspiration percentages similar to those of other karst areas (Table 3.1). Over a 505-day period, 68% of the rainfall returned to the atmosphere as evapotranspiration. The remaining 32% of the rainfall falling on the HQ Flat basin recharged with 26% infiltrating through the soils into the underlying bedrock and about 6% flowing into the cave drain at the lowest point of the sinkhole as discrete recharge (Figure 3.8). The 160 cm of rainfall measured over the 1.4 year reference interval was 21% above the local annual average rainfall of 81 cm. Over a single 2002 rain event, during which the ground was near saturation prior to precipitation, the amount of discrete recharge to HQ Flat Cave was 42% of the rainfall.

Preliminary measurements from a 348-day water balance of ET of 58%, diffuse infiltration of 34%, and discrete recharge of 8% were reported for this research by Hauwert et al. (2005; Table 3.3). The difference in results can be attributed to the longer 505-day interval, over which rainfall declined from 30% above average to 21% above average. For the longer 505-day water balance the ET data was refined by correcting

directly measured ET by eddy covariance to match ET measured by energy balance, as recommended by Twine et al. (2000).

A test period was selected to compare the percentage of rainfall constituting discrete recharge in the other internal drainage sinkhole basin, Flint Ridge, which has a catchment area that is 150% that of HQ Flat. A 1,140-day interval from July 15, 2003 to August 29, 2006, was used because this was the longest interval commencing after both sinkhole flow stations were operating where rainfall averaged typical precipitation amounts of 81 cm (32 inches) per year. Over the 1,140-day interval, discrete recharge at HQ Flat measured 3.4% of rainfall while 2.6% of rainfall entered Flint Ridge Cave, which are essentially identical values.

No measureable change in soil-moisture storage occurred over the 505-day water balance interval. The volumetric soil moisture was 20% $\pm$ 2% at the start and end of the selected water balance. In addition, the potential error of change in soil moisture storage can be examined using a theoretical example of the 505-day water balance where the starting and ending soil moisture was very different. The potential error to the water balance can be calculated for a 505-day interval for a hypothetical case where large change in soil moisture storage had occurred and assuming an average soil depth and porosity. Typical soil thickness depths within the HQ Flat basin were 60 cm or less on the northern half of the catchment basin, and about 12 to 30 cm or less on the southern portion (Figure 3.9). Over the water-balance interval, the maximum change in soil moisture storage of a hypothetical homogeneous soil from a very wet period to a dry period (or vice versa) is 20% of the soil volume, excluding the uppermost 2 cm depth which varied by 50% of the soil moisture volume. Assuming an average 30-cm soil depth, during the 505 day water balance interval, the change in soil moisture storage would theoretically be 11,170 m^3 of 55,850 m^3 total soil volume, or 3.8% of the 297,850 m^3 of rainfall over the HQ Flat catchment basin. The maximum possible error in a theoretical water balance where large changes in soil moisture storage had occurred declines to 2.3% of the 485,600 m^3 of rainfall over the 1,140 day (three year) water balance interval. This theoretical example shows that the potential error of changes in soil moisture storage becomes less significant as the water balance interval increases.

However, the combination of selecting an interval with identical starting and ending soil moisture and a sufficiently long water balance interval lowers the possible effects of changes in soil moisture storage to be within the ±2% potential maximum soil moisture measurement error or 0.4% of the 505-day water balance and 0.2% of the 1,140-day water balance.

TxDOT dug soil trenches along a north-to-south transect during the week of October 2, 2006, which was at least 2 weeks after a September 18, 2006, rain. Soil samples also were analyzed from a canopy and open site near the ET tower. The trenches revealed some variation in soil depth and soil moisture across the sinkhole catchment that reflects heterogeneity. Most of the trenches excavated from October 2 to 4, 2006 had overall increasing soil moisture with depth, which suggests evapotranspiration processes are predominant in the soils compared to deeper infiltration on the day the trenches were excavated (Figure 3.10). A few of the trenches or holes showed decreasing gradients near the middle of the soil profile that may reflect water diversion by roots or macropore drainage. Much of the drainage to bedrock occurs shortly after precipitation events such that the proportion of soil moisture contribution to recharge diminishes as ET increases over a single soil moisture recession cycle. Shallow cave drips were continuously monitored in a separate study by Cowan et al. (2007), and were found to drain from the soil and shallow epikarst in Flint Ridge and Barker Ranch Caves on the Tabor research site, except during some drought conditions.

The movement of water through the soil can be examined by increases in soil moisture following a rain event. Figure 3.11 depicts the effects of two rain events (August 10 and September 11, 2005) on soil moisture at various depths. Gravimetric soil moistures in test pits at depths up to a maximum of 37 cm increased in less than 8 hours after the start of the rain event. The deepest sensors at 9 cm showed increasing soil moisture less than 30 minutes after the start of the rain. Soil moisture data from the September 2005 cycle show an upward soil moisture gradient down to a 30 cm depth where the gradient reverses to an overall downward gradient. The shallow sensor data indicates a downward soil moisture gradient that reverses 5 days after the rain event, although there are no associated shallow gravimetric soil moisture analysis from depths

of 3 cm to verify the sensor readings during this interval. From limited observation of the variation in soil moisture, it appears that, following a sufficient precipitation event, infiltration penetrates the entire soil column within a matter of hours. Within hours or days of a rain event, evaporation draws moisture from the soil to a depth that varies from as deep as 12 cm at some sites and times, but as deep as 30 to 47 cm at other sites and times. The ability of the soils to infiltrate rainwater rapidly was verified by a separate study on the Tabor tract, which observed that tracers poured on the surface penetrated the entire soil column into a 5-m deep cave within hours following natural rainfall events (Cowan et al., 2007).

3. 3.3. Estimation of Recharge From Chloride Concentrations

Chloride concentrations increase from rainfall and runoff to shallow cave drips (5-m deep Barker Ranch Cave) to deeper cave drips (47-m deep Flint Ridge Drip Pit), to spring samples (Table 3.4). A plot of chloride versus sulfate/chloride concentrations of various water sources over and within the Barton Springs Segment is presented in Figure 3.12. The arithmetic mean runoff value of chloride was 0.95 mg/l (n=22) after two outliers were removed. The Barker Ranch Cave drips were collected from a depth of 5 m and had arithmetic mean chloride concentrations of 2.46 mg/l (n=38).

The ratio of sulfate to chloride peaks in cave drips samples compared to ratios from rainfall (except Sonora ratios which were all the highest), runoff, deep cave drip, and spring ratios, which is interpreted here to reflect a change in processes that increase chloride concentration from evapotranspiration process to another process such as rock dissolution. Such a process shift could account for increases in chloride concentration within the vadose and phreatic zones beyond the expected depth of significant evapotranspiration. The ratio of chloride concentrations in the runoff to cave drips, rainfall to cave drips, and Attwater rainfall to Barker Ranch Cave drips were 0.49, 0.39, and 0.26, respectively (Table 3.4).

Although chloride concentrations in the Tabor site runoff were on the average 0.31 mg/l lower than concentrations in the two rainfall samples, sulfate concentrations in the runoff averaged about 1 mg/l lower than in the rainfall. The reasons for this could be

that the runoff undergoes significant interflow through the clay-rich soils, leading to some reduction in sulfate by partitioning. A second reason could be there is atmospheric variation in sulfate concentrations not characterized by two rainfall samples.

3.4. Discussion

It is not surprising that much recharge to the Barton Springs Segment would occur within the major creek channels. Stream flow generated within the relatively large, upstream contributing area flows over the Edwards outcrop area through the major creek channels. In addition, much of the intervening upland area of the Edwards outcrop area generates flow to the major creek channels. However, because the 1980s water budget was based on limited data, recharge from the upland areas was underestimated. Smart and Hobbs (1986) suggested that in karst areas it is possible to quantify recharge from major creeks through flow loss measurements, but that an aquifer-wide water balance required measurements of upland recharge. Critical data missing from the original water budget were tracing of groundwater divides, measurement of upland recharge on the Edwards outcrop area, changes in storage over the water balance interval, lack of complete flow-loss data from the major creeks, and discharge to Cold Springs.

Flow loss measurements on Barton Creek from 1979 to 1981 between Loop 360 and Lost Creek were used to estimate its contribution to Barton Springs (Slade et al., 1986). Additional recharge occurs in Barton Creek downstream of Loop 360, although this recharge was considered insignificant. Since 1996, groundwater tracing during high- and low-flow conditions show that recharge from Barton Creek upstream of Loop 360 and downstream of Lost Creek flows to Cold Springs and not Barton Springs (Hauwert et al., 1998; Hauwert et al., 2004a). If the 1978 to 1981 water balance volumes were modified to assume that only 10% to 50% of the flow from Barton Creek originally attributed actually discharges from Barton Springs, then the water budget requires an additional 27% to 36% of recharge above the measured major creek-bottom flow loss (Table 3.2). The 10 to 50% range of the original 24% recharge contribution assumed from Barton Creek to Barton Springs is an upper and lower range of my best estimate. Assuming that the 1980s water balance is representative, this 27% to 36% of Barton

Springs discharge then could potentially be from upland recharge, instead of the 15% originally estimated. This study does not suggest that this reinterpretation creates an adequate water balance for the Barton Springs Segment, but rather, suggests that upland recharge is higher. In order to refine this aquifer-wide water budget, a new water budget is required over a longer interval where minimal change in storage occurs, that incorporates correct groundwater basins and includes flow loss from all major creeks and sample upland areas. Such a water budget should be verified and include recharge sources delineated by geochemical methods.

In Slade et al. (1986), the amount of rainfall that was assumed to recharge over the intervening areas between the main channels of some major creeks over the Edwards outcrop area (0.9%) was significantly smaller than values measured in other karst areas over the world or over the adjacent Trinity Aquifer (see Table 3.1). The Edwards Aquifer has relatively well-developed karst compared to the Trinity (Elliott and Veni, 1994) and 250 times greater average yield (Mace et al., 2000b). Consequently, the Edwards Aquifer must have a more efficient recharge structure and higher recharge to rainfall ratio than less karstic limestones, sandstones, and shales. In fact the 0.9% of rainfall allocated to recharge of the intervening areas by Woodruff (1984a) was less than the 1.0% of recharge from rainfall estimated for the Eagle Ford Shale outcrop, based on a one-year water balance in Bell County (Harrison, 1996). The assumption that the recharge of the intervening Edwards outcrop area is 0.9% (Woodruff, 1984a) is contrary to observations by early investigators (Hill and Vaughan, 1898; DeCook, 1957; Appendix A) that the Edwards Aquifer has a well developed recharge structure. The underestimation of upland recharge may have significantly affected the results of the 1980s water balance study for the Barton Springs Segment. The relatively small proportion of total recharge attributed to upland areas by Woodruff (1984a) has been used as the rationale for lower levels of protection for upland recharge features (TxDOT, 1989; URM, 1983; Woodruff, 2001). Thus, it is important to understand the role of upland recharge in the water budget of the Barton Springs Segment.

Internal drainage sinkholes are some of the most mature surface karst features on the Edwards outcrop area of the Barton Springs Segment. They show relatively high

efficiency for transferring a given rainfall volume per catchment area into recharge. This efficiency (32%) is much higher than larger-scaled studies of the Barton Springs Segment have previously recognized (0.87%, Senger, 1983; Woodruff, 1984; Slade et al., 1986). Most recharge (28% of rainfall) occurred on the sinkhole slopes that are similar in many aspects to other slopes across the Edwards outcrop area. Over average rain conditions, 3% of rainfall enters the cave drain of internal drainage basins that distinguishes internal drainage basins from other upland areas. In this regard, the results of the current study might be more representative of upland recharge within the Barton Springs Segment, particularly until more recharge data from across the Edwards outcrop area becomes available. The reasons that internal drainage sinkholes and upland areas in general are relatively efficient compared to creek-bottom recharge may be a combination of a number of factors:

1) In well-developed bowls of mature sinkholes within internal drainage basins, nearly all of the runoff generated within the catchment area can be stored if not immediately transmitted through the sinkhole. On the J17 HQ Flat Research site this runoff constitutes 3% of rainfall under average rainfall conditions, though during individual events when the soils are previously saturated half of the rainfall may become runoff within a sinkhole basin. Very little, if any, surface runoff contributes to downstream creeks inside internal drainage basins. In contrast, many creek-bottom swallets experience flows that exceed their recharge capacity. In addition, the proximity of the water table to creek-bottom swallets increases the potential that some recharge will be rejected. Upland internal drainage sinkholes can play an important role in capturing runoff during large rainfall events or following rainfall events when the major creeks are already flowing.
2) Through surface piracy, as well as bowl and drain enlargement through dissolution, mature sinkholes transmit surface water relatively rapidly below the surface to a depth where the water is not subject to significant evaporation and transpiration.

3) The majority of upland recharge occurs during and shortly after rain events when humidity is relatively high and evapotranspiration is relatively low (see Figure 3.13).
4) Most upland recharge directly infiltrates through the soils despite the presence of clay-rich layers. The soil, epikarst, and vadose zone serve to store water, and this storage is a particularly important source during dry periods when the major creeks are dry.

Based on the two basins monitored, the volume of discrete recharge through the primary sinkhole drain(s) varies directly with the catchment area over the Edwards Aquifer. Over the same reference period, large internal drainage basins show a similar or identical ratio of discrete recharge to rainfall. Based on the findings of this study, the following methods (in addition to methods described in Section 3.21) can be used to determine if the estimated catchment area is reasonable:

1) The simplest check is to measure the bowl volume and examine what catchment area is expected from the relation presented in Figure 3.7.
2) Measure the water flow into a cave and corresponding rainfall after the soil is sufficiently saturated from previous rains. Does the flow to the cave exceed the aerial catchment of immediately preceding rainfall?
3) In addition to the presence of a well-define solutional bowl, the presence of well defined channels and flood debris should provide an intuitive sense of the catchment area.

Flow data from this study indicate that the discrete recharge component increases during periods of higher rainfall when the soils and macropores are already saturated, analogous to Hortonian runoff in a watershed. The total recharge occurring in internal drainage basins may or may not vary greatly under average conditions, although a longer period of measurement is required to examine shifts in recharge patterns because of varying rainfall patterns. It is also important to recognize that the pattern of rainfall and recharge in Central Texas is not evenly distributed, and properly functioning upland internal drainage basins play an important role in capturing flows from storms that

otherwise would run off or evaporate, thereby maximizing recharge to the aquifer. Under dry soil conditions in both HQ Flat and Flint Ridge sinkhole basins, rain events of about 5 cm and more did not produce runoff to the cave drains monitored. During dry periods it is the upland soils that infiltrate precipitation, such that even under relatively high precipitation events any runoff generated often does not reach the major creeks. In essence there is variability of Texas climate that directly influences where recharge occurs.

The water balance revealed that 32% of the rainfall on the HQ Flat basin recharged the aquifer (Figure 3.8). The measured recharge from runoff falls well within the ranges seen in karst areas worldwide (Table 3.1). Of the total recharge, only 17% entered HQ Flat Cave as discrete recharge. The remaining 83% of the recharge is "diffuse" infiltration through the soils and macropores. The degree of soil infiltration that is actually diffuse versus macropore infiltration requires deeper investigation. The finding that most recharge infiltrates through karst soils rather than though sinkhole drain on upland karst plains is consistent with similar results found by Gunn (1983) in New Zealand. Recharge measured at other sites across the Edwards outcrop area may vary from recharge measured here, although these results are the most direct measurement of upland recharge to date for the Barton Springs Segment. Based on the recharge values of 32% recharge from rainfall derived from HQ Flat sinkhole, a gross estimate of 3.3% of the 176,000,000 m^3 of cumulative discharge from Barton Springs over the 1,140 day average rainfall interval originated as recharge from known internal drainage sinkholes that constitute 10% of the Edwards outcrop area contributing to Barton Springs. Assuming gross upland Edwards outcrop areas outside of internal drainage basins have 28% recharge from rainfall, then upland Edwards outcrop areas contributed 29% of Barton Springs flow.

Chloride concentrations increase from rainwater, to runoff, to cave drips, to phreatic groundwater through evapotranspiration, residence time/rock-water interaction, and aquifer mixing. Minimal evaporation of surface runoff is expected during and shortly after sufficient rain events because the air is water saturated. Significant ET is improbable

below the epikarst zone so comparison of rainfall and runoff to cave drips is the most suitable comparison to eliminate most rock/water interaction and aquifer mixing influences. Chloride and sulfate concentrations increase with decreasing flow at Barton Springs because of increasing contribution from the Saline-Water Zone (Hauwert et al., 2004b). Because aquifer mixing results in elevated concentrations of chloride and sulfate in at least three of the springs, spring geochemistry is not included in the discussion of chloride concentrations as an approach for calculating recharge

By sampling chloride in rainfall, runoff, and cave drips and comparing chloride calculations of evapotranspiration to eddy-covariance derived evapotranspiration, this study overcomes many potential limitations of the chloride method in the Barton Springs Segment. Only two rainfall samples were collected to characterize local rainfall quality although the standard deviation of the two samples was 0.01 for chloride concentrations. Austin rainfall chloride concentrations were 0.31 mg/l higher than the arithmetic mean of 22 Tabor site runoff samples. Local rainfall quality is expected to decrease from the Gulf of Mexico inland toward west Texas as coastal marine salinity is depleted (Bennett, 2009, personal communication; NADP, 2009). The chloride concentrations in two Austin rainfall samples (arithmetic mean = 1.21 mg/l) were higher than Attwater (arithmetic mean = 0.64 mg/l) and Sonora (arithmetic mean = 0.21 mg/l), and it is unknown why local chloride concentrations do not lie within this range. Consequently, measurement of chloride in rainfall likely is the largest potential error for calculating recharge using the chloride balance method in this study. A range from 26 to 49% recharge from rainfall, take into account the range of chloride concentrations from Attwater, Tabor runoff, and two local rainfall samples is calculated for the Tabor site. The range of Sonora rainfall chloride concentrations was exclusive of the range of any locally measured rainfall or runoff concentrations (n=24) so Sonora chloride concentrations are not representative of local rainfall chloride concentrations and were not used for recharge calculation (Figure 3.13).

A comparison of chloride in Austin-area rainfall, Tabor tract runoff to Flint Ridge Cave, and cave drips on internal drainage areas of the Tabor research site suggests that 51 to 74% of rainfall becomes ET while the remaining 26% to 49% of rainfall

becomes recharge. With an understanding of the limits in the chloride mass balance, the test serves as a separate measurement of recharge to supplement the water-balance method. The estimate of 32% recharge from water balance in the J17 HQ Flat sinkhole basin is encompassed between the 26% to 49% recharge estimated from chloride in Tabor cave drips. Variation in recharge across the Barton Springs Segment from site to site is expected.

3.5 CONCLUSIONS

Large catchment internal drainage basins characteristically have concave upward, solution-formed bowls with a bowl volume proportional to the size of the catchment area, its recharge significance, and karst maturity. The bowl volume provides quantitative measurement of surface solution processes associated with a karst feature and, therefore, is an excellent indicator of its recharge significance. Within the Barton Springs Segment the catchment area of a natural, internal drainage solution sinkhole is 300 times its bowl volume, with an R^2 of 0.9. Sinkhole bowl volumes are suppressed relative to their catchment areas where:

(1) their development is in less soluble hydrostratigraphic units, such as the RDM, Grainstone, and Basal Nodular Members;

(2) the sinkhole is filled;

(3) the sinkhole type is not an internal drainage basin, but another type such as a creek swallet; or

(4) multiple solution sinkholes are present within a catchment area.

Internal drainage sinkhole catchment areas are suppressed relative to their bowl volume if:

(1) the catchment area has been anthropogenically dissected;

(2) the sinkhole has been artificially excavated, such as an artificial internal drainage basin; or

(3) the sinkhole was largely shaped by collapse rather than dissolution.

Quantification of bowl volumes in karst assessments can help identify significant features by quantifying the catchment area for internal drainage basins. In nearly all cases, a large bowl volume defines the presence of an internal or at least partial internal drainage basin. In cases where sinkholes discovered in topographically high areas with little catchment nevertheless appear to have large bowl volumes, a closer inspection may reveal these are actually *collapsed* sinkholes and that the apparent bowl volume is actually a collapsed cave passage.

Collapsed sinkholes are characterized by convex upward cross section and relatively small catchment areas. Nevertheless, collapsed sinkholes are equally likely as solution sinkholes to have a strong hydraulic connection with the aquifer. A number of collapsed sinkholes (such as Midnight Cave, Salamander Mountain Cave, and Tabor Bat Cave) are observed as convergent points for shallow epikarst flow that exceeds direct flow to their entrance, and this epikarst flow uses the cave to descend towards the water table. Their recharge significance increases from natural and anthropogenic diversion of surface water into the collapsed sinkholes. Also, collapsed sinkholes may provide stable habitat sites for cave species, in part because they are less prone to flooding.

Open internal drainage basins, ponded internal drainage basins, and manmade depressions that intercept surface drainages make up at least 8%, 2%, and 0.4% respectively of the Edwards outcrop area of the Barton Springs Segment. These areas rarely, if ever, contribute to local downstream drainages. The results of a 1.4 year water balance of two large open internal drainage basins under higher than average rainfall conditions indicated that about 68% of the rainfall evaporates, about 6% enters the cave as discrete recharge, and about 26% diffusely recharges the aquifer through the soil or other lesser recharge features. For short periods under wet conditions, over 40% of the precipitation from a single rain event can enter HQ Flat Cave as discrete recharge. The portion of discrete recharge from rainfall increases over intervals of higher rainfall as the soils are relatively saturated and high humidity reduces the relative evaporative losses. The proportion of discrete recharge into the cave draining the base of large internal drainage sinkhole basins is 10% of rainfall when rainfall is 30% above average and 5% of rainfall when rainfall intervals are 20% above normal. Under average rainfall conditions

the discrete portion of recharge declines to 3% of rainfall. An estimated 32% of its rainfall recharged the HQ Flat sinkhole basin over the 505 day test interval, and preliminary results suggest that internal drainage basins are relatively efficient recharge areas.

Variation in upland recharge can be expected across the Edwards outcrop area. A better understanding of upland recharge requires aquifer-wide examination of upland recharge and additional site scale measurements over a longer time and in different locations. A chloride concentration comparison between Austin rainfall, runoff on the Tabor site, and cave drips on the Tabor site suggests that about a quarter to half of the rainfall recharges over that tract. The 51% to 74% range of evapotranspiration from rainfall measured with chloride concentrations on Tabor site compares with the 68% of rainfall measured for evapotranspiration at the HQ Flat site flux tower are both much lower than the 85% previously estimated for the Barton Springs Segment. The scale of the examination was insufficient to characterize the degree of heterogeneity of the infiltration through upland soils.

The measurements collected in this study are the first estimates of total recharge at a site scale within the Barton Springs Segment and indicate that most upland recharge occurs on the slopes rather than at discrete identifiable caves. From the water balance, the diffuse infiltration measured on slopes of internal drainage basins, or 28% of rainfall, maybe most representative for overall upland recharge outside of internal drainage basins. Outside of internal drainage basins, the 3% of rainfall measured as discrete recharge at a site scale may represent a measure of runoff entering the major creeks at larger scales.

When comparing recharge measurements from karst areas across the world, 20% to 60% of rainfall would be expected to recharge karst aquifers that varies with karst maturity, allogenic recharge from upstream areas, evapotranspiration, and other factors. The karst maturity of the Barton Springs Segment is higher than the Trinity Aquifer and should exceed the estimated 7% of Trinity Aquifer recharge from rainfall. Furthermore, the 1980s water balance overestimated creek recharge for the aquifer-wide water balance (Slade et al., 1986) because the source area had not yet been defined with tracing

(Hauwert et al., 1997). A correction to the original water balance results for less recharge from Barton Creek leaves 32 to 36% of total recharge to Barton Springs unaccounted for by the recharge from the six major creek channels and could come from upland recharge. Based on recharge measurements in HQ Flat sinkhole and extrapolating the results across the Edwards outcrop area, 29% of Barton Springs flow originates from upland area recharge. Hence, the recharge of specific internal drainage basins as well as the intervening upland areas is greater than previously reported.

Table 3.1. Recharge estimates from various karst aquifers.

% Recharge/ Direct Precip.	% Upland Recharge/ % Major Creek Recharge	Location	Aquifer, Basin, or Region	Source
28-32%		**Barton Springs Seg.**	**Edwards**	presented here
0.89%*	**15% / 85%**	**Barton Springs Seg.**	**Edwards**	Slade et al 1984, Woodruff, 1984
>10%		San Antonio Seg.	Edwards	Huang and Wilcox, 2005
	56% / 44%	Bexar Cty TX	Edwards	Ockerman, 2002
1.5%		Central TX	Trinity	Muller and Price, 1979
4%		Central TX	Trinity	Ashworth, 1983
11%		Central TX	Trinity	Kuniansky, 1989
6.7%		Central TX	Trinity	Bluntzer, 1992
7%		Central TX	Trinity	Mace et al., 2000
30%		Uvalde Cty TX	Trinity	Dugas, 1998
54%	100%/0%	Mendip Hills, England	Carboniferous Limestone	Atkinson, 1977
33%		Crimea, Ukraine		Dublyanskii et al., 1984
15-20%		Barbados	Uplands	Jones et al., 2000
25-30%		Barbados	Below 2nd Cliff	Jones et al., 2000
60%		Guam		Mink and Vacher, 1997
67%		Guam		Jockson et al., 2002
14-19.5%		Morocco	Plio-Plest.	Bolelli, 1951
23-42%		Tunisia		Tixeront et al., 1951
36-91%		Tunisia	Eocene Ls	Schoeller, 1955
10-45%		Israel	W. Galilee	Goldschmidt, 1960
53%		Israel	Na'aman Spr	Mere, 1958
41%		Syria	Damascus	Burdon, 1960
45%		Syria	Ghab	Voute, 1961
52%		Greece	Lilaia	Aronis et al, 1961
51%		Greece	Parnassos-Ghiona	Burdon and Papakis, 1961
12-124%		Hungary	Tettye	Kessler, 1957

*upland direct recharge only, total recharge estm. to be 5.95% which includes recharge of Contributing Zone flows

Table 3.2. Estimated recharge contributions from previous water balances.

Source	Percent Total Creek Recharge		Percent Total Aquifer Recharge		Max. Recharge Rate		Percent Total Aquifer Recharge	
	A* (%)	B* (%)	A* (%)	B* (%)	A* (m^3/s)	B* (m^3/s)	C*low (%)	C*high (%)
Barton	28	31	24	26	0.85-2.0	7.1	2	12
Williamson	6	3	5	3	0.4	0.4	5	5
Slaughter	12	6	10	5	1.5	1.5	10	10
Bear	10	7	9	6	0.9	0.9	9	9
Little Bear	10	7	9	6	0.8	0.9	9	9
Onion	34	46	29	39	3.4	3.4	29	29
Intervening Areas			15	15			**36**	**27**

A* - source Slade et. al., 1986

B* - source Barrett et. al., 1996

C* - Slade et al. (1986) results readjusted based on Barton Creek tracing results and the assumption that 10% to 50% of the original 24% Barton Creek contribution discharges from Barton Springs.

Table 3.3.Results of internal drainage basin water balance

Component	Interval Start	End	Interval Duration (days)	Amount/ Unit Area (cm)	(% of rainfall)	Water Volume (m^3)	Potential Error (% of total)	rainfall/avg (%)
HQ Flat Microbasin	**4/2/2004**	**8/20/2005**	**505**					121%
Rainfall				160	100.0%	297,850	5%	
Evapotranspiration				109	68.1%	202,910	3.4%	
Soil Moisture Storage				0	0.0%	0	0.4%	
Discrete Recharge				8.8	5.5%	16,300	+0.1 to -0.8%	
Diffuse Recharge				42	26.4%	78,640	(±11%)	
Total Recharge				51	31.9%	94,940	5%	
Flint Ridge Microbasin	**4/2/2004**	**8/20/2005**	**505**					
Rainfall				165	100.0%	237,587	5%	
Discrete Recharge				6.7	4.0%	18,600	+0.1 to -0.6%	
HQ Flat Microbasin	**7/16/2003**	**8/29/2006**	**1,140**					100%
Rainfall				261	100.0%	485,603	5%	
HQ Flat Discrete Recharge				8.8	3.4%	16,322	+0.1 to -0.5%	
Flint Ridge Microbasin	**7/16/2003**	**8/29/2006**	**1,140**					
Flint Ridge Discrete Recharge				6.8	2.6%	18,890	+0.1 to -0.4%	
Barton Springs Discharge	**7/16/2003**	**8/29/2006**	**1,140**			176,505,749	5%	
HQ Flat Microbasin	**7/1/2002**	**5/26/2003**	**329**					150%
Rainfall				70	100.0%		5%	
HQ Flat Discrete Recharge				7.2	10.3%	13402	+0.2 to -1.5%	

HQ Flat Catchment Area	186,156	m^2
Flint Ridge Catchment Area	279,200	m^2

Table 3.4. Water-quality summary for recharge calculation.

Water Type	Number of Samples	Arithmetic Mean			Standard Deviation			Ratio $Cl_{rain}/Cl_{cave\ drip}$		
		Cl	SO_4	SO_4/Cl	Cl	SO_4	SO_4/Cl	Based on Austin Rain Cl	Based on Runoff Cl	Based on Attwater Cl
Rainfall (Austin Area)	2	1.21	2.09	1.72	0.01	0.02	0.04			
Rainfall (Sonora)	22	0.21	1.04	5.08	0.05	0.18	1.12			
Rainfall (Attwater)	24	0.64	1.03	1.68	0.17	0.19	0.37			
Runoff (Tabor Tract)	22	0.95	1.06	1.23	0.33	0.29	0.42			
Barker Ranch Cave Drip (5 m)	38	**2.46**	5.12	2.12	0.54	0.70	0.19	**49%**	**39%**	**26%**
Flint Ridge Drip Pit (47 m)	3	6.34	18.60	0.34	0.38	0.98	0.01	19%	15%	10%
Upper Barton Springs	90	16.08	23.82	1.50	5.05	7.46	0.29	8%	6%	4%
Main Barton Springs	294	27.57	30.56	1.15	1.50	5.52	0.22	4%	3%	2%
Eliza Springs	101	28.06	31.8	1.18	12.8	12.5	0.19	4%	3%	2%
Old Mill Springs	146	50.0	47	0.95	13.6	8.9	0.13	2%	2%	1%

* Note two runoff outlier values were excluded.

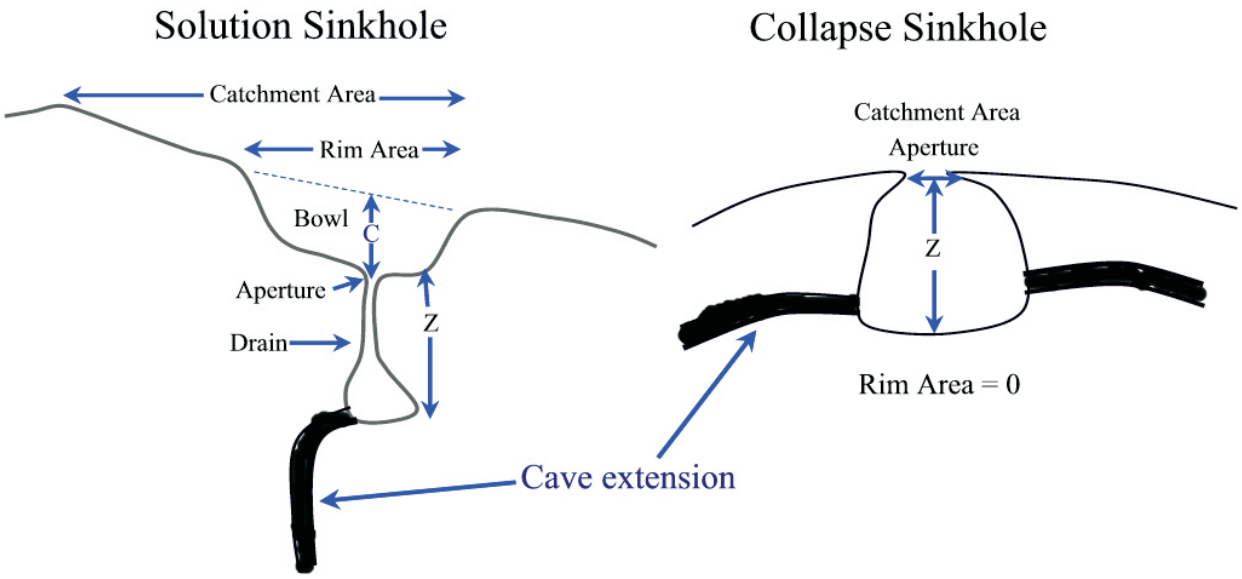

Figure 3.1. Sinkhole dimensions. Morphological characteristics were used to distinguish solution and collapse sinkholes. The rim area and C dimension were used to calculate the bowl (see glossary). Modified from Hauwert et al., 2005.

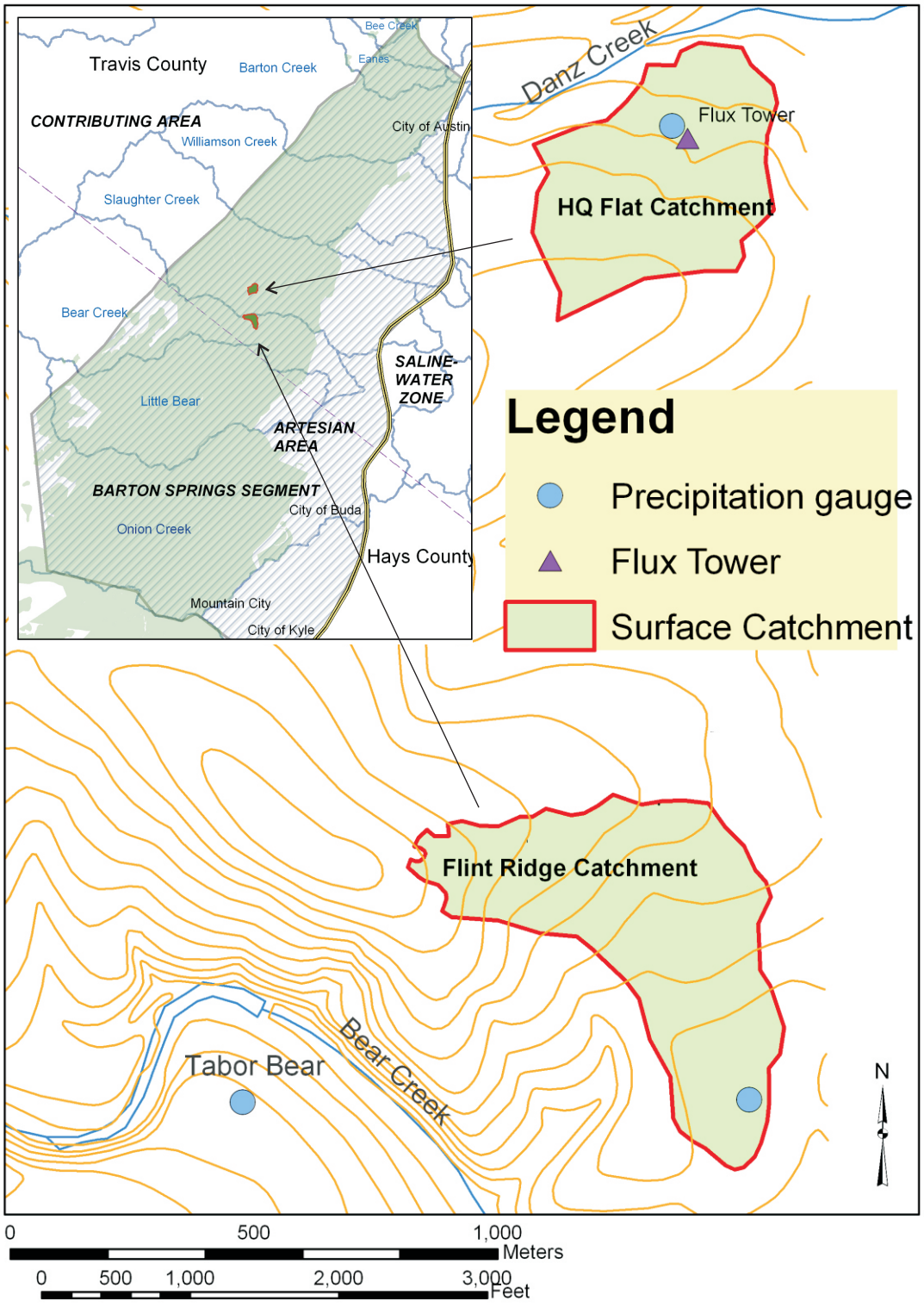

Figure 3.2. Research sites. The HQ Flat catchment is located on the J17 site. The Flint Ridge catchment is located on the Tabor site. Both sites are located near the center of the Barton Springs Segment.

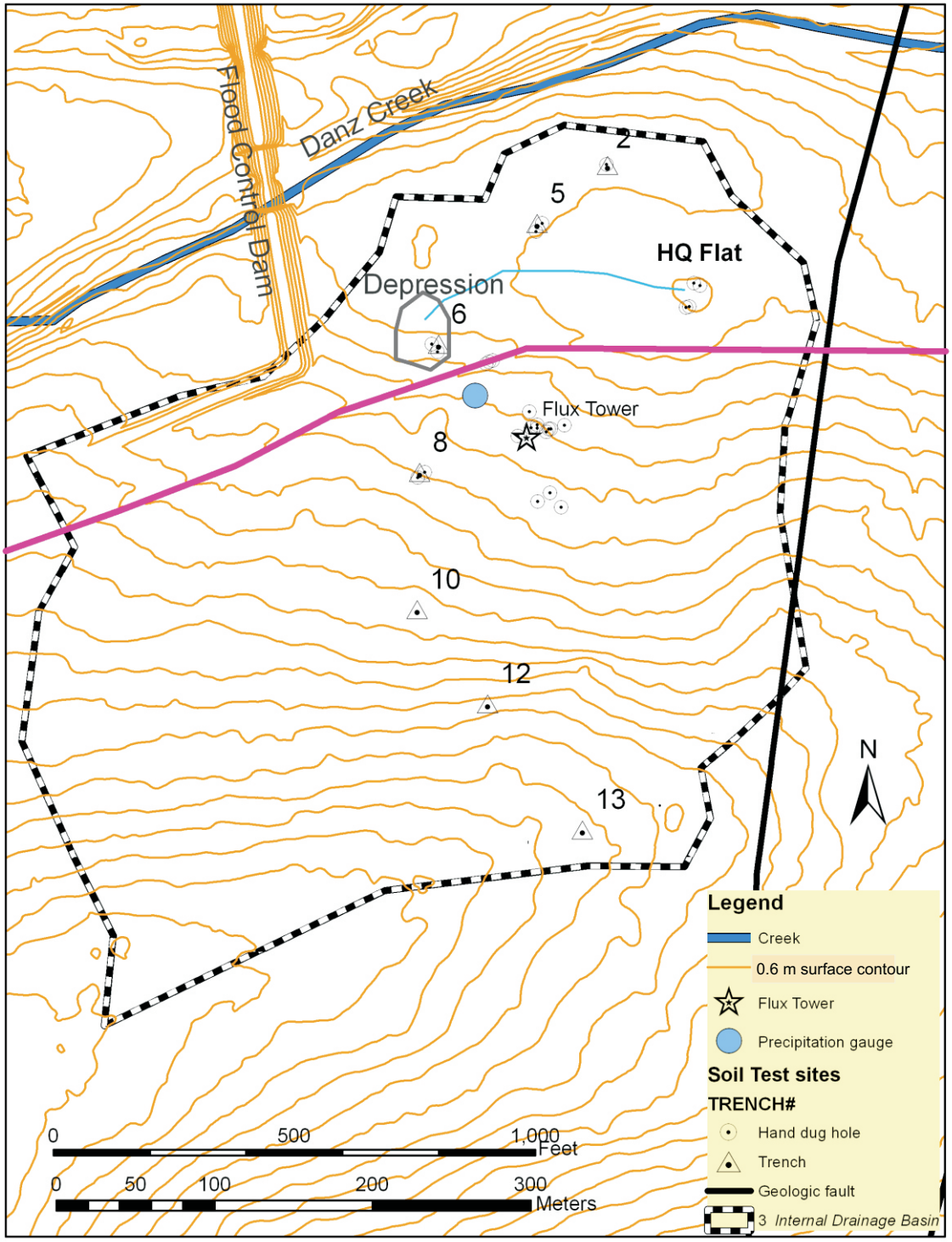

Figure 3.3. HQ Flat catchment. A paved private road crosses the north side of the catchment. A depressed area on the north side of the catchment must fill with runoff before additional runoff is diverted along a channel to HQ Flat Cave.

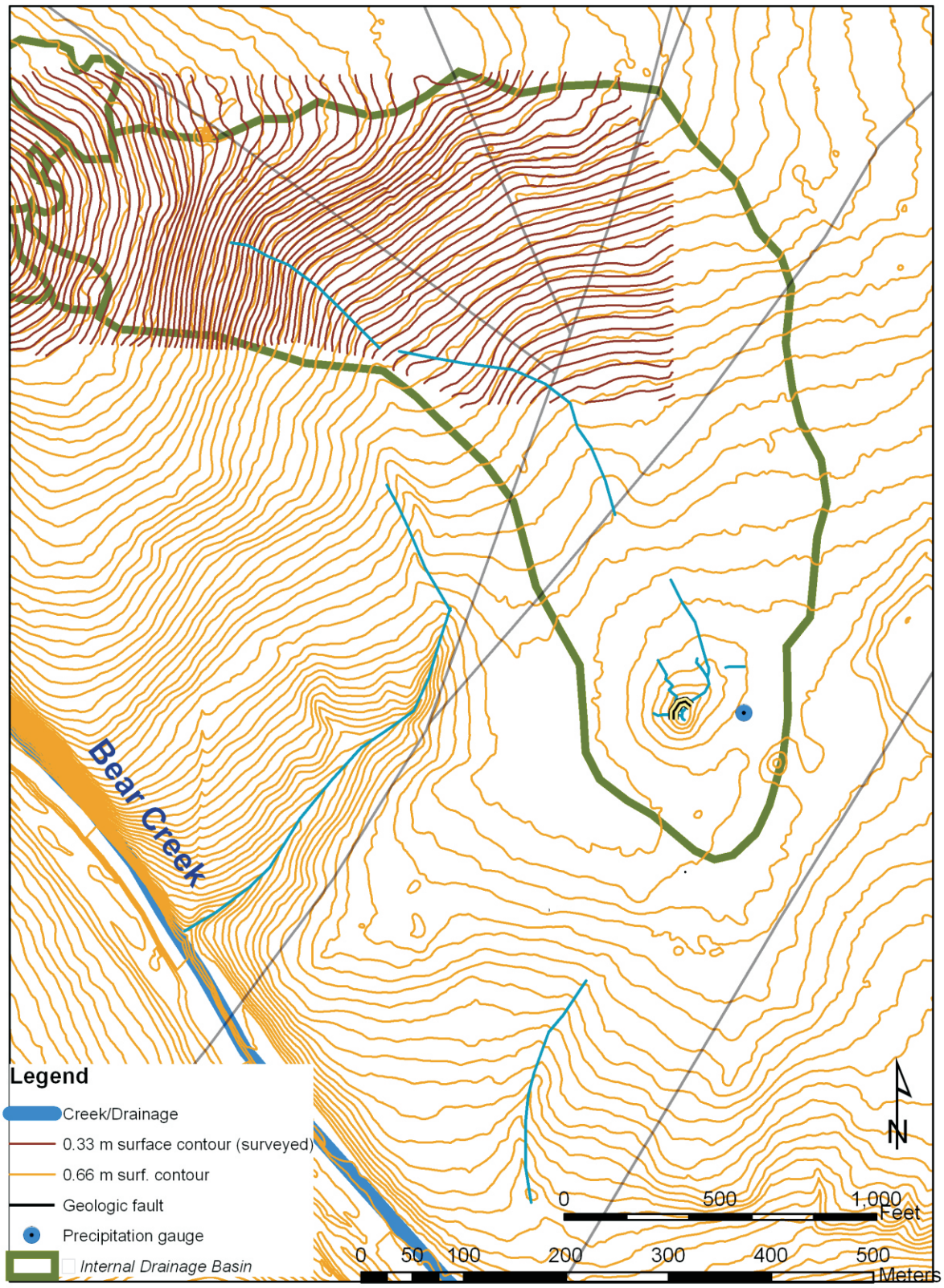

Figure 3.4. Flint Ridge catchment.

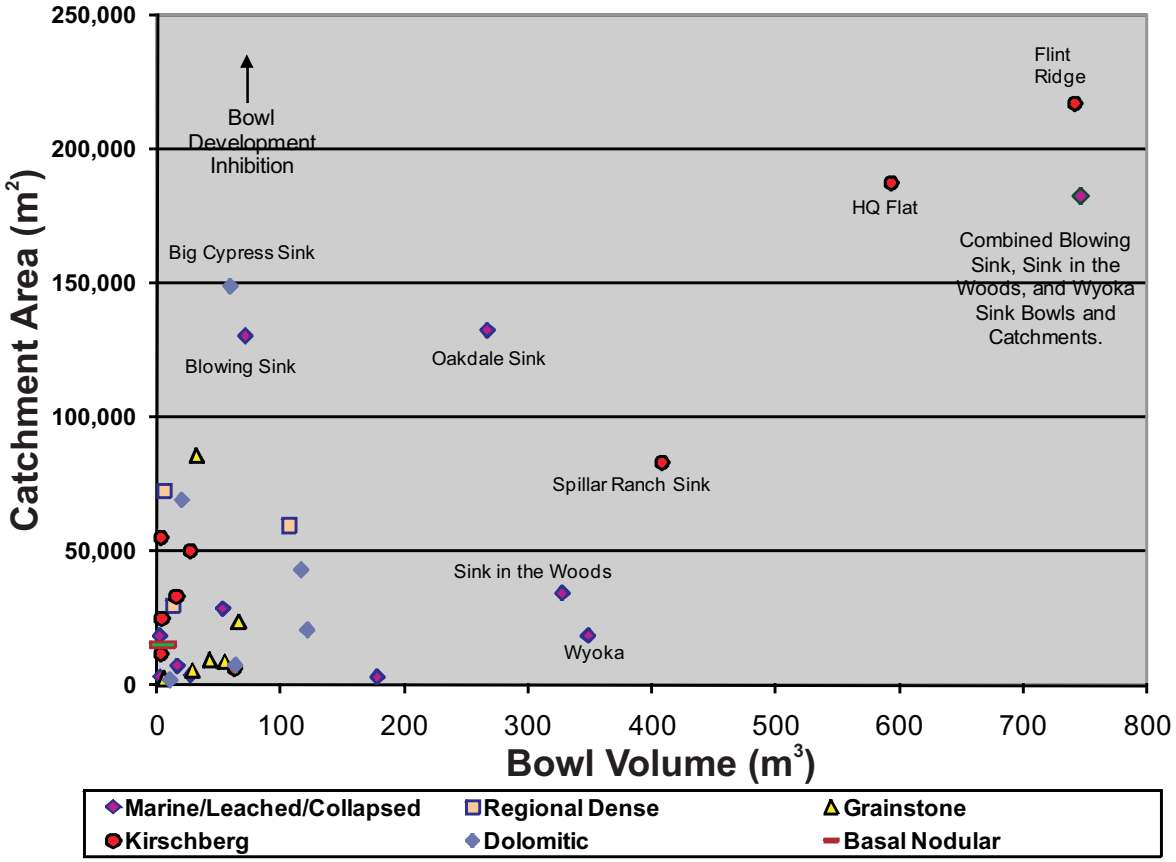

Figure 3.5. Sinkhole bowl volumes and surface hydrostratigraphic unit.

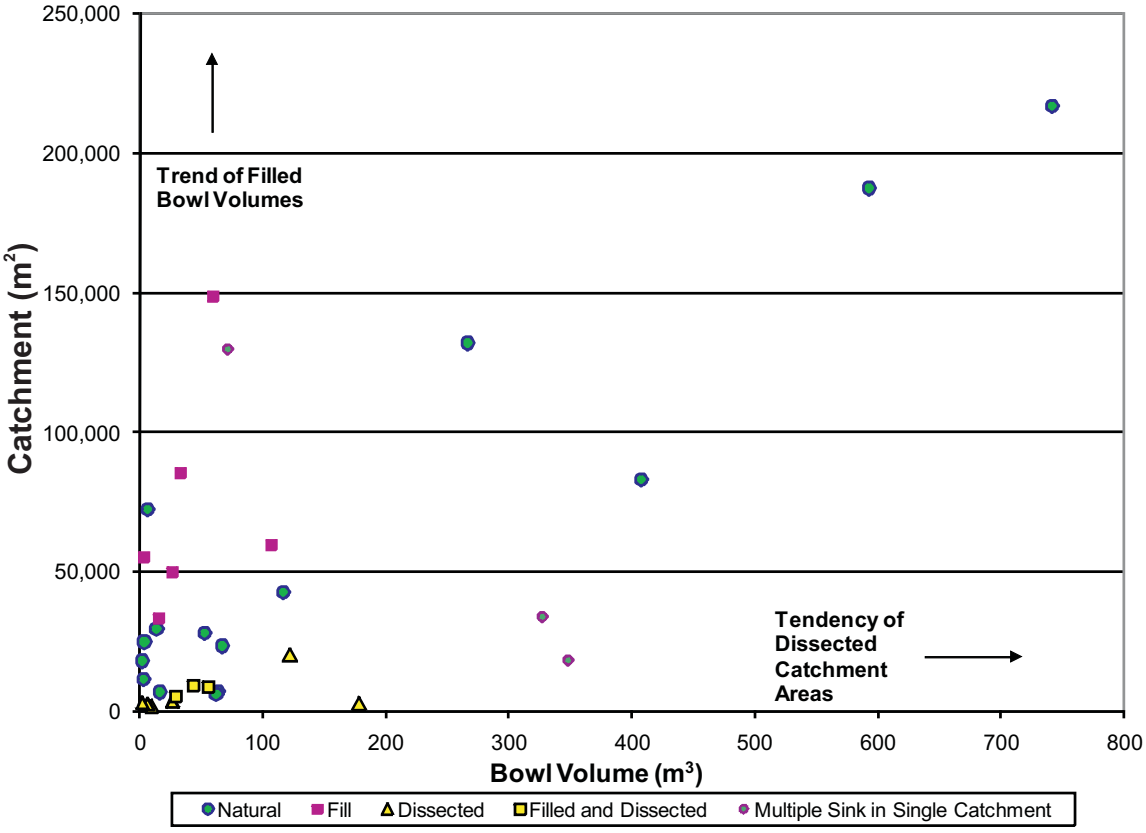

Figure 3.6. Anthropogenic influences on sinkholes.

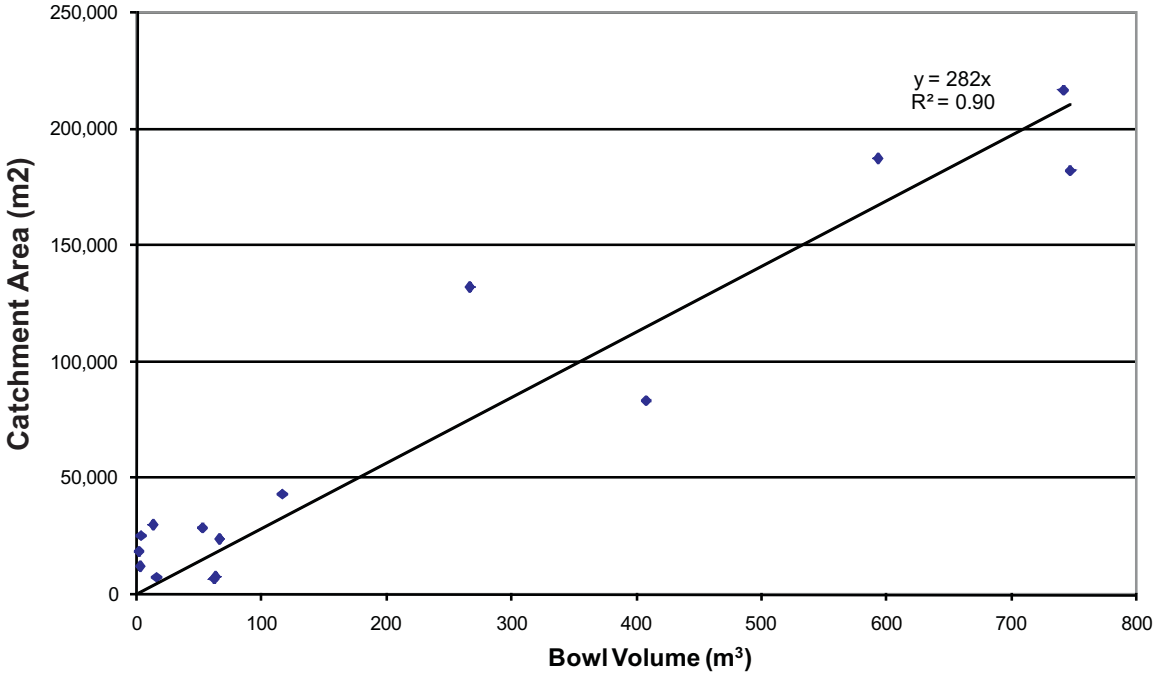

Figure 3.7. Sinkhole bowl volume and catchment (filtered).

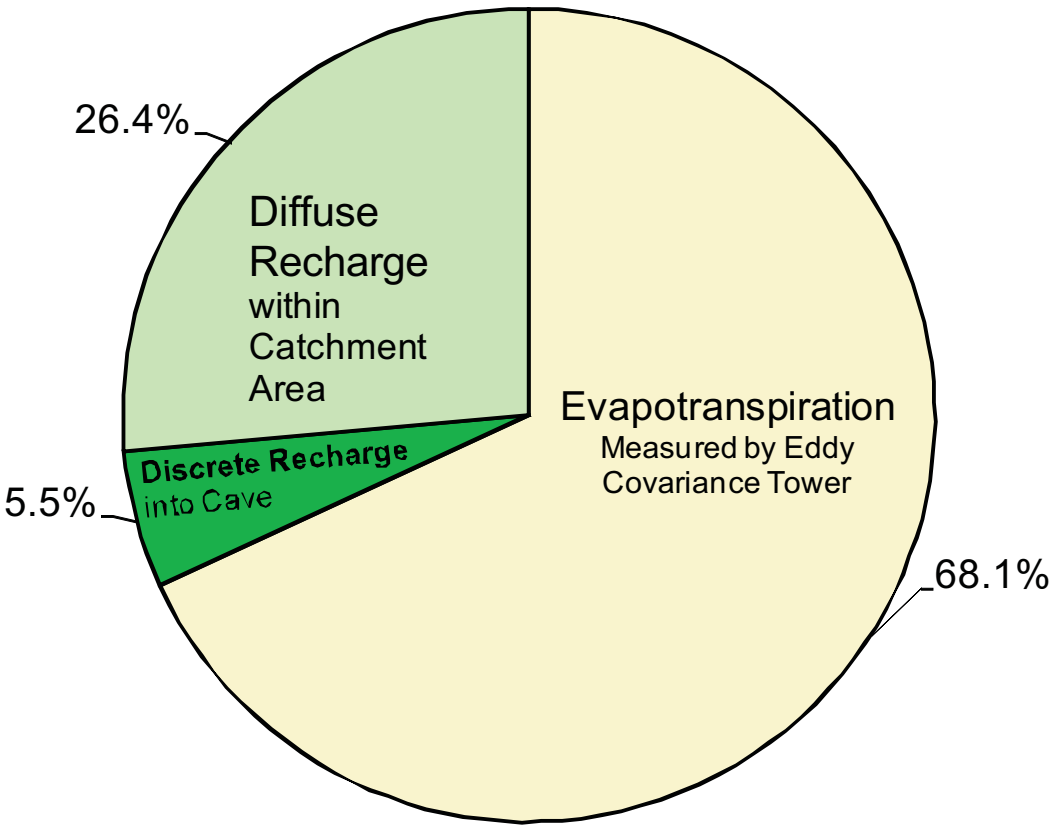

Figure 3.8. Water balance summary for HQ Flat basin: 505-day interval. This interval from April 2, 2004 to August 20, 2005 had 21% higher than average precipitation. The starting and ending soil moistures measured 20%±2%.

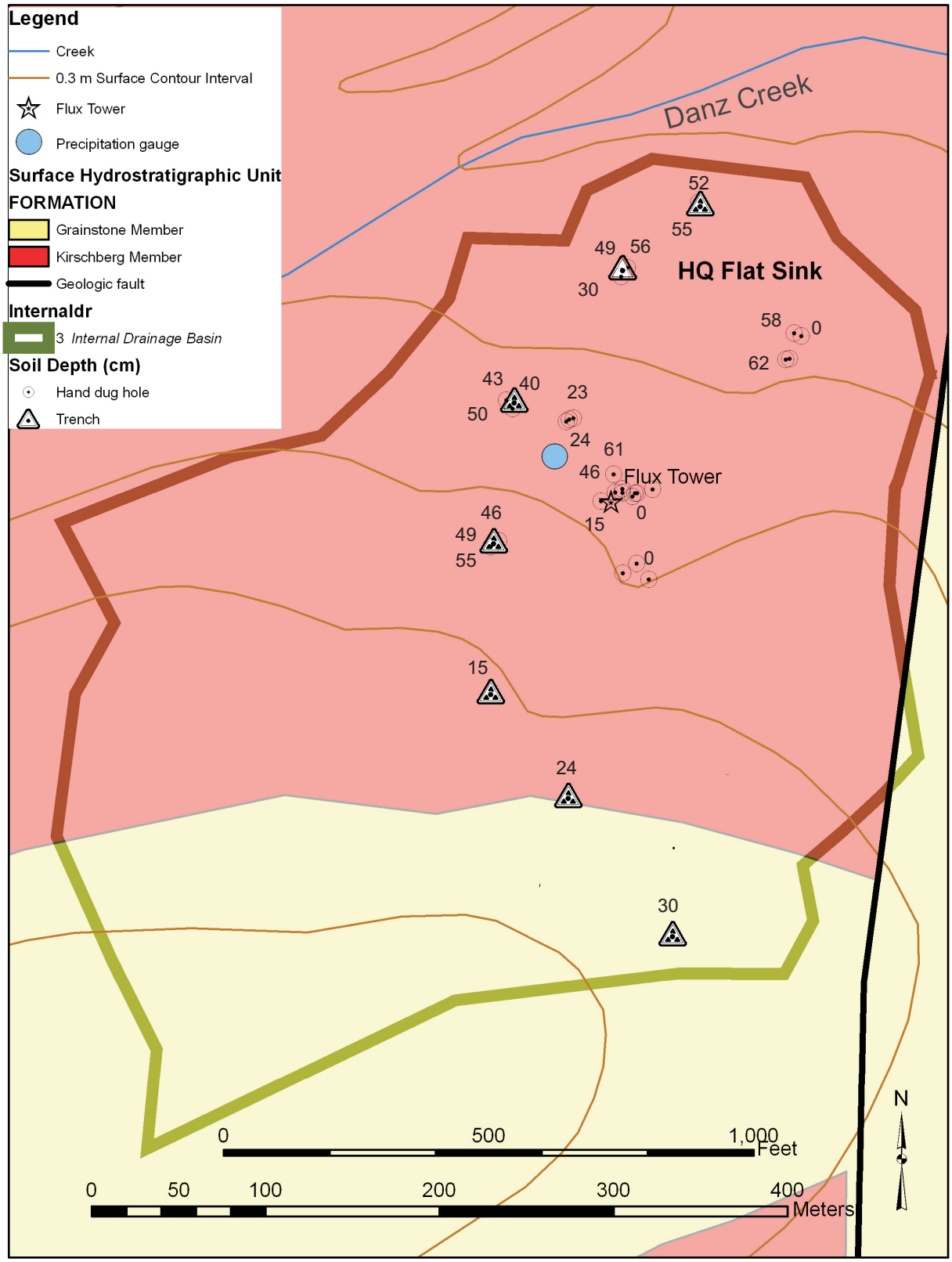

Figure 3.9. Soil thickness across HQ Flat catchment.

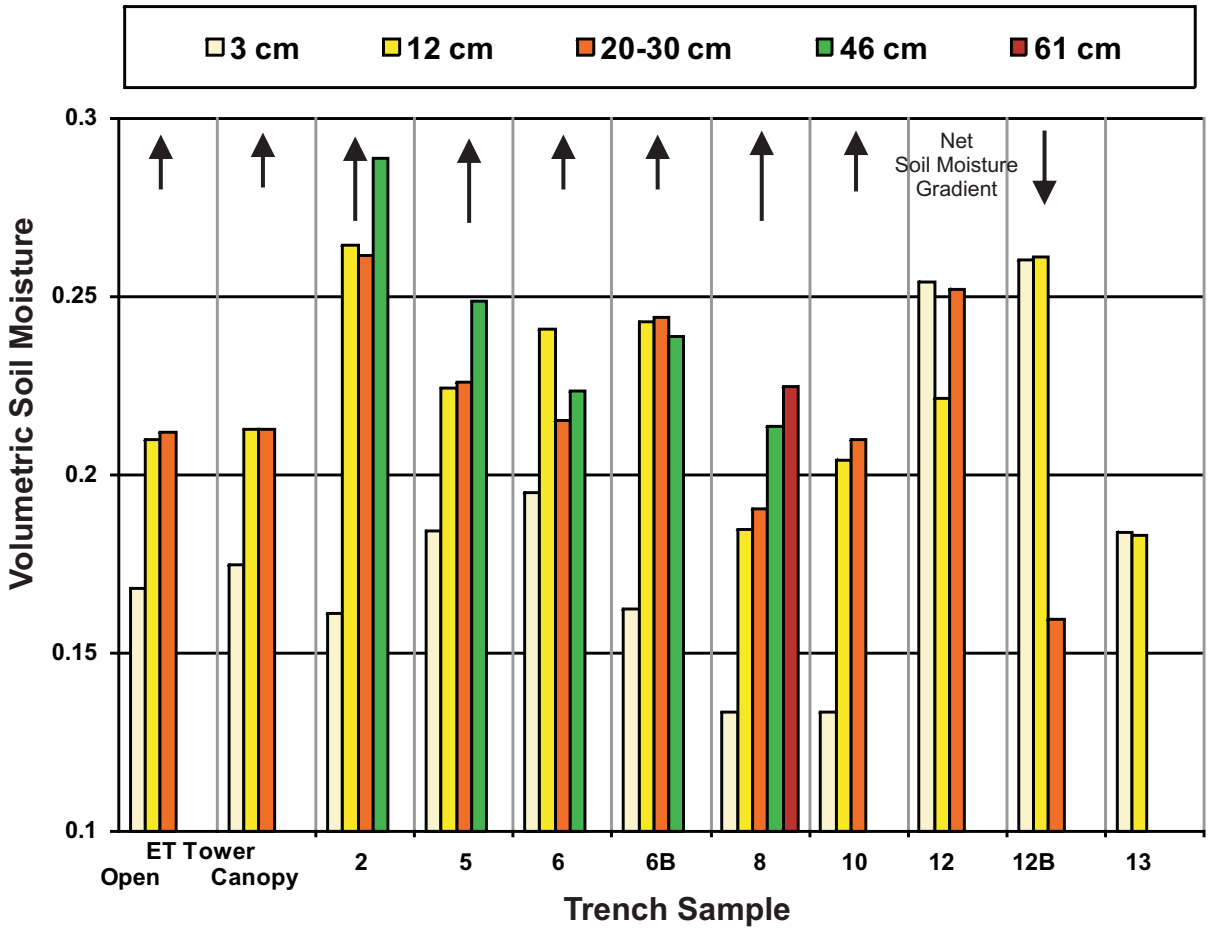

Figure 3.10. Soil moisture variation in trenches across HQ Flat catchment. All samples were collected between October 2, 2006 to October 4, 2006. Canopy samples were collected within tree covered areas, all others are open grassland. "B" samples are duplicate samples from same numbered trench at different location. Based on the soil moisture readings the net soil moisture gradient is upward (ET losses) at that time.

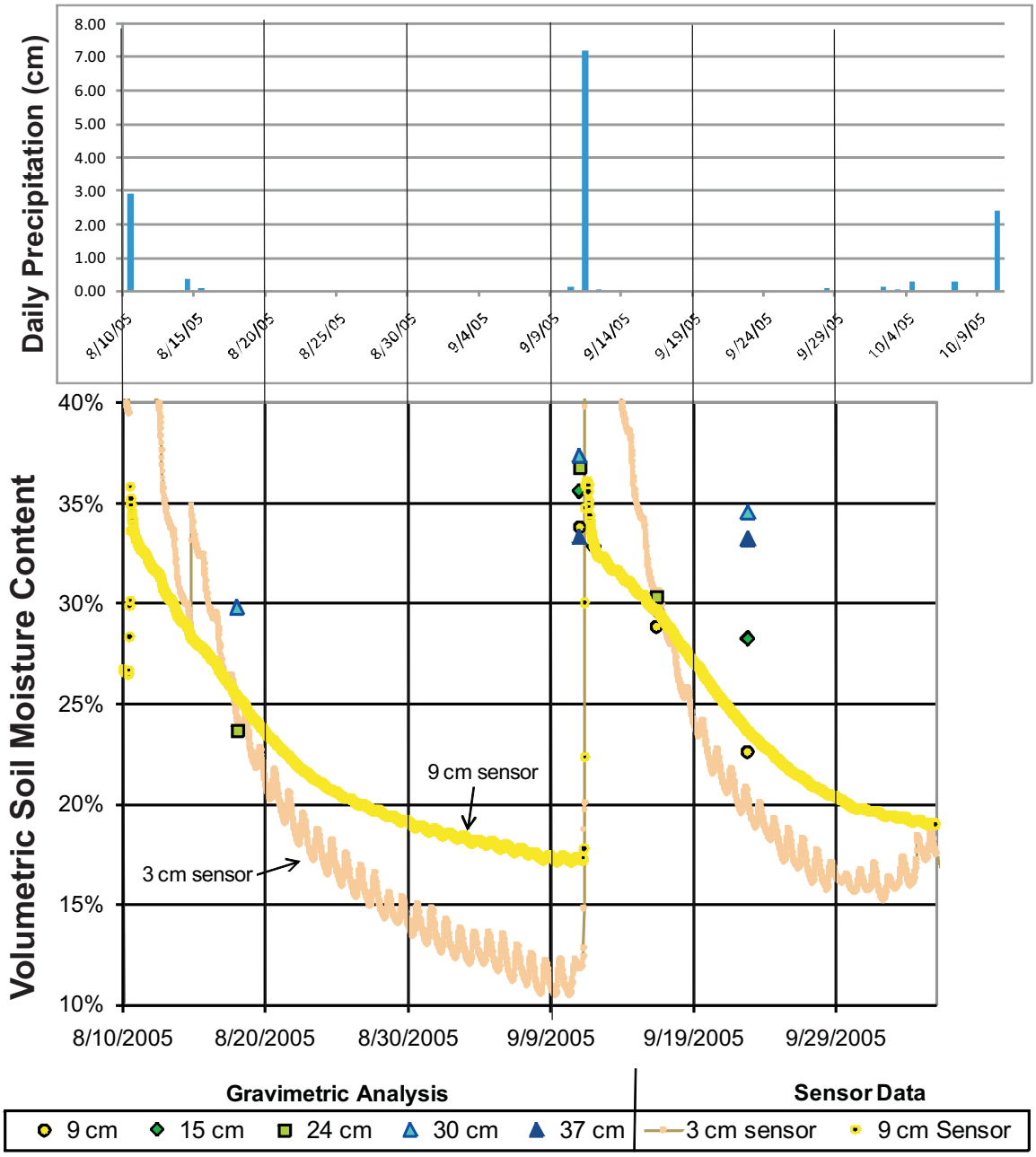

Figure 3.11. Volumetric soil moisture recession after rains.

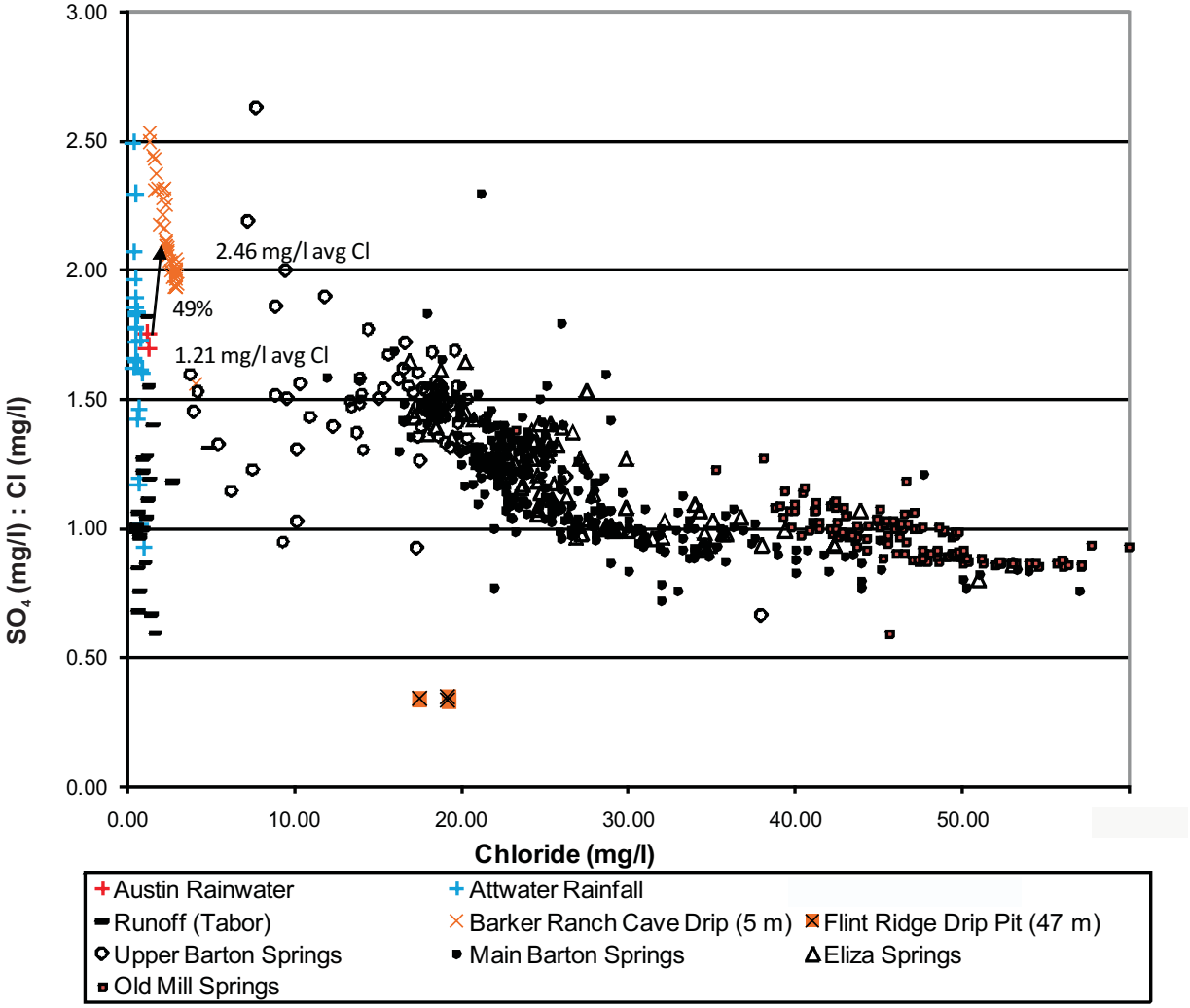

Figure 3.12. Comparison of chloride concentration and sulfate/chloride ratio. Chloride increases from rainwater and runoff sites to deeper cave drips and springs. Large evapotranspiration is not anticipated between cave drips and the water table and measured increases in chloride are attributed to rock interaction. Main, Eliza, and Old Mill are in hydraulic communication with the Saline-Water Zone, while Upper Barton Springs is not. The arrow indicates the shift from Austin rainfall quality to Barker Ranch Cave drip quality. This comparison suggests a recharge of 49% from rainfall based on assumptions including that the chloride enrichment results completely from evapotranspiration and that the rainfall quality is representative.

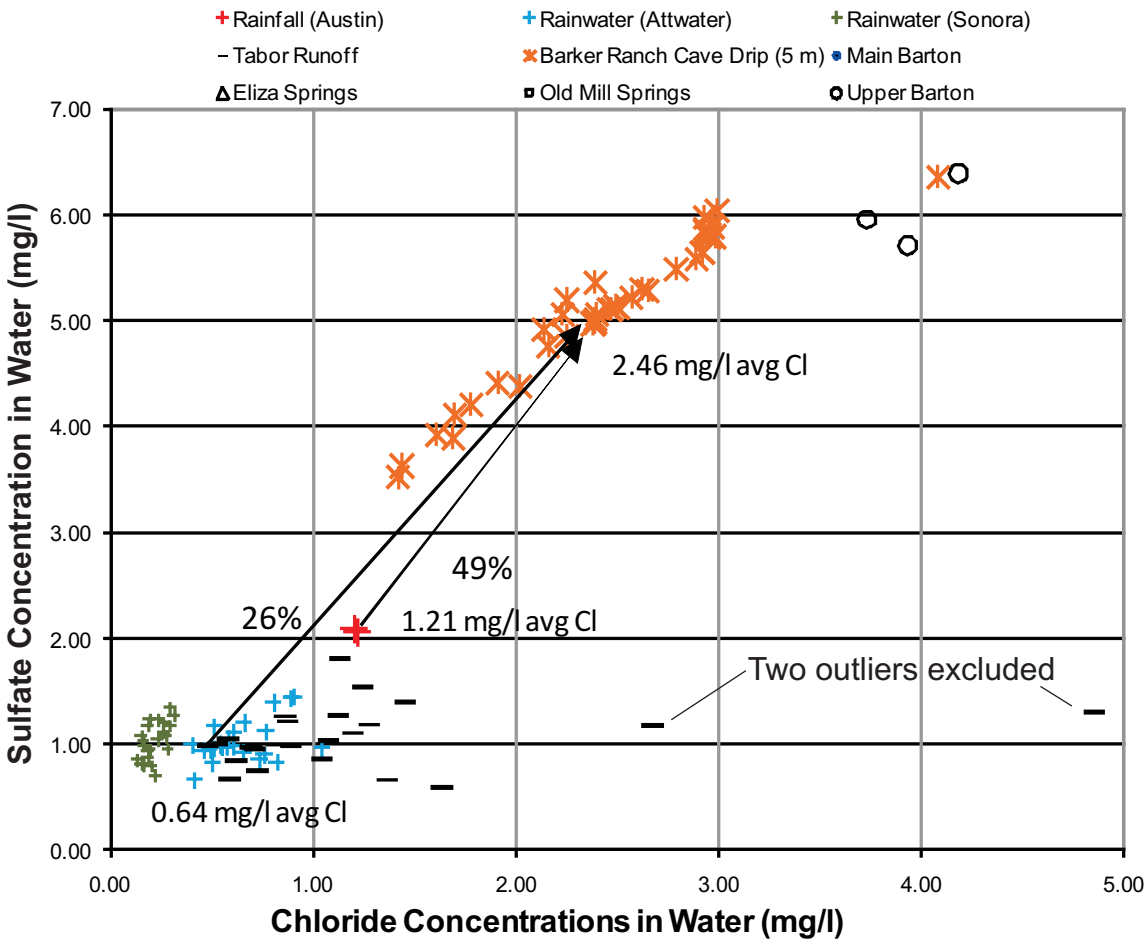

Figure 3.13. Chloride and sulfate concentration comparison. Two Austin area rainfall quality samples suggest that 49% recharge from rainfall occurs to the 5-m deep Barker Ranch Cave Drip. The same recharge calculation using the arithmetic average chloride concentrations from the Attwater National Atmospheric Deposition site is 26% of rainfall.

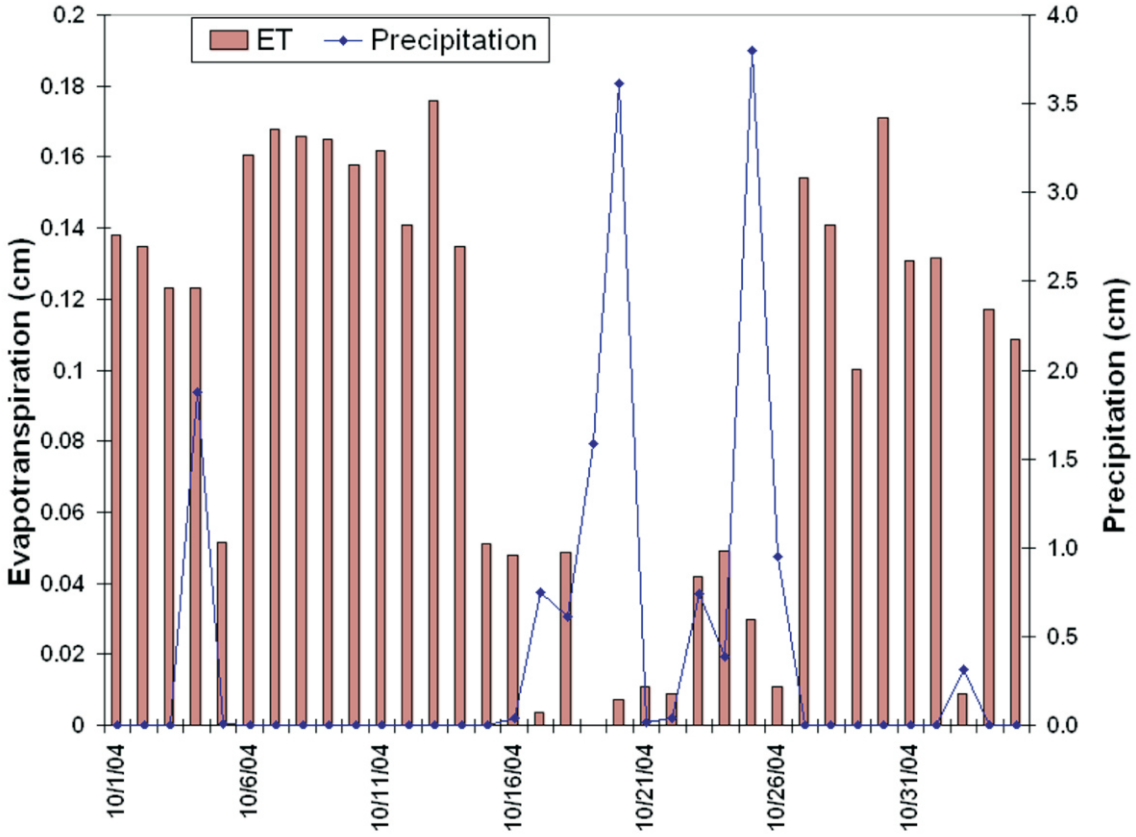

Figure 3.14. Variation in ET with precipitation.

Chapter 4. Groundwater Flow in the Edwards Aquifer

4.1 INTRODUCTION

This chapter examines groundwater flow through the Barton Springs Segment. An overview of prior investigations is presented.

4.1.1. Objectives and Scope

The objectives of this study are to characterize groundwater flow within the Barton Springs Segment. Field work, research, and analysis for this dissertation began in Fall 2000, although it builds on investigation that commenced in 1993. The groundwater system of the Barton Springs Segment, including discrete flow paths, groundwater basins, and transport characteristics, is examined with groundwater tracing, geochemistry, speleology, pump tests, and potentiometric-surface mapping. Groundwater tracing results between 2001 and 2005 are considered in combination with earlier tracing results. The flow rate of Cold Springs is estimated using creek flow losses in its traced source area. The hydrogeologic properties of the Barton Springs Segment, transmissivity, advection, dispersion, diffusion, and retardation, are quantified using tracer breakthroughs. Water-level data from wells and caves are used to interpret major flow path locations. Geochemical data are integrated to examine the localization of specific water-quality constituents along flow paths and to characterize drainage from the matrix. Aquifer test data are analyzed to calculate transmissivity and deviations in drawdown response to examine traced groundwater flow paths in the radius of influence.

4.1.2. Groundwater Flow in Karst Aquifers

Karst aquifers such as the Barton Springs Segment can be described as dual- or triple-porosity systems, because groundwater flow is influenced by matrix, fracture, and conduit flow (Ford and Williams, 1992; ASTM, 1995, Halihan et al., 2000, Kiraly, 2002). Groundwater flow in karst aquifers differs from other aquifers in that flow commonly converges into a few well-defined flow paths (Katzer, 1909; Martel, 1910). Convergent groundwater flow can also occur in non-soluble pseudokarst terranes, such as lava tubes

in basalt (White, 1988) and man-made trenches (Garcia-Fresca and Sharp, 2005). Most of the storage but little of the flow is thought to occur in the matrix (Worthington, 1999).

Quinlan (1989) described common methods for characterizing karst aquifers, including groundwater tracing, potentiometric-surface mapping, cave-stream mapping, and water-quality sampling. Worthington (1999) stressed that information from wells alone is not sufficient for characterizing karst aquifers. He listed several applications for well investigations in these areas:

(1) wells can serve as monitor/injection sites for tracers;

(2) aquifer test analyses (but with the understanding that the main channels of flow likely are not represented);

(3) variable rate aquifer tests, which show a nonlinear specific capacity if there are major groundwater flow conduit pathways within the cone of depression;

(4) packer tests can evaluate the fractures and matrix;

(5) the symmetry of the cone of depression will be irregular where well-connected conduit pathways are nearby;

(6) continuous water-level monitoring can characterize hydraulic connection of the system;

(7) spatial water-level measurements can indicate potentiometric troughs (or mounds) that indicate major conduit systems and changes in the hydraulic gradient in the downgradient direction can suggest (equivalent) porous media flow where the gradient increases or a karst system where the gradient decreases;

(8) frequent sampling can note variations in solute concentrations that indicate connections to major conduit networks and water-quality variations after rain events; and

(9) environmental isotopes may show younger water below older water in the major conduit pathways.

4.1.3. Sources of Subsurface Recharge to the Barton Springs Segment

Water leakage is defined in a hydrogeological sense as “the flux of fluid into or out of an aquifer or reservoir” that “commonly refers to cross formational flow” (Sharp, 1999). The presence of leakage from different water sources to the Barton Springs

Segment reflects discontinuities of the aquifer framework. Possible sources of subsurface leakage into the Edwards Aquifer are from the Saline-Water Zone and from the Trinity Aquifer.

4.1.3.1. Saline-Water Zone

The Saline-Water Line marks a relatively abrupt increase in chemical constituents directly east of the Barton Springs Segment (Clement and Sharp, 1988), approximately following Interstate 35 and Congress Avenue toward Barton Springs (Flores, 1990). The Saline-Water Zone east of the Barton Springs Segment is enriched in sodium, chloride, sulfate, and strontium (Clement and Sharp, 1988). The higher salinity in this area may be the result of more intense faulting at the San Marcos Arch, creating offsets that could strongly restrict the Saline-Water Zone (Clement and Sharp, 1988). Maclay and Small (1984) suggested that faults that offset 50% or more of the Edwards Aquifer can restrict lateral flow sufficiently to influence the position of the Saline-Water Zone. Offsets of this magnitude are observed near the Saline-Water Zone in cross sections along Barton Creek (Figure 2.3). Abbott (1973) explained that the Saline-Water Zone was groundwater from the Edwards Aquifer that filled a relatively static field outside of the well-developed flow paths to Barton Springs within the freshwater portion. The Saline-Water Line is irregular and does not follow any fault trend for any significant distance (Abbott, 1973). Land and Prezbindowski (1985) ruled out a connate origin for the Saline-Water Zone. They found no evidence of selective loss or gain of chemical species, or membrane filtration, that would be expected from upward leakage through shale layers, and the waters were depleted rather than enriched in deuterium relative to Standard Mean Ocean Water (SMOW). The downdip undersaturation with respect to dolomite, the enrichment in chloride, and high dissolved solids relative to other limestone brines led them to infer that the brines originated from updip movement of deeply buried and pressurized Jurassic evaporate-derived brines that were heavily diluted with downdip-moving meteoric water (Edwards Group brines). These Edwards Group brines could be Luling Fault Zone or Karnes Trough brines moving updip.

Rightmire et al. (1974; Kehew, 2001, p. 275-277) characterized water quality in the Edwards Aquifer as having low and gradually increasing sulfate concentrations and sulfate isotope ratio, and having essentially no sulfide. Rightmire et al. (1974) infer that the sulfates in the Edwards Aquifer probably originated from gypsum dissolution. A distinct high sulfate and sulfate-isotope-ratio sulfide-bearing water type was interpreted to be influenced by the migration of brines from a down-dip source (Rightmire et al., 1974).

Oetting (1995) compared the chemistry of the Saline-Water Zone to fresh water of the Barton Springs Segment and suggested its source to be a mixing of Edwards Group brines with highly evolved meteoric water with long residence time. Some Saline-Water Zone samples had higher Na/Cl than mixing models indicate and several possible sources were suggested: (1) dissolution of halite deposits, (2) mixing with waters from underlying units, or (3) Na-Cl exchange occurred across clay-rich layers. All of the chloride measured could originate from Edwards Group brine sources hypothesized by Land and Prezbindowski (1985; Oetting et al., 1996). An average mixture of about 30% underlying Glen Rose saline groundwater, 69% evolved meteoric water, and 1% Edwards Group brines provides a close match for the Saline-Water Zone quality adjacent to the Barton Springs Segment.

There is interaction between the Barton Springs Segment and the Saline-Water Zone. Senger (1983) estimated a roughly 5% to 10% contribution when Barton Springs flows declined as low as 20 ft^3/s. Hauwert et al. (2004b) estimated a maximum flow contribution of 3% at Old Mill Springs and 0.5% at Main and Eliza Springs combined from the Saline-Water Zone, when Barton Spring flows declined to 17 ft^3/s. Although both Senger (1983) and Hauwert et al. (2004b) referred to chloride concentrations from well 58-50-301 for the Saline-Water Zone end member, Senger (1983) used a 332 mg/l value measured in 1949 under moderate-flow conditions while Hauwert et al. (2004b) used 3,640 mg/l chloride concentrations measured in 1948 under low-flow conditions, hence the difference in their estimates. Garner (2005) estimated that Old Mill Spring received 4% to 9% of its water from the Saline-Water Zone using an unknown end member for comparison, but presumably the same value Senger (1983) used from well

58-50-301 under moderate-flow conditions. Johns (2006) extrapolated the Saline-Water Zone contribution to Main and Old Mill Springs would increase to 1 - 1.25% and 3 - 3.25%, respectively if Barton Springs declined to flows of 0.142 m^3/s (5 ft^3/s).

Although water-quality data from the Saline-Water Zone are limited, the lower contributions of about 3% or less, based on well water quality from 58-50-301 during low-flow conditions, are more representative of the Saline-Water Zone component of Old Mill Springs. Because waters from the Saline-Water Zone are nonpotable, few wells are located near the Saline-Water Line. Even fewer wells are completely inside the Saline-Water Zone and some of these wells near the boundary contain a mixture of fresh and saline waters under higher flow conditions. Therefore, the Saline-Water Zone quality may be best represented in wells near the Saline-Water Line during low-flow conditions when fresh Edwards Aquifer flows are low.

Garner (2005) inferred from geochemical analysis that the Saline-Water Zone persisted at lower levels of the Barton Springs Segment and extended in some places far into the Sunset Valley groundwater basin (well 58-50-406) and farther west into the Cold Springs groundwater basin (well 58-50-211). However, these wells lie in urban areas and are elevated in nitrate (arithmetic mean of 5.10 and 1.83 mg/l, respectively) so the elevated chloride and sulfate are interpreted here to originate from anthropogenic sources (COA, 1997) and not from the intrusion of the Saline-Water Zone through complex multi-level crossing of groundwater flow paths. Tracers injected in a well near the western edge of the Edwards outcrop area appeared in well 58-50-211 (Section 4.2; Figure 4.1), demonstrating that its source area is from the south rather than the east.

During high-flow conditions, the freshwater portion of the Edwards Aquifer intrudes into the Saline-Water Zone (Garza, 1962). During drought periods, contribution from the Saline Water Zone to Barton Springs is reflected by increases in mineral constituents such as sodium, chloride, strontium, and fluoride (Senger, 1983; Senger and Kreitler, 1984; Hauwert and Vickers, 1994; COA, 1997).

4.1.3.2. Trinity Leakage

The flow of Trinity Aquifer waters to the Edwards Aquifer was originally hypothesized by Hill and Vaughan (1898) based upon sites on the western side of the Edwards outcrop area where faults bring the Middle and Lower Trinity Aquifer into direct contact with the Edwards Group. Trinity Aquifer contributions to the Edwards Aquifer potentially can occur laterally across faults that have sufficient displacement to place permeable beds in the Trinity Aquifer next to permeable portions of the Edwards Aquifer (Senger and Kreitler, 1984). Slade et al. (1986) noted that 13 of 140 tested wells across the Barton Springs Segment showed chemical signature of Trinity Aquifer leakage, and that each of the 13 wells was near a fault where leakage may localize. Trinity Aquifer water can be geochemically distinguished by differences in strontium, sulfate, fluoride, chloride, and sodium (Brune and Duffin, 1983, p. 94-97; Senger and Kreitler, 1984; Slade et al., 1986, p. 61). Some areas of the Edwards Aquifer, including Barton Springs, are enriched in constituents that are characteristic of the Trinity Aquifer (Senger and Kreitler, 1984; Slade et al., 1986; Hauwert and Vickers, 1994; Oetting, 1995; Hauwert et al., 2004b; Garner, 2005). In the Northern Segment, the Saline-Water Zone shows a close chemical similarity to the lower Trinity Aquifer (Clement and Sharp, 1988).

Water-level maps suggest that Trinity leakage to the Barton Springs Segment occurs, although sufficient water-level data is lacking to show where this leakage occurs. To simulate potentiometric heads in the middle Trinity Aquifer, a considerable amount of simulated leakage to the Edwards Aquifer is required (Mace et al., 2000b). In areas on the western side of the Edwards outcrop area, the Edwards Aquifer potentiometric heads are higher than Trinity Aquifer water levels under all flow conditions in a few locations where direct comparisons are possible, so that the potential exists for downward leakage into the Trinity Aquifer rather than vice versa (Smith et al., 2007). Farther to the east, Trinity Aquifer data are not available on the eastern side of the outcrop area, eastern drainage, or artesian areas to determine whether Trinity Aquifer heads are indeed higher there.

The fact that Trinity Aquifer waters have one or two orders of magnitude less total dissolved solids than the Saline-Water Zone suggests that Trinity waters circulate more rapidly with less rock-water interaction. This circulation likely is created by Trinity leakage to the Edwards Aquifer because there are no other significant natural discharge points (east of the contributing area where the top of the Trinity Aquifer lies below the base level of the local rivers and creeks). Base flow generated within the contributing area originates from Trinity Aquifer springflow. This Trinity Aquifer discharge recharges the Barton Springs Segment though the major creeks and possibly through the Blanco River.

Tracing and cave mapping have shown direct connection between the Edwards and Trinity Aquifers in some areas. Major cave development can be observed in the Walnut/Basal Nodular Member both north and south of the Barton Springs Segment. This potentially could allow vertical leakage in some areas between the Edwards and Trinity Aquifers (Kastning, 1986; Russell, 1993; Veni, 1999). In fact, cave streams developed within the Walnut Formation in North Austin have been traced to discharge from a Glen Rose spring (Hauwert and Warton, 1997). Schindel (2006, personal communication) reported injecting dye on the Upper Glen Rose Formation at Camp Bullis and recovering the dye miles away in an Edwards Aquifer well. Klimchouk (2004) suggests that hypogene leakage from underlying aquifers across assumed aquitards are common in karst aquifers.

4.2. Tracing of Groundwater Flow System

Tracing reveals details of the groundwater flow system that cannot be obtained by other methods. Tracing studies require an accurate conceptual model of possible alternative recharge and discharge conditions; non-detection of an injected tracer more often than not reflects a poor understanding of the system (Smart, 1988; Field, 2002a). If wells downgradient of the injection site are available and monitored, then tracers can be recovered in them (Quinlan, 1989). If all potential discharge sites from the injection site are monitored and sampled at sufficient frequency at the time the tracer arrives for the duration of its discharge, then the breakthrough can be measured (Fields, 2002a).

Loading, or total mass of discharged tracer, can be calculated if the discharge rates and concentrations of tracer discharge are known accurately.

Interpretation of tracing results transcend simple positive or negative recovery at a monitored site. Differences in concentrations and multiple arrival peaks can reveal details about flow paths and water sources. Atkinson et al. (1973) used multiple peaks on breakthrough curves to infer divergent flow paths with varying travel times. Multiple peaks also can result from release of stored tracer that is flushed by rain events.

4.2.1. Groundwater Tracing Methodology

The methodology for groundwater tracing in the Barton Springs Segment from 2000 to 2005 was essentially the same as methodology used from 1996 to 2000 (Hauwert et al., 2004a). Groundwater tracing involves the introduction of non-toxic materials (*tracers*) into surface drainages or the subsurface (*injection points*) and monitoring the movement of these materials at wells and springs (*receptor sites*). The general methodology of tracing and an evaluation of various tracers are described by Aley (2002) and Smart and Laidlaw (1977). The procedures and criteria of the laboratory analysis for the tracer were described in detail by Aley (2000a).

The tracers used in this study are traditional, well-documented organic dyes, acquired from Ozark Underground Laboratory (OUL) in Protem, Missouri. The tracers used in this study are eosine, fluorescein, rhodamine WT, sulforhodamine B, and pyranine; these names are used throughout the report. Dye quantities identified in the report represent the dye mixture used.

Eosine is Acid Red 87 and its Color Index Number is 45380. It is also called eosin. The eosine mixtures used contained approximately 75% dye equivalent and 25% diluent. The dye mixture was purchased as a powder.

Fluorescein (Fl) is Acid Yellow 73 and its Color Index Number is 45350. It is also known as sodium fluorescein and uranine. The fluorescein mixtures used contained approximately 75% dye equivalent and 25% diluent. The dye mixture was purchased as a powder.

Rhodamine WT (RWT) is Acid Red 388 and it does not have an assigned Color Index Number. The rhodamine WT mixtures used contained approximately 20% dye equivalent and 80% diluent. The dye mixture was purchased as a liquid.

Sulforhodamine B (SRB) is Acid Red 52 and its Color Index Number is 45100. The sulforhodamine B mixture used contained approximately 75% dye equivalent and 25% diluent. The dye mixture was purchased as a powder.

Pyranine was purchased as Drug and Cosmetic Green 8. Its Color Index Number is 59040. The pyranine mixture used contained 77% dye equivalent and 23% diluent. The dye mixture was purchased as a powder.

Tracer monitoring at Barton Springs using charcoal receptors has been nearly continuous since 2000. Once dye concentrations are sufficiently low or nondetectable, a new tracing phase may commence once funding is available and specific objectives are identified. Tracing phases require at least 3 months of monitoring and are separated by 6 months to 3 years. The tracers selected are not necessarily rare substances but may be present in some quantity in stormwater runoff, automotive coolants, sewage, hydraulic fluids, cooling tower emissions, fluorescent stationary, and other sources (Aley, 2002).

To monitor the movement of the tracers, charcoal receptors were placed in springs, creek and river sites, and accessible wells. Monitored wells with active pumps were fitted with receptors at a point prior to any water treatment systems. These active well sites were either allowed to flow continuously at a low rate or pumped for a period of time each day. For active well systems, a small seep or drip of flow from a periodically pumping well was diverted through a standard garden hose and into specially constructed polyvinyl chloride (pvc) holders, designed by OUL, where charcoal receptors were placed. The receptor holders were often placed in pairs to allow for duplicate samples, although it was difficult to insure both receptor holders received the same quantity of flow. Open wells without pumps were monitored by lowering a receptor to a depth where flow was believed to enter the well bore. The optimal monitoring depths within these *passive well sites* were estimated from downhole camera observations of void intervals within the well or from available caliper logs of the well bore. Any springs that represented likely discharge points for the injection sites were monitored. Springs might

exist within the channel of the Colorado River that are not obvious, so receptors were placed in the Colorado River at numerous locations during some phases. Creeks were monitored downstream of the injection point where necessary to determine if creek flow subsequent to injection could move the tracers along surface flow routes to other recharge points. As the study progressed, monitoring sites were added and dropped to better fit monitoring needs and accessibility of that phase. Continued and regular access was one of the most limiting factors to selecting or sustaining a monitoring site.

Receptor sites were monitored using a combination of adsorbent activated charcoal packets (receptors) and grab samples. Receptor sites were monitored for 2 weeks prior to tracer injection to detect any background presence of tracers. Several receptors were placed at each receptor site and collected at intervals ranging from several hours to 3 weeks. Short-term receptors, those collected over hours or days, were often overlapped by a long-term receptor. The long-term receptor was analyzed initially and if a tracer was detected the short-term receptors were analyzed for that interval. This procedure reduced analytical costs and allowed refinement of the arrival times for tracers. Breakthrough curves were prepared from the laboratory results, from which the initial travel time, duration, and peak concentrations were calculated. To allow comparison of results from receptors placed over varying periods of time, the cumulative concentration of the results were divided by the number of days in that time period. Because of this mathematical adjustment of the cumulative concentrations, some receptors may show an average daily concentration below the cumulative concentration detection limit.

Water samples, known as grab samples, were collected in plastic bottles at the time the receptors were replaced and provided information on the instantaneous tracer concentrations in the water. After 2000, ISCO model 3230 automatic samplers were deployed at Eliza Springs, and occasionally at Main and Old Mill Springs, so that grab samples could be collected between 4-hour and 1-day intervals for limited periods following injections. Because the concentration of tracers measured in the charcoal receptors is cumulative, higher concentrations of tracer can be expected to be present in an adsorbent receptor than are measured in instantaneous grab water samples from the same site. Consequently, the tracers are more easily detected in receptors than in grab

samples. Grab samples also served to verify positive detections measured on corresponding receptors.

The Rules and Bylaws of the BS/EACD requires the submittal of an operations plan and subsequent authorization from the BS/EACD prior to any groundwater trace in the Barton Springs Segment of the Edwards Aquifer where materials are introduced into surface or groundwaters (BS/EACD, 1997). This rule was enacted so the BS/EACD could track tracer studies within the Barton Springs Segment, avoid interference between groundwater traces, and evaluate the proposed injection materials for possible detrimental affects. Access for all sites was obtained in advance from the site owner or authorized representatives. Identified well users in close proximity to the injection points were notified in advance of the test to prepare for possible visible levels of the tracers.

The quality control and assurance procedures utilized in this study incorporated trip blanks, field duplicates, laboratory-spiked standards, and the testing of a portion of the sample containers for possible contaminants. Trip blanks, consisting of wetted charcoal packets handled by field personnel during the course of sampling, were submitted to the lab from each team recovering receptors in order to test periodically for cross contamination between sites or contamination from other materials the teams were exposed to. Over 12 percent of the total charcoal samples submitted to the OUL for analysis included a field duplicate sample in order to allow two independent measurements of the same sample for comparison. Between 1996 to 2000, a portion of the duplicates and blanks submitted to the laboratory were blind, so that the lab did not know their purpose. OUL tested standard solutions of the tracers daily as described in its procedures and quality control document. Laboratory blank samples were analyzed on each twentieth sample. OUL tested one percent (1%) of the unused sample containers to assure that tracer contaminants were not present. Grab samples were collected to verify the results of the receptors, and to measure the concentration of tracers at a single point in time.

Primary or secondary flow paths were mapped to reflect groundwater discharge rates under average flow conditions. Figure 4.1 shows an interpretation of the primary and secondary groundwater flow routes active during moderate and high-flow conditions.

These are based in part on measured flow losses at discrete swallets in creek channels as well as location and estimated average flow losses over larger identified upland internal drainage basins. The primary and secondary flow paths mapped are not all inclusive; I infer that more secondary and tertiary flow paths will be discovered with further investigation. Mapped potentiometric troughs during recession periods indicate strong hydraulic connection with discharge areas.

The tracer recovery is the mass of tracer that is estimated or calculated to discharge from the aquifer system. Tracer recoveries were calculated using measured concentrations at wells and springs and calculated springflows and pumping rates at each receptor site where the tracer was detected to estimate the mass of discharging tracer. The percent recovery is the ratio of recovered tracer mass to the mass of tracer injected. The tracer masses described in this report refer to dye mixture amounts. Because there is no direct comparison between receptor and water-sample results, only the grab-sample results (and not the charcoal receptor results) were used to calculate tracer recoveries. Consequently, the calculated recoveries may be underestimated, because many of the traces showed detectable tracer concentrations on receptors for months after the grab-sample concentrations declined below detection limit. Sampling frequency also will affect tracer recovery. Daily and weekly water samples tend to miss the peak of the tracer arrival, when most of the tracer typically will discharge. Therefore, less frequent sampling will result in underestimation of the actual tracer recovery. Calculation of percent recoveries also can be affected positively or negatively by errors in the estimation of springflow at each outlet. Recovery data are also important for modeling groundwater constituent transport, to insure monitoring sites are properly located on downstream preferential groundwater flow paths, and to insure that all major discharge sites from the aquifer were monitored (Field, 2002b). Jones (1976) listed several factors that can account for failure to recover a tracer at its discharge site including: (1) the discharge site(s) were not monitored, (2) an insufficient amount of tracer was used, (3) complete sorption losses occurred on fine-grained sediment or organic matter, (4) very slow, diffuse groundwater flow causing the tracer to arrive at a concentration below the detection limit, (5) the duration or frequency of sampling was insufficient, (6) high

background concentrations obscured the tracer arrival, (7) the receptors were coated or saturated, (8) the tracer concentration was reduced by photo-decay or other degradation, (9) the tracer was diluted due to flooding, and (10) an inadequate amount of time was provided to allow purging of the same tracer from previous tests.

Quantitative tracer tests (Mull et al., 1988; Field, 2002a) can quantify the hydrogeologic parameters of the Barton Springs Segment. Five traces from varying injection distances across the aquifer were analyzed including one short trace from Barton Creek in 1999 and three longer traces from 2005. These traces were selected because they had relatively well-defined breakthrough curves from samples collected at intervals of 1 to 4 hours. The tracer concentrations from these four traces were quantified by Ozark Underground Lab (OUL) in Protem, Missouri. The fifth trace selected was the Rhodamine WT trace reported by Senger in 1983. The concentrations were reported to be derived from a Turner fluorimeter and were estimated from a chart presented in Senger (1983).

Transmissivity can be calculated from the hydraulic conductivity derived from mean tracer velocities through the following relation:

Hydraulic conductivity = $K = vn_e/I$	(m/s)	(6)
Transmissivity = $T = K/m$	(m^2/s)	(7)

where:

v = mean tracer velocity (m/s)

n_e = effective porosity assumed to be 0.001 (Smith and Hunt, 2004)

I = potentiometric gradient from injection site to Barton Springs

m= saturated thickness, which was assumed to be 130 m (Hauwert, 1997)

The effective porosity of 0.001 is consistent with aquifer tests described in this chapter and groundwater models conducted by BS/EACD (Smith and Hunt, 2004).

The longitudinal dispersion between an injection and discharge site can be quantified using the Chatwin (1971) method, which does not assume Fickian diffusion

(Field, 2002a). The Chatwin method computes the importance of advection compared to longitudinal dispersion (the Peclet number) along the traced flowpath. First, the ratio of advection to dispersion is calculated by deriving Chatwin values for each breakthrough concentration measurement as:

$$Y = t * \ln((C_p*(t_p)^{1/2})/(C*(t)^{1/2})) \quad (8)$$

where:

Y = Chatwin values (sec $^{1/2}$)

t = elapsed time (sec)

t_p = elapsed time to peak concentration (sec)

C= instantaneous concentration (ppb)

C_p = peak concentration (ppb)

The Chatwin value intercepts (Y_{int}) are graphically derived from a plot of Chatwin values versus elapsed time (min). A straight line extrapolation from the early tracer recoveries plot indicates a y-intercept Chatwin value (Figure 4.2) at zero elapsed time to calculate the longitudinal dispersion coefficient with the relation:

$$D_L = (L/ Y_{int})^2 \quad (9)$$

where:

D_L= the longitudinal dispersion coefficient (m^2/s)

L = distance from injection point (m)

Y_{int} = y intercept of extrapolation from early Chatwin values versus elapsed time

The Peclet number is the ratio of advective transport to hydrodynamic dispersive transport. The hydrodynamic dispersion is the combination of bulk diffusion and mechanical dispersion:

$$Pe = (v*L)/D_L \quad (10)$$

where:

v = mean tracer velocity (m/s)

D_L = the longitudinal dispersion coefficient (m^2/s)

L = distance from injection point (m)

Typically the dyes are assumed conservative, but tracer properties vary (Aley, 2000a; Aley, 2002; Hauwert et al., 2004a; Appendix I). Consequently, the advective component may be less because of the sorptive properties of the tracer, particularly when sulforhodamine B (SRB) is used. The greater sorption of SRB causes a lower recovery of about 20% compared to an identical injection mass of sodium fluorescein (Aley, 2007, personal communication). Rhodamine WT dye is composed of two isomers, one of which is conservative, and the other having high sorption (Rochat et al., 1975; Hofstraat et al., 1991; Sabatini and Austin, 1991; Shiau et al., 1992; Shiau et al., 1993). Consequently, about 50% of rhodamine WT is typically sorbed compared to fluorescein (Aley, 2007, personal communication). Rhodamine WT and SRB sorb readily on clays, while fluorescein and eosine have a greater affinity for limestone surfaces (Sabatini, 2000; Appendix I). All of the dyes used in this study sorb readily on organic materials, which is a desired property for recovery on charcoal receptors (Milulla et al., 1997). The tracer properties are further described in Appendix I.

4.2.2. Review of Tracing Efforts

In the early 1980s, groundwater tracing was applied successfully on a number of traces to San Marcos Springs south of the Barton Springs Segment (Ogden et al., 1986). One trace injected near the southern divide on the Blanco River was injected under high-flow conditions (Barton Springs flow reported between 1.98-2.26 m^3/s or 70-80 ft^3/s) and arrived at San Marcos Springs a year later under low-flow conditions (Barton Springs flow about 0.85 m^3/s or 30 ft^3/s). Barton Springs was not monitored during this trace. A trace of the same cave on the Blanco River under low-flow conditions (Barton Springs

flow of 0.82 m^3/s or 29 ft^3/s) similar to those during the original trace arrival did not yield definitive recovery at monitored sites between San Marcos and Barton Springs although injection mass (6.8 kg or 15 lbs of 75% sodium fluorescein mixture) was probably too low to reach Barton Springs (site Q; Hauwert et al., 2004a; Hauwert et al., 2004b; Figure 4.1).

Dye injected in well 58-42-903 traveled 61 m (200 ft) to arrive at Main Barton Springs within 20 minutes (Senger, 1983; Figure 1.3). The breakthrough curve of this short trace and low discharge recession coefficient were used to characterize the Barton Springs Segment as having "a very large hydrodynamic dispersion" but the flow velocity was high compared to porous media aquifers (Senger, 1983). Subsequent analysis of these tracing results in this chapter show that dispersion actually is very low compared to advection. After an unsuccessful trace from upper Barton Creek (site B in Figure 4.1) to Barton Springs however, Senger and Kreitler (1984) considered tracing "unreliable" for use in the Barton Springs Segment because of the large distances across the aquifer and assumed dispersive characteristics.

Beginning in 1996, groundwater tracing was reapplied successfully across the Barton Springs Segment through regular tracing programs. From 1996 to 2000, a tracing study by the Barton Springs/Edwards Aquifer District (BS/EACD) and City of Austin Watershed Protection and Development Review Department (COA), with partial funding from EPA 319H program administered through TCEQ, traced sites across the outcrop area of each watershed (Hauwert et al., 1998; Hauwert et al., 2004a). From 2000 to present these traces continue at regular intervals carried out by the BS/EACD and COA (Hunt et al., 2004; Smith et al., 2006). Since 2005, a City of Austin Capital Improvement Project has partially funded tracer studies across the Barton Springs Segment for the purpose of simulating accidental spills of hazardous materials. Since 2000, groundwater tracing was included as a portion of this dissertation study. Table 4.1 presents a list of traces conducted through 2007 and sources with detailed methodology and results. Traces conducted in 2006 to 2009 have not been analyzed in this dissertation. A number of repeated traces were conducted in the Blanco River watershed in 2008 and may continue

in 2009. The Blanco River traces were performed cooperatively by the Edwards Aquifer Authority, BS/EACD, COA, Zara Environmental and Ozark Underground Labs.

The tracing studies commenced in 1996 demonstrated that tracing could map groundwater flow paths. In the 20 traces conducted from 1996 to 2000, 17 were recovered at some monitored sites, which indicate that properly conducted tracer tests are appropriate tools of investigation within the Barton Springs Segment. In 1996, the BS/EACD and COA Tracers reinjected at the same site B previously utilized by Senger (1983) and were successfully recovered in the Colorado River just downstream of Cold Springs. The tracer was not detected at Barton Springs (Hauwert et al., 1998). Cold Springs and portions of the Colorado River upstream of Barton Creek may not have been monitored in the 1982 trace.

From tracer injections, the groundwater flow rate of initial arrival of tracer from natural recharge features along traced flow paths varied from 1.6 to 11 km/day (1 to 7 mi/day, traces C, F, A', H, J, D, E, N, and G in Figure 4.1) during moderate, high, and overflow conditions. Traces from Onion Creek required as little as three days to traverse the entire Edwards outcrop area and initially discharge at Barton Springs. Flow conditions affect the groundwater flow rate by increasing hydraulic gradients and drying of upper-level conduits. During low-flow conditions, groundwater velocities of 1.1 to 1.6 km/day (0.7 to 1 mi/day; traces A, B, L, O, and P in Figure 4.1) were measured.

Recovering tracers during low-flow conditions is difficult because: (1) many areas from the western side of the Edwards outcrop area are transiently unsaturated; (2) potentiometric surfaces near preferential groundwater flow paths are discrete troughs instead of mounds, hence wells near but not directly on the flow paths may not recover dye; and (3) the advective gradient is low so that travel times are slower and breakthroughs show a relatively higher dispersion than during moderate-flow conditions (Hauwert et al., 2004a).

Three of the tracers injected during low-flow conditions (sites I and R on Figure 4.1, site Q is further south on the Blanco River) were never recovered at monitored sites. Despite previous non-recovery of trace R under low-flow conditions, the same dye was reinjected at a cave (10d) 600 m from site R under high-flow conditions in 2007 and was

clearly detected at Barton Springs within 3 days. Traces B, K, M were injected during low-flow conditions and recovered from wells or rivers but not in spring discharge.

4.2.3. Groundwater Basins and Preferential Groundwater Flow Routes

Based primarily on injected tracer information, the Barton Springs Segment can be separated into three groundwater basins: Manchaca, Sunset Valley, and Cold Springs (Figure 4.1; Hauwert et al., 2004a). These preferential groundwater flow routes reveal significant anisotropy and heterogeneity within the Barton Springs Segment. The presence of preferential flow paths within the Barton Springs Segment is apparent by observations of groundwater convergence, such as the appearance of tracers injected in different watersheds appearing at a single well and not other wells (Hauwert et al., 2004a).

Some flow paths change location or reverse flow under different flow conditions. During overflow conditions, overloading of regular flow paths causes diversion of some or all of the new recharge to other flow paths (Hauwert et al., 2004a; Hauwert et al., 2004b). During overflow conditions, recharge is diverted in several places from eastern flowpaths to more western flow paths to the north or south. Overflow conditions may be localized and are not necessarily aquifer-wide. During low-flow conditions, some flow paths probably combine or be dry.

4.2.3.1. Manchaca Groundwater Basin

The Manchaca groundwater basin is the largest groundwater basin in the Barton Springs Segment (Figure 4.1). The Edwards outcrop and eastern drainage areas of the Manchaca groundwater basin are 181 km^2 (70 mi^2) and its artesian area is 129 km^2 (50 mi^2) in area (see Figure 2.6). It is dominated by two preferential flow routes, the Manchaca Flow Route and Saline-Line Flow Route. The Manchaca Flow Route discharges at Eliza, Main, and to a lesser extent at Old Mill Springs. It represents by far the largest flow contribution to Barton Springs. The convergence of flow along the Manchaca Groundwater Flow Route is demonstrated by multiple tracer recoveries from injections in different sites of Bear, Little Bear, and Onion Creek watersheds at a single well (58-50-742) but not other monitored wells nearby. The Manchaca Flow Route is

indicated by a broad potentiometric trough, such as those mapped by Brune and Duffin (1983), Slade et al. (1986), and Hauwert and Vickers (1994).

The presence of a Saline-Line Flow Route (Figure 4.1) is inferred from an injection at site O (Figure 4.1) in Onion Creek where a 10-day delay in the arrival of a tracer at Old Mill Springs was observed after its initial arrival at Main and Eliza Springs (Figure 4.2). Dye injected within the Manchaca groundwater basin south of Bear Creek and west of the Manchaca Flow Route arrived at much lower concentrations at Old Mill Springs than at Eliza and Main Barton Springs, suggesting dilution of Old Mill Springs from a separate source (Figure 4.3). A number of tracers injected in Site M on Onion Creek were detected in wells eastward and northeastward toward and adjacent to the Saline-Water Zone instead of converging with the Manchaca Flow Route (Figure 4.1). From tracer recovery, only a single well (58-58-209) is inferred to be the closest identified well to the Saline-Line Flow Route (Figure 4.1). Tracer detections in wells along this flow route are sparse because there are few wells along the Saline-Water Line and those that exist have not been the focus of monitoring until after the flow path was recognized in 2002. For mapping purposes, this flow route is assumed to follow the Saline-Water Line as defined by Flores (1990). Garza (1962) and DeCook (1963) mapped a potentiometric trough through the Kyle area and trending southeast of the Buda that may correspond to a portion of the Saline-Water Flow Route. Abbott (1973) and Senger (1983) hypothesized that mixing of saline water with fresh Edwards groundwater could result in undersaturation with respect to calcite and dolomite that could enhance dissolution along the Saline-Water Line. Dilution from the Saline-Line Flow Route is interpreted by lower tracer concentrations in Old Mill Spring than in Eliza Springs of tracers following the Manchaca Flow Route (Figures 4.2 and 4.3; Hauwert et al., 2004b).

During low-flow conditions, it is possible the Saline-Line Flow Route (Figure 4.1) converges with the Manchaca Flow Route, similar to the convergence of the Sunset Valley Flow Route and Manchaca Flow Route. This alteration in the Saline-Line and Sunset Valley Flow Routes is indicated by the historic drying of Old Mill and Upper Barton Springs (which consist largely or entirely of flows from the Saline-Line and Sunset Valley Flow Routes, respectively) during low-flow conditions. The potential

variation in groundwater divides under low-flow conditions is not sufficiently understood to allow precise mapping of the convergence sites.

During certain high-flow conditions, an overflow condition occurs as the Saline-Flow Route backs up from excessive recharge, causing diversion of water to the Manchaca Flow Route and to San Marcos Springs. This condition is described in in section 4.5 and is mapped in Figure 4.4.

The Saline-Line Flow Route appears to be fed solely by the Onion Creek watershed and a relatively small proportion (< 3 %, see section 4.1.3.1) of saline-water leakage, although the Blanco River watershed may be a possible recharge source under certain flow conditions.

The southern divide lies between Onion Creek and the Blanco River (Andrews et al., 1984; Slagle et al., 1986). Traces conducted between the Blanco River and San Marcos Springs have discharged at San Marcos Springs and other springs south of the Blanco River (Ogden et al., 1986; Schindel, 2006). Traces in Onion Creek through 2002 discharged from Barton Springs and not San Marcos Springs (Hauwert et al., 2004a and b). A trace from Crippled Crawfish Cave (Site S on Figure 4.1) in Onion Creek under high-flow conditions was recovered from both Barton Springs and (to a lesser extent) San Marcos Springs. This suggests that under some overflow conditions portions of Onion Creek correspond to the southern divide. This groundwater divide fluctuates between the Blanco River and Onion Creek and is not fixed along a surface-water divide. For most purposes, however, the current delineation of the southern divide along the surface water divide between the two watersheds (Guyton and Assoc., 1964; Andrews et al., 1984) is a reasonable approximation, but it may not be sufficient for purposes such as a water balance of recharge to Barton or San Marcos Springs or for predicting the fate of spills in the Blanco River. Currently investigations are underway by BS/EACD, EAA, and COA to determine if the Blanco River contributes flow to Barton Springs under low-flow conditions. The southern divide is discussed further in Section 4.3.

4.2.3.2. Sunset Valley Groundwater Basin

The Sunset Valley groundwater basin is about 30 km^2 (12 mi^2) in size, and consists entirely of Edwards outcrop and eastern drainage areas. The basin was defined by the area of tracer injections that were recovered at Upper Barton and Main Barton Springs, but not Eliza, Old Mill, or Cold Springs. The tracer concentrations in grab samples were five to ten times higher at Upper Barton Springs than at Main Barton Springs, suggesting that Main Barton receives most of its flow from water sources other than the Sunset Valley groundwater basin.

The Sunset Valley Flow Route focuses flow from the Sunset Valley area to Barton Springs and understanding of its presence was originally based on interpretations of the Barton Springs fault and the presence of a 12-m (40-ft) deep potentiometric-surface trough crossing Loop 360 just east of Barton Creek (City of Austin, 1991; Hauwert and Vickers, 1994; Hauwert, 1995). Subsequently, injected dye traces verified the presence of this flow route and its role in providing flow to Upper and Main Barton Springs (Hauwert et al., 2004a; Hauwert et al., 2004b). Mahler et al. (2006) verified the presence of the Sunset Valley Flow route by comparing concentrations of organic contaminants in Upper Barton Springs and wells in the Sunset Valley area. Based on spring flow measurements and differences in dye concentration and chemistry, the flow contribution to Barton Springs averages about 0.28 to 0.42 m^3/s (10 to 15 ft^3/s; Hauwert et al., 2004b). Sites on or near this major flow route include Upper Barton Springs and wells 58-50-231, 58-50-221, and 58-50-2N3 (now plugged).

The divides of the Sunset Valley Groundwater Basin vary with flow condition. During low-flow conditions, when Upper Barton Springs is dry, the Sunset Valley Flow Route may shift its location to the east and converge with the Manchaca Flow Route prior to discharging at Main Barton and Eliza Springs (Hauwert et al., 2004a). This convergence is indicated by the drying of Upper Barton Springs under low-flow conditions and the occasional appearance of tracers injected in the Sunset Valley groundwater basin in Eliza Springs during low-flow conditions. Under some overflow conditions, groundwater from the Slaughter Creek watershed of the Manchaca

groundwater basin is diverted to the Sunset Valley groundwater basin through Blowing Sink Cave, as described in Section 4.4 (Figure 4.4).

4.2.3.3. Cold Springs Groundwater Basin

Part of the groundwater divide between the Cold Springs and Barton Springs basins was delineated with water-level responses to the draining of Barton Springs pool in wells by Senger (1983). Slade et al. (1986) suggested that one possible cause for a 12% difference between measured discharge and recharge in his water budget calculation could be that portions of Barton Creek could actually contribute to Cold Springs. The assumption that the entire Edwards outcrop area portion of the Barton Creek watershed contributes recharge to Barton Springs has been proved inaccurate by groundwater tracing conducted during both low and high groundwater flow conditions (Hauwert et al., 2004a). In fact, most of the outcrop area of the Barton Creek watershed overlies the Cold Springs groundwater basin. Low-flow surveys of Barton Creek indicate that most flow loss in Barton Creek also occurs over the Cold Springs groundwater basin (Smith et al., 2001).

The Cold Springs groundwater basin is about 30 km^2 (12 mi^2) in size and also consists entirely of Edwards outcrop area. As delineated by tracing under moderate or higher flow conditions, Barton Creek channel has 3.5 km in the Cold Springs groundwater basin, 2.5 km along the Cold Springs and Sunset Valley groundwater basin divides, 3 km within the Sunset Valley groundwater basin, and about 0.7 km within the Manchaca groundwater basin (Figure 4.5). The lower 1.5 km of Barton Creek channel is a gaining stretch except during low- flow conditions and under those conditions recharge losses are limited. This basin was delineated by injecting tracers into swallets in the Barton Creek and Williamson Creek watersheds and in one well in the Williamson Creek channel (Figure 4.1). All of the swallet injections were accomplished under dry or drying creek conditions, using fire trucks, water hydrants, or the receding creek flow to flush the tracer. This tracing determined that Edwards outcrop area portion of the Barton Creek watershed upstream of Loop 360 overlies the Cold Springs groundwater basin, but at least some of the flow loss downstream of Loop 360 contributes to Barton Springs. The

vicinity of the Barton and Cold Springs groundwater divide was traced under low (0.5 m^3/s or 18 ft^3/s Barton Springs flow), moderate (1.73 m^3/s or 61 ft^3/s Barton Springs flow), and high (3.0 m^3/s or 107 ft^3/s Barton Springs flow) conditions.

In 1997, dye was poured into a USGS monitor well (Site F, Figure 4.5) in Williamson Creek using diverted creekwater to flush the dye. The dye injected in the Williamson Creek well was recovered from Cold Springs and later from a well in Travis Country (well 58-50-211, Figure 4.5). The flow path from this well to Cold Springs corresponds to a potentiometric-surface trough that delineates the Cold Springs Flow Route. The portion of Williamson Creek from just upstream of Highway 290 to the Brush Country road crossing was traced only once and during high-flow conditions. Until further tracing data are available, I infer that this area contributes to Cold Springs during other recharge conditions. Low-flow measurements along Williamson Creek suggest limited flow-loss of about 0.14 m^3/s (5 ft^3/s) upstream of the Brush Country Road. Most creek recharge on the main channel of Williamson Creek occurs downstream of Brush Country Road within the Sunset Valley groundwater basin.

Although no tracers were injected in the Eanes Creek watershed, it is assumed that recharge from this watershed contributes to Cold Springs or smaller springs discharging directly into the Colorado River. Eanes Creek is within the Cold Springs groundwater basin and the Colorado River is at the lowest base elevation. The lower 1 km of Eanes Creek channel approaches within 0.8 km of Barton Springs.

The map of the Cold Springs groundwater basin divide could be further delineated by additional tracing under varying flow conditions, particularly in Barton Creek channel downstream of Loop 360, in Williamson Creek upstream of Loop 1, and along the western edge of the outcrop area in the Slaughter and Bear Creek watersheds. Except for a few injections into swallets in Onion Creek and one injection into flowing Bear Creek, all of the tracers were injected when the creeks were dry or carried only a small flow. Consequently, it cannot be ruled out that under higher creek flow conditions when most recharge is occurring, mounding beneath the creek could divert some flow upstream of Loop 360 towards Barton Springs (Raymond Slade, personal communication, 2005).

4.2.3.3.1. Estimation of Cold Springs Discharge Rate

The most precise flow measurements of Cold Springs are taken as the difference in upstream and downstream flow of the Colorado River during drought conditions when the river flow is very flow. On August 10, 1918, the U.S. Geological Survey gauged the Colorado River and discovered a 0.1 m^3/s (3.7 ft^3/s) increase between Tom Miller dam (0.58 m^3/s or 20.5 ft^3/s) and 0.4 km (0.25 mi) below Deep Eddy (0.68 m^3/s or 24.2 ft^3/s). This increase in flow is attributed primarily to the flow of Cold Springs because it is the only known major spring along this reach. On the same day, a flow of 0.4 m^3/s (14.3 ft^3/s) was measured discharging from Barton Creek, which can be attributed to Barton Springs. The 1918 flow measurement was taken during a drought and probably represents one of the most accurate instantaneous measurements of Cold Springs, but does not reflect average conditions. Because the flow of Cold Spring is a fraction of the larger Colorado River flows, a precise measurement of Cold Springs from upstream and downstream flow is possible only during drought periods when Colorado River flows were sufficiently low.

Brune (1981) described Cold Springs as consisting of at least seven springs, but only two are above the normal level of Town Lake. He listed four discharge measurements varying from 0.08 to 0.12 m^3/s (2.9 to 4.2 ft^3/s), some of which were measured by the USGS from upstream and downstream measurements of Colorado River flow. It is possible that some of the reported direct flow measurements by Brune represent only part of the flow of Cold Springs, and do not include the submerged portions of Cold Springs that he observed. The flow measurements compiled by Brune (1981) indicate that Cold Springs is a relatively constant-rate spring whose flow varies from about 0.08 to 0.11 m^3/s (3 to 4 ft^3/s). However, observations of the portion of Cold Springs above the Colorado River reveal variable flow, with additional outlets becoming active during moderate- to high-flow conditions.

Measurements of partial flow by the City of Austin in 1997 and 1999 measured exposed Cold Springs discharge of 0.14 m^3/s during high-flow conditions in 1997. At times of relatively low-flow conditions (Barton Springs discharge of 0.85 m^3/s or 30 ft^3/s) exposed Cold Springs discharge measured between 0.13 and 0.19 m^3/s (4.8 and 4.5 to 6.8

ft^3/s). Hauwert et al. (2004a) correlated partial flow measurements of Cold Springs with Barton Springs flow and suggest that minimum average Cold Springs flow may exceed 0.23 m^3/s (8 ft^3/s), although the great majority of measurements included only part of Cold Springs flow. Town Lake was lowered for 2 weeks in early 2008, exposing more but not all of the discharge points for Cold Springs. On January 29, 2008, I measured 0.35 m^3/s (12.4 ft^3/s) discharging from the exposed portions of Cold Springs and 1.87 m^3/s (66 ft^3/s) from Barton (Main, Eliza, and Old Mill) Springs.

A water balance for Town Lake was conducted by Don Rauschuber and Associates for BS/EACD (COA, 1992). The balance considered measured flows between Tom Miller Dam and Longhorn Dam, as well as measured flows from Barton Springs and measured diversion by the City of Austin Green Water Treatment Plant. The balance indicated an average excess of 0.82 m^3/s (29 ft^3/s), which could be attributed to unmeasured springs (such as Cold Springs) and other sources feeding Town Lake.

Groundwater tracing studies conducted between 1996 and 2000 delineated the groundwater basin for Cold Springs to be 30 km^2 (12 mi^2) in area (Figure 4.5). Based on the tracing data, the watershed source area for potential recharge to Cold Springs is estimated to be about 340 km^2 (130 mi^2) in size and includes:

1) the entire Barton Creek watershed contributing area. The drainage area upstream of the Lost Creek Flow Station is about 277 km^2 (107 mi^2).
2) the Barton Creek Edwards outcrop area that recharges to Cold Springs. The area between Lost Creek and Loop 360 flow stations is about 23 km^2 (9 mi^2).
3) the Williamson Creek watershed source for Cold Springs, which includes the 18 km^2 (7 mi^2) square mile drainage area upstream of Brush Country Road USGS flow station.
4) the entire 9.3 km^2 (3.6 mi^2).square mile Eanes Creek watershed, which is ungauged and has few flow measurements.
5) smaller creeks and drainages that flow directly to Colorado River, between Bee Creek and Eanes Creek. This drainage area is only about 3.8 km^2 (1 mi^2).

A first approximation of the expected Cold Springs groundwater basin discharge is estimated by comparing the size of the outcrop areas over the groundwater basins contributing to Barton Springs (211 km^2 or 82 mi^2), the average flow of Barton Springs (1.42 m^3/s or 50 ft^3/s), and the size of the outcrop area over Cold Springs groundwater basin (30 km^2 or 12 mi^2):

Cold Springs proportional flow based on groundwater basin size =

$$\frac{\text{Area (km}^2\text{)*flow (m}^3\text{/s)}}{\text{Area (km}^2\text{)}} = \frac{30 * 1.42}{211} = \mathbf{0.20\ m^3/s \text{ or } 7.1\ ft^3/s} \qquad (11)$$

The catchment area for Barton Creek extends about 300 km^2 above the Edwards outcrop area. Also, since the Cold Springs groundwater basin lies on the western edge of the Edwards outcrop area and upstream portion of Barton Creek, it will receive more sustained baseflow than eastern and artesian portions of the Manchaca and Sunset Valley groundwater basins. Artesian areas may not significantly contribute to flow except through subsurface leakage. Based on these factors, we would expect the flow of Cold Springs groundwater basin to be greater than the flow contributed by similar area of groundwater basin contributing to Barton Springs.

Another estimation of discharge from the Cold Springs groundwater basin is calculated from measured flow losses in portions of Barton and Williamson Creeks known through tracing to contribute flow. The average daily flow measured at USGS Loop 360 and Lost Creek flow stations were downloaded from the U.S. Geological Survey Web site for the period of Sept. 28, 1988, to Sept. 28, 1998. For this 10 year interval, the flow measured at the downstream Loop 360 station was subtracted from the upstream Lost Creek station. Following a rain event, the difference between upstream and downstream flow stations commonly was negative (greater at the downstream station) as a result of the local generation of runoff on the Edwards outcrop area. The difference between upstream and downstream flow stations, or potential flow loss, following storms was extrapolated back to peak flow from the trend of diminishing flow

loss that occurred after the effects of local runoff ceased. The potential flow loss is corrected only for data gaps and for post-storm runoff to create corrected flow loss that represents infiltration in the main channel of Barton Creek.

The flow loss between Lost Creek and Loop 360 flow stations is about 2.8 m^3/s (100 ft^3/s) within a few days of floods. Then flood waters are stored in bank alluvium and reach higher recharge features and higher hydraulic head increases recharge to swallets. Subsequently, the flow loss upstream of Loop 360 stabilizes at about 0.85 m^3/s (30 ft^3/s), and eventually declining to about 0.28 m^3/s (10 ft^3/s) over time. For the 10-year period of record, the average daily flow loss along the main channel of Barton Creek upstream of Loop 360 is 0.4 m^3/s (14 ft^3/s). The flow loss on Barton Creek is frequently limited by the amount of upstream allogenic flow. The creek bottom of Barton Creek is also limited by the recharge capacity of a relatively few sites where creek flow loss or recharge gain occurs (Smith et al., 2001). Any additional runoff beyond its limited recharge capacity will flow downstream of Loop 360 where it potentially can contribute to Barton Springs or flow directly to the Colorado River.

The USGS flow station at Brush Country Blvd. has a record from March 11, 1993, to September 30, 2003. A recharge loss of roughly 0.14 m^3/s (5 ft^3/s) was measured along the main creek channel of Williamson Creek upstream of Brush County in the Cold Springs groundwater basin using instantaneous flow measurements with a Marsh McBirney flow meter. Flow loss to Cold Springs within the Williamson Creek channel was calculated by estimating a daily flow loss of 0.14 m^3/s (5 ft^3/s) for each day where the average creek flow was greater than zero. It is likely that this flow loss would vary, such as increase during storms or diminish as specific features plug temporarily. However, insufficient upstream flow data were available. The average flow loss to Cold Springs from Williamson Creek over the 6.5-year period from March 11, 1993, to September 30, 1999, was only about 0.02 m^3/s (0.65 ft^3/s).

Additional unmeasured contributions to the recharge of Cold Springs were not estimated because the possible errors would be significant compared to their possible contributions. These contributions include recharge from direct infiltration over the Cold Springs groundwater basin, and urban contributions such as infrastructure leakage

through water lines, wastewater lines, septic tanks, and lift station releases (Garcia-Fresca, 2004). The City of Westlake operates at least one floodwater injection well that is a converted internal drainage sinkhole.

Given the traced size of the Cold Springs groundwater basin, the flow loss occurring within its groundwater basin, and the flow gain estimated to the Colorado River, it is not possible to accept that Cold Springs flows at a relatively constant 0.08 to 0.11 m^3/s (3-4 ft^3/s) or that this range approaches its flow average. A water balance for the Cold Springs groundwater basin suggests that its minimum average discharge is about 0.42 m^3/s (15 ft^3/s) or more. The Barton Creek watershed contributing area may be the largest source for potential recharge to Cold Springs. The Cold Springs groundwater basin contains only about 31 km^2 (12 mi^2) of the 340 km^2 (130 mi^2) Cold Springs source area that extends into the contributing area of the Barton and Williamson Creek watersheds.

An alternate method for determining Cold Springs flow is constructing a rating curve from water levels of a well in the Cold Springs basin using a number of instantaneous flow measurements derived by tracer dilution tests (Kilpatrick and Cobb, 1985; Bennett, 2000, personal communication), or possibly by mapping thermal or chemical plumes from Cold Springs into the Colorado River.

4.2.3. Hydrogeologic Parameters Derived from Dye-Tracing Data

The Chatwin analysis of longitudinal dispersion yields Peclet values greater than 1,000 for all five of the traces examined (Table 4.1). The Barton Springs well test reported by Senger (1983) showed the highest of the five traces, with a Peclet number of about 10^8. Peclet numbers below 0.4 would suggest a dispersion-dominated system, while values over 6 indicate a system dominated by advection (Fetter, 1992). The Peclet values from five tracer tests in the Barton Springs Segment are two to seven orders of magnitude above six. Thus, this aquifer can be characterized as having a strong component of advection, where the molecular diffusion and transverse dispersion are small and the longitudinal dispersion is very low compared to the advective component of transport. This result is intuitively obvious considering that a relatively low mass of

injected dye (16 kg) can be readily recovered across the extent of the Barton Springs Segment. The low dispersion found in the five tracer tests contradicts Senger's (1983) impression that dispersion was very high within the Barton Springs Segment.

Some studies have looked at increases in longitudinal dispersion with scale. Based on 59 studies worldwide, Gelhar et al. (1992) found an increase in dispersivity with scale; however, once the low confidence tests were filtered out the trend was not significant. Domenico and Schwartz (1998) summarized that small-scale column tests show a typical range in dispersion from 10^{-2} to 1 cm while dispersions from larger scale field measurements typically range from 0.1 to 2 m. The discrepancy between scales is attributed to heterogeneities present at larger scales. The relation between increasing dispersion and scale within the Barton Springs Segment is insignificant based on four of the five tracer tests examined (Figure 4.6b).

Sorption depends on the properties of the rock surfaces or fracture skins, the properties of the solute being sorbed, as well as advective gradient. Sorption of dye from the traces cannot be precisely derived except as a maximum possible value since many factors, including dye properties influence how much is recovered. Recoveries of 0% to 77% in traces shown on Table 4.1 can be potentially affected by factors including the following:

(1) effects of sampling interval on quantification of the tracer loading, particularly during the peak breakthrough,
(2) long-term storage in the aquifer discharged below detection limit or in pulses between sampling events,
(3) relatively low mass of injected tracers,
(4) accuracy of measurement of spring flow rates,
(5) sorption by fracture skins and conduit walls,
(6) sorption of dye by organic constituents in the groundwater,
(7) adsorption of non-conservative dyes by fine-grained fill materials,
(8) the potential that unknown discharge sites of the dye were not monitored,
(9) flow conditions,

and

(10) the potential for insufficient number of monitoring sites traced and analyzed.

The amount of dye injected is likely a large factor for how much is recovered. Consequently, the recovery of a small mass of dye may not reflect the sorption of a large spill volume of substance with different properties.

Hauwert et al. (2004a) hypothesized that groundwater flow from the western side of the Edwards outcrop area may be through more immature flow paths with smaller recharge areas and more limited poorer hydraulic connection. The traces from the western side of the outcrop area to discharge springs prior to 2001 with poor recovery were all conducted during low-flow conditions. However, post-2001 traces injected under moderate or higher flow conditions, including J, K, 10a, showed very strong hydraulic connection to the western side of the outcrop area. One exception was tracer T, whose lack of recovery is attributed to the tracer being trapped in a mud plug at the bottom of the injection cave. Zara Environmental, City staff, and volunteers who cleaned out the cave in 2007 encountered the dye in mud excavated from the bottom of the cave. Therefore, poor hydraulic connections along flowpaths to the western side of the outcrop area may be the result of dried conduit connects or low hydraulic gradients during low-flow conditions and there is no evidence that western flow paths are less developed.

4.3. FLOW PATHS DERIVED FROM WATER-LEVEL DATA

Water levels in wells and caves provide valuable information about groundwater flow paths. Potentiometric surfaces in the Barton Springs Segment can have considerable relief. For this reason, water-level data are considered together with more definitive groundwater-tracing data to derive flow paths.

4.3.1. Water-Level Measurement Methodology

Water-level measurements were collected from well and spring sites during the course of the study so that potentiometric maps could be prepared. A potentiometric surface represents the elevation that water would rise in a well screened within the aquifer of interest. The potentiometric-surface elevation is different from a water table, because within the artesian area, the water level in an Edwards Aquifer well will rise above the top of the Edwards Aquifer. This map serves to estimate the groundwater-flow paths between injection sites and monitored sites where the tracer is detected. The depth to water within a well was measured using an electric water-level meter read to the nearest 0.003 m (0.01 ft) from the top of casing or other reference point. This resolution is necessary when comparing changes in water level within the same well. Some potential errors in mapping the potentiometric-surface elevation include inaccurate measurement of the elevation of the reference point; changes in the potentiometric surface over time; short-term, localized changes in water level due to pumpage; mixing of separate aquifer-producing units because of well construction; and extrapolation of the potentiometric elevation between measured sites.

The top of casing or spring surface elevation of nearly all of the sites from which water-level measurements were taken were measured by a Trimble XRS or Pathfinder Global Positioning Unit (GPS). The GPS data was postprocessed to achieve maximum horizontal and vertical errors of about 1 m (3 ft). A comparison of 10 elevation measurements collected at a first order benchmark on different days by this GPS unit indicated an average accuracy of $\pm$ 0.75 m (2.47 ft) in elevation measurements with a maximum vertical error of 1.27 m (4.17 ft.) For other sites, the elevation of the reference point was either estimated from a 7.5 minute, 10- to 20- ft (3.05-to 6.1-m) contour

interval USGS topographic map, surveyed relative to sea level to within 0.003 m (0.01 ft), measured with a digital altimeter, or estimated from City of Austin 2-ft (0.61 m) contour interval topographic surveys or other site-survey maps. The surface elevation of a flowing spring was used as the potentiometric-surface elevation if the spring likely represents discharge of the water table from the Edwards Aquifer. The resolution of one meter (3 ft) is adequate for mapping 3 m (10 ft) interval potentiometric surfaces.

The span of time over which the water-level data were collected for a potentiometric map ranged from 2 days for a local area to several weeks for the complete map. Continuous water-level measurements were available from 9 to 15 water-level monitor wells maintained throughout the Barton Springs Segment of the Edwards Aquifer by the BS/EACD and USGS. The water-level data from wells not screened within the Edwards Aquifer were not used for the potentiometric-surface maps. However, on the western side of the study area, wells commonly are screened in both the Edwards and upper Trinity Aquifers to the extent that these cannot be fully evaluated without further information. In addition, wells on the eastern side of the study area commonly do not fully penetrate the Edwards Aquifer. However, there is no evidence that the upper and lower portions of the Edwards Aquifer are not well connected hydraulically.

4.3.2. Applications of Water-Level Analysis

Davis and Deweist (1966) suggested that the angle between potentiometric surfaces and actual flow directions quantifies the anisotropy of an aquifer. Sayre and Bennett (1942) and Arnow (1963) noted that apparent discrepancy between water-level surfaces and flow directions actually is caused by insufficient distribution of water-level measurements. Focused or discrete recharge through a swallet can create potentiometric mounding underneath a creek, which in some cases, where insufficient water-level data are present, can lead to the interpretation that flow lines are parallel or upgradient of the mapped potentiometric table slope (Thrailkill, 1968).

Quinlan and Ray (1981) mapped potentiometric troughs and groundwater basins in the Mammoth Cave area using 1,400 well and 500 dye traces. Their study showed that

groundwater flow paths converged similar to stream tributaries and carried flow at rates up to 10 km/day.

Thrailkill (1985) examined water-level measurements from 65 wells in Kentucky, and, when used in conjunction with groundwater tracing data, they indicated the general groundwater basins and interbasins. The potentiometric lows may suggest major conduits of groundwater flow in karst areas. Thrailkill recommended that in karst areas researchers should not rely solely on widely spaced well data averaged together to determine groundwater-flow directions, or to discount water-level data points simply because they differ abruptly from other water-level data. White (1999b) illustrated the flow from major phreatic groundwater conduits to the surrounding aquifer during peak recharge periods and flow from the surrounding aquifer to conduits during recession periods.

Water tables are not planar in karst aquifers and the determination of downgradient directions can be complicated by numerous factors creating gradients. Potentiometric mounding, which occurs during the rising limb of the Barton Springs flow hydrograph and for some time after its peak, produces gradients both into the adjacent aquifer from major flow paths and toward the discharge springs. Potentiometric troughs form during the recession period of Barton Springs flow and drain storage from the aquifer into the major flow paths. Figure 4.7 illustrates multiple downgradient flow paths during mounding conditions: 1) gradients on either side of focused recharge sites such as creek swallets, 2) gradients from preferential flow routes into aquifer storage, 3) gradient along the preferential flow paths to discharge springs, and (4) bifurcation gradients through periodically saturated upper-level conduits. Mounding and recession troughs create the challenge of finding "relevant" groundwater water-quality and water-level monitoring sites as discussed by Quinlan (1989 and 1990). During high-flow conditions of 2005 tracing from Site S on flowing Onion Creek (Figure 4.1), mounding along the preferential flow path was evident from the recovery of tracer in wells 430 m (1,400 ft) southeast and 210 m (700 ft) northwest of the flow path (Figure 4.4). However, tracers injected in Site O on dry Onion Creek during low-flow conditions in 2000 were recovered only from wells very near the flow path. Many random well locations intercept

a relatively small amount of groundwater flow from mixed sources or generated from a relatively small source area or isolated source.

The development of potentiometric mounds and troughs causes high variation in water levels along preferential flow routes inside the artesian area. Consequently, the greatest sensitivity to water-quality and water-level changes is found on or near preferential flow routes. This is best indicated by the strong recovery of a distant tracer injection (Milanović, 1981, p. 128). Conversely, on the Edwards outcrop area where conduits are only partially filled, water levels remain relatively static unless flood flows are sufficient to fill the cave and conduits.

The depth of a potentiometric trough varies, but the maximum depth determined from available wells reflects its the significance as a flow route. Detailed mapping of the water table between the City of Sunset Valley and Barton Springs revealed a 12 m (40 ft) deep potentiometric trough corresponding to the Sunset Valley Flow Route (Figure 4.8; Hauwert and Vickers, 1994; Hauwert et al., 2004a).

Additionally, the water level of 58-50-2N3, a sediment-laden well at the lowest point of the trough in the Sunset Valley Flow Route, showed a peculiar lack of variation at lower flow conditions (Hauwert and Vickers, 1994; Figures 4.9). Compared to water levels in well 58-50-301 (Figure 4.9), water-levels in well 58-50-2N3 fluctuate very slowly between 131 and 133 m above mean sea level, which may be interpreted as resulting from a partially water-filled conduit of the Sunset Valley Flow Route. Thus, the vertical height of the conduit is estimated to be about 2 m or more in diameter and its base elevation about 130 m msl. From this information, the primary conduit of Sunset Valley Flow Route is positioned in the uppermost pulverulitic bed at the top of the Kirschberg Member. Bonacci (1995) found similar delayed responses that revealed the elevation and dimensions of a major cave conduit when he compared the discharge of Ombla spring in Croatia to water-level response of wells within the karst aquifer and

Relatively constant water levels are observed in a second well near a major partially-filled cave conduit associated with a preferential flow path. Well 58-50-411 is located near the extension of a perennial southeast-flowing cave stream known as Eileen's River passage (Figures 4.10 and 4.11). The water-level elevation is about 163 m

(535 ft msl) in the siphon closest to the well and must rise roughly 5 m (15 ft) before it can enter a higher "Dark Side of the Moon" passage: a large, circular passage that slopes northeast toward Barton Springs. In well 58-50-411 the water-level elevation generally varies from 165.0 m to 165.5 m above mean sea level, which is higher than in the nearby flowing stream passage (Figure 4.12). Blowing Sink Cave and well 58-50-411 lie near the general groundwater divide between the Manchaca and Sunset Valley groundwater basins. However, a tracer injected at site H was detected in well 58-50-417 across this approximate divide within the Sunset Valley groundwater basin. The tracer was not detected in well 58-50-417 until after a large rain event and 1 month after the tracer had already arrived at Barton Springs through the Manchaca Flow Route. It is interpreted that the limited recharge area and the high hydraulic conductivity of the southeastward flowing cave stream causes the water level in the cave stream and well to be maintained at a stable elevation. Only under short-term large rain events and associated rising water levels within the Manchaca groundwater basin and flooding on Slaughter Creek does the southeastward flowing cave stream become overwhelmed and water-filled, such that flow is diverted through the upper-level Dark Side of the Moon passage, and into the adjacent Sunset Valley groundwater basin. The temporary southward shifting of the groundwater divide appears to occur under local overflow conditions (Figure 4.4).

The hydraulic condition of the Saline-Line Flow Route is gauged from abundant monitoring records from well 58-50-301 located near and at times within the Saline-Water Zone (Figure 4.13). Relative to Barton Springs flow, water levels in the well recede rapidly but demonstrate a delayed response on the rising end of the hydrograph. Once recharge has ceased, water-levels in 58-50-301 remain relatively static as Barton Springs flow declines, then follow a predictable recession until the next recharge event. The lack of water-level decline relative to Barton Springs during recession suggests that the Saline-Line Flow Route is less transmissive than the Manchaca Flow Route, as observed in delayed tracer arrival from Onion Creek to Old Mill Springs (Figure 4.2). Hauwert and Vickers (1994) attributed slight water-level responses of well 58-50-301 after rainfall to be the result of "diffuse flow through smaller pores and fractures" but I

now attribute the well's response to a relatively small and isolated conduit associated with the Saline-Line Flow Route.

Under some overflow (B) conditions (Figures 4.13 and 4.4), Onion Creek recharge overwhelms the Saline-Line Flow Route, causing flow to back up and divert all flow to the Manchaca Flow Route and a smaller amount to San Marcos Springs. During high-flow conditions in May 2005 similar to the previous 2002 injection, eosine tracer was again injected into Cripple Crawfish Cave (Site S), but with a different result (Figure 4.1). Under these "B" overflow conditions, when the Saline-Line Flow Route is obstructed by excess flow, the second or late tracer arrival from Onion Creek injections does not occur. At the time of injection, Onion Creek flow loss was about 0.6 to 0.85 m^3/s (20 to 30 ft^3/s), which was considerably lower than the 2.3 to 2.8 m^3/s (80 to 100 ft^3/s; Smith et al., 2001) loss normally measured across the Edwards outcrop area. Tracer recoveries in unusual locations were interpreted to indicate diversion flow from the Mountain City area across Onion Creek to a western secondary flow path of the Manchaca Flow Route (Figure 4.4). Another explanation (Smith et al., 2006) for the diversion of Onion Creek flow to San Marcos is that the Blanco River flow and San Marcos Springs flow were lower during the 2005 traces than during 2002 injections, even though Barton Springs flow was about the same flow during both injections. This could have allowed southward flows in 2002 but not 2005. Based on existing tracing and water-level data, this relatively rare overflow condition occurs when water depths in well 58-50-301 are less than 41 m (130 ft), shown as area B in Figure 4.13. In well 58-50-301, water depths less than 41 m occurred 944 days over a 5,157-day period from November 4, 1991, to November 15, 2006, of daily readings by BS/EACD (or 18% of the 15 year record). The precise quantification of this overflow condition requires additional refinement with additional tracing from Onion Creek, particularly under high-flow conditions.

Other methods are used in wells to detect caves that could be associated with preferential flow paths. Well log methods such as downhole camera and caliper logs have been applied in the Barton Springs Segment. Airflow commonly is observed blowing into or out of wells, although the airflow may cease or greatly diminish under high-flow

conditions when the cave discharging the air is submerged. Consequently, the depth of the cave can be determined by the water depth at which the airflow ceases, as water levels rise at a later date. The airflow depth should be verified by multiple observations on different days, because of changes in airflow resulting from temperature and pressure differences between the surface and subsurface. Strong airflow in a well is an indication of a relatively well-connected conduit and large unsaturated porosity. Perhaps the most direct means of examining caves in wells or boreholes is to drill or excavate a sufficient sized borehole connection to the cave, such as Honey Creek Cave, where a cave-radio located borehole shaft and well were drilled to intercept a known cave (Veni, 1997), and Inner Space Caverns, where a 0.6 m (2 ft) diameter borehole shaft allowed human exploration (Sansom and Lundelius, 2005).

Basing groundwater flow directions on potentiometic surface maps alone can yield erroneous results when not verified with groundwater tracing. A potentiometric-surface mound beneath Onion Creek led Stein (1995) to conclude that groundwater south of Onion Creek did not flow to Barton Springs under high or moderate-flow conditions, but instead flowed to City of Kyle wells or San Marcos Springs. The potentiometric data upon which the interpretation was based were accurate, but widely spaced water-level measurements do not show the details necessary to reveal destinations that are revealed by tracing (Figure 4.14). Groundwater flow does bifurcate and even trifurcate around Onion Creek, but all flow paths lead to Barton Springs except under rare occasions where a relatively small portion of flow is directed to San Marcos springs (Figure 4.1; see Saline-Water Zone description above). In this case, the choice of test (potentiometric-surface mapping versus groundwater tracing) can lead to two different interpretations. When a smaller area north of Onion Creek is mapped with a greater density of water-level measurements supported with geological mapping and groundwater tracing, details such as potentiometric troughs are discernible that are not detected with wider-spaced measurements (Figure 4.15).

4.4 WATER-QUALITY DERIVATION OF FLOW PATHS

Aquifer geochemistry is only examined superficially herein for the purpose of characterizing groundwater flow paths in the Barton Springs Segment. Abbott (1973) and Senger (1983) found the Barton Springs Segment to be generally unsaturated with respect to calcite and dolomite, while the Saline-Water Zone was supersaturated with respect to calcite and dolomite. Geochemical modeling revealed that mixing of these two water types decreases the carbonate saturation indices, which could enhance dissolution of the Edwards Aquifer along the mixing zone (Abbott, 1973). Abbott (1973) offered the explanation that an undersaturated condition for Barton Springs waters with respect to calcite and dolomite resulted from fast groundwater flow and insufficient residence time. Garner (2005, see section 4.6) showed that well water-quality in 58-50-211 on the western side of the outcrop area became undersaturated with respect to calcite for several days following a rain event.

The differences in sulfate and chloride concentrations between the Barton Springs outlets were consistent with the delineation of groundwater basins from tracing data and the relative contributions from major flow path sources (Hauwert et al., 2004b). Examining specific conductance data from Main Barton Springs for 1999 to 2003, Massei et al. (2007) distinguished different source contributions to Barton Springs that were interpreted to represent recent recharge, the Saline Water Zone, and the matrix. The relative contributions from these sources vary from year to year.

Garner (2005) and Garner and Mahler (2007) used major ion data collected by the USGS in 26 wells across the Barton Springs Segment to interpret which wells were on major and minor flow paths, as well as wells influenced by Trinity Aquifer and Saline-Water Zone mixing (Figure 4.16). Garner's major flowpath wells were characterized by relatively low specific conductance, diminished Mg/Ca concentration ratios during high-flow conditions, decreased downgradient Mg/Ca concentration ratios, increased Ca-HCO_3 concentrations, and increased sensitivity to contamination sources. Minor flowpath wells were characterized by Garner by decreasing specific conductance during flowing creek conditions. He found that minor flow path wells have a lower vunerability to contamination than major flowpath wells as indicated by nitrate nitrogen concentration

less than 2 mg/l. His findings are that of 26 randomly-located wells used in USGS sampling, four wells intersect major flow paths, five wells intersect minor flow paths, five wells across the Barton Springs Segment receive flow from the Saline-Water Zone, and six wells receive flow from the Trinity Aquifer. Therefore, Garner's (2005) geochemical designation of wells as being on major flowpaths agrees with the interpretation presented in Figure 4.1 for 8 of 10 wells. For 6 of the 10 wells designated on major or minor flowpaths were within 1 km of a primary or secondary flowpath interpreted on Figure 4.1. It is possible that some wells whose geochemistry suggested flowpath influence by Garner and Mahler (2007) are discovered later through tracer recovery to be on primary, secondary, or tertiary groundwater flow paths. Geochemical characterization of existing data using the Garner and Mahler (2007) approach may be a useful screening tool to identify the optimum wells for monitoring tracer recovery because all wells cannot be monitored in any trace. The application of geochemical characterization of flow paths is intriguing, brings forward new information, and bears further study.

Geochemical analyses of the Barton Springs Segment have indicated that urban degradation is localized to specific areas of the aquifer, along major flow paths, and springs (Hauwert and Vickers, 1994; Hauwert, 1995; Barrett and Charbeneau, 1996; Hauwert et al., 2004a and b; Garner, 2005; Mahler et al., 2006). Hauwert and Vickers (1994) and Hauwert (1995) showed the localization of poor water-quality based on elevated indicator bacteria, sediment, trace metals, and organics along the Sunset Valley Flow Route. Hydrocarbon contamination also was detected beneath a site of surface petroleum contamination indicating that surface contaminants could be detected in the underlying groundwater. Low levels of pesticides have been also detected at sites across the aquifer. The City of Austin collected regular samples from Barton Springs and Cold Springs and documented anticipated decline in local groundwater with urbanization and correlated creek water quality with levels of impervious cover (Johns, 1994; Johns and Pope, 1998). These results suggested that poor water quality was a useful criteria for identifying flow paths when the contaminants are sufficiently far from the source.

Similar to the downstream convergence of injected tracers, point and non-point-source contamination is more likely to be encountered along a preferential groundwater flow path (Hauwert et al., 2004a and b). Because primary flow routes discharge at a spring, springs will have more poor water-quality constituents than most wells in the same aquifer. Tracing and geochemical data showed greater advective transport to the discharge spring than to a well than within a small karst watershed of Bushkill Creek in Pennsylvania (Toran et al., 2007).

Key contaminants also can serve as tracers from source areas along major flow paths to their discharge springs. The USGS refined contaminant sampling of the Barton Springs Segment to include: (1) consistent annual sampling of wells; (2) sampling of selected sites following rain events; (3) the development of very low detection limits and sophisticated sampling methods; and (4) the expansion of water-quality and sediment-quality parameters with the National Water Quality Assessment program (Mahler et al., 2006). Mahler et al. (2006) and Mahler and Massei (2007) reported that water chemistry differences between wells and spring orifices revealed separate flow paths. Although the mean nitrate-nitrogen concentration of Main, Eliza, and Old Mill varied only by 0.05 mg/l, the difference in concentrations between springs collected after a recharge event on the same day suggested that different groundwater flow routes within the same groundwater basin were being followed. Tetrachloroethene and chloroform concentrations were similar in Main and Eliza springs and slightly lower in Old Mill Springs. Following storm events, a 5-hour delay in specific conductivity response at Old Mill Springs compared to Main and Eliza springs was observed. The nitrate-nitrogen, atrazine, simazine, prometon, and bromodichloromethane concentrations in Upper Barton Springs always were considerably higher, suggesting a separate and more urbanized source area. Chloroform and freon concentration similarities between Upper Barton Springs and a well in Sunset Valley suggested a flow path between those areas. The results of this geochemical analysis overall were consistent with flow path and groundwater basin interpretations presented in Figure 4.1.

The presence of persistent and heavy sediment loading in wells and springs has proved to be a reliable criterion for the presence of major groundwater flow paths in the

Barton Springs Segment. Quinlan (1989) suggested that wells where high turbidity was observed after rains were likely sites to recover tracers along fast-flowing groundwater flow paths. A turbid plume discharged from Barton Springs following a 10-cm storm in 1980 (Slade et al., 1986). Other sediment plumes were observed discharging from Barton Springs in the 1990s; most were in association with rain events. Sediment-laden wells are occasionally encountered that can produce high turbid loads sufficient to fill a number of boreholes by as much as 50 m and a municipal water storage tank up to 0.5 m (Hauwert and Vickers, 1994). This amount of sediment is too large to originate simply by sloughing of adjacent loose materials around a wellbore. Furthermore, the sediment largely has a consistent composition of euhedral dolomitic silt, which is correlated to specific pulverulic layers in the Kirschberg Member (Mahler, 1997; Mahler and Lynch, 1999; Lynch et. al., 2004). The occurrence of sediment-laden wells is interpreted to be limited to sites where groundwater velocity is sufficiently rapid to transport and erode sediment for long distances through the aquifer (Hauwert and Vickers, 1994; Mahler, 1997).

The presence of sediment-laden wells was used as criteria for mapping possible primary or secondary groundwater flow paths (Figure 4.1). To determine which wells qualified as sediment-laden, all BS/EACD well purging files from 1993 to 2000 that document changes in field parameters such as turbidity using a calibrated Horiba U-10 prior to sampling were examined. Turbidity measurements and visual observations suggested the presence of sediment was readily distinguishable, even without a detailed mineralogical analysis. A threshold of 40 nephelometric turbidity units (NTU) was selected to identify sediment-laden wells. Wells were not considered sediment-laden for this study if: (1) the turbidity diminished and remained below 40 NTU over the purging period; (2) turbidity was observed in association with large declines in water levels within the well or even drying of the well; and (3) the sediment appeared to be short term, such as during well development shortly after well drilling. It has been observed that wells directly on a preferential flow path (such as 58-50-2N3, Figure 4.8) have high suspended solids, while others near the flow path may have sediment only occasionally and frequently during changing flow conditions. In addition to measurement of turbidity

with a field meter, evidence of heavy sediment loading episodes may be seen from diminished total well depths, discarded sediment filters, sediment-filled water tanks, and piled sediment at well discharge points. Some wells are reported as being unusually sediment-laden by a driller or well owner. Typically, well owners and drillers have handled the sediment problem to varying degrees of success by installing sediment filters, by waiting for seasonal changes, or by plugging the well and drilling a new well.

4.5. AQUIFER TESTING

Aquifer testing provides information on the local anisotropy and heterogeneity of aquifers. The shape of the cone of depression formed around tested well fields can reveal anisotropy. The lateral distribution of drawdown also provides insight as to how pumping wells are influenced by the major flow routes and the surrounding aquifer. The mapped cone of depression was used to delineate the source area for a well field in a karst aquifer of Pennsylvania (Barton and Risser, 1991). Palmer (1999) mapped the highly elongate cone of depression resulting from a 31-hour aquifer test in the carbonate Beekmantown Formation of Pennsylvania. A 5-hour aquifer test in West Virginia showed the growth of an anistropic cone of depression parallel to the direction of stratigraphic strike in a karst aquifer (Jones, 1999). Hantush (1966a and b) described the growth of elliptical cone of depression from well pumping in an anisotropic media. The major axis of the cone of depression lies in the direction of greatest hydraulic conductivity. Hantush warned that using traditional analytical methods that assume isotropic conditions can yield erroneous values of transmissivity and storativity.

In many cases, deviations from typical type curves for confined, unconfined, leaky, and/or double-porosity conditions result from boundaries such as recharge, barriers, well-bore storage, partial penetration of wells, and interference from other pumping wells (Kruseman and deRidder, 1990; Barton and Risser, 1991). Ogden (1986) observed the effects of barrier boundaries, water-filled conduits, and other recharge boundaries reflected in deviations from Cooper-Jacob and Theis-type curves in the San Marcos area of the San Antonio Segment of the Edwards Aquifer. The cone of depression from a pumping well expands and, given time, it may eventually draw from a significant

water-filled conduit, causing the rate of drawdown to diminish in a response similar to that expected for a test conducted near a recharging creek. Mikels (2001) observed the recharge boundary effects of Onion Creek during a test of the nearby City of Buda municipal wells in the Barton Springs Segment.

Fracture (or fissure) flow can be considered as an intermediate flow regime between open conduit flow, which is turbulent, and continuum or porous media flow, during which Darcian (laminar) flow occurs through small pores within the matrix. Various analytical approaches can quantify the hydraulic properties of a fracture flow system and evaluate the application of different conceptual models. The cubic law assumes that discharge through a fracture is directly proportional to the cube of its aperture, and that no significant flow occurs through the matrix (Romm, 1966; Witherspoon et al., 1980; Neuzil and Tracy, 1981; Tsang and Witherspoon, 1981). In a double-porosity system that is dominated by matrix and fracture flow, mineral deposition on the fracture surface or fracture skins can restrict flow from the matrix into the fractures, which can result in a pseudo-steady state which appears as a deflection from a standard Theis curve (Moench, 1984).

Some studies (Razack and Huntley, 1991; Huntley et al., 1992) indicate that aquifer testing underestimates transmissivity in heterogeneous alluvial aquifers but overestimates transmissivity in fractured aquifers because of well efficiency and turbulence. Robins (1993) notes that the transmissivity of a fractured aquifer is underestimated because the wells tested do not intersect fractures, fissures, or conduits, which are primary elements of regional flow. However, if the wells tested are only those that intercept conduits/fissures, then the transmissivity could be overestimated. Rovey (1994) suggested that in karst areas, hydraulic conductivity increases with area scale, up to some representative elemental volume that represents regional scale. This is attributed to the increasing dominance of the "larger but rarer conduits" in the flow system. Rovey (1994) believed that the regional average hydraulic conductivity value could be obtained by averaging a large number of small-scale aquifer tests.

An explanation for the apparent increase in hydraulic conductivity with scale is the focusing of flow along conduits, and the small likelihood of any well producing

directly from the few conduits that carry most of the flow, values of transmissivity derived from aquifer tests underestimate those estimated by groundwater tracing of the conduits where most flow occurs (ASTM, 1995).

Within the Barton Springs Segment, Alexander (1990) found a general correlation between increasing specific capacity measured in 27 well tests, including 6 measurements he collected, and decreasing distance from 938 lineaments interpreted by either Charles M. Woodruff, Fred Snyder, or Albert Ogden, but no correlation with the 48 lineaments interpreted by all three investigators. He found that 10 of the 13 wells with highest specific capacities were positioned to the southeast of the nearest lineament. None of the 13 wells with the lowest specific capacity values were located within 305 m (1000 ft) southeast of a lineament.

4.5.1 Aquifer Test Analysis Methodology

Since 1989, the BS/EACD has required aquifer testing of permitted wells in order to measure the potential for impacts on nearby wells and the hydraulic parameters of the aquifer. After 1993, the tests involved measuring existing wells radially around the test well at varying distances up to 4 km away (BS/EACD, 1994). The author participated on behalf of BS/EACD in the design, monitoring, and independent analysis of 10 of these tests up to the year 2000, and three after 2000. The well owner is responsible for selecting a period for the test when rain events, flowing creeks, and local well interference are minimized and the well fields are fully recovered from previous pumping. The BS/EACD-required aquifer tests rely only on existing wells where nearby well owners volunteer cooperation. Further, not all tests have sufficient maximum drawdown data to map the cone of depression in detail.

I analyzed the data collected during all of the tests in which I participated. The maximum drawdown for each monitored well during the aquifer tests was calculated where sufficient measurements were made. In some cases it was necessary to correct drawdown for background rise or fall of water levels. During many tests, one of the monitored wells was being pumped by a resident or was influenced by another local high-capacity well at some point during the test. This well interference required corrections or,

in some cases, preventing useful data from being collected from the monitored well. A common challenge is collecting sufficient background water-level data in each monitored well prior to aquifer testing to clearly show whether any drawdown was created by the test well. Monitoring of the recovery phase after the test well was shut off allowed verification when increases in water levels of the monitor wells were observed. Although recovered water levels were not always the same as water levels measured prior to the test, when properly corrected for background fluctuations, the total recovery should approximately reflect the total drawdown. A map of the cone-of-depression surface was prepared by mapping of maximum drawdown observed in wells around the pumping well. Local anisotropy was measured as the ratio of minimum to maximum distances from the pumping well to a selected drawdown contours (Figure 4.17). The aquifer test results are summarized in Appendix E. The detailed test data are on file at BS/EACD.

Well efficiency is affected by the cased intervals, the materials used in a filter pack and well screen, and drilling mud caked along the borehole (Kresic, 1997). Mace (1997) found that typical corrections to drawdown for well efficiency were unrealistically high for pumping tests in the Edwards Aquifer, to the extent that corrections to drawdown exceeded measured drawdown 10 to 20% of the time. The vast majority of Edwards Aquifer wells are open-hole construction and contain large voids, so the drilling fluids are unlikely to plug water-producing intervals. However, most aquifer tests focus on high-capacity water-supply wells that are cased and screened and, therefore, poor design could affect by well efficiency. No measurement of well efficiency was made in the tests reported here, which requires drawdown measurement at different pumping rates (or step-drawdown test), so it is possible that in some tests the transmissivities are underestimated.

Analytical modeling was performed on the test results from wells that were relatively free of interference effects to measure the aquifer parameters of transmissivity and storativity. Most of the pumping and recovery phases of the tests were examined using analytical solutions, including Theis (1935), Cooper-Jacob (1946), and Moench (1984). A description of these methods and their assumptions are provided in Appendix D. The software Aqtesolv for Windows was used to calculate most of the transmissivity

and storage values. This allowed simultaneous correction for partial penetration and varying pumping rates (Duffield, 2000). On tests performed within the artesian area, most wells are partially penetrating to some extent; consequently, the transmissivity may be underestimated, particularly where wells did not penetrate through the Kirschberg Member.

From 1993 to 2000, about 160 specific-capacity measurements were collected from wells throughout the Barton Springs Segment (Appendix F). Most of these measurements were collected from wells during groundwater sampling or in response to concerns of water loss for well owners. Water levels were measured before and after pumping using an electric marked conductor line (or eline). The test typically lasted for 20 to 40 minutes, although some were as short as a few minutes or as long as several hours. A longer duration allows the well to reach its maximum drawdown. Therefore, duration is likely the best single gauge of the accuracy of the test. Short test durations underestimate drawdown and overestimate specific capacity and transmissivity. On rare occasions, the well was already pumping on arrival, in which case the pumping rate and pumping water level were measured before the pump was shut off so the water levels could recover. Pumping rates for specific-capacity tests most often were measured by the time required to fill a 20-l (5-gal) bucket. In other cases, a dedicated flow meter was used to measure the volume of water discharged over a 1-minute interval. Nearly all specific-capacity measurements were collected from domestic wells supplying single households. The measurement of specific-capacity (pump rate/drawdown) was converted to transmissivity using empirical relations developed by Mace (1997) from other Edwards Aquifer pumping tests:

$$T = \text{Transmissivity} = 0.76 * (\text{Specific capacity})^{1.08} \qquad (12)$$

where both T and specific capacity are in m^2/day

The distance from wells with aquifer test and specific-capacity measurements to closest mapped primary or secondary groundwater flow paths was measured. Because the

saturated thickness may influence the relation between distance to flow path and transmissivity, the hydraulic conductivity values were calculated by dividing transmissivity by estimated saturated thickness:

The relation between hydraulic conductivity and distance to nearest estimated flow path is affected by:

1) The fact that the location of the groundwater flow paths shown on maps in some areas is not known with great precision. Actual locations could be a hundred meters or more from estimated locations where well or spring data are scarce.
2) The existence of other primary, secondary, or tertiary flow paths that are not yet known or mapped.
3) The variability of the hydraulic influence of nearby flow paths, which are affected by flow conditions in the unconfined Edwards outcrop area. Water-bearing conduits connecting flow paths and wells may dry during low-flow conditions.
4) The accuracy of the transmissivity measurement and (for hydraulic conductivity) the estimated saturated thickness.
5) The fact that most specific-capacity test wells are pumped at low rates of about 50 m^3/day for short periods of time and, therefore, test only the local aquifer conditions.

The distance from the wells to the nearest flow primary or secondary flow path were plotted against measured hydraulic conductivity values and evaluated for linear correlation.

Deviations in pumping and recovery levels from type curves often reflected the presence of barrier and recharge boundaries, and assisted in characterizing the local aquifer conditions. To test for recharge or barrier boundaries, the drawdown data were plotted versus the log of elapsed time to calculate Cooper-Jacob approximation for transmissivity and storage. Deviations from straight-line trends with increased drawdown were interpreted as barrier boundaries, while decreasing drawdown anomalies were interpreted as recharge boundaries. Barrier boundaries are expected where the cone of

depression reaches a fault that juxtaposes lower permeability units. Recharge boundaries include primary and secondary groundwater flow paths and flowing creeks on the Edwards outcrop area near the pumping well. Recharge boundaries were interpreted based on the time of deviations on semilog plots, restriction of the cone of depression in observation wells, flowing creeks in the Edwards outcrop area, and mapped primary or secondary groundwater flow routes. Barrier boundaries were estimated based on the aquifer framework derived from the geologic map (Chapter 2) and mapped groundwater flow paths (Figure 4.1).

4.5.2 Aquifer Test Results

The hydraulic conductivity of nine aquifer test wells decreases exponentially with distance to primary groundwater flow paths (R^2 correlation of 0.82; Figure 4.18). The correlation between 10 wells to the closest secondary mapped flow routes also has an exponential correlation ($R^2 = 0.8$).

The 41 specific-capacity tests closest to mapped primary flow paths and 98 specific-capacity tests closest to secondary flow paths individually show no correlations with hydraulic conductivity. The lack of correlation probably reflect that small domestic well systems do not draw sufficient flow to show the influence of major flow paths; that the wells tested are influenced by much smaller groundwater conduit, fissure, fracture, and matrix features than other wells, or indicate that the accuracy of the specific capacity tests are too poor for this analysis.

A few aquifer tests selected for more detailed examination of results are described below.

4.5.2.1 Cimarron Park 1996 aquifer test

The Cimarron Park test ran for 9.4 hours on September 11, 1996, at a pumping rate of 3,300 m^3/day (600 gpm, Vickers., 1996, Figure 4.19). Measured water-level declines in the pumping and observation wells are presented in Appendix E. At the time, the Barton Springs Segment was in a drought. Barton Springs flow was 1 m^3/s (35 ft^3/s) on September 11, 1996. Although the Cimarron Park system is located well within the mapped artesian area, water-level declines brought the area to unconfined conditions.

The anisotropy of the Cimarron Park cone of depression is 0.33 (1:3) to 1.2 (1:8; Figure 4.19). During this test, 0.6 meter (1.7 ft) of drawdown was clearly observed 2 km (1.25 mi) to the northeast. To the southwest and west, drawdown appeared to be restricted. Tracer injections in Onion Creek (Site M, Figure 4.1) south of the Cimarron Park system were recovered in the westernmost well monitored for drawdown in the 1996 aquifer test, indicating that a flow path tributary to the Manchaca Flow Route is present that would potentially restrict drawdown to the west.

A semi-log plot of the time versus drawdown data suggests a distinct increase in transmissivity 90 minutes into the test, which resembles a recharge boundary (Figure 4.20). Using a Cooper-Jacob (1946) analytical solution, the transmissivity increased from about 450 m^2/day to 550 m^2/day. The recharge boundary is interpreted to be the primary groundwater flow route to the west (Figure 4.18).

4.5.2.2 Creedmoor Maha Aquifer Tests

The 2001 Creedmoor Maha Site 1 test ran for 4 days beginning June 5, 2001 at a rate of 6,770 m^3/day (1,240 gal/min) diminishing to 6,500 m^3/day (1,190 gal/min). Analysis of this test was complicated by recovery of the pumping well from previous pumping, interference from a local pumping well, and changing water levels in monitor wells prior to the test. As a result, the maximum drawdown in observation wells was subject to interpretation of which corrections to apply. Maximum drawdowns interpreted here are nearly always greater than drawdowns presented by Collier Consulting Inc (2001). The water-level measurements and drawdown interpretations are presented in Appendix E. The pumping well could not be monitored during the test, so drawdown within the wellfield was based on an observation well (58-50-850) within the same well field, which declined 3 m (15 ft, corrected to 7 m or 21 ft for incomplete recovery) during the test. The resulting mapped cone of depression is oriented northeast-southwest, parallel and proximal to local mapped faults (Figure 4.21). Beyond the first 20 minutes of well-bore depletion, the pumping wells showed three increasing shifts in transmissivity, interpreted as drawing from the local aquifer for the first 80 minutes, and thereafter the cone of depression extended to a secondary flow path (Figure 4.22). After about 1,100

minutes into the test the drawdown essentially ceased in the pumping field, as the cone of depression likely reached the Saline-Line Flow Route to the east. The cone of depression continued to expand over the duration of the test in area monitoring wells. Based on the data from 20 monitored wells the anisotropy of the cone of depression is 1:4 to 1:8. By the end of the test, the cone of depression grew such that 1.5 m (5 ft) of drawdown was measured in two monitored wells about 3.2 km (2 mi) to the southwest of the pumping wells. A similar 1.5 m (5 ft) of drawdown occurred only a half mile away northeast of the pumping wells. Its cone of depression is subparallel to and overlapping with the cone of depression interpreted from the 1996 aquifer test of the Cimarron Park well system.

The Creedmoor well site 2 shows ranges of transmissivity (resulting from pumping interference effects and possible background water-level declines) from about 472 to 633 m^2/day (38,000 - 51,000 gpd/ft) and a storativity of 0.03 to 0.045. The cone of depression is suppressed to the east, presumable from the nearby Saline-Line Flow Route.

4.5.2.3 Sunset Valley 1997 Aquifer Test

A test of the Sunset Valley municipal well was conducted on May 14, 1997, by the staff of Sunset Valley with monitoring assistance and verification from BS/EACD staff. The well was pumped at 820 m^3/day (150 gpm) for 510 minutes. A maximum water depth of 14.5 m (48 ft) was measured in the pumping well. The relatively low pumping rate and lack of local wells limited definition of the cone of depression (Figure 4.24). Three deflections appeared in the time drawdown curve, interpreted to reflect the transmissivity of the local aquifer, the nearby Sunset Valley Flow Route, followed by a third deflection that may reflect the cone of depression reaching a secondary groundwater flow route or flowing Barton Creek (Figure 4.25).

4.5.3. DISCUSSION

Primary and secondary flow paths control the hydraulic conductivity of the Barton Springs Segment. Hydraulic conductivity (K in m/day) declines by: $K = 340 \times L^{-10}$ with distance (L in m) away from primary or secondary flow path. The drawdown responses of the Cimarron Park, Creedmoor, and Sunset Valley well systems are

anisotropic inhibited by local primary and secondary flow paths that serve as recharge boundaries.

Recession analysis of springs or water levels is another tool for characterizing aquifer properties. Hydrograph recessions from three karst or fractured rock sites in three states were used to estimate the matrix transmissivity (Powers and Shevenell, 2000). The recession values were compared to transmissivities from aquifer and slug tests. Advantages of the recession method include: (1) the aquifer parameters could be obtained under natural conditions without stressing the aquifer and (2) no pumping was necessary. The hydrograph recession and aquifer test estimates of matrix transmissivity agreed very well. Based on recession analysis Senger (1983) estimated a range of transmissivity values from six wells in the Barton Springs Segment to be 0.10 to 0.40 m^2/sec (Table 4.2). Storativity for these six wells ranged from 0.001 to 0.023. Based on the change in storage at Barton Springs during one recession period, he estimated an overall storativity of 0.0075.

Transmissivity measured from well cores, water-level recession analysis, aquifer tests, and tracer tests can be compared for scale effects (Figure 4.26). Mace and Hovorka (2000a) measured permeability in well cores at values from 8.4×10^{-6} to 8.3 m/day with a arithmetic mean of 1.3×10^{-3} m/day. The scale of the tracer tests is simply the distance between injection and discharge sites. For comparison purposes the scale of the well cores, aquifer tests, and recession analysis is assumed to be 1 m, 2 km, and 5 km, respectively. It cannot be ruled out in this study that different methods (permeameter tests, aquifer tests, water-level recession, and tracer tests) account for some of the apparent scale differences (ASTM, 1995; Halihan et al., 2000; Kiraly, 2002).

4.6. CONCLUSIONS OF THE GROUNDWATER-FLOW ASSESSMENT

The Barton Springs Segment is composed of three groundwater basins, each with identified prominent preferred groundwater flow routes. Primary and secondary groundwater flow routes are highly transmissive and are where most transport is localized. The primary and secondary flow routes are associated with potentiometric-surface mounds during surface recharge periods and longer-lived potentiometric-surface troughs during recession periods, during which the local aquifer storage drains back in the flow routes. The locations of primary and secondary flow routes are best determined through groundwater tracing but are supported from other criteria, including potentiometric troughs and mounds, sediment-laden wells, geochemistry, aquifer testing, geologic mapping, creek-flow measurements, and cave mapping near the phreatic zone.

Groundwater tracing is an essential tool for verifying the flow route locations, advective velocity, dispersion, and discharge sites for recharge areas under tested flow conditions. The advective transport was 1,000 times greater than the hydrodynamic dispersion in five groundwater traces across the Barton Springs Segment.

Preferential groundwater flow routes are delineated based on:

(1) tracer recovery sites from injections a kilometer or more away;

(2) potentiometric surface mounds and troughs;

(3) groundwater samples with heavy sediment loads;

(4) groundwater samples with contamination is detected sufficiently far (such as more than 2 km) from its source;

(5) recharge features of major recharge importance, particularly creek swallets and large upland internal drainage basins;

(6) wells with high transmissivity;

(7) spring discharge sites;

(8) areas of high head variability within the artesian area; and

(9) areas of subdued head variation in the unconfined portion of the aquifer during recession or minor recharge periods.

The aquifer-testing results of the Cimarron Park and Creedmoor well systems show anisotropy ranging which is between 1:4 and 1:8. The direction of greatest transmissivity parallels local faulting and preferential groundwater flow routes oriented northeast-southwest. Measured cones of depressions and drawdown shifts on semi-log plots consistently show increasing transmissivity towards and along secondary and primary groundwater flow paths. As pumping progresses in the karst aquifer, the cone of depression expands primarily along conduits hydraulically connected to the pumped well. Preferred groundwater flow paths represent the convergence of groundwater flow through a few master conduits. Three tested pumping system wells are not directly intercepted by a primary or secondary flow-route conduit, as suggested by lack of recovery during separate tracer tests, yet each of these wells is influenced by these flow routes after sufficiently long pumping periods. Hydraulic conductivity (K in m/day) is highest along primary and secondary flow paths and declines with distance (L in m) away from the flowpaths by: $K = 340 \times L^{-10}$.

Table 4.1. Summary of tracer injections.

Site	Phase	Site Name	Watershed	Injection Date	Barton Springs Flow (cfs)	Barton Springs Flow (m^3/s)	Tracer	Tracer Mass OUL mixture (lbs)	Tracer Mass OUL mixture (kg)	Mass Recovery	Min. Distance to Discharge (miles)	Min. Distance to Discharge (km)	First Detection at Discharge (days)	Discharge Site	Best Report Source
		PHASE I													
A	1	Mopac Bridge	Barton Creek	8/13/1996	18	0.51	RWT	10	4.5	59%	3.4	5.5	5	Cold	Hauwert et al., 2004a
B	1	Mt Bonnell Fault	Barton Creek	8/13/1996	18	0.51	Fl	10	4.5	---	2.7	4.3	6	Cold	Hauwert et al., 2004a
		PHASE II													
A'	2	Mopac Bridge	Barton Creek	8/5/1997	107	3.03	Eosine	5	2.3	77%	3.4	5.5	0.79	Cold	Hauwert et al., 2004a
C	2	Dry Fork Sink	Williamson Creek	6/17/1997	101	2.86	Fl	3	1.4	4.2%	4.8	7.7	<1.25	Barton	Hauwert et al., 2004a
F	2	Brush Country	Williamson Creek	6/24/1997	110	3.12	RWT	10	4.5	---	5.3	8.5	<8	Cold	Hauwert et al., 2004a
		PHASE III													
H	3	Brodie Sink	Slaughter Creek	4/27/1999	83	2.35	Eosine	7	3.2	7.4%	8.6	13.8	1-2	Barton	Hauwert et al., 2004a
J	3	Midnight Cave	Slaughter Creek	4/27/1999	83	2.35	RWT	5	2.3	16.6%	11	17.7	7-8	Barton	Hauwert et al., 2004a
D	3	Whirlpool Cave	Williamson Creek	6/16/1999	68	1.93	Eosine	5	2.3	0.07%	5.6	9.0	3-4	Barton	Hauwert et al., 2004a
E	3	Westhill Drive	Barton Creek	6/16/1999	68	1.93	SRB	2	0.9	7%	2	3.2	0.4	Barton	Hauwert et al., 2004a
		PHASE IV													
I	4	Hobbit Hole	Bear Creek	9/28/1999	37	1.05	Fl	5	2.3	0%	not recovered				Hauwert et al., 2004a
K	4	Spillar Ranch	Bear Creek	9/28/1999	37	1.05	RWT	10	4.5	0.0002%	1.3	2.1	22-28	well 58-50-742	Hauwert et al., 2004a
L	4	Dahlstrom Cave	Little Bear Creek	9/28/1999	37	1.05	Eosine	10	4.5	0.7%	14.9	24.0	21	Barton	Hauwert et al., 2004a
		PHASE V													
M	5	Antioch Cave	Onion Creek	3/28/2000	26	0.74	RWT	20	9.1	<0.0001%	3.3	5.3	8-22	well 58-58-128	Hauwert et al., 2004a
N	5	Barber Falls	Onion Creek	3/29/2000	26	0.74	Fl	10	4.5	0.04%	15.7	25.3	14-16	Barton	Hauwert et al., 2004a
P	5	Marbridge Sink	Bear Creek	3/28/2000	26	0.74	Eosine	20	9.1	<0.001%	11	17.7	36-43	Barton	Hauwert et al., 2004a
		PHASE VI													
G	6	Loop 360	Barton Creek	6/23/2000	61	1.73	Pyranine	5	2.3	1.1%	3.3	5.3	<2	Cold	Hauwert et al., 2004a
Q	6	Tarbutton Cave	Blanco River	8/3-5/2000	29	0.82	Fl	15	6.8	0%	not recovered at San Marcos or Barton Springs				Hauwert et al., 2004a
O	6	Crooked Oak	Onion Creek	8/12/2000	28	0.79	Eosine	25	11.3	13%	18.6	29.9	23	Barton	Hauwert et al., 2004a
R	6	Recharge Sink	Slaughter Creek	10/6/2000	24	0.68	SRB	12	5.4	0%	not recovered				Hauwert et al., 2004a
M'	6	Antioch Cave	Onion Creek	11/21/2000	81	2.29	RWT	24	10.9	<0.001%	recovered only in wells				Hauwert et al., 2004a
		PHASE VII													
M"	7	Antioch Cave	Onion Creek	8/2/2002	98	2.78	Fl	25	11.3	80%	14	22.5	7.1	Barton	Hunt et al., 2004
S	7	Crippled Crawfish	Onion Creek	8/6/2002	99	2.80	Eosine	35	15.9	1%	17.5	28.2	3.5	Barton	Hunt et al., 2004
		PHASE VIII													
T	8	Hoskins Hole	Onion Creek	5/4/2005	104	2.95	SRB	35	15.9	0.0%	not recovered (trapped in mud)				Smith et al., 2006
S'	8	Crippled Crawfish	Onion Creek	5/4/2005	104	2.95	Eosine	35	15.9	5.2%	17.5	28.2	2.4	Barton	Smith et al., 2006
U	8	HQ Flat Cave	Slaughter Creek	5/5/2005	103	2.92	RWT	30	13.6	41.7%	9.5	15.3	4.1	Barton	Smith et al., 2006
K'	8	Spillar Ranch Sink	Bear Creek	5/5/2005	103	2.92	Fl	20	9.1	10.5%	11.5	18.5	3.3	Barton	Smith et al., 2006
		PHASE IX													
9a	9	Barton Hills Trib	Barton Creek	3/1/2006	31	0.88	Fl	10	4.5	not calc.	0.7	1.1	not calculated	Barton	report pending
9b	9	Skunk Hollow	Barton Creek	3/3/2006	31	0.88	RWT	25	11.3	not calc.	1.9	3.0	not calculated	Cold/Barton	completion
9c	9	Seismic Wall	Barton Creek	3/6/2006	31	0.88	Eosine	50	22.7	not calc.	2.8	4.5	not calculated	Cold/Barton	of Barton Creek
9d	9	Frech well	Barton Creek	3/30/2006	31	0.88	SRB		0.0	0.0%	not recovered				traces
		PHASE X													
10a	10	Hangtree	Slaughter Creek	4/10/2007	96	2.72	Eosine	30	13.6	not calc.	14	23.2	3-4	Barton	report to be
10b	10	Sandbur	Bear Creek	4/11/2007	96	2.72	RWT	45	20.4	not calc.	11	18.1	2.7	Barton	completed
10c	10	Bear Creek Tabor	Bear Creek	5/1/2007	96	2.72	Fl	5	2.3	not calc.	12	19.4	2-3	Barton	by COA/BSEACD
10d	10	Wildflower Cave	Slaughter Creek	4/9/2007	96	2.72	SRB	30	13.6	not calc.	10	16.1	2.46	Barton	in 2009

Table 4.2. Tracer precision and accuracy.

Tracer	Normal Acceptable Emission Wavelength Range (nanometers)	Detection Limit (parts per billion)	Practical Quantity Limits (PQL) (ppb)	Precision Limits (RPD) (%)
Elutant Extractions from Charcoal Receptors				
Fluorescein	510.7 to 515.0	0.01	0.03	26-34
Eosine	533.0 to 539.6	0.035	0.0105	29-36
Rhodamine WT	561.7 to 568.9	0.275	0.825	37-49
Sulforhodamine B	567.5 to 577.5	0.15	0.45	35-46
Pyranine	499.1 to 503.9	0.055	0.165	**
Water Samples				
Fluorescein	505.6 to 510.5	0.0005	0.0015	1.7-2.7
Eosine	529.6 to 538.4	0.008	0.024	3-4.5
Rhodamine WT	569.4 to 574.8	0.05	0.15	4.5-6
Sulforhodamine B	576.2 to 579.7	0.04	0.12	4.2-5.5
Pyranine*	501.2 to 505.2	0.03	0.09	**
* pH adjusted water with pH of 9.5 or greater.				
** insufficient data for generalizaton.				
All data provided by Ozark Underground Labs, Protem, Missouri				

Table 4.3. Hydrologic parameters measured from selected tracer tests.

Injection Site		**K**	**S**	**U**	**E**	BS Well *
Feature Name	Units	Spillar Ranch	Crippled Crawfish	HQ Flat Sink	Westhill	58-42-903
Distance to Barton Springs	(km)	19	29	16.8	2.6	0.061
Dye		Fluorescein	Eosine	RWT***	SRB**	RWT***
Mass	(lbs)	20.0	35.0	30.0	2.0	0.26
	(kg)	9.1	15.9	13.6	0.9	0.1
Inj Date/Time		5/5/05 13:15	5/4/05 15:00	5/5/05 9:00	6/16/99 19:00	Mar-82
Initial Arrival (Main Barton)	(days)	3.28	2.38	4.13	0.42	0.01
Mean Residence Time	(days)	9.7	2.0	5.4	0.8	0.1
MeanTracer Velocity	km/day	2.0	14.7	3.1	3.1	0.5
Time to Peak	(days)	4.45	2.54	4.79	0.63	0.05
Barton Spr. Flow (USGS)	(cfs)	104	103	104	68	47 ± 4
Mass Recovered						
Main Barton	(kg)	1.00	0.84	3.00	0.11	0.14
Eliza	(kg)	0.27	0.17	0.49	Added above	---
Old Mill	(kg)	0.11	0.05	0.21	0.007	---
Upper Barton	(kg)	0.00	0.00	0.00	0.00	---
Total Rec. @ Barton Spr.	(%)	**15%**	**7%**	**27%**	**13%**	**115%**
Chatwin Value	($s^{1/2}$)	3,900	6,100	8,900	1,000	67
Long. Dispersion (Chatwin)	(m^2/s)	5.9	5.7	0.9	1.7	6.6E-08
Peclet Number	(m^2/hr)	1,747	21,008	16,231	1,314	140,684,644
Potentiometric diff.	(m)	108	85	82	5	0.3
GW Gradient		0.0057	0.0029	0.0049	0.0019	0.0049
Hydraulic Conductivity	(m/s)	0.0040	0.0580	0.0073	0.0188	0.0013
Transmissivity	(m^2/day)	420,300	6,108,000	774,000	1,980,000	135,000

* Calculated from injection and breakthrough information reported by Senger (1983)

**Sulforhodamine B

***Rhodamine WT

Table 4.4. Transmissivity values from water-level recession analysis.

Well	T (m^2/s)	T (m^2/day)	S*
58-50-216	0.17	14,688	0.023
58-50-301	0.1	8,640	0.012
58-50-518	0.14	12,096	0.003
58-50-704	0.14	12,096	0.001
58-50-801	0.14	12,096	0.003
58-50-219	0.4	34,560	0.001
average	0.18	15,696	0.0075

* Storativity

From Senger (1983)

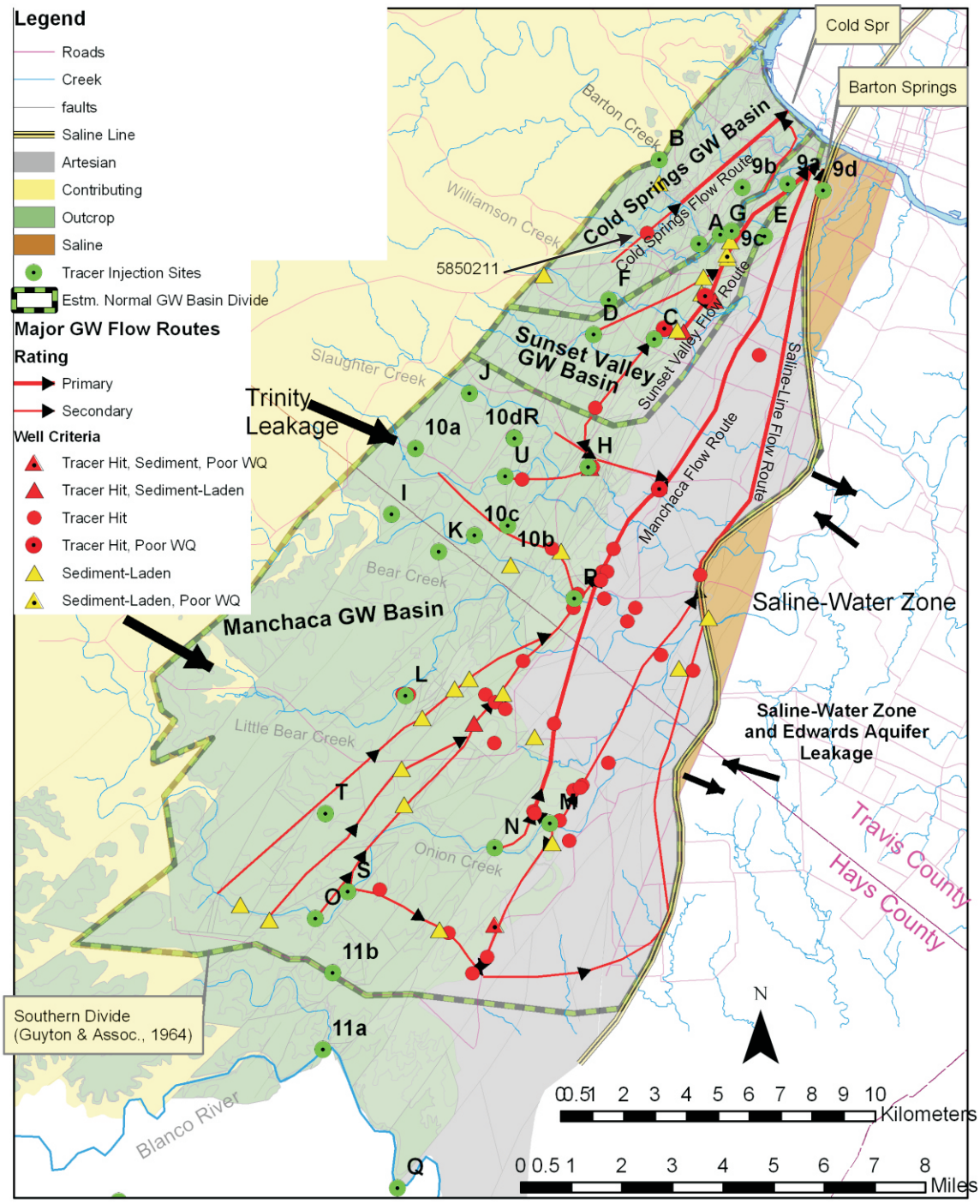

Figure 4.1. Groundwater flow routes: moderate to high-flow conditions. The flow paths are interpreted based on criteria including sites of tracer recover; major creek flow-loss; sediment-laden wells; poor water-quality originated from distant sources; potentiometric troughs and mounds; geologic faults, the Saline-Water Line; and differences in tracer concentrations in wells and springs. Numbered injection sites have not been analyzed to date.

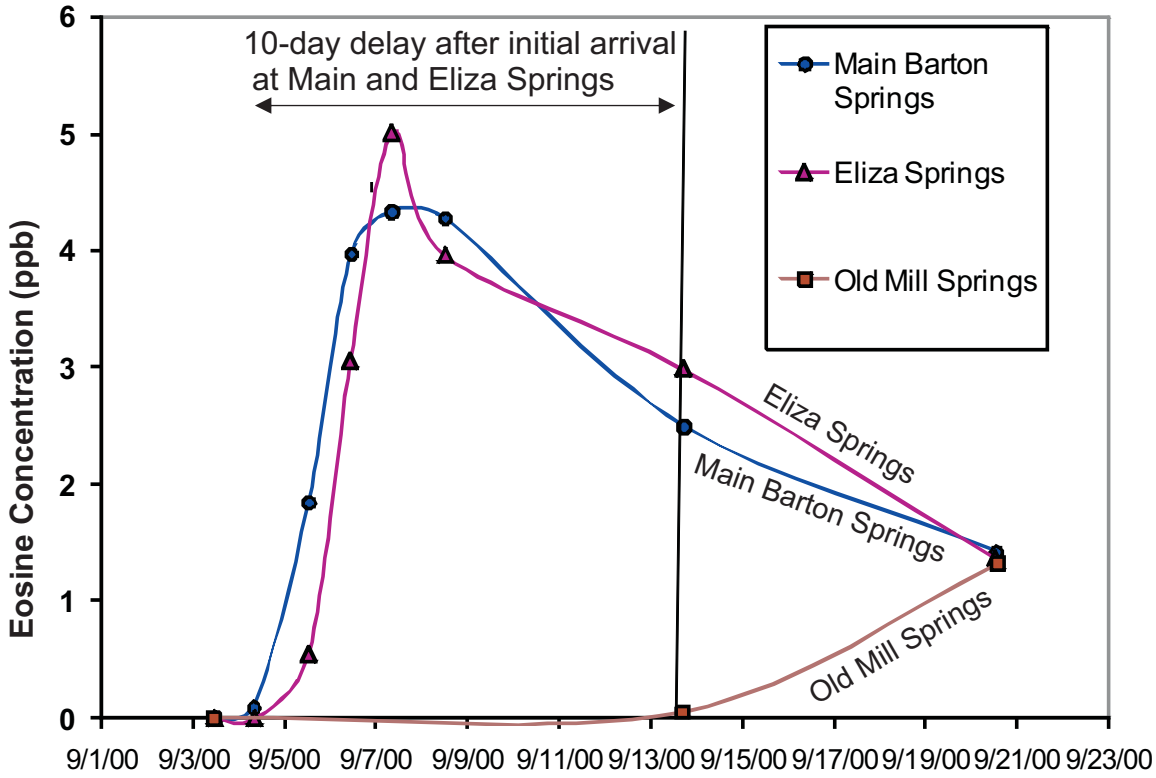

Figure 4.2. Delayed arrival of tracers to Old Mill Springs. Following a 2000 trace from Site O on Onion Creek, the tracer is not detected at Old Mill Springs until more than 10 days after initial arrival at Main and Eliza Springs. Weekly charcoal receptors from Old Mill Springs show no detection of eosine prior to September 6, 2000, only borderline detection until after September 13, 2000 and peak eosine concentrations the week of September 20 to 28, 2000 (Hauwert et al., 2004a, Appendix A-VI-14). This delayed response is interpreted to result from a bifurcation of flow paths from Onion Creek to the Saline-Line Flow Route (to Old Mill Springs) and the faster Manchaca Flow Route (to Main and Eliza Springs). Barton Springs Low-flow conditions of 0.82 m^3/s (28 ft^3/s) were occurring during the August 12, 2000 injection at Site O.

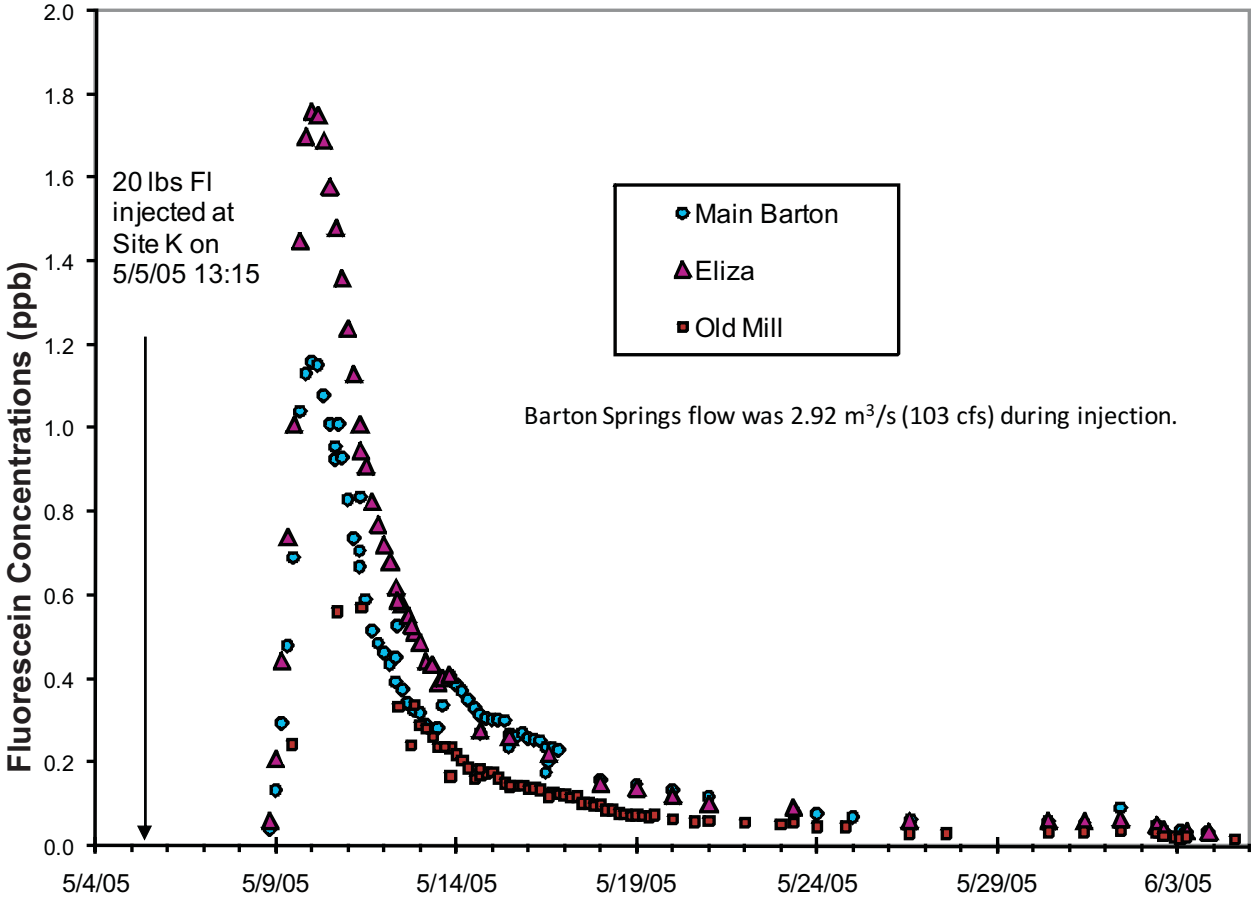

Figure 4.3. Tracer breakthroughs from Manchaca Flow Route. Following injection at Site K within the Manchaca GW Basin north of Onion Creek and west of the Manchaca Flow Route, tracer concentrations at Eliza Springs are greater than at Main Barton and Old Mill Springs, suggesting dilution of Main and Old Mill Springs by other sources. Here the dilution is attributed to flows from the Saline-Line diluting Old Mill and Main Barton springs, as well as separate flows from the Sunset Valley Groundwater Basin diluting Main Barton Spring. No fluorescein was detected at Upper Barton Springs during this trace.

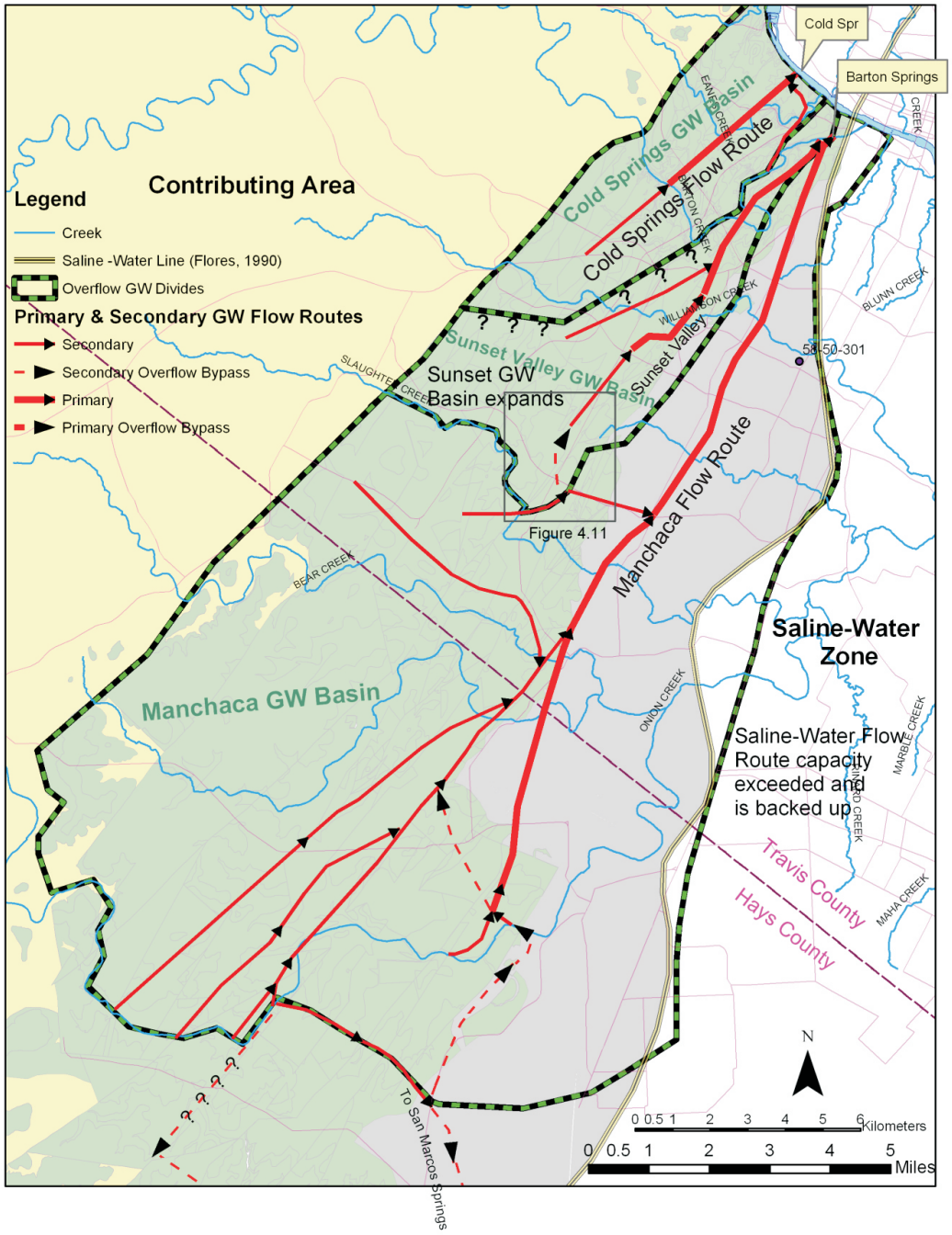

Figure 4.4. Mapped Groundwater Flow Routes: Overflow Conditions. Under some excessive recharge conditions, certain flow paths become backed up and flow is diverted to other conduits. The groundwater divide between the Sunset Valley and Manchaca Groundwater basins may shift to Slaughter Creek. The Southern Divide shifts north to portions of Onion Creek. The Saline-Line Flow Route appears to become blocked under some overflow conditions.

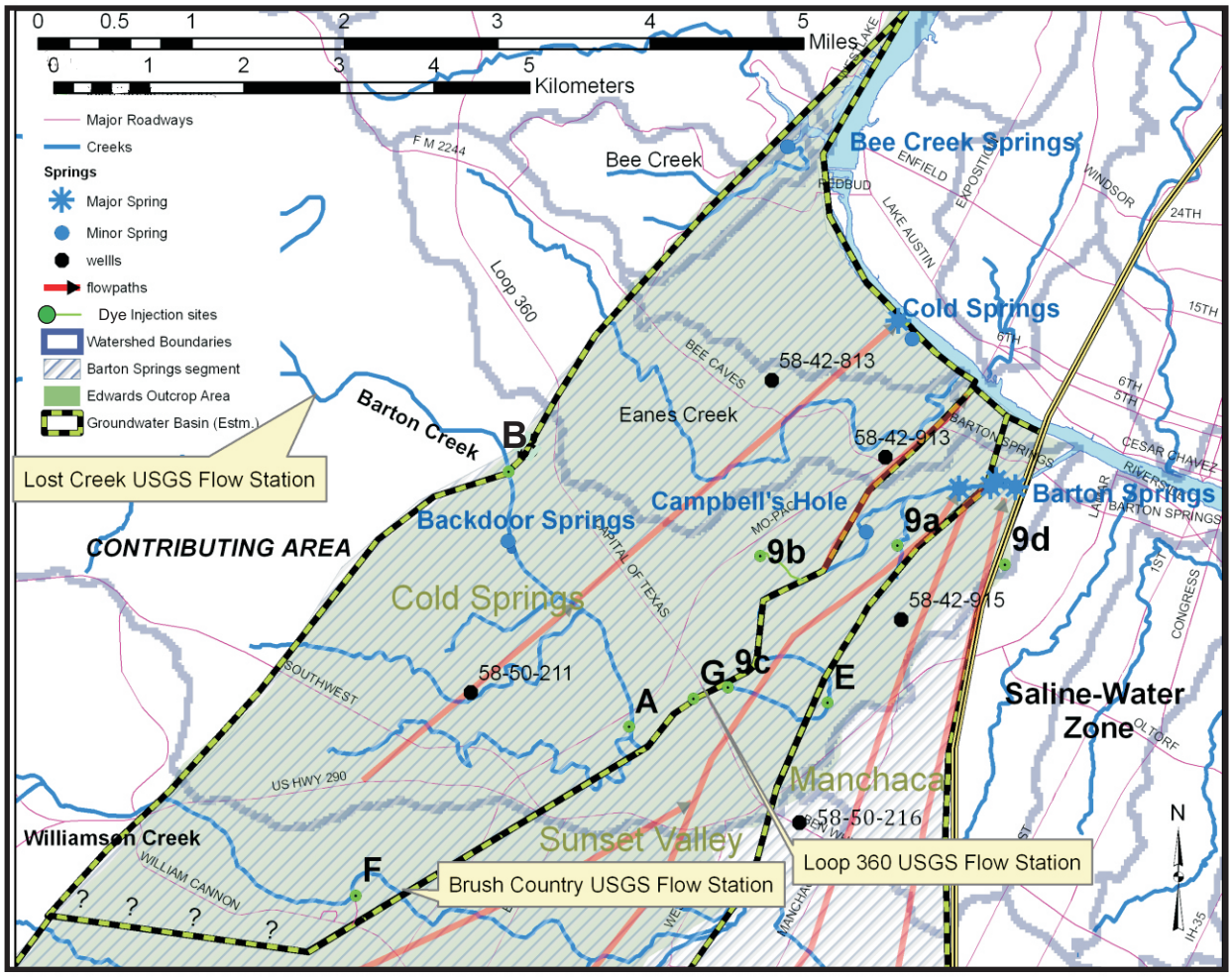

Figure 4.5. Cold Springs Groundwater Basin Source Area. Groundwater tracing from 1996 to present defines the Cold Springs groundwater basin. Senger (1983) found water-level responses in wells 58-50-216 and 58-42-915 to the draining of Barton Springs pool. however water levels in 58-42-913 did not respond. Traces A, G, F, 9b, and 9c discharged from Cold Springs. Tracer B was recovered in the Colorado River just downstream of Cold Springs. Traces 9a and E discharged from Barton Springs.

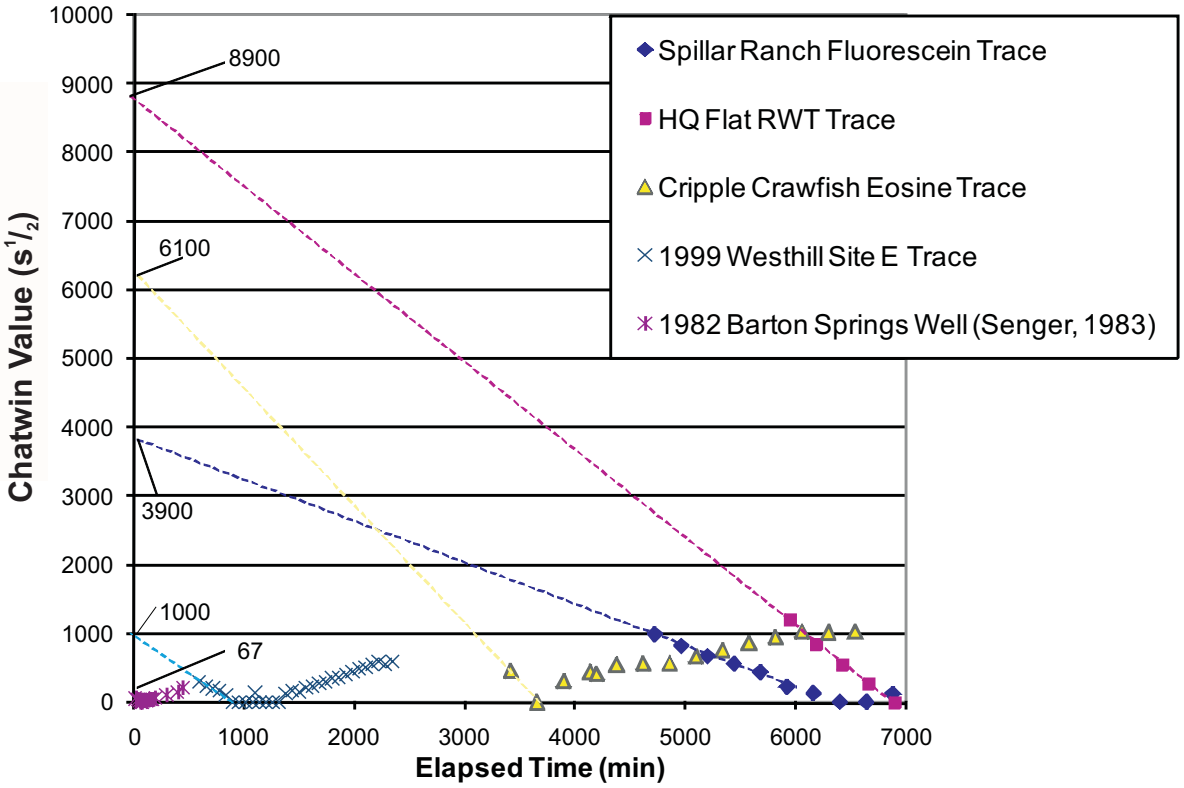

Figure 4.6. Chatwin extrapolations from the early tracer arrivals are used to extrapolate Chatwin intercept values for zero elapsed time.

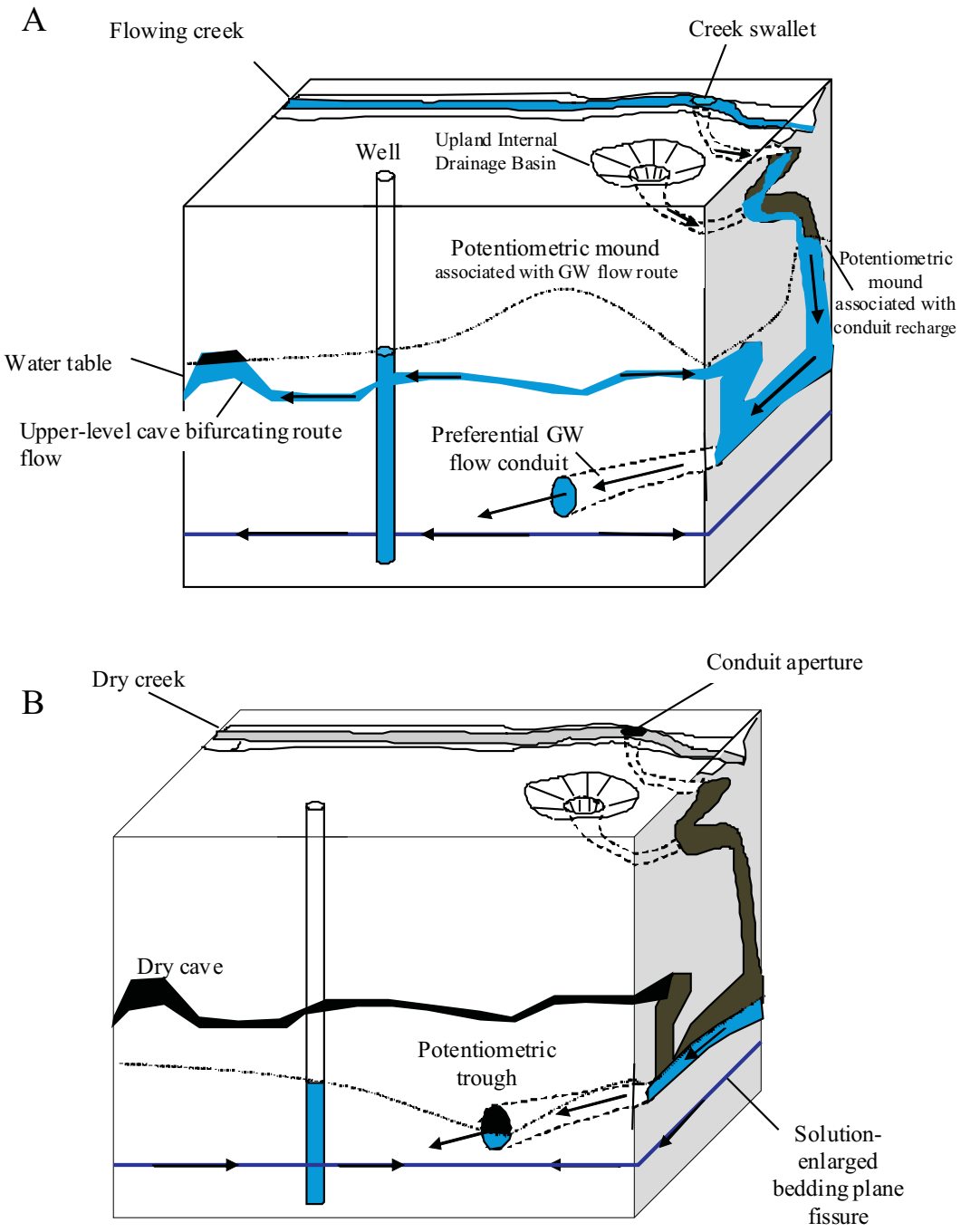

Figure 4.7. Hypothetical groundwater flow paths. During flowing creek or upland precipitation scenario A, mounds potentially form below the major recharge sources (swallets and internal drainage basins). Potentiometric mounds also potentially form along preferential groundwater flow conduits. The recharge waters are dispersed laterally into the aquifer and to discharge springs. Under scenario B, the recharge sources are depleted and potentiometric troughs form along the preferential groundwater conduits and draws storage from the aquifer. Note that the well draws flow from the preferential groundwater conduit in scenaio A but stored water or groundwater from other sources under scenario B.

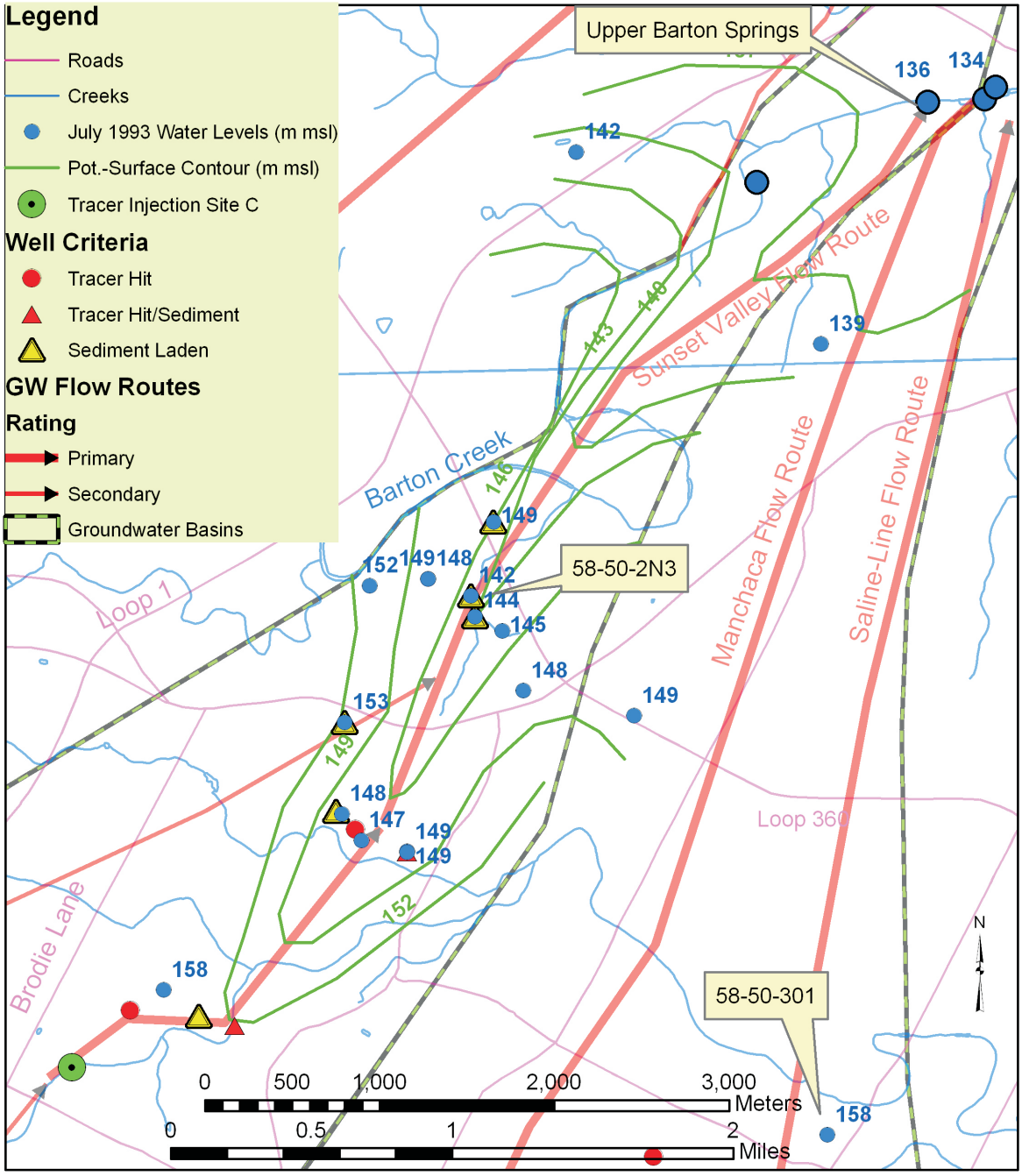

Figure 4.8. Potentiometric-Surface Trough of Sunset Valley Flow Route. Water levels measured in July 1993 indicated a 13-m-deep potentiometric trough that initially identified the Sunset Valley Flow Route (Hauwert and Vickers, 1995). The heavily sediment-laden wells here were found to be pulverulitic sediment naturally eroded by rapid groundwater velocities (Mahler, 1997). Tracing conducted at site C was recovered in several wells in the Sunset Valley area and Upper Barton and Main Barton Springs. Some key wells, such as 58-50-2N3 were plugged prior to the 1997 trace. Figure modified from Hauwert and Vickers, (1995) and Hauwert et al. (2004a.)

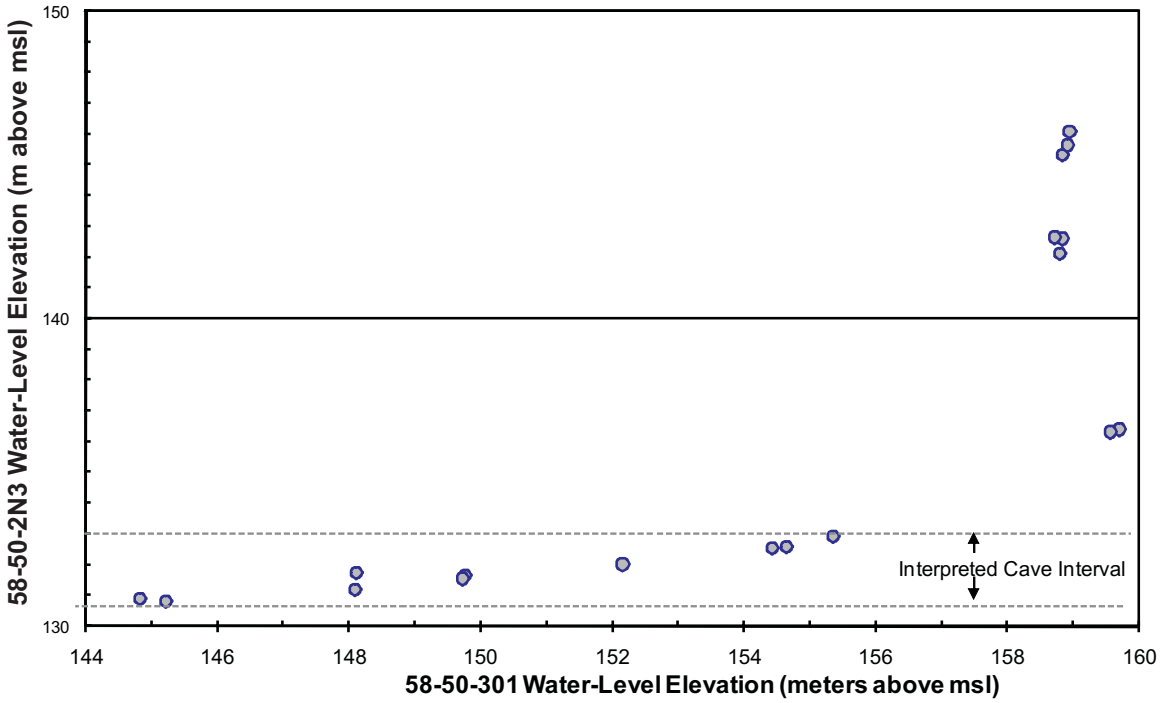

Figure 4.9. Correlation of water-level elevations in 58-50-2N3 and 58-50-301. Water-level changes in a well can be used to estimate the elevation and height of a partially water-filled cave. Well 58-50-2N3 appears to be near the Sunset Valley Flow Route, based on anomalous sediment deposition filling its uncased interval and low water-level elevation (Figure 4.8). When water levels in well 58-50-2N3 exceed 133 m msl, its water levels change 10 m while associated water levels in 58-50-301 vary by only 4 m. This response can be explained by a water-bearing cave located near 58-50-2N3 at least 2 m high with roof elevation at 133 m msl or slightly lower. When water levels exceed 133 m msl in well 58-50-2N3, the local cave is completely filled and the local aquifer behaves more like a confined aquifer well similar to well 58-50-301.

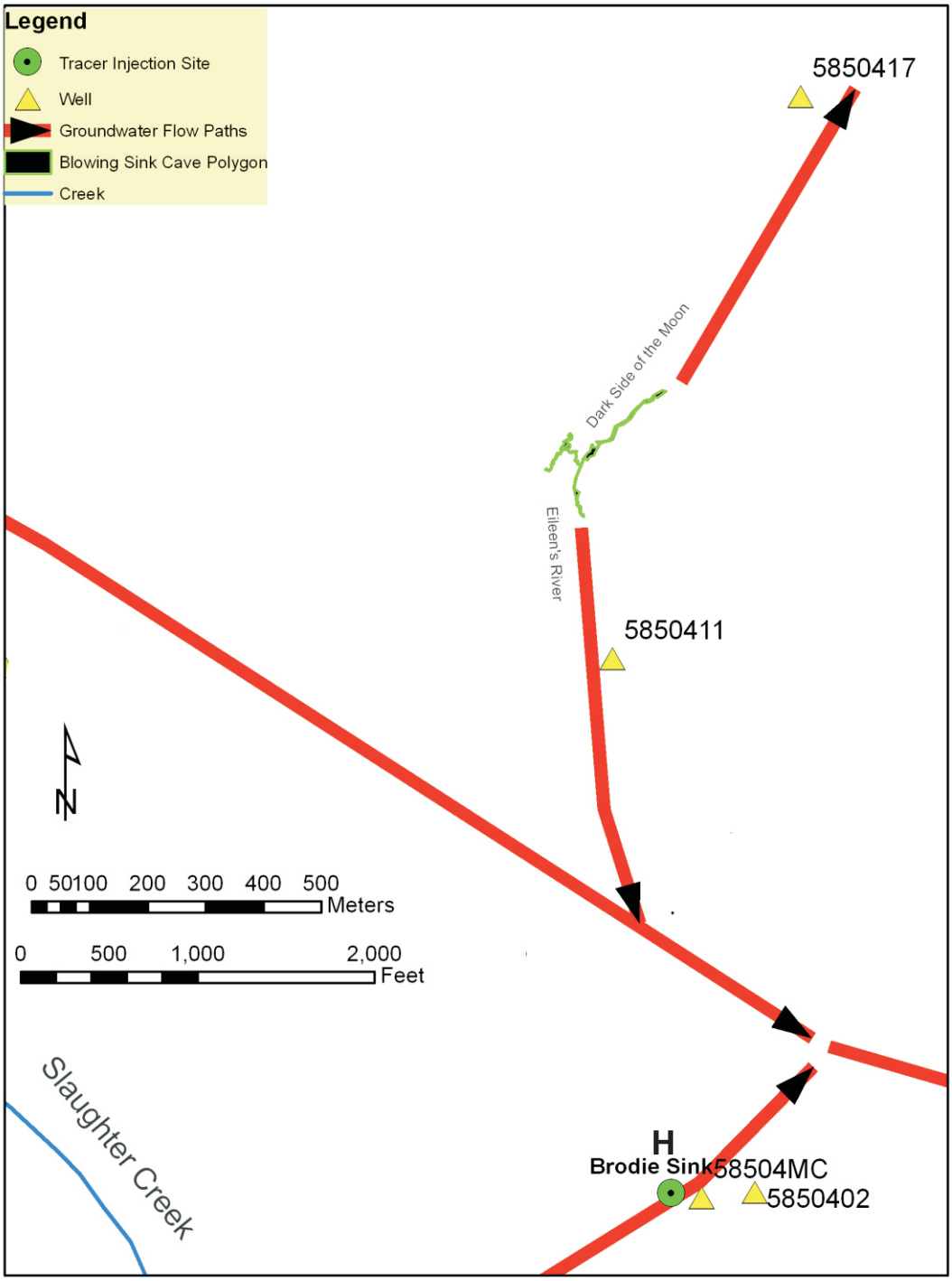

Figure 4.10. Groundwater flow paths interpreted near Blowing Sink Cave. Eileens River cave stream flows perennially south, presumably towards an eastward flowing secondary flow path of the Manchaca groundwater basin. Tracers injected at site H reached Main, Eliza, and Old Mill Springs within 30 hours after injection. Yet a month after injection, following heavy rain and local flooding, the tracer was detected in well 58-50-417. That this dye was not detected at Upper Barton Springs or other flow path wells monitored in the Sunset Valley groundwater basin is interpreted to mean that under overflow conditions, the groundwater divide shifts south to Slaughter Creek. The amount of diverted flow was relatively small following the H injection.

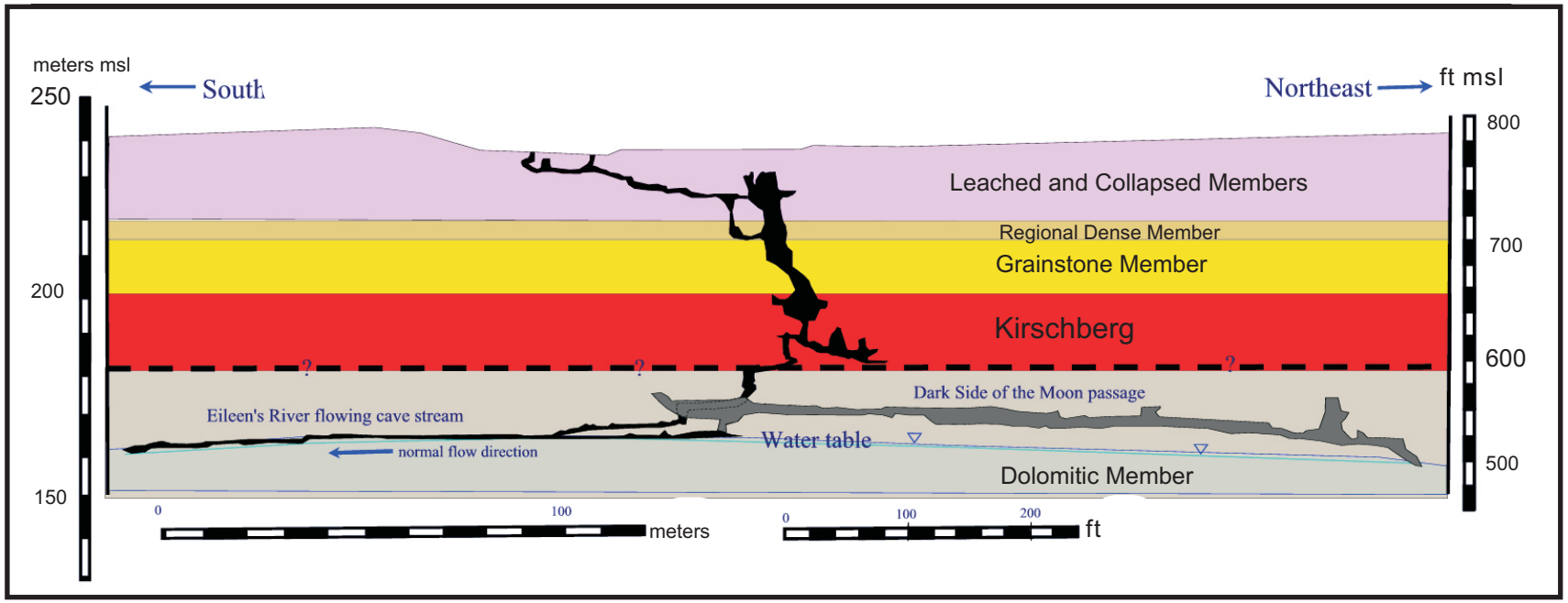

Figure 4.11. Blowing Sink Cave Cross Section.
Cross section cut south to northeast along the trend of Blowing Sink Cave, extending to the water table. During infrequent inspections when the cave is not flooding, Eileens River flowing cave stream can always be observed flowing south, even during droughts. During local overflow and surface flooding conditions, flow appears to rise into the Dark Side of the Moon passage, causing a reversal of flow to the northeast. The cave cross section is modified from Blowing Sink Cave map by Russell (1996). Hydrostratigraphic units from Blowing Sink measured section by Nico Hauwert in 1995 (Appendix C).

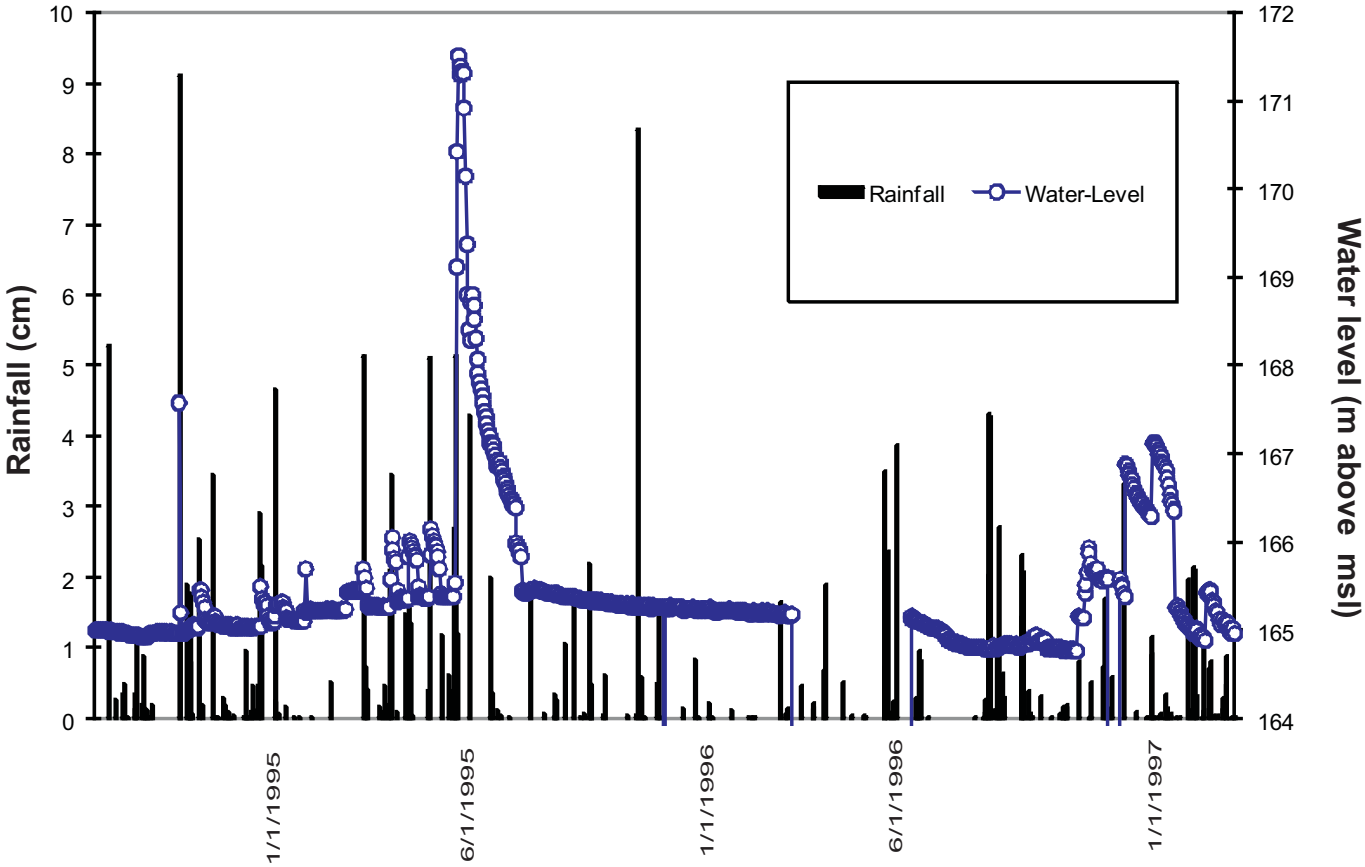

Figure 4.12 Water-level variation in well 58-50-411. Well 58-50-411 is located about 230 m south of the mapped extent of Eileen's River cave stream in Blowing Sink. Based on infrequent observations during nonflooding conditions, Eileen's River cave stream flows southeast perennially and has a water elevation of about 163 m (535 ft) above mean sea level. Well 58-50-411 is normally downgradient of Eileen's River cave stream, yet has a higher and relatively constant water level, generally varying between 165.0 and 165.5 m above msl. When water levels in Blowing Sink Cave exceed about 168 m above msl, flow from Eilleen's River backs up into the Dark Side of the Moon passage and groundwater flow reverses to the northeast into the Sunset Valley groundwater basin. This groundwater reversal may account for the late appearance where dye injected at Site H appeared in another well (58-50-417) to the northeast after heavy rains and a month after the dye arrival at Barton Spring outlets supported by the Manchaca groundwater basin.

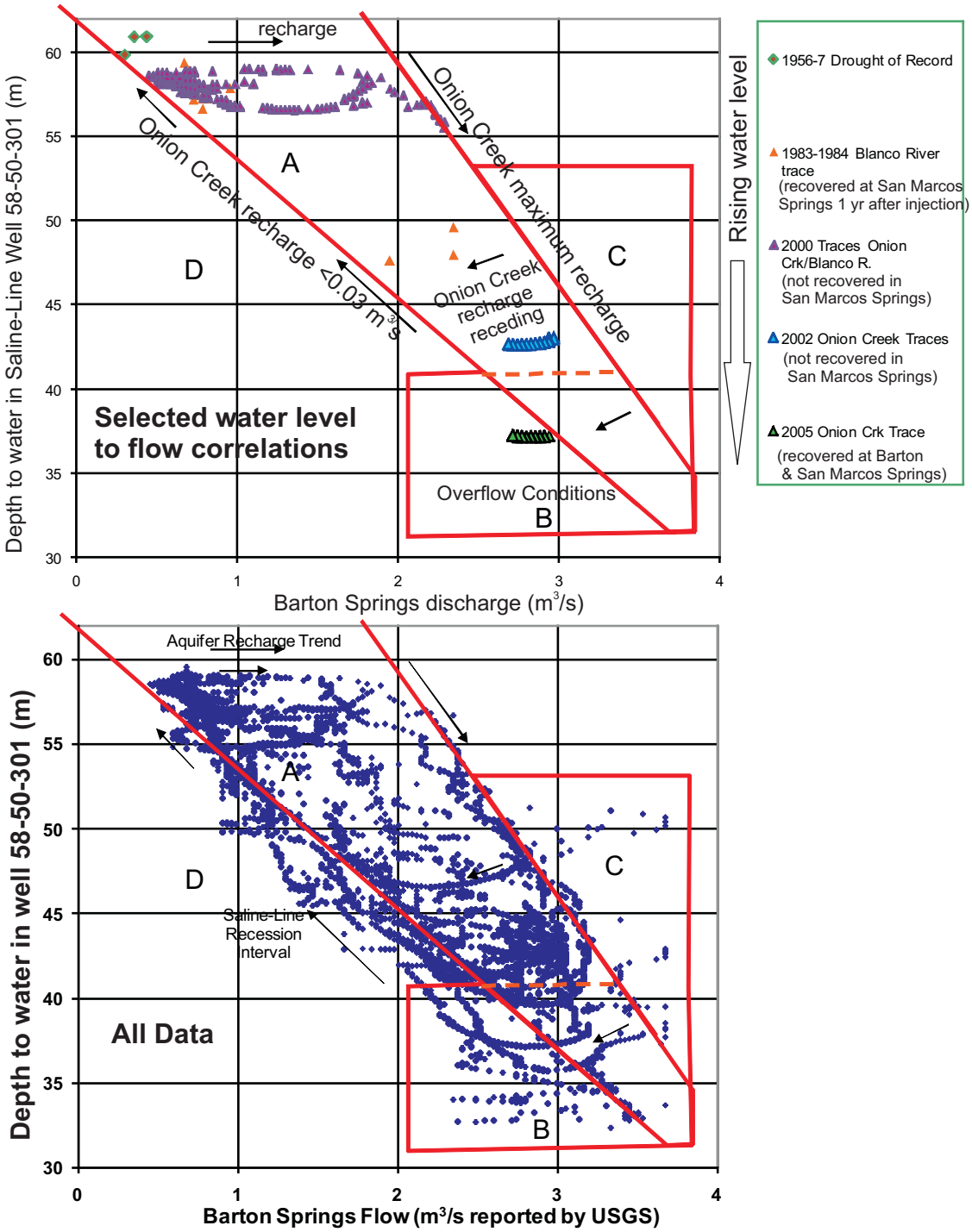

Figure 4.13. Saline-Line water levels and Barton Springs flow. Well 58-50-301 water-level data from BS/EACD and TWDB reflect conditions of Saline-Line Flow Route when compared to Barton Springs flow reported by USGS. Condition A reflects normal delayed response in the well following recharge and recession cycles of Onion Creek. Recession along the D and A boundary reflects the drying of contributing area contributions below 0.03 m^3/s. Condition B reflects overflow conditions under which recharge exceeds the capacity of the the Saline-Line Flow Route resulting in diversion of some Onion Creek flow to San Marcos Springs.

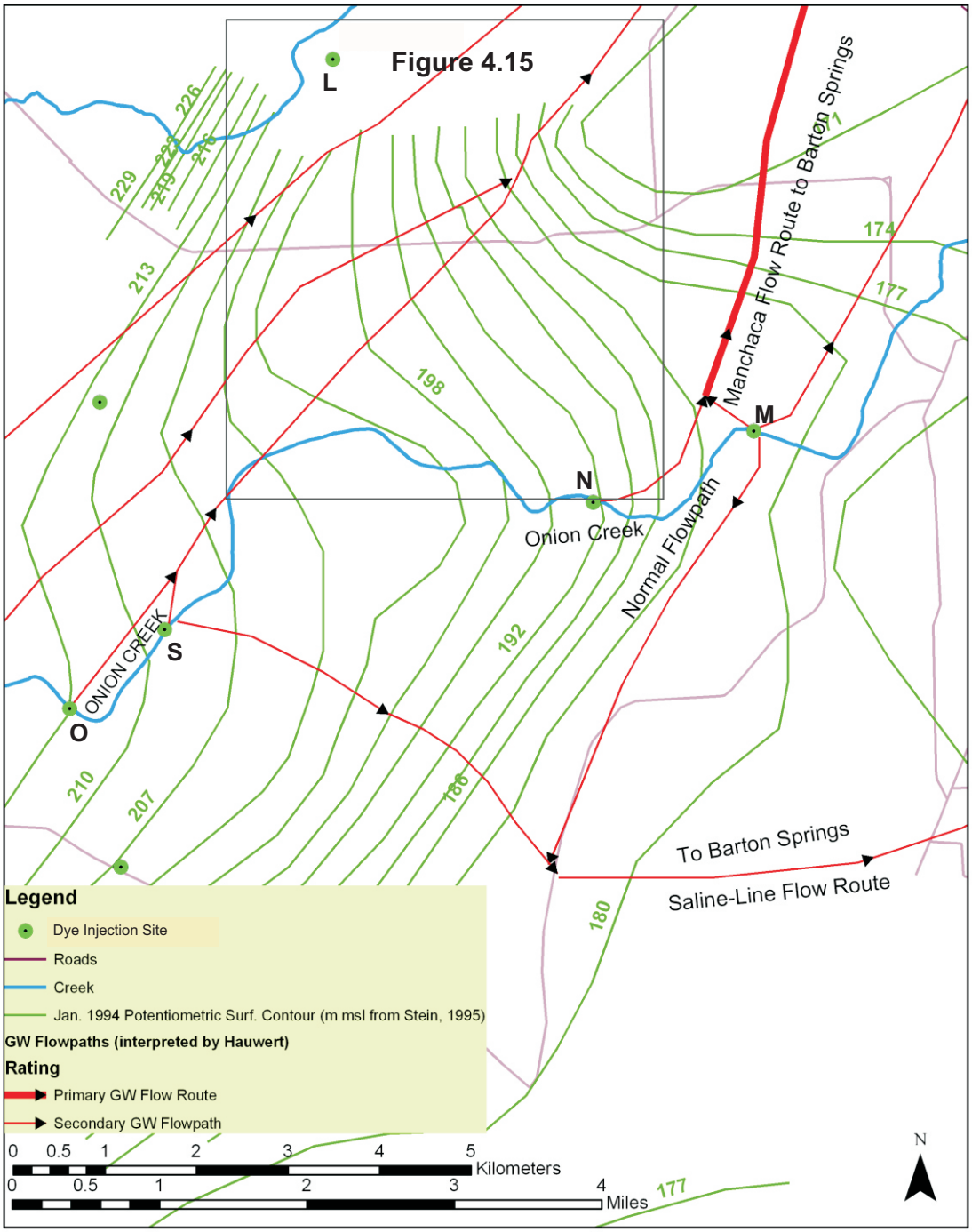

Figure 4.14. 1994 Potentiometric-Surface Map Along Onion Creek. Based on potentiometric-surface data alone, a groundwater divide between San Marcos Springs and Barton Springs was interpreted to follow Onion Creek (Stein, 1995). However, later groundwater tracing showed that under most (low to high) flow conditions, the potentiometric mound actually corresponds to a bifurcation between the Manchaca and Saline-Line flow route that both paths arrive at Barton Springs. During infrequent overflow conditions portions of Onion Creek temporarily serve as the divide between Barton and San Marcos Springs.

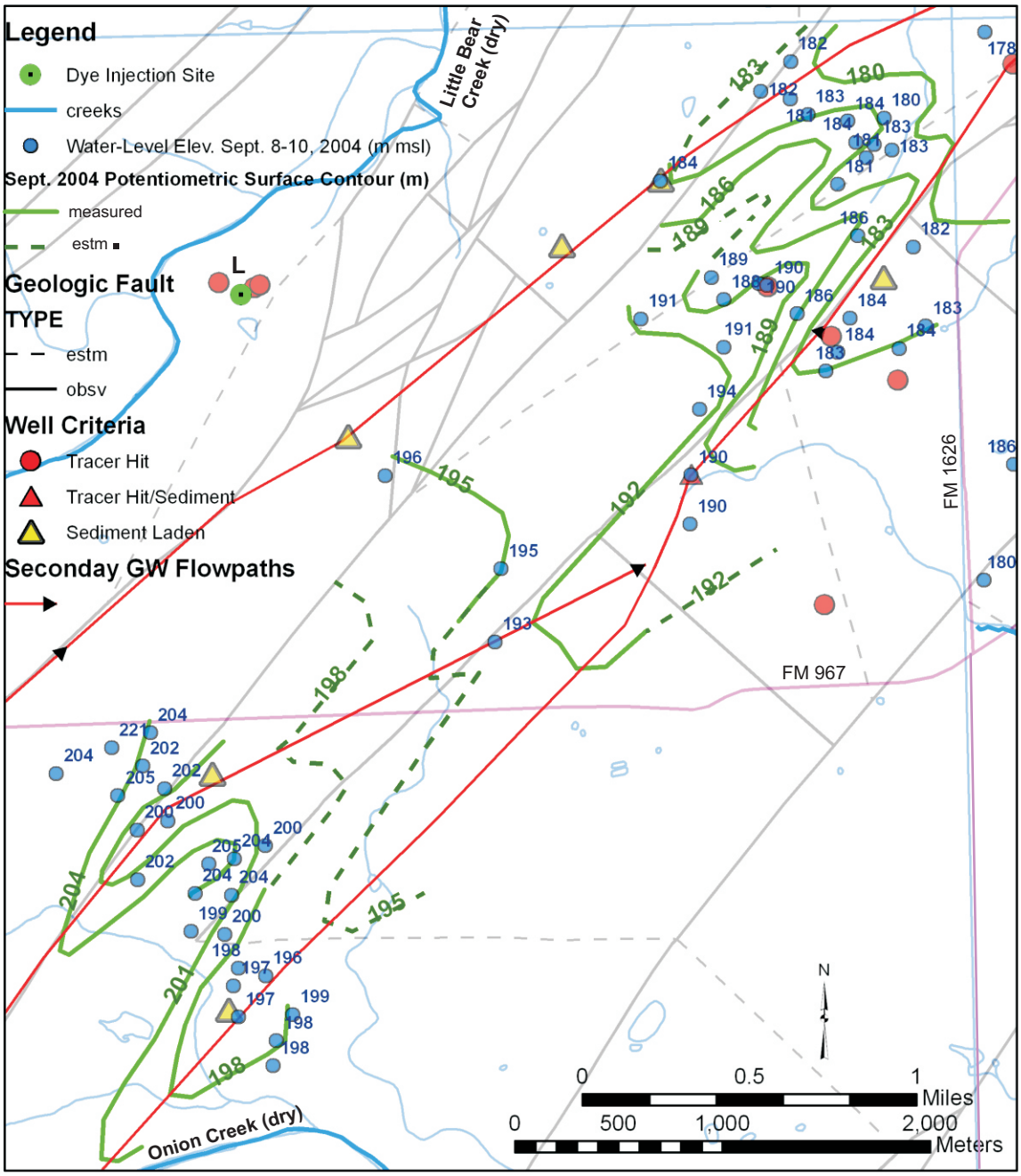

Figure 4.15. Sept. 2004 potentiometric-surface map west of Buda. Water levels measured September 8 to 10, 2004, by Joe Beery (BS/EACD) and the author. During the survey, Onion Creek was discharging at 0.17 m^3/s (6 ft^3/s) from the upstream USGS gauge station and the flow did not reach this stretch. Tracing from Onion Creek in 2005 targeted verification of flow paths tentatively identified by potentiometric troughs, sediment-laden wells, major creek swallets, and connecting fault locations. Detailed water levels suggest more complexity in water-level surface and flow paths than indicated by widely-spaced measurements.

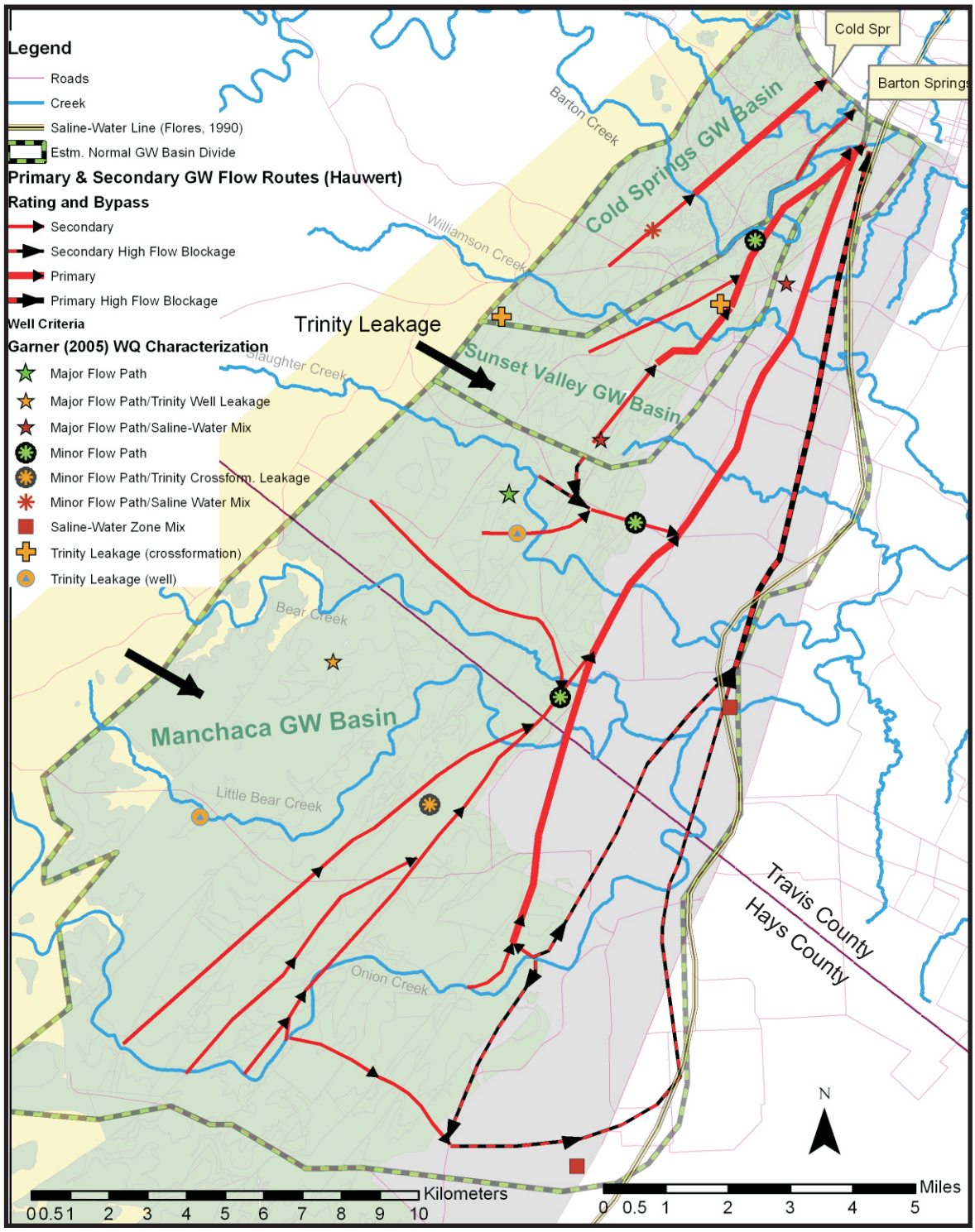

Figure 4.16. Map of Garner (2005) water-quality analysis interpretation. Groundwater flow paths interpreted in this study are overlaid with water-quality characterization of selected wells by Garner (2005) and Garner and Mahler (2007).

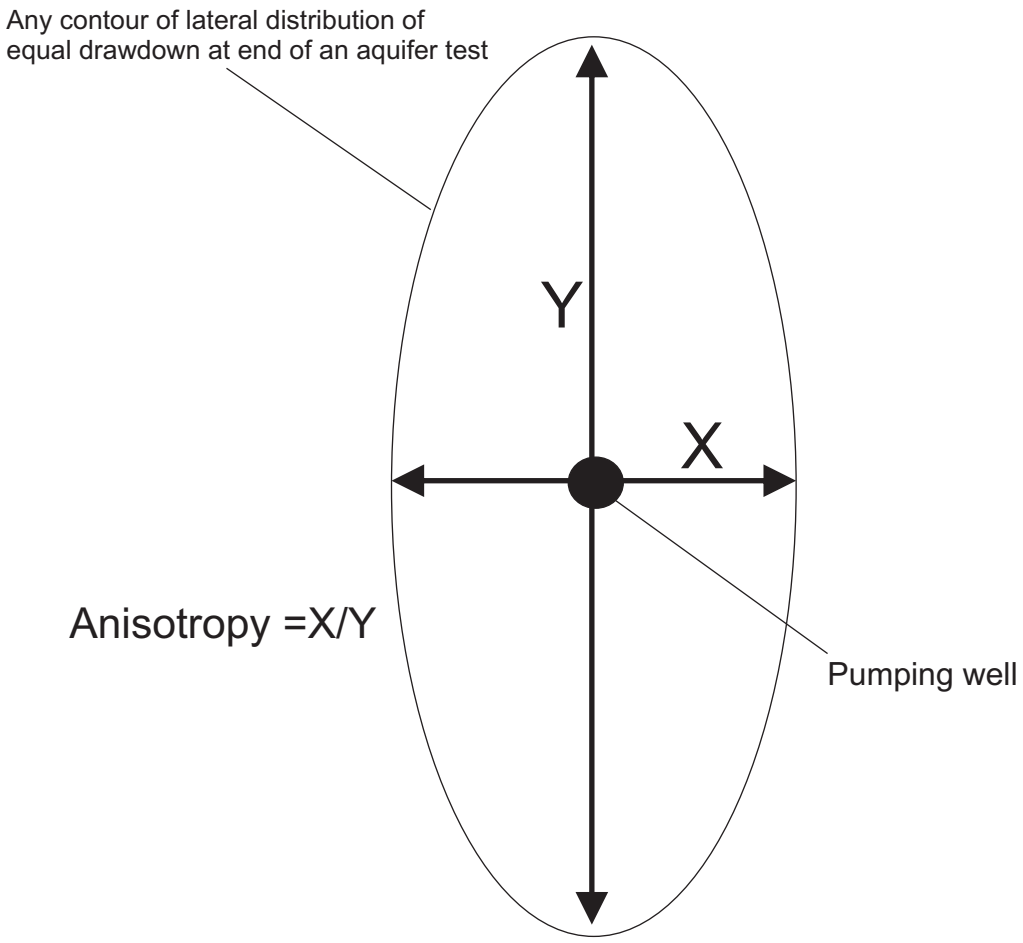

Figure 4.17. Hypothetical anisotropic cone of depression. Contour maps of the cone of depression can be mapped based on the drawdown measured or extrapolated in wells at the end of an aquifer test. The anisotropy of a cone of depression at the end of an aquifer test can be quantified by the ratio of shortest diameter to the longest diameter.

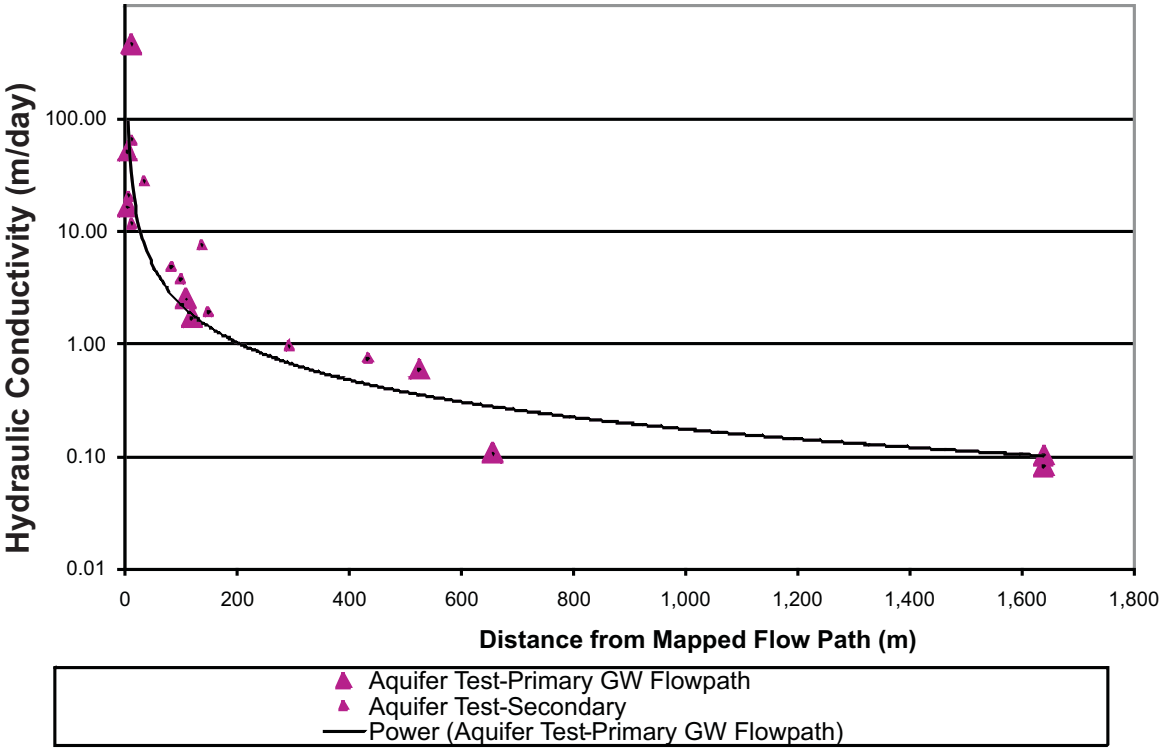

Group	Best fit trend	R^2
Aquifer Tests-Primary FP	$K = 340\ L^{-1.097}$	0.82
Aquifer Tests-Secondary FP	$K = 190\ L^{-0.84}$	0.76
Aquifer Tests-Combined FP	$K = 340\ L^{-1.04}$	0.8

L = distance from flow path (m)

K = hydraulic conductivity (m/day) =transmissivity/saturated thickness

Figure 4.18. Aquifer test hydraulic conductivity and distance to flow path. Hydraulic conductivities derived from aquifer tests (triangles) decrease exponentially away from mapped groundwater flow paths. The aquifer test correlation suggests that high hydraulic conductivity areas of the Barton Springs Segment are directly associated with primary and secondary groundwater flow paths.

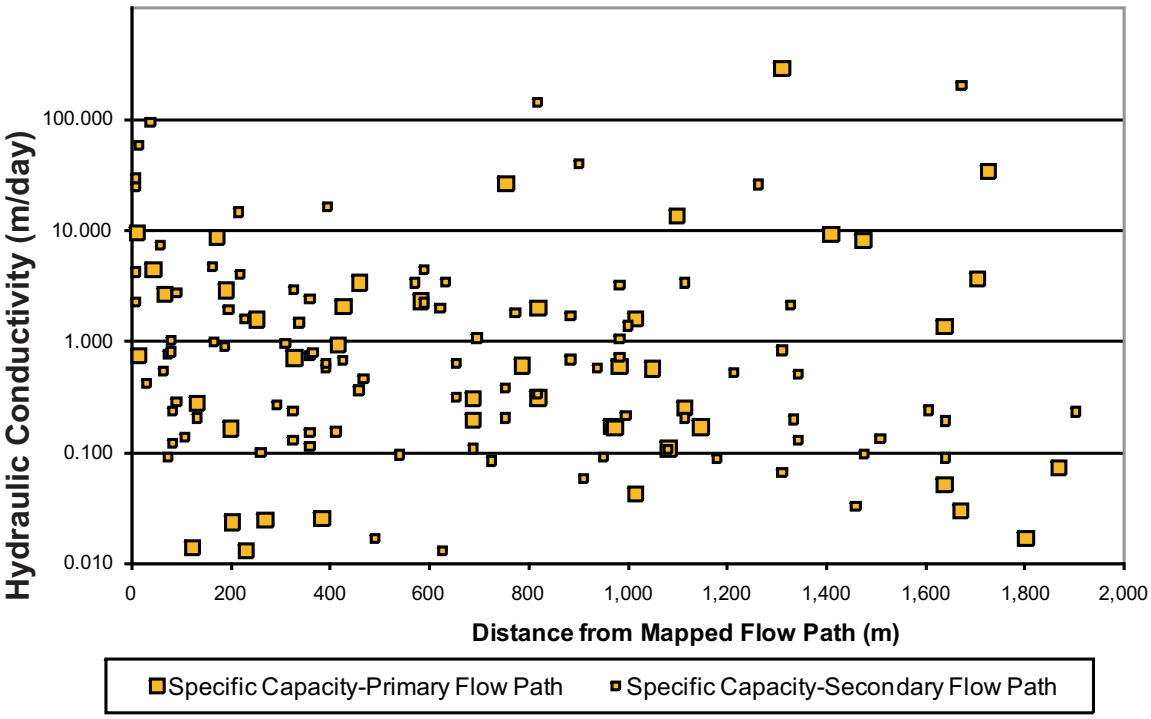

Figure 4.19. Specific-capacity test hydraulic conductivity. Hydraulic conductivity derived from specific-capacity tests show no correlation to distance from mapped primary and secondary groundwater flow paths. The specific-capacity tests are short term, pump at relatively low rates, and measure hydraulic conductivity less accurately than aquifer tests. Because they test only a small area around the well, specific-capacity tests are highly influenced by local aquifer variability.

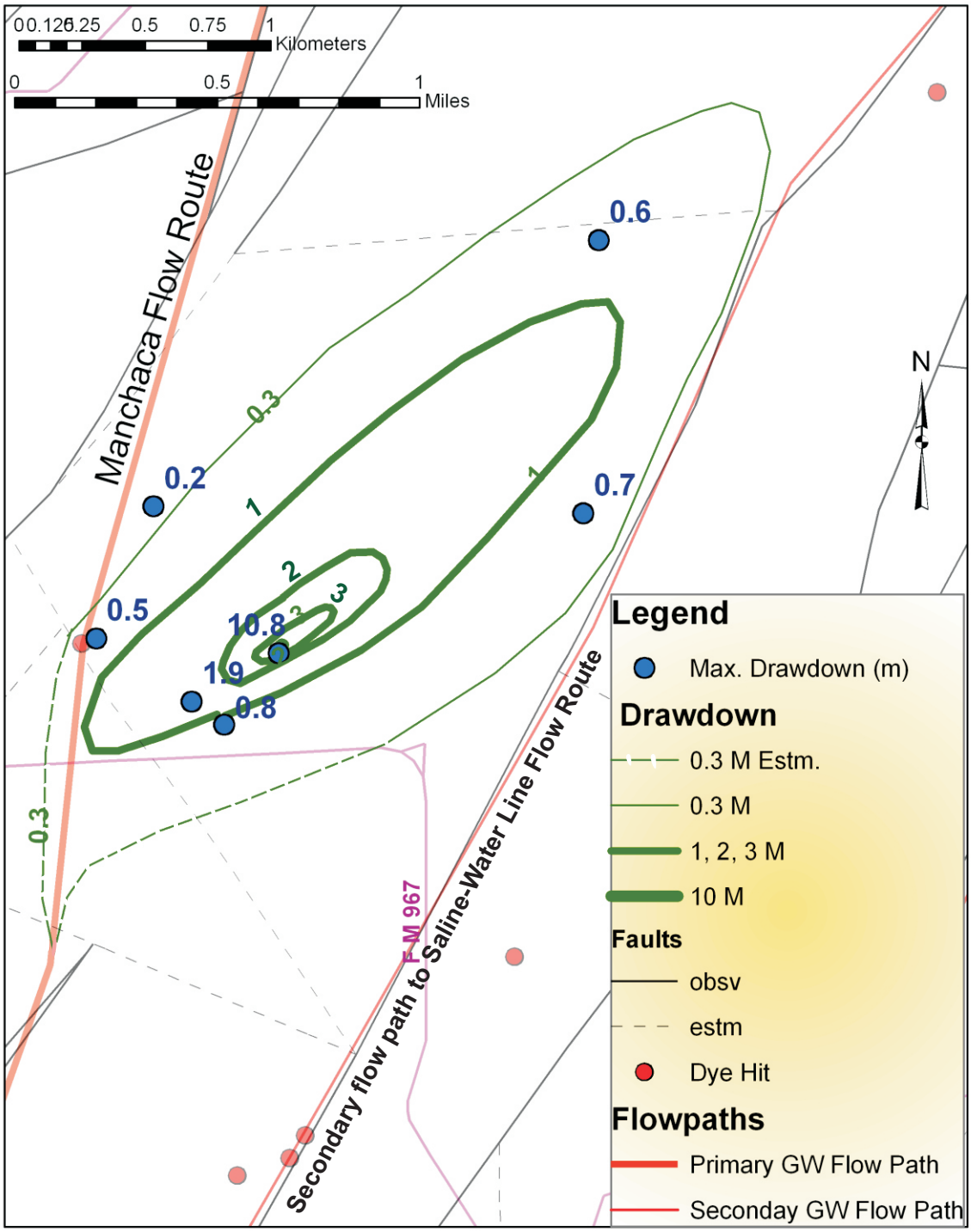

Figure 4.20. Cimarron Park 1996 aquifer test. Final drawdowns for the 1996 Cimarron Park aquifer test on Sept. 11, 1996. Two major groundwater flow paths are mapped on either side of this system, the primary Manchaca Flow Route to the west and a secondary flow path contributor to the Saline-Line Flow Route to the east. The cone of depression is interpreted to follow and diminish across these flow paths, although drawdown data was not collected to demonstrate this. The drawdown data does indicate an anisotropy of 0.12 to 0.33.

Δs_1 = 1.6 m; Δs_2 = 1.1 m
Q = 2.3 m^3/min
pi = 3.14159265

Cooper-Jacob (1946) Solution
T = (Δs*4pi) /2.3Q

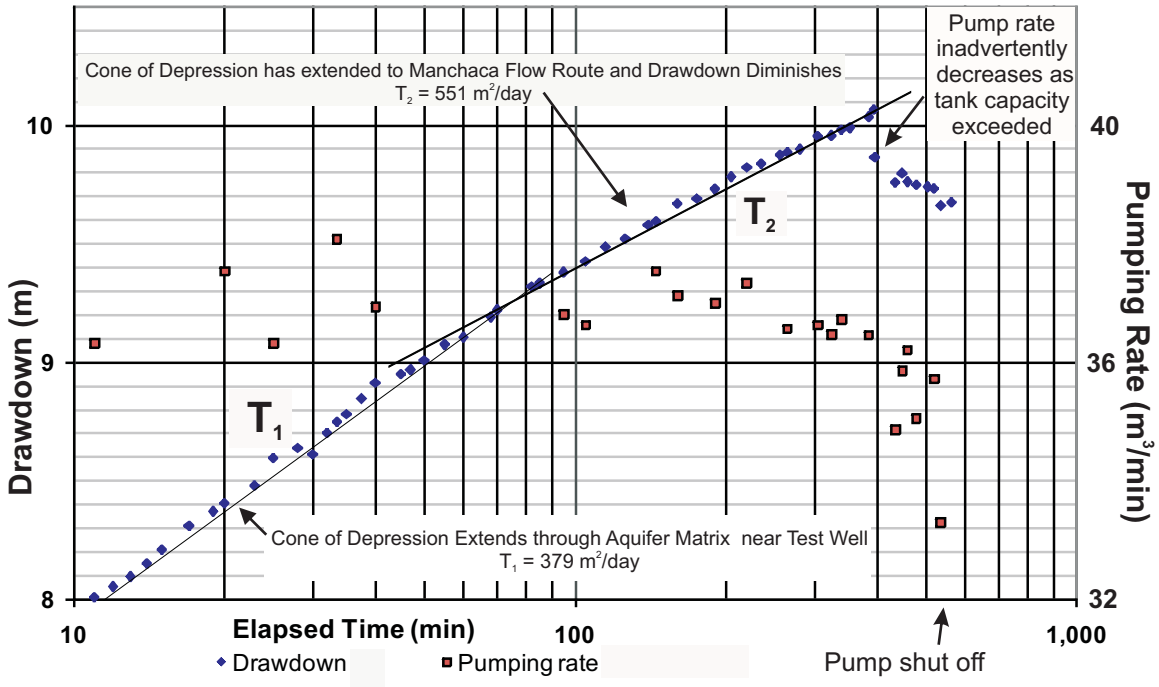

Figure 4.21. Cimarron Park 1996 aquifer test time-series drawdown. A semi-log plot of drawdown data collected during the Cimarron Park 1996 aquifer test indicates distinct shifts in transmissivity as the cone of depression expands from the pumping well 58-58-102. T_1 is interpreted to reflect the local aquifer while T_2 is interpreted to reflect the extension of the cone of depression to a major flow path, likely the primary Manchaca Flow Route about 0.8 km west.

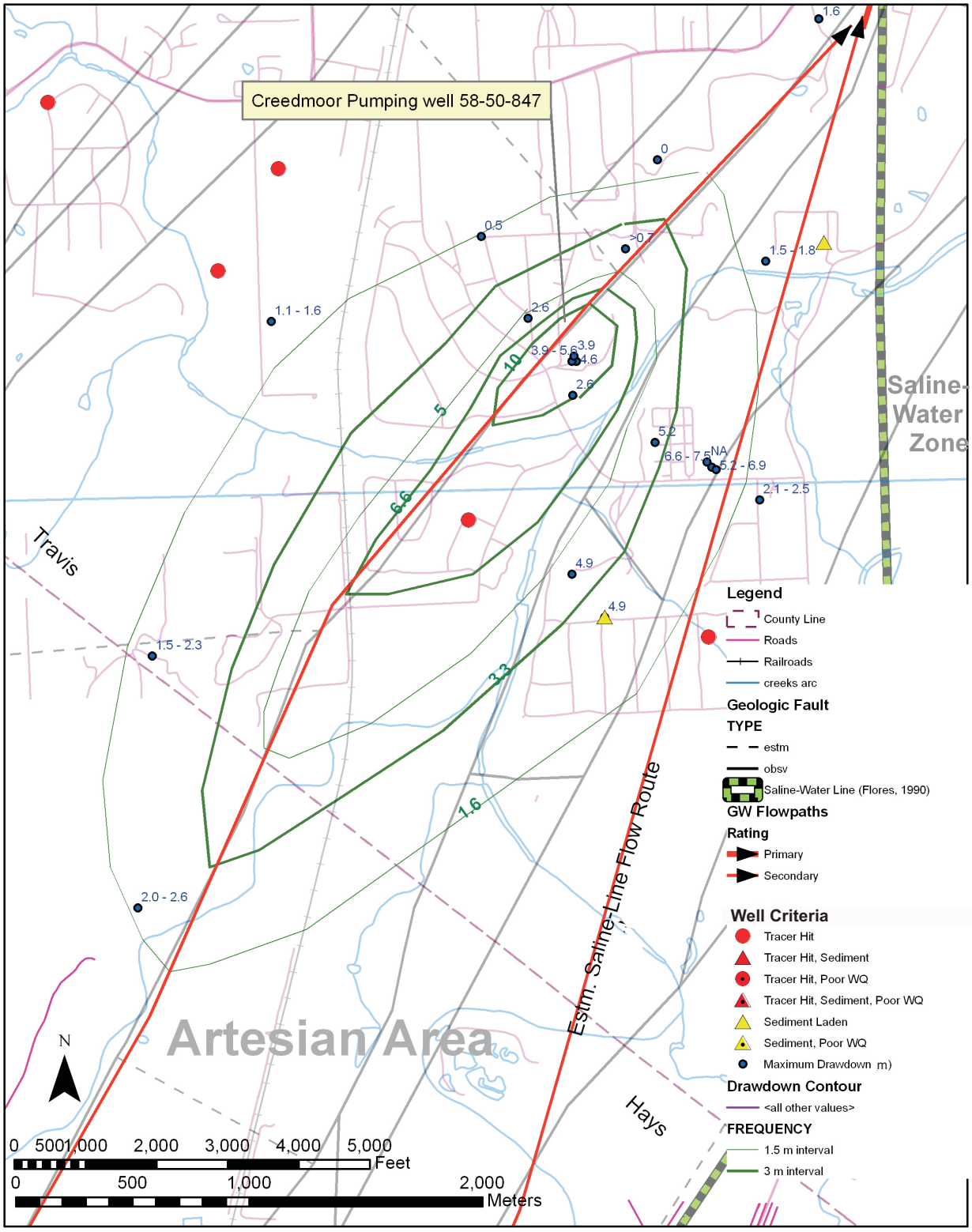

Figure 4.22. 2001 Creedmoore site 1 aquifer test. The cone of depression from the 2001 site 1 Creedmoore System aquifer test is anisotropic, following a secondary flow path to the Saline-Line Flow Route.

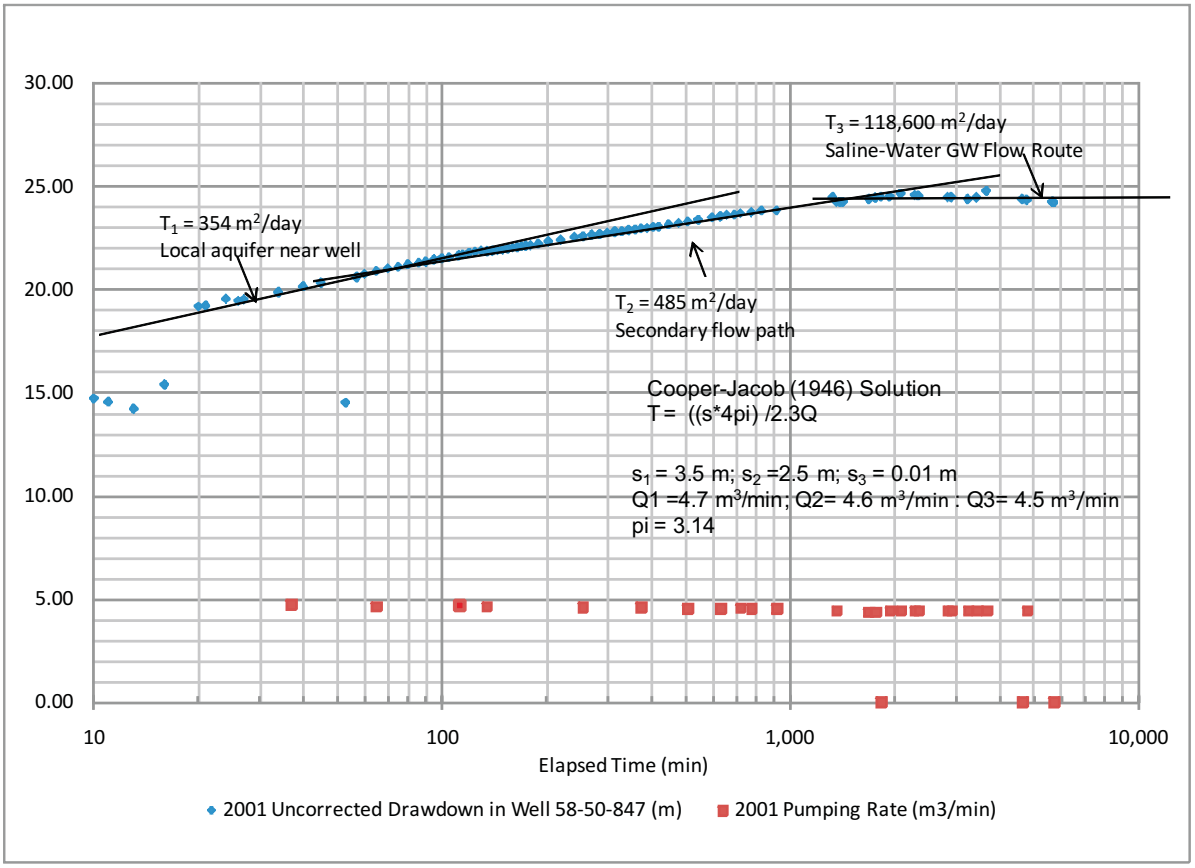

Figure 4.23. 2001 Creedmoor Site 1 aquifer test time-series drawdown. Shifts in increasing transmissivity are interpreted to reflect the brief expansion of the cone of depression through local aquifer, into a secondary groundwater flow path, and finally to the Saline-Line Flow Route 800 meters to the east.

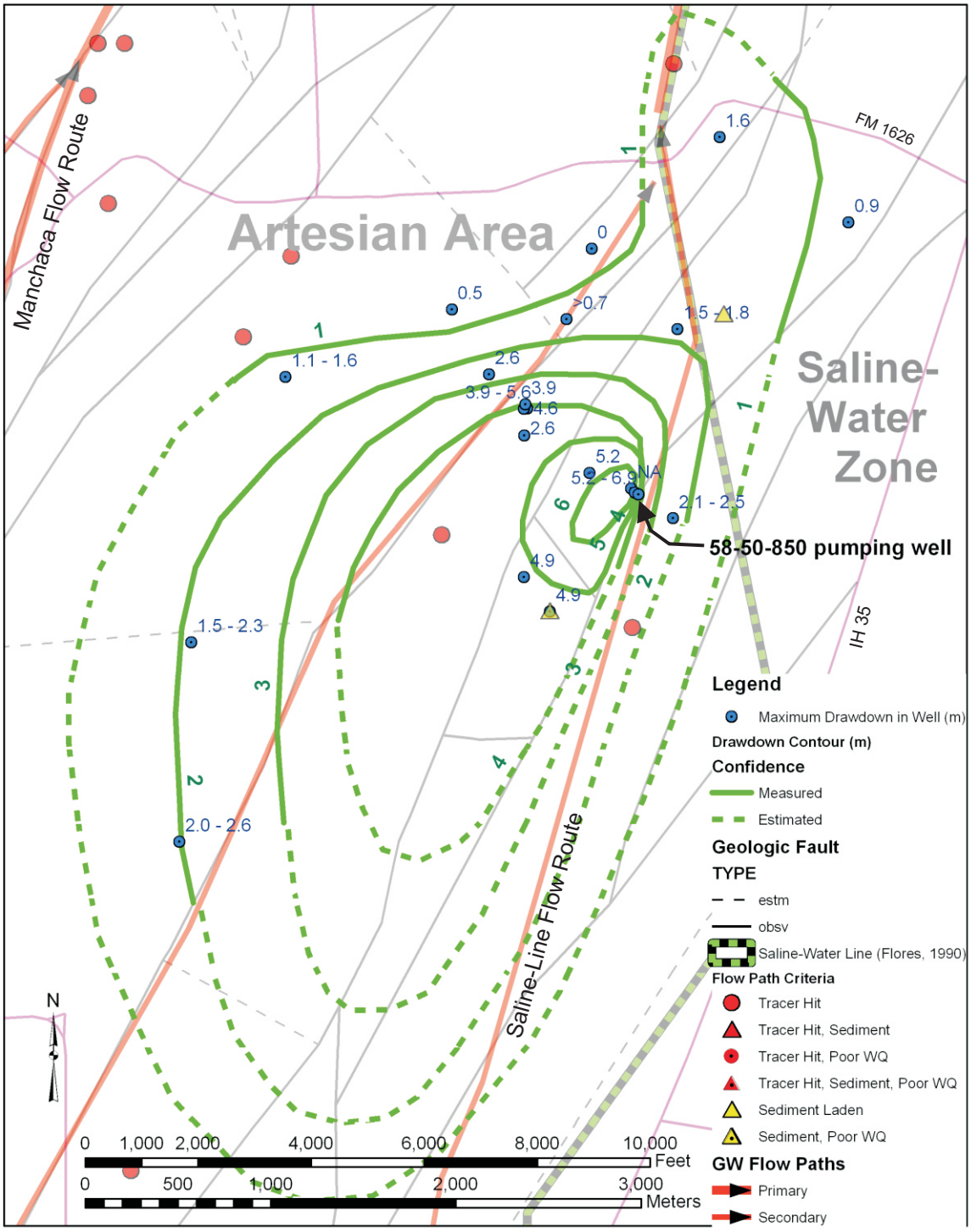

Figure 4.24. 2001 Creedmoore site 2 aquifer test.

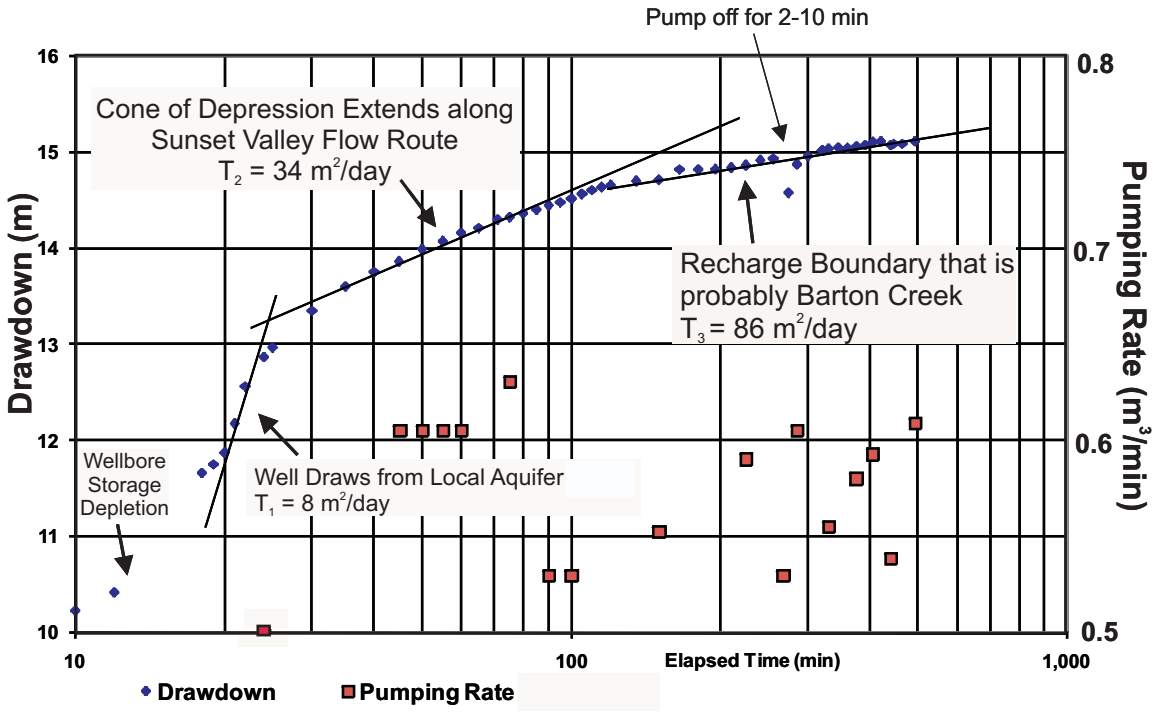

Cooper-Jacob (1946) Solution
T= (Δs*4pi) /2.3Q
Δs_1 = 19 m; Δs_2 = 4.4 m; Δs_3 = 1.75 m
Q = 0.57 m^3/min
pi = 3.14

Figure 4.25. Sunset Valley 1997 aquifer test time-series drawdown.Shifts in drawdown on a semilog plot is interpreted to reflect the cone of depression extending through the local aquifer matrix (T_1), the Sunset Valley Flow Route (T_2) 300 m to the east, and Barton Creek 1,700 m to the south.

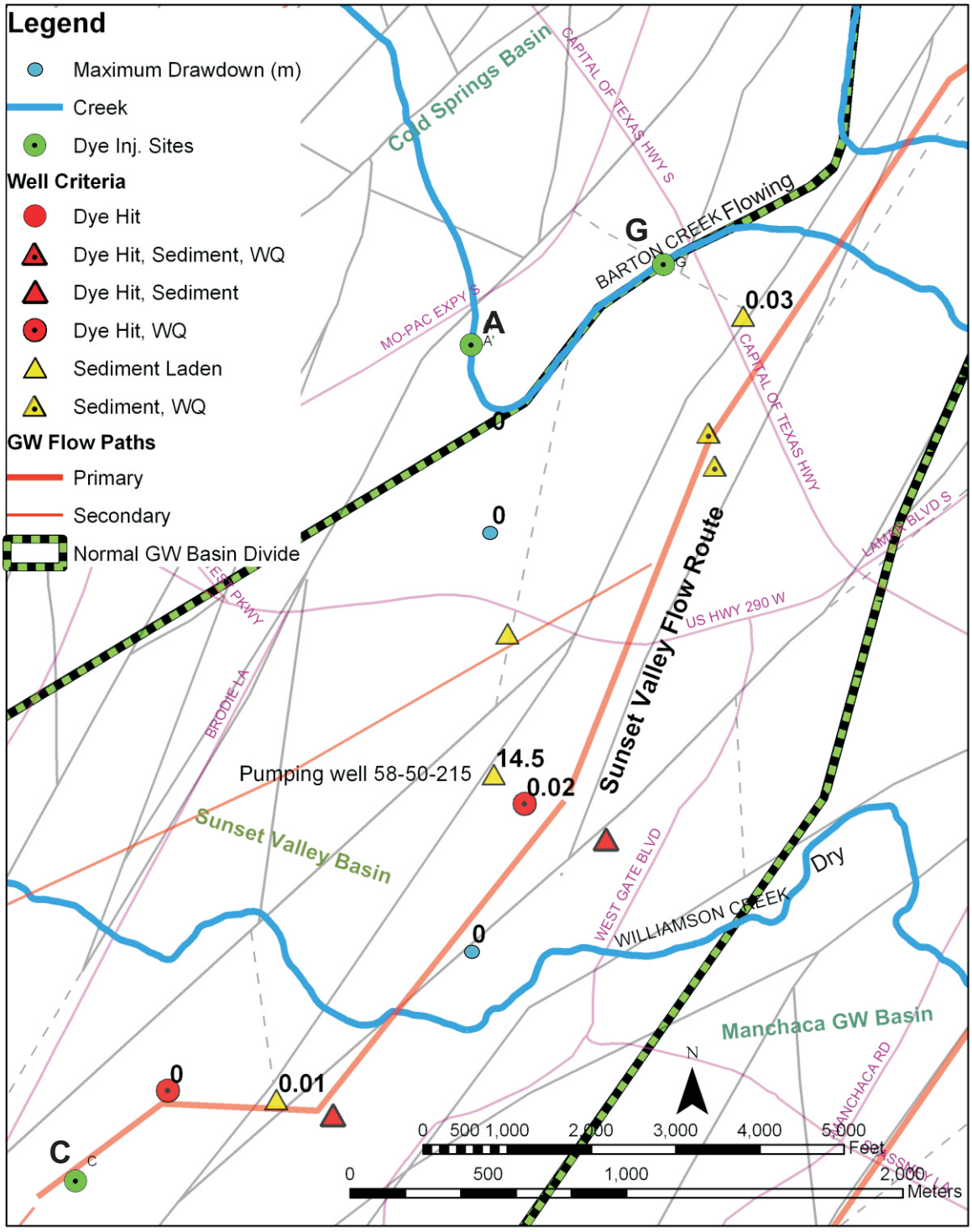

Figure 4.26. Sunset Valley test results. The maximum drawdowns measured in pumping and observation wells reflect the growth of a cone-of-depression along the Sunset Valley Flow Route, located 300 m east. Corresponding transmissivity are interpreted from drawdown shifts on a semi log plot. Barton Creek was flowing during the test.

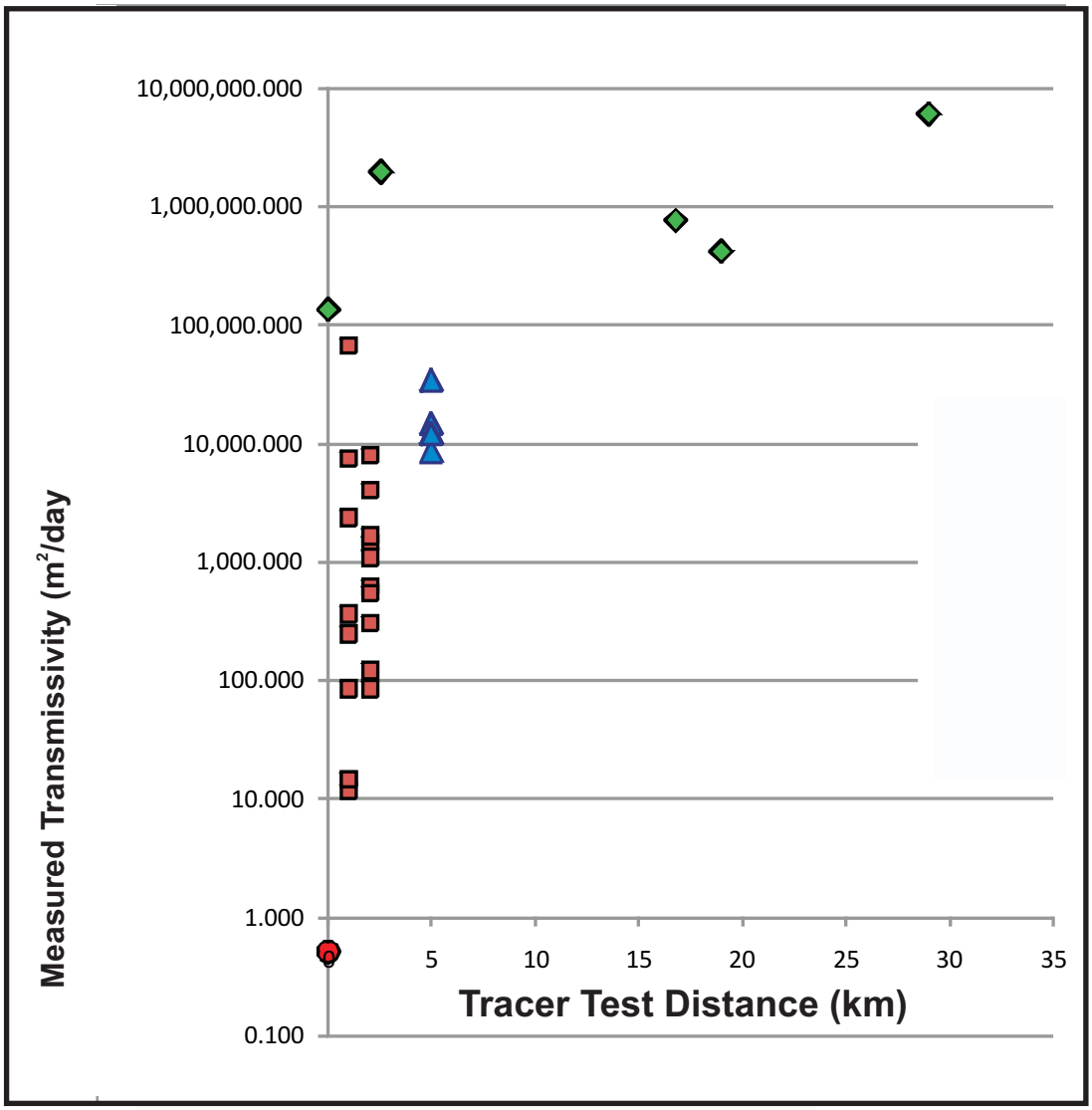

Figure 4.27. Range of transmissivity measurements. The scale of the tracer tests was calculated as the distance between injection and discharge sites along mapped flow paths. The scale of the well cores, aquifer tests, and recession analysis is assumed to be 1 m, 2 km, and 5 km, respectively. The increase in transmissivity with scale may represent decreasing transmissivity with greater distance away from primary and secondary groundwater flow paths.

5.0 CONCLUSIONS

A number of methods were used to evaluate groundwater flow and recharge in the Barton Springs Segment of the Edwards Aquifer. Faults were mapped across the Barton Springs Segment to examine their effects on groundwater flow and aquifer test drawdown. A water balance examined recharge on a research site. Groundwater tracing and other flow-path criteria defined primary and secondary flow paths and groundwater basins. Aquifer tests were conducted to examine the wellfield scale hydraulic properties. The following conclusions were drawn:

1) The quantity of recharge from upland internal drainage basins varies directly with catchment area and is reflected in the localized dissolution that creates sinkhole bowls. For natural internal drainage basins, the sinkhole catchment area is about 300 times its bowl volume. Bowl volumes may be subdued in the RDM, Grainstone, and Basal Nodular Members and Georgetown Formation, although large sinkholes are found in the Kirschberg, Leached and Collapsed Members. Recharge contributions from sinkholes can be reduced as a result of anthropogenic impacts such as sediment and debris deposition, impervious cover, and dissection of natural catchment areas.
2) Internal drainage basins defined as areas where runoff is completely captured and constitute at least 10% of the Barton Springs Segment. Internal drainage basins were distinguished as natural, ponded, and artificial.
3) Upland and intervening area recharge was measured using four different methods including: the measurement of water balance components on an upland sinkhole site for 505 days; chloride concentration comparison between rainfall and shallow cave drips; compilation of recharge measurements from other karst areas worldwide; and reinterpretation of an existing water balance based on stream-flow losses and Barton Springs discharge. For an instrumented internal drainage basin (HQ Flat) over a 505-day period when rainfall was 21% above average, 32% of rainfall recharged the aquifer and the remaining 68% left as evaporation or

transpiration to the atmosphere. 17% of the recharge (5% of rainfall) entered the cave drain to the sinkhole, and 83% infiltrated through soil-covered areas (26% of rainfall). The rapid increase in soil moisture following storm events and high portion of diffuse infiltration measured by water balance verified that soils on the J17 research site are relatively permeable. During a longer period of average rainfall, the discrete recharge to both HQ Flat Cave and a second monitored sinkhole, Flint Ridge Cave, diminished to 3% of rainfall. Comparison of chloride concentrations in local rainfall and runoff to a shallow (5 m) cave drip suggests that 26 to 49% of rainfall recharges the Tabor site. Worldwide 20% to 60% or more of rainfall can be expected to recharge mature karst aquifers. A 1980's water budget for Barton Springs, based on streamflow loss and Barton Springs discharge, was reinterpreted based on recent tracing data and found that 27% to 36% of Barton Springs discharge was unaccounted for by streamflow loss and could constitute intervening area recharge.

4) Cave morphology and groundwater tracing data indicate the groundwater flow is largely discrete with predominantly advective flow and low hydrodynamic dispersion.
5) Across the Edwards outcrop area, the major groundwater flow routes trend southeast along the gradient created by down-dropped fault blocks. Within the artesian area, the Manchaca Flow Route localizes along a few fault trends to the northeast. Groundwater flow on the far eastern side of the artesian area does not appear to follow to fault tends.
6) Primary and secondary flow routes convey flow from major recharge areas to springs. High transmissivity and rapid flow are localized along these routes within the Barton Springs Segment. Hydraulic conductivity (K in m/day) declines from the primary and secondary flow paths with increasing distance (L in m) by $K = 340 \times L^{-10}$.
7) When excessive recharge or flooding occurs, localized overflow conditions divert backup up flow to other flowpaths farther north or west. Infrequent overflow conditions may divert Onion Creek flow to San Marcos Springs.

The heterogeneity of the Barton Springs Segment will require additional characterization. Several factors that may affect the heterogeneity and anisotropy of the Barton Springs Segment were not examined fully. Further investigation should include:

1) Further quantification of recharge sources to and discharge sites from the Barton Springs Segment, including direct recharge through swallets within the major creeks, recharge through intervening areas, recharge and discharge to and from adjacent segments of the Edwards Aquifer, recharge to and discharge from the Trinity Aquifer and Saline-Water Zone, anthropogenic sources and losses, and recharge and discharge to or through overlying confining units through hypogenic processes.
2) A more detailed site-scale examination of heterogeneities of infiltration through soils, perhaps using tracers. A study of this type is currently being conducted on the Tabor WQPL research site by UT graduate student Brian Cowan.
3) Further quantification of the aquifer characteristics and flow paths using groundwater tracing.
4) The actual agents and processes of dissolution, such as the role of carbonic acid, hydrogen sulfide reducing agents and processes, and the role of microbial processes, both past and present.

APPENDICES

APPENDIX A

ESSAY: HISTORICAL OBSERVATIONS AND CONCEPTUAL PARADIGMS

A.1. HISTORICAL OBSERVATIONS AND CONCEPTUAL MODELS OF THE BARTON SPRINGS SEGMENT

In the course of my Ph.D. studies, I was intrigued by the evolution of hydrogeological concepts on the Edwards Aquifer. Historical views of groundwater flow and recharge of the Barton Springs Segment are varied. Mulkay (1979b) points out that scientific interpretations and validation criteria are "socially variable", but that they are not necessarily invalid. Geologists try to look at Earth systems objectively, but success depends on the methodologies and tools that are available or accepted at the time. The Edwards Aquifer and its Barton Springs Segment are introduced in a historical context in order to examine how views have varied. Some early investigators invested considerable effort in the study of this area, and many features that were visible in the past have since been covered by the urban landscape.

Recorded observations beginning in the middle 1800s reflect a conceptual understanding of the Edwards Aquifer as discrete networks of conduits. Roemer (1849a) describes the Edwards outcrop area of the Edwards Aquifer:

> The tableland in general is an arid region whose terrain is composed in many places of fissured, hard, limestone beds. The atmospheric precipitation which takes place, sinks through the fissures and crevices of the limestone to the impermeable stone layer, collects in large subterranean channels and breaks out in large springs where the limestone hills end abruptly. The impermeable bed is the clayey Cretaceous marl, which outcrops at the surface everywhere near New Braunfels and apparently extends as the underlying formation under the hard limestone bed of the higher plateau.

In 1898, Hill and Vaughan remarked on the Edwards Aquifer:

> There are many interesting caverns in the Edwards Plateau, and inasmuch as their occurrence, together with the general question of limestone solution, has great bearing upon the distribution of underground water, it is essential that

> they be briefly mentioned. They are of three general types: (1) small cavities within individual limestone strata, giving them what is locally termed a honeycombed structure; (2) open caverns occurring in certain bluff faces along the stream valleys; and (3) underground caverns of vast extent dissolved out of many strata…. The method of rock solution here shown is especially interesting to students of underground water, as it gives an insight into related problems discussed in later pages of this paper…. The limestone, as exposed in cliffs, may appear hard, durable, and of homogeneous nature, but the interior when examined may prove to be very heterogeneous…. The irregular cavernous decomposition of the Edwards limestone is well shown in the bluffs along the Colorado River west of Austin…. While water is distributed horizontally by thin pervious beds, separation planes, and cavernous strata or honeycombed rock, it is also distributed vertically in the Edwards limestone by joints, fissures, and crevices.

Hill and Vaughan held that the size and connectivity of subsurface caverns was evident from the presence of "peculiar cave-inhabiting animals" including "eyeless salamanders" in the Austin, San Antonio, and San Marcos area. They also reported that the entire Nueces River disappears into the Edwards Aquifer through a fissure at one location, which would be recognized as a sinking stream in other karst areas.

In 1922, Taylor and Schoch reported to the City of Austin on the feasibility of using various long-term water sources. They defined a "conveyance region" named as "Hardscrabble Country" that constitutes the Edwards outcrop and artesian areas, limited on the west by a "Main fault" (the Mount Bonnell Fault and its extensions) and on the north by the Colorado River. Taylor and Schoch believed that groundwater from the San Antonio area discharged from Barton Springs. They based this on the northward decline in potentiometric head and gradual increases in salt content. Potentiometric surface maps and groundwater tracing data (presented in Chapter 4) show a groundwater divide in the Kyle area under most conditions tested, but cannot rule out whether northward groundwater flow occurs from San Antonio to Barton Springs under extreme drought conditions. These early scientists also calculated the maximum sustainable pumping yield of the Barton Springs Segment to be one-fifth the normal flow of Barton Springs (or about 0.34 m^3/s or 12 ft^3/s), which is remarkably close to the current estimated pumping limit of 0.28 m^3/s (10 ft^3/s), calculated from observations of the later 1950s drought and groundwater models (Sharp and Banner, 1997; Smith and Hunt, 2004).

Taylor and Schoch (1922) evaluated the water quality of Barton Springs for a possible City of Austin water supply. In 1917, the presence of *E. coli* was detected only occasionally in Barton Springs. However, daily sampling in 1922 found bacterial contamination in every sample collected in June, July, and five daily samples taken in October and November after a light rain showed the presence of *E. coli* bacteria (Burns and McDonnell, 1922; Taylor and Schoch, 1922). These investigators concluded that the contamination originated from people living far from the springs and that Barton Springs was too sensitive to be relied on as a water source for the City of Austin.

The severe droughts of 1918 and the 1950s increased interest by the USGS and the predecessors of the Texas Water Development Board (TWDB), the Texas Board of Water Engineers and later the Texas Department of Water Resources to inventory wells, intermittently measure water levels and water quality, and periodically measure Barton Springs discharge (DeCook, 1963; Brune and Duffin, 1983). These data are vital for establishing background conditions prior to the urban growth experienced later over the Barton Springs Segment, to establish severe drought records, and to provide a long period of record.

DeCook (1957) made the following observations about recharge of groundwater to the Edwards Aquifer in Hays County:

> Of the precipitation that falls on the outcrop, a part may run off on the surface to other areas, but this amount is relatively small, as the topography is subdued in profile and stream-cut valleys are widely spaced. An undetermined amount of the rainfall is returned to the atmosphere by evaporation, intercepted or transpired by vegetation, or absorbed as replenishment to the soil moisture. The remainder infiltrates to the underground reservoir. Although data are not at hand to illustrate how much of the precipitation ultimately reaches the Edwards ground water, it is generally believed that it is a relatively high percentage in limestones such as the Edwards as compared with that in other rock types. In the San Marcos area, the soil veneer on the Edwards is relatively thin, and differential solution has produced many open spaces in the rock for the reception of water.

Guyton and Associates (1964) noted that the Barton Springs Segment and its contributing area ("Edwards Reservoir") was 960 km^2 (370 mi^2) in area and was recharged by direct infiltration on the outcrop areas and stream infiltration. Creek bottom

recharge through Barton, Onion, Bear, Slaughter, and Williamson Creeks was inferred to be the most important source of recharge. Guyton noted that even though Cold Springs discharged to the Colorado River at a lower elevation than Barton Springs, Barton Springs discharged at a much higher rate. The Barton Springs Segment was "envisioned as a complex three-dimensional network of pipelines through which water moves," and that at that time the "individual paths of movement cannot be predicted." If sufficiently large and well-connected conduits were present, then contaminants could move to Barton Springs from "relatively long distances with little or no natural purification."

Rose (1972) and Abbott (1973) described the hydrostratigraphic properties of the Edwards Aquifer as related to their depositional environment and evolution. The development of the Edwards Aquifer involved primary porosity present during deposition, dissolution of relatively thick and pure limestone sequence during the Cretaceous (paleokarst), selective dissolution of specific hydrostratigraphic beds by groundwater flow, and groundwater circulation enhanced by faulting (Abbott, 1973). Master conduits developed that pirated groundwater flow from other conduits and the matrix, and which directed flow to a few large springs. The lack of travertine deposits at the spring orifices indicated that residence time within the aquifer was not long enough to reach equilibrium with respect to aragonite (Abbott, 1973).

The late 1970s brought more effort to quantify hydraulic parameters of the Edwards Aquifer and was a period of renewed discovery of the Barton Springs Segment. This renewed interest may have grown from the desire for expansion of a growing population over the only readily available water supply for most of the Barton Springs Segment. Since 1978, the USGS measured Barton Springs flow and major creek channel flows continuously on the upstream edge of the Edwards outcrop area. Beginning in 1989, the BS/EACD began continuous measurement of water levels in a number of selected wells across the Barton Springs Segment. Cooperative support from the City of Austin, Texas Water Development Board, and Texas Natural Resource Conservation Commission, as well as research at the University of Texas at Austin has fueled collection of new data on the Barton Springs Segment.

Slade et al. (1986), Senger (1983), Senger and Kreitler (1984), and Baker et al. (1986) introduced quantification of hydraulic parameters in the Barton Springs Segment. Slade et al. (1986) and Baker et al. (1986) presented geologic cross sections that illustrated the geologic framework, conducted flow surveys of major creeks to show specific stretches where creek recharge was focused, and created potentiometric maps where large broad troughs gave indications of the presence of preferential flow paths.

A test for anisotropy reported by Senger (1983) and Slade et al. (1986) measured the anisotropic distribution of drawdown in wells following the drawdown of Barton Springs pool. During low-flow conditions, a 1-m (3 ft) water-level decline was observed in a well (58-42-915, see Figure 4.6) 1.7 km away, in a direction of fault trends, following the draining of Barton Springs pool. Farther south along the trend of faulting, a well (58-50-216) 2.7 km from the pool displayed a 0.15-m (0.5 ft) drawdown after the pool draining. Another well 1 km to the west (58-42-913) showed no response to the pool draining. The pool draining responses demonstrated the anisotropy of flow present in the Barton Springs Segment and allowed the approximate delineation of the "Rollingwood portion" (Cold Springs groundwater basin) and the source basin to Barton Springs. Senger tested the anisotropy of the area near Barton Springs with a porous media model and found that simulated heads could reasonably approximate observed water levels but did not show the extent of actual declines. Senger (1983, p. 59) noted that in "a carbonate aquifer, the groundwater flows in general through conduit-like fractures and fissures and inertial flow conditions are not uncommon" and that groundwater storage in bedding planes and solution collapse zones gave the Edwards Aquifer isotropic characteristics. Like Senger (1983), Ellis (1985) acknowledged that "good hydraulic connection through large underground conduits throughout the aquifer" was evidenced by relations between discharge, water levels, and rainfall. Slade et al. (1986) attributed variations in well yield directly to the presence or absence of cavities.

Andrews et al. (1984) described the groundwater flow network of the Barton Springs Segment:

> "A network of steeply dipping faults and joints, especially in the Balcones fault zone; large caverns; and underground channels afford the rapid movement of

ground water through the aquifer. These avenues make this part of the Edwards Aquifer in the Austin area particularly susceptible to pollution from natural or human sources during storm runoff."

Some literature from 1970s through the 1980s suggested an overall shift in viewpoints toward the Edwards Aquifer from a discrete to a perceived diffuse system. Senger (1983) and Slade et al. (1986) concluded from recession curve analysis and a dye trace that the Barton Springs Segment responded as a diffuse aquifer at large spatial scales. Well contamination in the 1970s and 1980s was attributed generally to poor well construction in those specific wells, rather than transport through conduits over distances in the aquifer (Reeves, 1976; St. Clair, 1979). According to St. Clair, contamination from many septic tanks in the Rollingwood area either did not reach the underlying water table of the Barton Springs Segment or reached it below measurable concentrations as a result of the thickness of the unsaturated zone (36 to 87 m), adsorption by clay-rich terra rossa, adsorption by rock surfaces in the bedrock, and dilution, dispersion, and chemical breakdown within the vadose and phreatic zones. Soils and fracture skins play a role in the adsorption and biological uptake of contaminants, as described in Chapters 3 and 4. The lack of groundwater contamination detected in other karst aquifers with septic tanks and urbanization, such as Dade County (Florida), San Antonio (Texas), and southeast West Virginia was presented in support of the hypothesis that Barton Springs Segment was relatively insensitive to surface contamination.

The data presented in St. Clair (1979), however, do not justify the conclusion that septic contamination did not reach the groundwater. In St. Clair (1979), some samples were intentionally taken shortly after rain events, which appropriately increased the chances of observing contaminants, but the relevance of sampling points was not established. By discounting the possibility of high anisotropy and heterogeneity, it was assumed that nearby wells were necessarily downgradient of the septic tanks. Since Quinlan (1990), karst hydrogeologists predict that the most representative sampling sites would likely be near springs, such as Cold Springs, but these were not monitored in the study, and that randomly spaced wells are unlikely to be downgradient of a single or even collective contamination source or sources. Many wells do not receive flow from

presumed sites of contamination, have only limited source areas, have distant recharge sources that differ from local sources, and have source areas that change with aquifer conditions. St. Clair (1979) assumed the Rollingwood recharge source area was local, but later tracing demonstrated that Barton Creek was the major recharge source for the Cold Springs groundwater basin (see Chapter 4).

Later sampling did reveal that contamination was indeed present in the Rollingwood area, although the specific sampling needed to determine the question of hydrologic connection between Rollingwood area septic tanks and groundwater may still be lacking. Cold Springs was sampled in several subsequent studies including by Parten (1991), COA (1997), and Hauwert and Vickers (1994) and showed doubling of nitrate-nitrogen and anomalously high ammonia concentrations (2.7 mg/l) after rain events that could represent flushed septic effluent from the unsaturated zone mixing with the relatively low-nitrate waters recharged from Barton Creek. Contamination in one of wells monitored by St. Clair, 58-42-813, was sufficient that the Texas Commission on Environmental Quality (TCEQ) refused to permit the well for water supply use in 1993 (Figure 1.4). In 1995, TCEQ performed a downhole survey on this well to assist the author (on behalf of BS/EACD) in planning its proper plugging. The downhole video revealed no cascading flows or other indications that borehole leakage was contaminating the well. COA (1997) noted that well 58-42-813 was elevated in chloride likely from anthropogenic sources. The assumption that earlier data collected by the Texas Water Development Board were necessarily representative of unimpacted groundwater is not valid, as Taylor and Schoch (1922) reported. Overall, the St. Clair study did not test for the type of karst conduit networks described by early investigators (Hill and Vaughan, 1898; DeCook, 1957; Taylor and Schoch, 1922; Guyton and Associates, 1964; and Abbott, 1973.) Based on nitrate-nitrogen enrichment within the groundwater in portions of the Barton Springs Segment, Barrett and Charbeneau (1996) suggested upland infiltration from septic tank leakage may be more important than previously estimated. Because natural sources of nitrate-nitrogen in limestone are limited to soils and vegetation, concentrations above 1.5 mg/l usually are derived from anthropogenic sources (Garner, 2005; Mahler et al., 2006).

Other studies from the 1970s and 1980s implied that the Barton Springs Segment was not particularly karstic and travel times for flow across the aquifer travel times were estimated to be much slower than later direct tracing data demonstrated. Brune (1981) estimated that "most of the water flows in a few days to a month through underground channeled and caverns to the springs", but believed that most flow originated from nearby Barton Creek. Ellis (1985) noted that groundwater flow rates in the Edwards "may be considerably slower than is generally believed" and "not as fast as formerly thought" based on point dilution tests reported by Maclay and Rettman (1972). These point dilution tests indicated groundwater flow rates of 0.55 to 15 m/day (1.8 to 51 ft/day) through interstitial pores. Later studies (Hovorka et al., 1998; Hauwert et al., 2004a) showed that these small-scale tests sampled only the relatively unused pores in the matrix and actual groundwater flow rates were more appropriately tested in other ways. Under normal flow conditions, Alexander (1990) estimated recharge from Onion Creek required about 3 to 5 years to discharge from Barton Springs. Slade et al. (1986, p. 39-40) noted that turbidity and bacteriological water-quality changes in Barton Springs and water-level changes in unconfined wells and Barton Springs indicated recharge from creeks reached the water table in a matter of hours. Even though the five monitored wells were unconfined, Slade et al. (1986) suggested that the discrepancy between inferred slow overall travel times and rapid water-level responses could be explained by pressurized groundwater in caves that allowed water-level changes to adjust rapidly through the aquifer as a pressure pulse. The turbidity and indicator bacteria in Barton Springs that increased within a few hours to several after storms were assumed to originate from local sewer-lines and from nearby Barton Creek since distant sources were thought impossible. Later tracing demonstrated that groundwater actual travels within days across the Barton Springs Segment under most conditions, such that contamination sources could rapidly reach Barton Springs from distant watersheds.

Unlike Hill's observations of the importance of caves and conduits in the aquifer system, some studies in the 1980s treated upland caves as localized phenomena and not important in the recharge contribution. Baker et al. (1986) noted that solution cavities, enhanced by faulting, allowed rapid infiltration and groundwater flow. However, caves

and sinkholes were inferred to be localized in only a few areas. Senger noted surface karst features existed in upland outcrop areas but suggested that "they cannot be considered important as recharge points to the aquifer." According to Senger (1983), all significant recharge occurred in major creekbeds as "most of the precipitation … is channeled as surface runoff into the creeks." The inference that caves were not relevant to aquifer yield was not universal, as Slade et al. (1986) directly connected well yields with the presence or absence of caves in wells.

A.1.1. Assumptions of Local Sources to Barton Springs

Because of the proximity of the Barton Creek channel to Barton Springs, its large catchment area, and demonstrated recharge loss under some conditions, workers in the 1970s and 1980s assumed that it was the most significant influence on the recharge and water quality of Barton Springs. Senger (1983) hypothesized that 90% of Barton Springs' flow was sustained by Barton Creek during high flow conditions. According to St. Clair (1979), increases in flow within several hours to a few days after rain events and associated sediment plumes could come only from Barton Creek. From geochemical analysis, St. Clair concluded that local sites in Barton Creek and the Colorado River were the major sources for Barton Springs. However, the elevated chloride and sulfate attributed to the Colorado River instead represents the breakthroughs from the Saline-Water Zone (Senger, 1983). Brune (1981) similarly perceived that the Barton Springs "are recharged chiefly by surface water in Barton Creek, and to some extent Onion Creek."

By mid-1980s it was generally recognized that Onion Creek and not Barton Creek was the principle recharge source for Barton Springs and the role of local recharge from Barton Creek has been found to be less over time. From three years of creek flow data, Slade et al. (1986) calculated that Barton Springs was fed by Barton, Williamson, Slaughter, Bear, Little Bear, and Onion creek watersheds, by 28%, 6%, 12%, 10%, 10%, and 34% respectively. Woodruff (1984) and Slade et al. (1986) further estimated that 85% of Barton Springs flow recharged within the major creek channels and that the remaining 15% recharged in intervening creeks and upland areas of the recharge area.

Later, groundwater tracing studies (described in Chapter 4) documented that most of the Edwards outcrop area portion of the Barton Creek watershed overlie the Cold Springs groundwater basin (Figure 4.3), although some runoff from upper Barton Creek does indeed flow along Barton Creek, recharge downstream of Loop 360, and discharge from Barton Springs. This recharge reaches Barton Springs faster than recharge from the other major creeks, as evidenced by an 8-hour tracer arrival from Barton Creek (Hauwert et al., 2004a). However, the differences in travel times of recharge from the major creeks are actually relatively small, as later tracing has demonstrated that some groundwater also can flow through the entire vadose zone and traverse the entire extent of the Barton Springs Segment within 3 days (Hunt et al., 2004; Hauwert et al., 2004b; Smith et al., 2006).

A.1.2. Implementation of 1980s Water-Quality Protection

The design of storm mitigation systems over the Edwards Aquifer in the 1980s reflected the prevailing understanding of the time. In 1979, the Shady Hollow sinkhole was engineered with a vertical culvert filled with gravel to filter the storm runoff from the neighborhood being built around it. The gravel failed from plugging during flood events in 1981, adjacent homes flooded, and the developer was sued by homeowners. Consequently, the gravel was removed to allow urban stormwater to recharge unimpeded (Green, 1984). Subsequently, the surface drainage for much of the Shady Hollow neighborhood was diverted untreated into numerous large sinkholes (URM, 1983) just east of the J17 and Tabor research sites discussed in section 3.7. Ironically, Shady Hollow is one of the "sole source" communities that rely on the Edwards Aquifer groundwater for its water supply. In the late 1980s, a storm-water drainage well was drilled into a sinkhole in Westlake Hills lined with sand as a "unique subsurface system" to manage storm water runoff in a "cost-effective, trouble-free, and efficient" manner (Kabir, 1987). Wastewater treatment plants built for new developments in Shady Hollow and Travis Country in the 1980s discharged "treated" wastewater to the Edwards outcrop portion of Slaughter and Barton Creek watersheds. These two plants were closed in the early 1990s and other surface discharge of treated wastewater to the Edwards outcrop

area has since not been permitted. Although subsurface drainage systems of urban storm water are no longer constructed, older existing systems still operate today and reflect the 1980s concept of the Barton Springs Segment as a diffuse aquifer with high dispersion where upland recharge is insignificant.

A.2. CURRENT PERCEPTIONS OF THE BARTON SPRINGS SEGMENT

In the 1990s, the Barton Springs Segment underwent another perception shift. Hauwert and Vickers (1994) compared features found in other karst regions, such as potentiometric troughs, to similar expressions of conduit flow in the Barton Springs Segment. Contamination identified in wells and springs verified the hydraulic connection to the surface and through the aquifer that would be expected from urban sources in a karst aquifer (Hauwert and Vickers, 1994). The City of Austin (1997) states the "flow in the BSEA [Barton Springs Segment] appears dominated by conduits based on the abundance of caves in the Edwards, rapid rises in water levels following rain, field observations of spring discharge points, spring responses to rain events, and rapid drops in water levels." The "rapid recharge and rapid migration characteristics" of the Barton Springs Segment allow "contaminants to enter the aquifer rapidly with minimum attenuation." Successful large scale groundwater traces began in 1996 and provided direct data on groundwater flow paths, travel times, and attenuation (Hauwert et al., 1997). Sources of sediment within the aquifer were distinguished using mineralogy and it could be demonstrated for the first time that particulates readily move across the Barton Springs Segment (Mahler, 1997).

A.3. POSSIBLE EXPLANATIONS FOR CHANGING CONCEPTUAL MODELS

The wide variation on perspectives of the Edwards Aquifer on even the same data sets and sites, begs for an explanation. Why do current conceptual models of the Edwards Aquifer more resemble views of the 1800s and early 1900s than in the 1970s and 1980s? Below some possibilities can be suggested.

A.3.1 Lack of data

One possibility could be an aliasing bias, where the magnitude of a time series appears smaller than when sampled at higher frequency (Agneni, 1992). The time-series bias easily applies to groundwater sampling for contaminates and injected tracers where a lower recovery of tracers or contaminates invariably occurs when loading pulses are missed by insufficient samples (Quinlan, 1990). Because some materials move as pulses through a limestone aquifer, sampling techniques selected may be insufficient to measure representative concentrations or loads. As a result of aliasing bias, the connection between surface constituents and the groundwater system may not be clear. Quinlan (1990) points out that the lack of detection of a contaminant is frequently the result of insufficient monitoring in karst areas. However, the absence of well known groundwater contamination still is cited today as evidence that the surface is not well connected to the subsurface. Because of the discrete nature of karst aquifers, insufficient groundwater sampling, including timing, frequency, methodology, parameters, and sampling locations, tends to obscure evidence of any surface and subsurface connections that exist.

A similar bias exists because complex systems appear more heterogeneous with more examination. Gomez-Hernandez (2006) wrote "the issue is not so much the degree of model complexity but, rather, how to address the uncertainty associated with model predictions due to lack of knowledge." Ford (1999) illustrated this point with a hypothetical example showing how karst systems can appear more discrete (i.e., heterogeneous) with deeper examination. Kiraly (2002) suggested that it is possible to model groundwater flow in a karst aquifer but only if a high degree of understanding is present.

Worldwide, the basic understanding of karst aquifer systems was relatively advanced by the 1940s (White, 2000). However, Hubbert's (1940) classic paper on groundwater flow influenced many to treat limestone aquifers essentially as forms of porous media systems in which caves had little practical significance in groundwater flow (White, 2000 and 2007). However, it is clear even at a large scale that the groundwater flow rate and contaminant transport of karst aquifers cannot be accurately simulated with a porous-media equivalent because of the dominant effects of preferential flow paths and

turbulent flow along conduits (Schindel et al., 1986; Huntoon, 1995; Quinlan et al., 1996; Halihan et al., 2000).

It is important to recognize there are biases toward direct observations on the surface by many versus those observed by a few or inferred in the subsurface. Ford (1999) noted that conceptual models of karst areas came from two widely divergent types of investigation. He suggested that groundwater hydrogeologists tend to examine karst through wells and cores and measure very localized hydraulic characteristics that typically suggest a system of diffuse groundwater flow and recharge. Speleologists and karst hydrogeologists typically focus their investigation on conduits large enough to enter and on spring discharges. These studies highlight the discrete nature of flow in karst aquifers. Klimchouk (2000) pointed out that even among speleologists and karst hydrogeologists there are historical preferences towards looking at karst morphology in terms of shallow epikarst processes, which can be more readily observed, rather than deep-seated hypogenic processes, which are more cryptic.

A.3.2. The Cryptic Nature of Caves

Cryptic refers to something concealed, hidden, mysterious, or not recognized and this term describes the nature of karst on the Barton Springs Segment. The cryptic nature of caves creates biases that tend to underestimate their presence. These biases include limited property access; the tendency for filled cave entrances; the difficulty of cave exploration; the limited efforts to examine and document caves; and physical constraints of passage size and the water table.

Access is limited to properties where caves can be examined. Some property owners value privacy, are hesitant to allow access to geologists they do not personally know, and may not understand how such assessment may help preserve their water supply. Many property owners envision eventually profiting from their land investment and perceive that discovery of caves or endangered species may prevent or limit the marketability of their land. Property owners of large tracts who might otherwise allow access have not been asked because of time constraints of the researchers, because the property has not been identified as useful to a specific research problem, or because of

lack of contact information. Most assessment effort is invested in tracts preparing for immediate development, where the developer hires a geologist to conduct an assessment and the state and or local municipality has a limited opportunity to review the assessment and site. The Texas Commission on Environmental Quality is allowed 30 days to review the plan, receive comments from local jurisdictions, and conduct its own site inspection. Although many caves are documented during development review on a site-by-site basis, many likely are not. The public acquisition of Water-Quality Protection Lands (WQPL) on the Edwards outcrop area by the City of Austin since 1999 has been a big step for providing access and understanding of the Edwards Aquifer. The acquisition of preserve lands has made caves and sensitive features more economically valuable, with the result that private property owners are more willing to point out known features. The WQPL also provide access for long-term studies.

Newly discovered caves within the Barton Springs Segment generally do not resemble the large, gaping openings of local, popular, commercially-developed caves. Most of the sinkhole entrances found and documented within the last 30 years within the Barton Springs Segment were discovered filled with trash, boulders, flood debris, fine sediment, or terra rossa. Being depressed features, sinkholes tend to accumulate debris, particularly where land disturbance is occurring within the catchment area. A study of sediment from Halls Cave in the Edwards Plateau suggested continuous soil erosion and natural cave filling during a period of strong seasonal rainfall that declined after the last glacial period in the late Pleistocene and middle Holocene, roughly 14,000 years ago, and ending about 5,000 years ago (Toomey et al., 1993; Musgrove et al., 2001; Cooke et al., 2003). Recent erosion (100 cm/1,000 yr) has increased by an order of magnitude over the relatively high climate-driven soil erosion rates of the post glacial period (2 cm/1,000 yr) as a result of abrupt land-use changes (Cooke et al., 2003). Subsequently, potential land disturbance activities, such as large-scale ranching, agriculture, and development of urban centers, increased sediment loading in runoff to creeks and sinkholes (Pimentel et al., 1995).

By the 1980s, much of the natural surface area in the Barton Springs Segment was been sufficiently modified by urbanization and ranching practices to the point that surface karst forms were not as evident as they had been earlier. Filling of open sinkholes was common practice on local ranchlands through the mid-1980s to eliminate possible hazards for cattle and other livestock, to create stockponds out of sinkhole depressions, and to dispose of wastes (Aley, 1972; Grimshaw, 1976; Elliott and Veni, 1994; Hauwert and Vickers, 1994). Many caves and sinkholes have been sacrificed to accommodate growing urban spaces. Skyway Cave (Appendix C) is an example of dozens of known caves later covered with building, parking lots, yards, and other urban spaces. A comparison of historical and current aerial photos in Pinellas County, Florida, showed that 87% of the original sinkholes were covered by urbanization (Brinkmann et al., 2007). As neighborhoods grew closer to discovered caves, these caves became magnets for potentially inexperienced and ill-equipped explorers. This frequently resulted in unnecessary fear or injury to the explorers, or damage to the cave or its inhabitants from vandalism (BCCP Karst Subcommittee, 2007). Such problems have led to the sealing of sinkholes and caves. As a result, the filling of sinkhole bowls or dissection of their catchment area may affect the ability to assess their natural condition.

Caves have an inherent bias in that, by definition, requires that they must be large enough for a person can enter (Jennings, 1985, p. 135). However, conduits and fissures smaller than human dimensions can play a significant role in transporting subsurface water. Although conduits and caves passable by humans generally are limited to dimensions of about 0.15-0.3 m (0.5-1 ft) in breadth, actual size limitation of access by an investigator is subjective. Some investigators may view a 1-m (3 ft) wide passage as being too small to enter. Coupled with the frequent need to remove loose material from portions of cave passages to make constrictions passable, most physically accessible caves in Austin are perceived as inaccessible.

Cave exploration, even in the unsaturated portions of the Edwards outcrop area, is relatively slow, grueling, dirty, potentially dangerous, and requires specialized skills. In general this exploration is carried out by a few experienced volunteers associated with the

Texas Speleological Survey (TSS), local cave clubs, and other cave management groups. Most cave discoveries in the Austin area still are made or supported by a small number of volunteers. The Texas Commission on Environmental Quality Edwards Aquifer Protection Program does not require geologic features to be entered and mapped in order to assess their sensitivity for proposed development. Most geologists have not acquired the skills or inclination to examine caves to the same degree as speleologists (Veni, 1999). As a result, relatively few cave discoveries are made each year within the Barton Springs Segment and the information available from accessible caves may not be fully utilized.

Roughly two-thirds of the aquifer volume of the Barton Springs Segment is water saturated, which makes it extremely difficult or impossible to examine the phreatic zone in the way the vadose zone can be examined. The Barton Springs Segment is unusual as an aquifer, in that a person can directly examine it as far down as the water table at only a limited number of sites. Consequently there is a bias for vadose caves over phreatic caves.

The factors influencing cave discovery tend to lead scientists, regulators, and the public towards believing that caves are not common or, more importantly, that conduit hydrologic connection is not developed within the Barton Springs Segment. In part to educate the public about the natural landscape, recharge, and cave ecosystems, a number of cave preserves have been created since the 1990s in the Austin area. These preserves are open to the public, although the caves themselves are restricted to supervised access. South Austin area parks and preserve with educational exhibits, public access to surface karst features, and possibly limited guided subsurface tours include the Goat Cave Karst Preserve, the Village of Western Oaks Karst Preserve, the Lady Bird Johnson Wildflower center, the Barton Creek Greenbelt, Dick Nichols Park, and the Slaughter Creek MetroPark.

A.3.3 Cultural Influences

It is possible that a scientist's views of the Barton Springs Segment are influenced by cultural and social environments of the time, as hypothesized by Mulkay (1979a and

1979b). Consider that a few decades ago, the practice of disposing trash into sinkholes was accepted and widespread across the United States, and it was commonly believed that contaminants associated with refuse were well attenuated by limestone aquifers (see section 3.7.4). Aquifer education was focused heavily toward convincing the public that "underground streams" espoused by dowsers did not in fact exist (Vogt and Hyman, 1979). In reality, as Meinzer (1923, p. 134) noted, "some of the large caverns contain streams that do not differ greatly from surface streams." Regardless of whether a hypothesis is correct or not, social pressures exist to accept certain paradigms and reject others. Mial and Mial (2002) describe the social perceptions that lead the geologic and scientific community to accept new paradigms in seismic stratigraphy and global sea-level cycles almost wholeheartedly with very little supporting data, relying instead on "assumptions about Exxon's resources, scientific expertise, authority, and credibility."

In the objective assessment of a site, it is difficult not to consider the perceived reactions of the public to the discoveries of heterogeneities and how such discoveries may affect the proposed use of sites, particularly where economic investments are perceived to be at risk (Adolf, 1961a; Adolf, 1961b; Wessel, 1982; Ashford, 1983; Bradley, 1983). Environmental scientists are frequently put in a position to characterize complex heterogeneous geology with pressures to produce the lowest bid, pre-determined desired outcomes by a client, and the need for continued work (Cehrs and Bianchi, 1996). Meehan (1984) saw that even previously known and active faults were frequently overlooked in geologic assessments for proposed nuclear plants and waste sites in California. In this case, the bias was attributed to a regulatory approval system that relied entirely on assessments by representatives of the proposed plant who were encouraged by clients to find that a preselected site was structurally and hydraulically homogeneous. Systematic biases frequently are perceived as influencing results of scientific studies in the pharmaceutical and energy industries (Washburn, 2003 and 2005). Lexchin et al. (2003) found that pharmaceutical studies funded by companies are four times as likely favor their products.

These pressures are also extended to oversight agencies. As an example, during the cholera epidemics in England during the mid-1800s, the diagnosis of virulent strains

of cholera and its origins was influenced by long-standing but erroneous perceptions, politics, fears of economic consequences, and corporate conflicts between powerful water districts (Morris, 2007). The erroneous understanding of cholera was ingrained by health boards whose members were politicians with little technical expertise and doctors who only supported traditional views (Morris, 2007).

The distribution of research funding may affect the extent to which complex systems are understood. In the early 1980s, federal environmental research was limited by sweeping personnel changes, budget cuts, and reductions in regulatory requirements (Vig and Kraft, 1984). In the mid-1990s, EPA funding supported groundwater tracing studies within the Barton Springs Segment.

It is not clear to what extent a multitude of conditions, such as limited data, the cryptic nature of caves, and political and economic pressures for development, contributed to the shift in the 1970s and 1980s to view the Edwards Aquifer as a relatively homogenous, diffuse aquifer with high sorption. Factors such as limited access to caves, the covering of cave entrances, the lack of cave discovery and mapping efforts, and the discrete nature of cave data limits our perception of the prevalence of karst. Some aspects of the Barton Springs Segment were presented by a wide range of published interpretation based on little data.

A.4 CONCLUSION

Understanding of the recharge and discharge processes of the Barton Springs Segment have benefited from over a century and a half of observations. Although geologists in the 1800s did not differ overall in their descriptions of the Edwards Aquifer, there are shifts in the perception of its karst development and heterogeneity over time. Efforts to quantify hydraulic parameters in the 1980s were limited by perceptions that the Barton Springs Segment could be treated as a diffuse aquifer system. In general, the perceived heterogeneity and karst maturity of the Barton Springs Segment has increased with greater examination. Assessments from the mid-1800s to 1970 saw the Edwards Aquifer as strongly influenced by conduits, from observations including disappearing streams, blind aquatic vertebrates, and water-quality impacts far from potential sources.

Assessments in the 1970s and 1980s generally saw the Barton Springs Segment as an overall diffuse aquifer with good hydraulic connection with localized and uncommon caves and conduits. In the 1970s and early 1980s some inferred Barton Springs as being supplied primarily or largely by Barton Creek, because it was the closest creek with a large catchment area. Although sediment from Barton Creek was thought to discharge at Barton Springs, other surface contamination was thought to be unable to reach the water table across the outcrop area because of attenuation and the minor role attributed to upland recharge. Observed instances of contamination were generally attributed to poor well construction within the well where contamination was observed. The 1990s introduced investigations using approaches including groundwater tracing. Literature after 1990 generally describe the Barton Springs Segment as an aquifer in which fractures, fissures, caves and solution cavities are very common and groundwater flow is localized through conduits. The role attributed to Barton Creek as a recharge source to Barton Springs diminished after tracing suggested most of the outcrop area of its watershed overlies the Cold Springs groundwater basin.

The changing paradigms of the Edwards Aquifer over time demonstrate that study of these karst systems is still a dynamic frontier for research. "Successive transition from one paradigm to another via revolution is the usual developmental pattern of mature science" (Kuhn, 1996). With each new finding, I see my earlier interpretations requiring refinement. The study of the Edwards Aquifer demonstrates that with scientific scrutiny, complex aquifers such as the Barton Springs Segment can be successfully characterized.

APPENDIX B

MEASURED SECTIONS

Measured Geologic Section of Barton Creek at Campbell's Hole, Deep Eddy (Cold Springs) Bluff, and Bee Creek

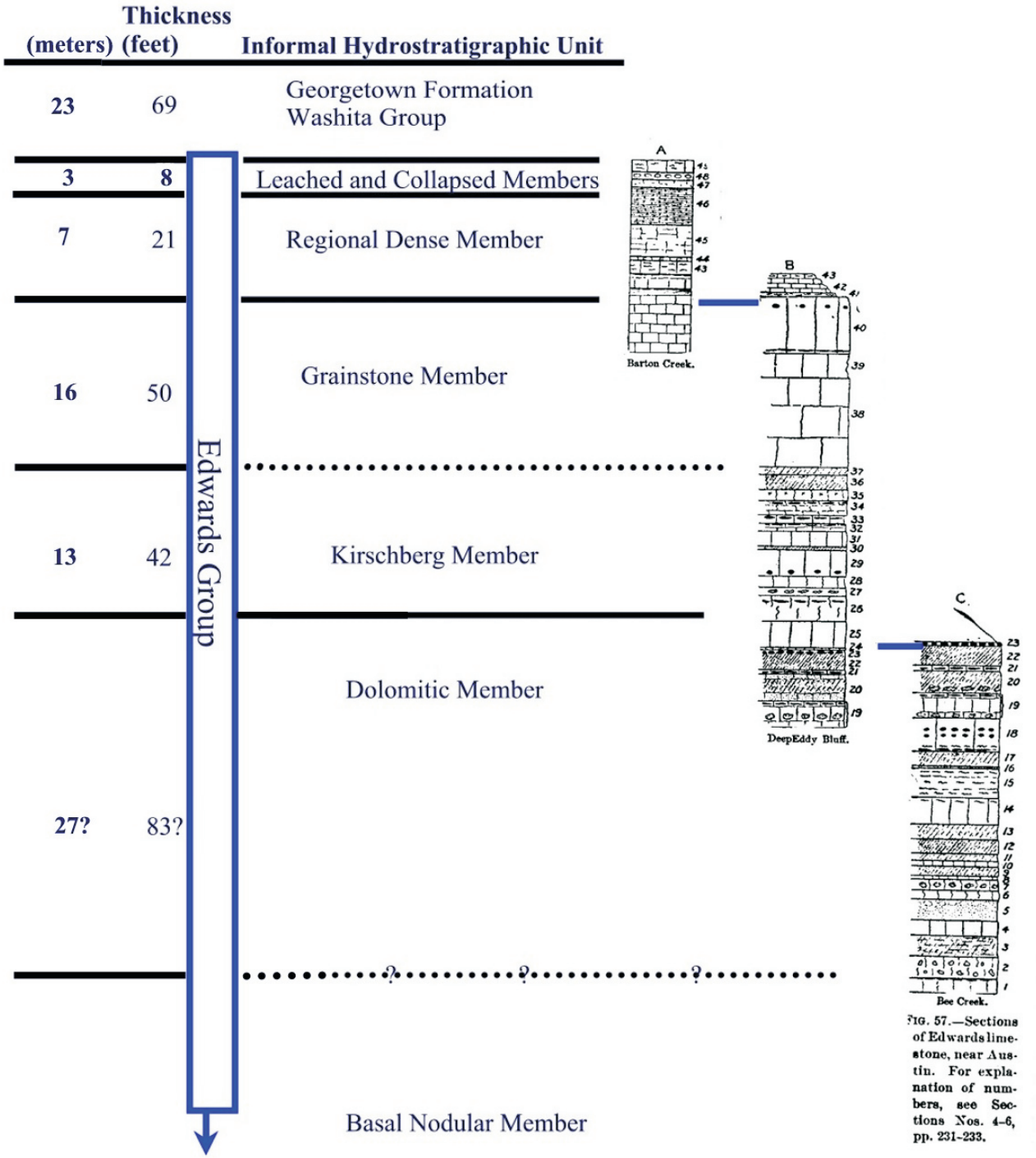

FIG. 57.—Sections of Edwards limestone, near Austin. For explanation of numbers, see Sections Nos. 4–6, pp. 231–233.

Measured section reported in Hill and Vaughan, 1899.
Interpreted by Nico Hauwert, City of Austin WPDRD, 2003

SECTION NO. 4.—*Bluff on Barton Creek, about 1 mile above Barton Spring, Travis County, Texas.* (Fig. 57, A.)

Fort Worth limestone:[1]

	Ft.	In.
5. Grayish limestone, irregular fracture, with *Alectryonia carinata* and *Gryphæa washitaensis*	1	0
4. Yellow or reddish calcareous shale	4	4
3. Alternating layers of hard and soft limestone with *Alectryonia carinata*, *Gryphæa washitaensis*, *Exogyra americana*, etc	18	0
2. Hard grayish limestone	33	0
1. Soft chalky limestone, with a saline taste	13	0
Total thickness of Fort Worth limestone	69	4

Edwards limestone:

49. Nodular limestone full of Requienia	3	0
48. Nodular limestone, nodules as large as one's head	2	0
47. Hard chalky limestone	3	0
46. Thinly laminated limestone (the so-called "lithographic flags")	8	9
45. White, sublaminated, chalky limestone. The lower part of Nos. 45 and 46 contain many fossils, *Exogyra texana*, *Pholadomya knowltoni*, etc.	8	5
44. Nodular limestone, no Requienia	1	0
43.[2] Nodular limestone with many Requienia (second Requienia bed)	3	9
e. Laminated limestone	1	0
d. A series of hard limestone ledges (eight in number) separated by the thinly laminated layers. There are some flints, about as large as a man's fist—Radiolites and *Ostrea? munsoni*	45	8
c. Flaggy layer with discoidal flints	2	4
29 *b*. Hard limestone, forming a shelf along this portion of Barton Creek and its bottom at the bridge below, eroded into deep pot holes. The lower 2 feet of this layer contains very large blue flints, often 1 foot across. Some of them are oval, others flattened out and very irregular in outline. The upper part of bed contains small flints	12	8
a. Limestone ledges with some flattened flints. All of the flints in this section belong to the blue variety	11	0
Base of *a* is Barton Creek bed.		
Total thickness of strata in bluff	171	11

SECTION NO. 5.—*Deep Eddy Bluff, south of the Colorado River, west of Austin.* (Fig. 57, B.)

	Ft.	In.
43. Nodular limestone with Requienia at top (the second Requienia bed of the Barton Creek section).		
42. Limestone ledges	5	0
41. Limestone ledges containing Requienia. The three layers above described form a slope to the top of the hill (or bluff) above the face proper of the bluff	1	0
40. Ledge of hard limestone, 10 inches above basal sheet flint. The upper part of the ledge contains rather small nodular flints	15	0
39. Limestone weathering out and giving rise to a good deal of red clay, apparently representing the zone of calcitized fossils found in the high bluff above McGill's Ford	6	6

[1] The Fort Worth limestone is assumed to be 70 feet thick at Austin. Future study may modify this estimate. The uppermost layers, characterized by *Kingena wacoensis*, are missing in the section.

[2] The beds in the Barton Creek section below 43 can not be correlated layer for layer with the Deep Eddy Bluff section; therefore numbers are not used in the description of the former section for beds below the one numbered 43 (except in one case, 29). The numbers in the different sections indicate equivalence.

From Hill and Vaughan, 1899.

	Ft.	In.
38. Massive thick ledges of limestone, detail not exposed	23	8
37. Soft, white, arenaceous limestone	2	2
36. Soft arenaceous limestone	3	10
35. Ledge of limestone, rather soft, emitting odor of petroleum	2	10
34. Chalky limestone forming little caves, composed of a good many small ledges; discoidal flints at top	4	0
33. Hard limestone, emitting odor of petroleum under blows of hammer. Texture of limestone rather mealy. Nodular flints, occasional discoidal flints in top	2	1
32. Two thin ledges of limestone; layer of sheet flint in top	1	2
31. Ledge of thick massive limestone	5	0
30. Hard yellowish limestone	2	0
29. Hard, thick, massive ledge of siliceous limestone, ringing under blows of hammer. At the base there is a layer about 9 inches thick of opalescent, pinkish or brownish flint. Apparently the limestone is being converted into flint by replacement, and the process has not yet been completed	6	0
28. Soft chalky limestone, dissolving and forming small caves	3	0
27. Soft chalky limestone with very large (may be 1 foot long), irregularly shaped blue flints at top	2	3
26. White chalky limestone, apparently siliceous; zone of flint near top. The flints blue, discoidal, and tending to form sheet	6	8
25. Massive ledge of hard bluish limestone	7	0
24. Very hard limestone	0	6
23. A layer of enormous blue flints, in some places over 1 foot thick	1	0
22. Thick massive ledge of limestone, rather soft, yellow in color, and slightly arenaceous	5	5
21. Ledge of hard yellowish limestone with a zone of flints tending to form a sheet at base	1	4
20. Soft, white, slightly arenaceous limestone, composed of thin ledges; upper 2 feet, middle 4 feet, lower 1 foot	7	0
19. Soft yellowish or whitish limestone with layer of flattish, bluish flints forming a sheet at top. This is really three ledges: upper ledge, with flints at top, 2 feet; middle, containing concretions of calcite in lower part, 4 feet; lower ledge, exposed at low water, 1 foot	7	0
Total, Deep Eddy section	121	5

SECTION NO. 6.—*Bluff at the mouth of Bee Creek.* (Fig. 57, C.)

	Ft.	In.
Limestone slope, detail not exposed	11	0
23. Layer of enormous blue flints	1	0
22. Arenaceous limestone	5	5
21. Hard yellowish limestone with sheet flint at base	1	4
20. Yellowish, rather hard limestone, somewhat siliceous; thin band of chalky limestone at top; calcite concretions near base.	6	0
19. Sheet flint at top (sheet flint at top of lowest ledge of Deep Eddy Bluff); three ledges of limestone: upper, 1 foot; middle, 2 feet 6 inches; lower (containing calcite concretions), 3 feet	6	6
18. Sandy limestone, with two zones of nodular flint near middle; sheet flint at base; mass of Requienia just above the sheet flint	10	0
17. Soft, yellow, calcareous sandstone, a part of the preceding ledge, about.	3	0
16. Yellow cherty limestone, about	0	6
15. Three or four ledges of rather soft, whitish or yellowish limestone; the upper ledge containing a great mass of Requienia, the others fewer	8	1

From Hill and Vaughan, 1899.

	Ft.	In.
14. Solid white limestone, granular, not very hard; contains a great many Requienia near top	6	11
13. Yellow arenaceous limestone	4	0
12. Blotched arenaceous limestone	3	8
11. Soft, yellow, arenaceous limestone	2	0
10. Hard, yellowish, granular limestone, with shell fragments, gray on fresh exposure	1	6
9. Soft, yellow, arenaceous limestone or calcareous sandstone	2	4
8. Ledge of nonindurated granular limestone, with indurated blotches, which are structureless and flinty looking	1	0
7. Ledge of white, rather soft limestone, with many very irregularly shaped flints in a zone about the middle of the ledge. The flints are mostly small, bluish in color, and do not show concentric banding; about	3	0
6. Ledge of white, rather soft limestone; no flints; a few fragmentary fossils	2	6
5. A soft arenaceous ledge. The lower 1 foot 10 inches is a subledge. In the upper part (near top) are concretionary bodies that in their form resemble flints, but are not flints in texture. These bodies are hard, apparently siliceous, and contain white blotches, some of which appear to be of foraminiferal origin	5	5
4. Hard limestone, whitish or bluish, without flint; not fossiliferous	4	0
3. Arenaceous limestone, has a tendency to lamination, but in the ledge the laminated character is not always evident. The upper part of the ledge by solution becomes porous. The rock has a considerable absorbent power for water, and has a dark (wet) appearance, due to water contained	5	9
2. Thick ledge of white limestone, not very hard, oxidizing yellow from contained iron. Contains a large number of irregularly shaped flint nodules. These may be as much as 1 foot long, but usually are rather small—3 or 4 inches in length. They are bluish in color and have a concentrically grained structure, resembling the graining of pine wood. Their long axes are not always parallel to the bedding planes of the limestone, an important exception to the usual position of the flints relative to the stratification of the limestone	5	9
1. Ledge of yellowish or whitish limestone, without flints; in a thin layer about 6 inches thick at the top of this ledge there is an enormous number of *Requienia texana*	4	0
Total, Bee Creek section	104	8

The total thickness of the Edwards limestone exposed in the vicinity of Austin, as determined from the foregoing sections, is as follows:

	Ft.	In.
Bluff on Barton Creek, beds 49 to 43	29	11
Deep Eddy Bluff, beds 42 to 24	99	8
Bluff at month of Bee Creek, beds 23 to 1	104	8
Grand total	234	3

In the Nueces section the upper 100 feet consist of flaggy layers of hard white limestone devoid of flints. Below this are ledges of yellowish limestone of considerable thickness, marked by numerous black flints. The central portion is of white limestone of homogeneous texture, in which large caverns occur. The lower portions consist of thick and thin ledges and flags containing considerable numbers of flint nodules or strata of flint and many honeycombed layers.

From Hill and Vaughan, 1899.

John Hanson's Generalized Measured Section of the Barton Springs Segment of the Edwards Aquifer

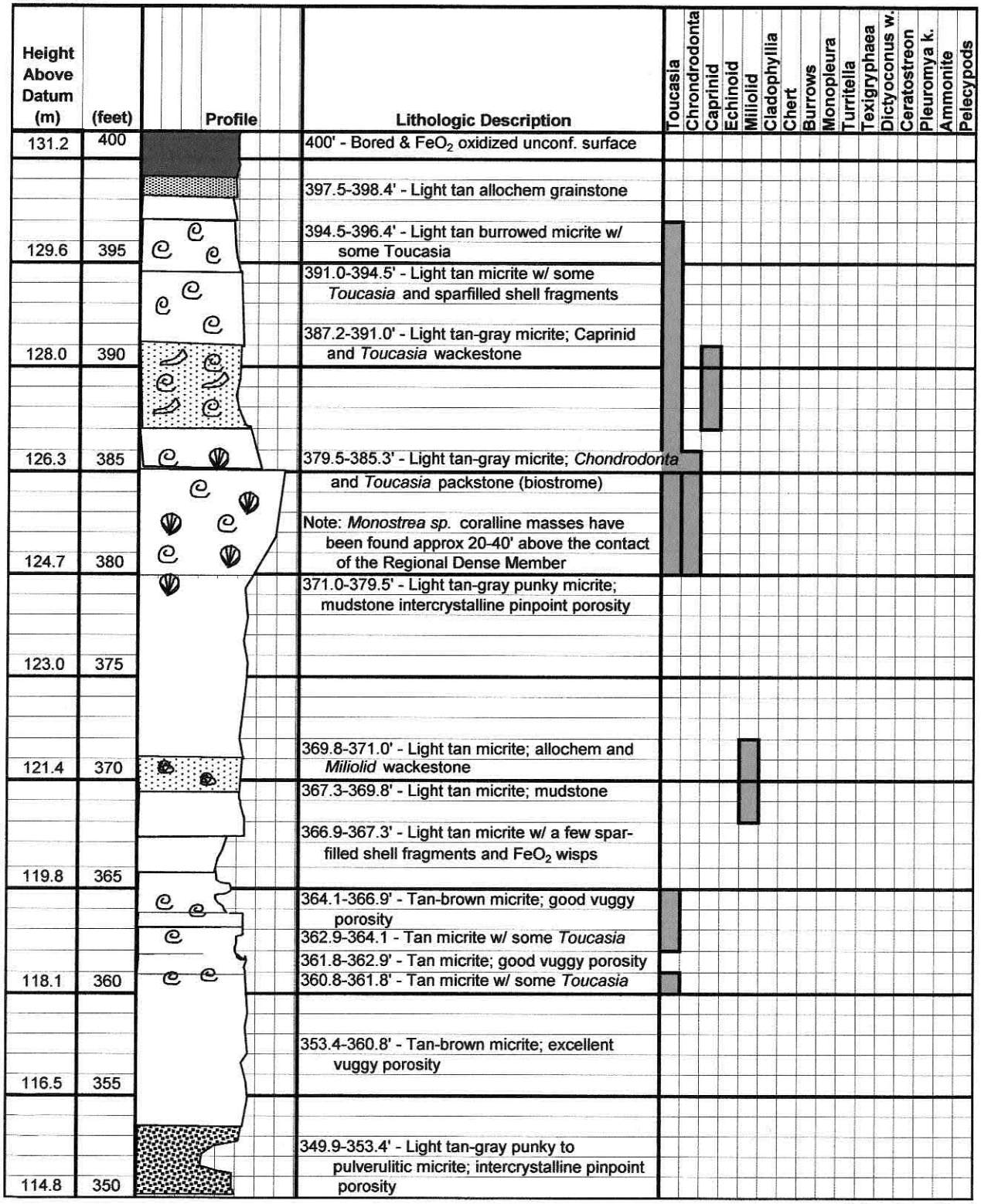

digitized by: Tim Ledet
2/12/96
Modified from Hanson, 1996

Geologist: John Hanson

John Hanson's Generalized Measured Section of the Barton Springs Segment of the Edwards Aquifer

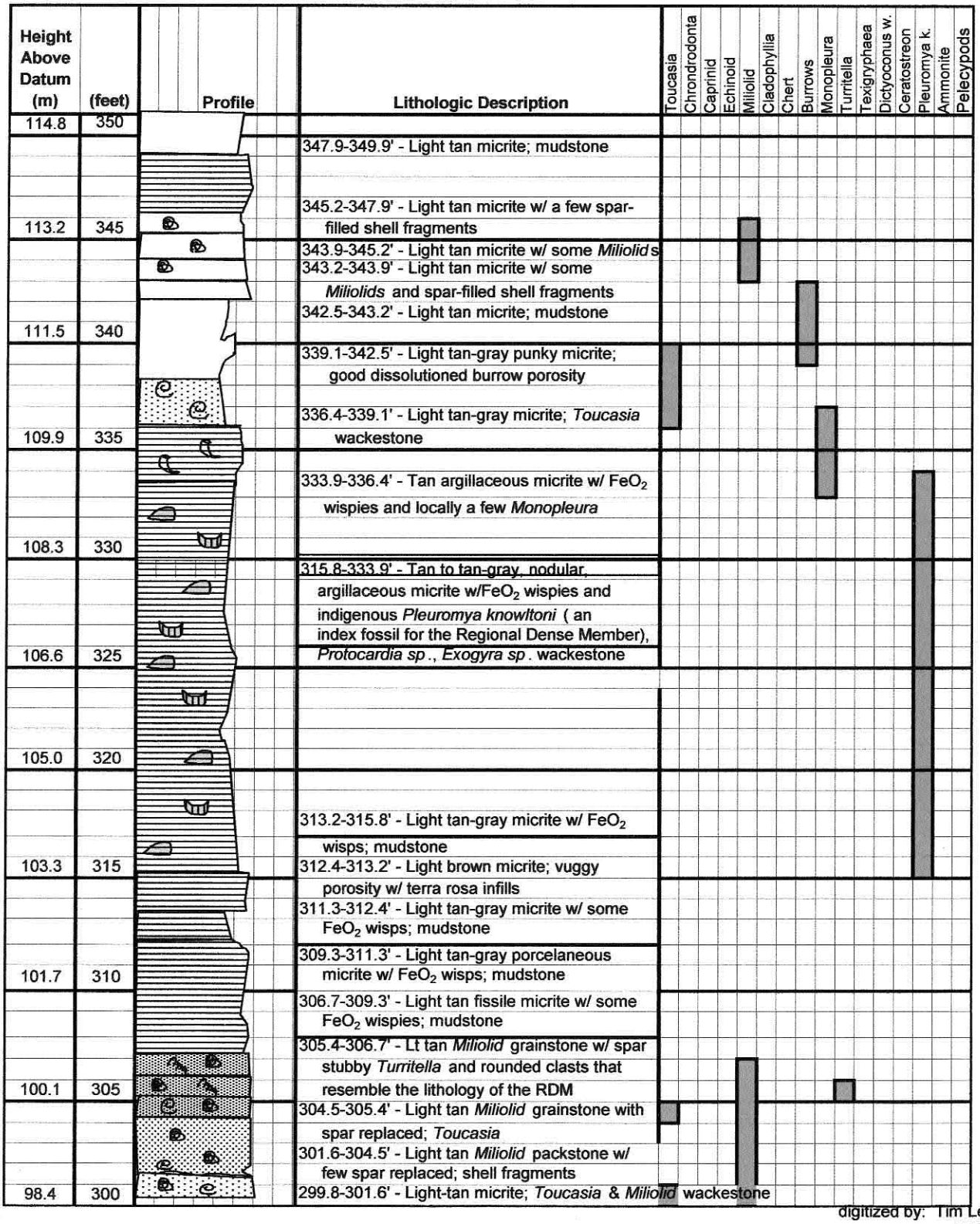

digitized by: Tim Ledet
2/12/96
Modified from Hanson, 1996

Geologist: John Hanson

John Hanson's Generalized Measured Section of the Barton Springs Segment of the Edwards Aquifer

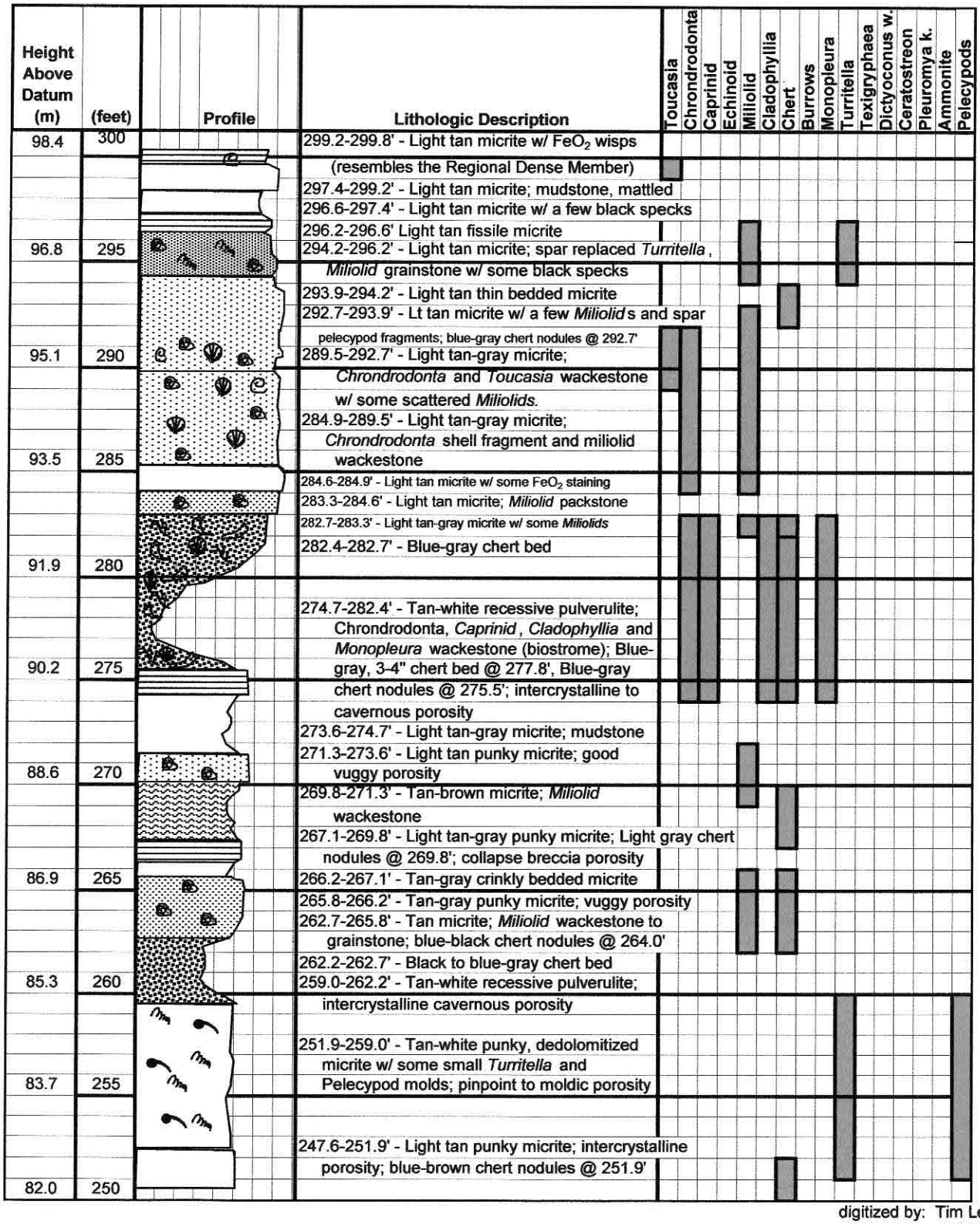

digitized by: Tim Ledet
2/12/96
Modified from Hanson, 1996

Geologist: John Hanson

John Hanson's Generalized Measured Section of the Barton Springs Segment of the Edwards Aquifer

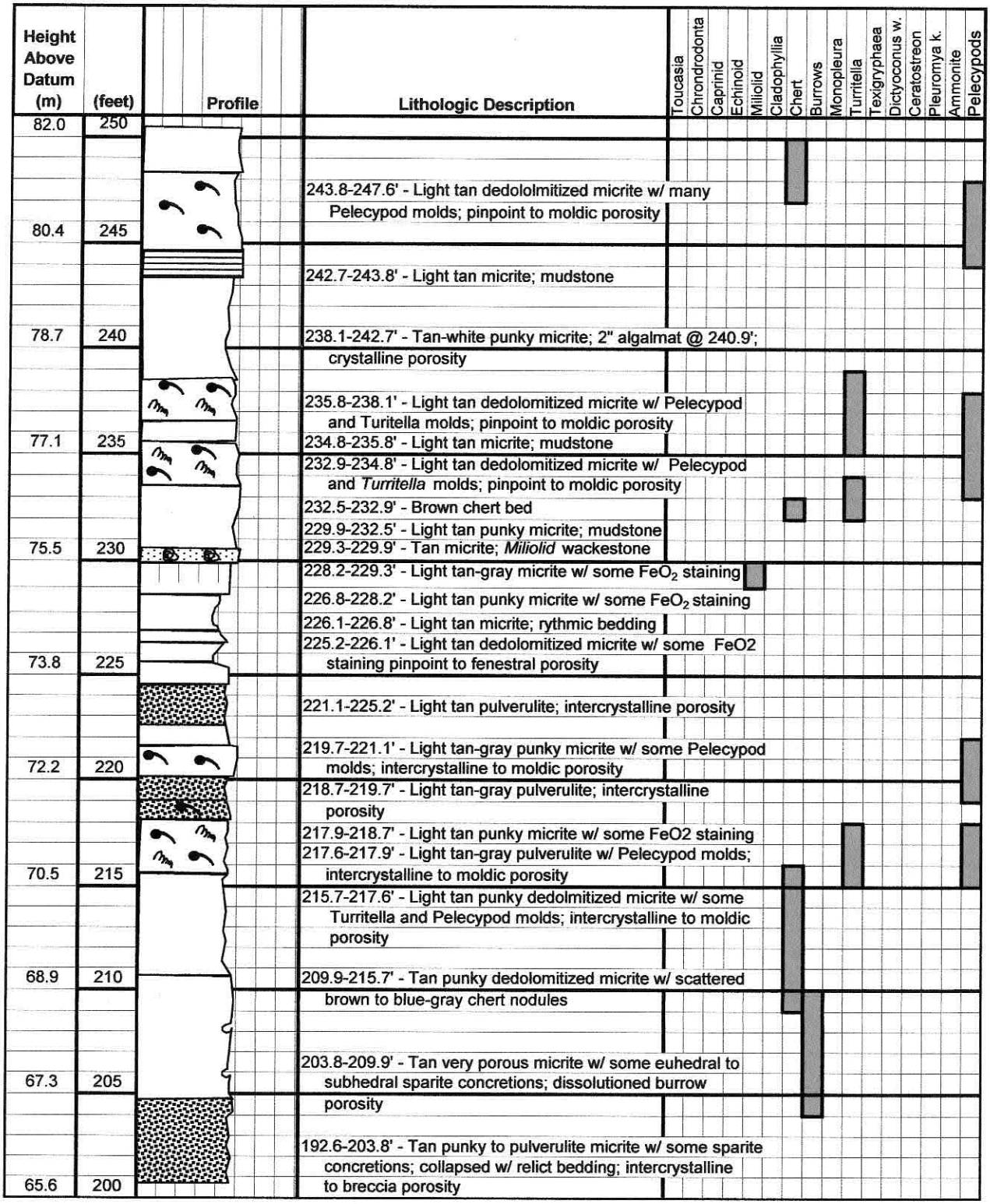

Geologist: John Hanson

digitized by: Tim Ledet
2/12/96
Modified from Hanson, 1996

John Hanson's Generalized Measured Section of the Barton Springs Segment of the Edwards Aquifer

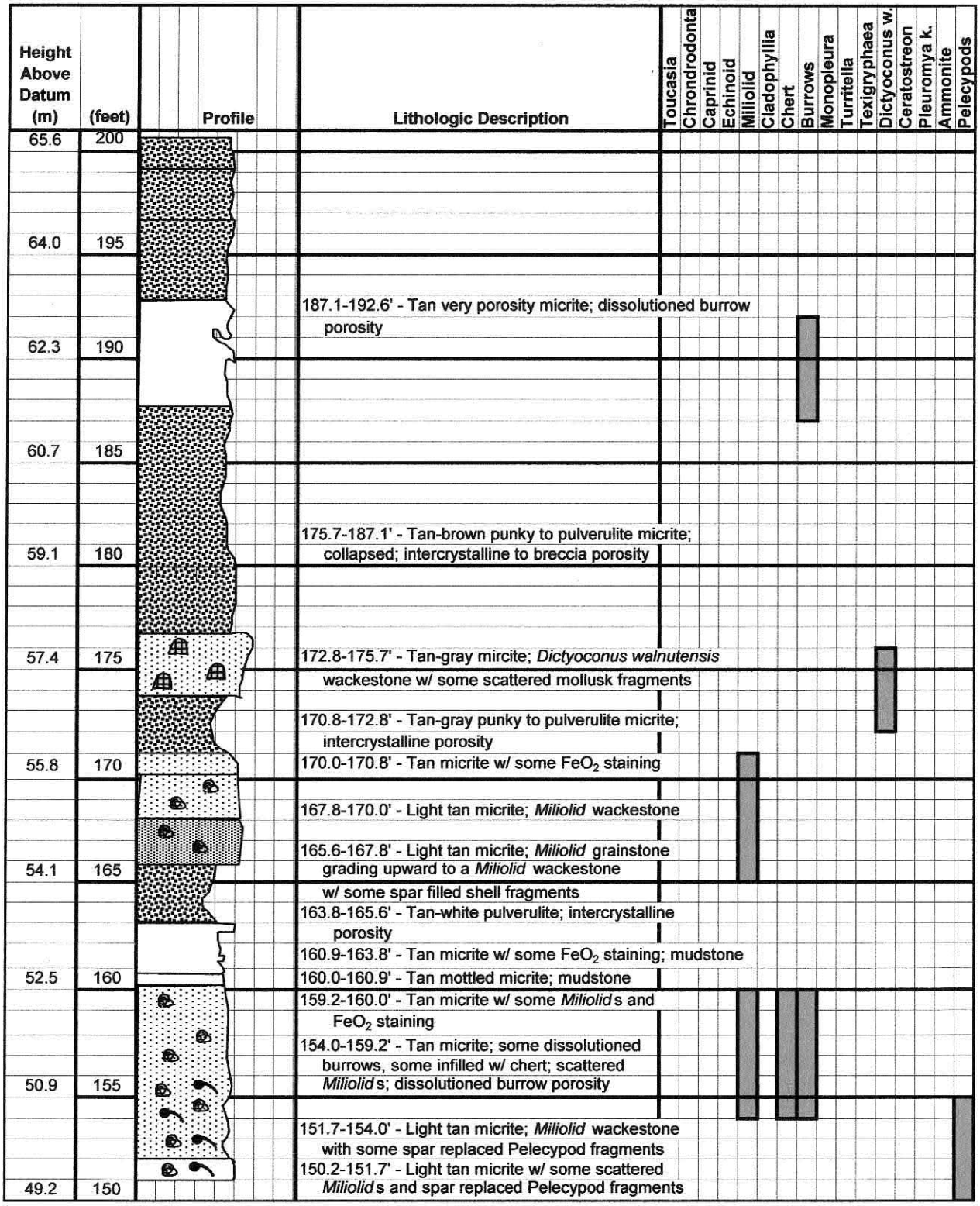

digitized by: Tim Ledet
2/12/96
Modified from Hanson, 1996

Geologist: John Hanson

John Hanson's Generalized Measured Section of the Barton Springs Segment of the Edwards Aquifer

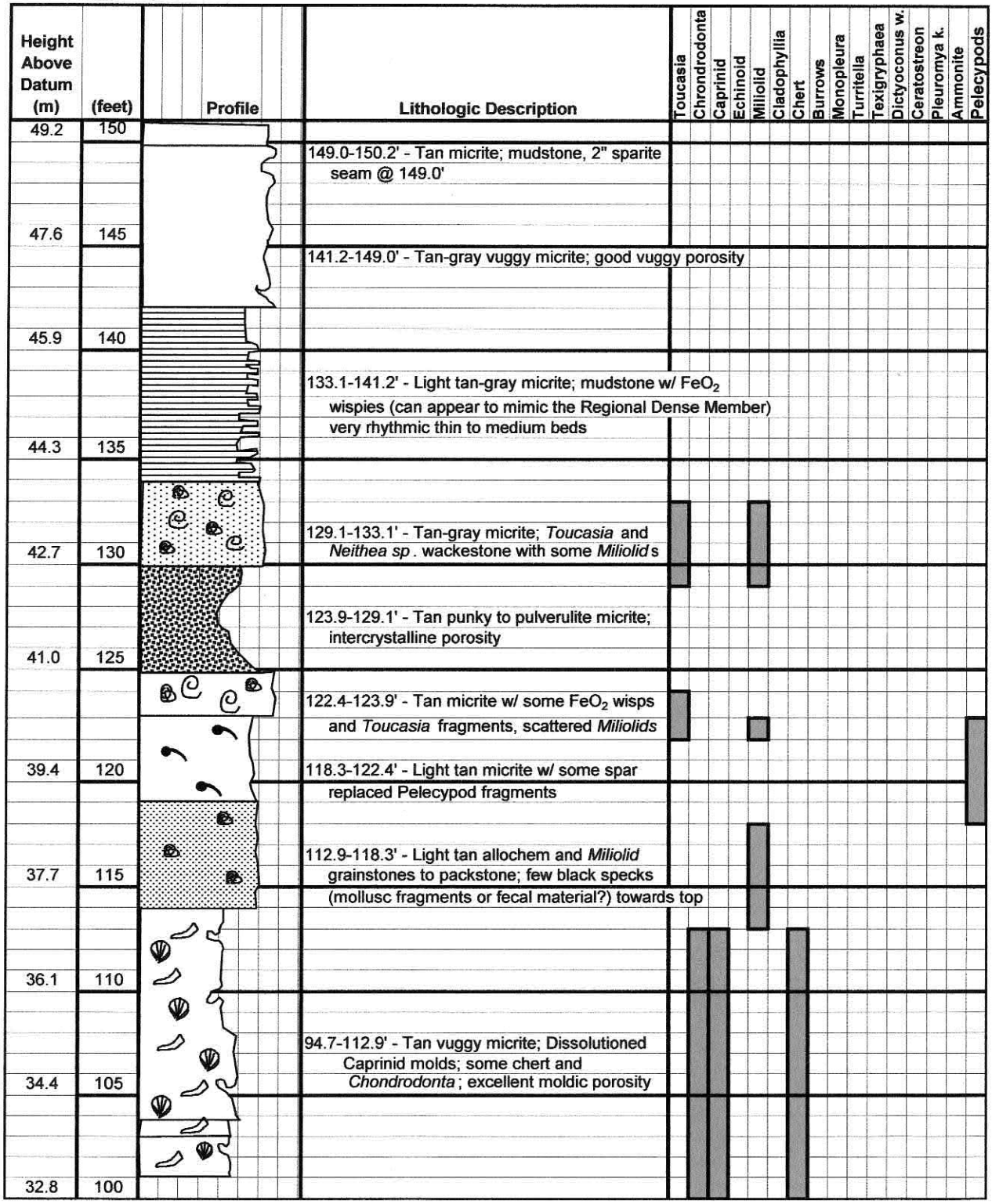

Geologist: John Hanson

digitized by: Tim Ledet
2/12/96
Modified from Hanson, 1996

John Hanson's Generalized Measured Section of the Barton Springs Segment of the Edwards Aquifer

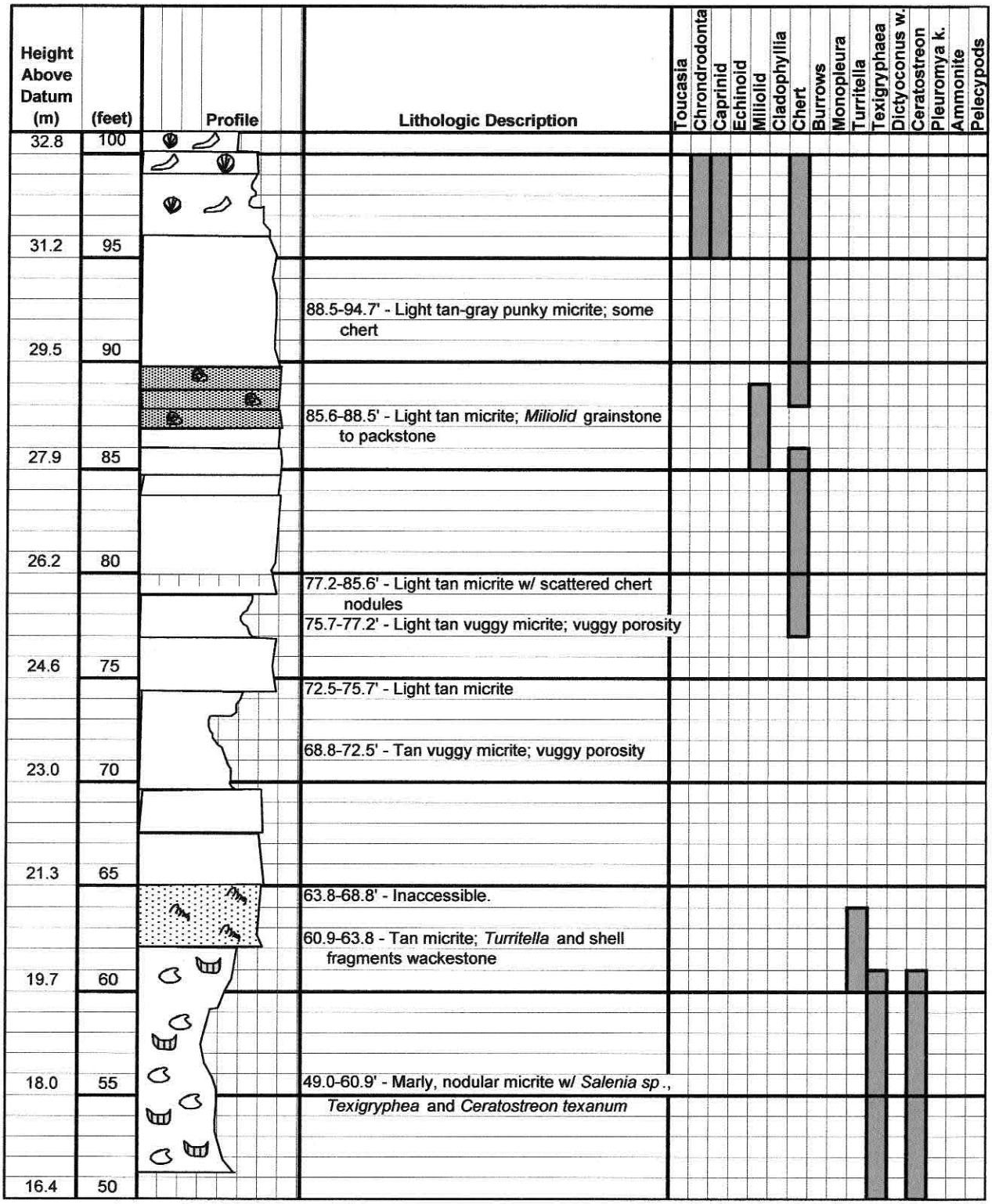

digitized by: Tim Ledet
2/12/96
Modified from Hanson, 1996

Geologist: John Hanson

John Hanson's Generalized Measured Section of the Barton Springs Segment of the Edwards Aquifer

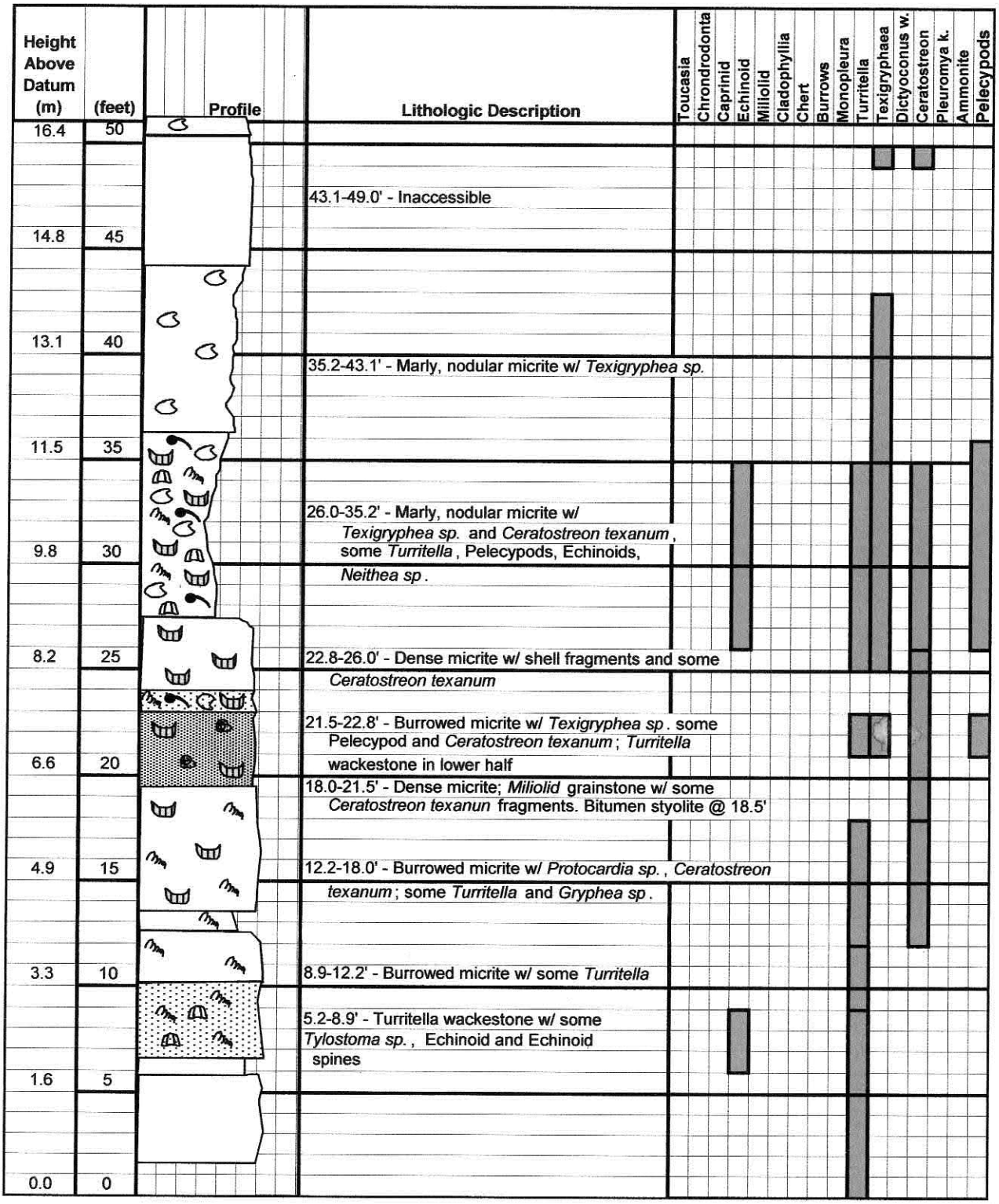

Geologist: John Hanson

digitized by: Tim Ledet
2/12/96
Modified from Hanson, 1996

John Hanson's Generalized Measured Section of the Barton Springs Segment of the Edwards Aquifer

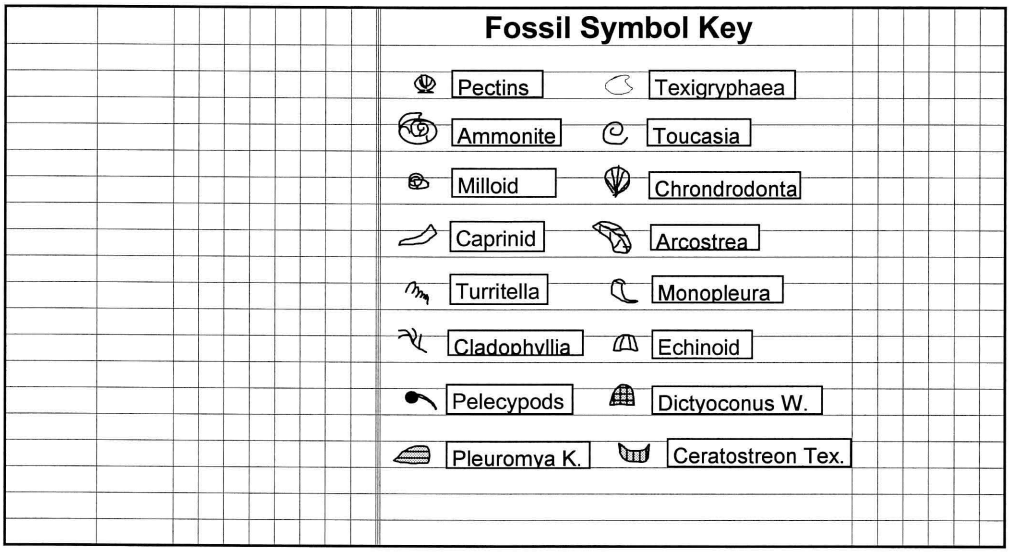

Red Bud Trail Measured Section

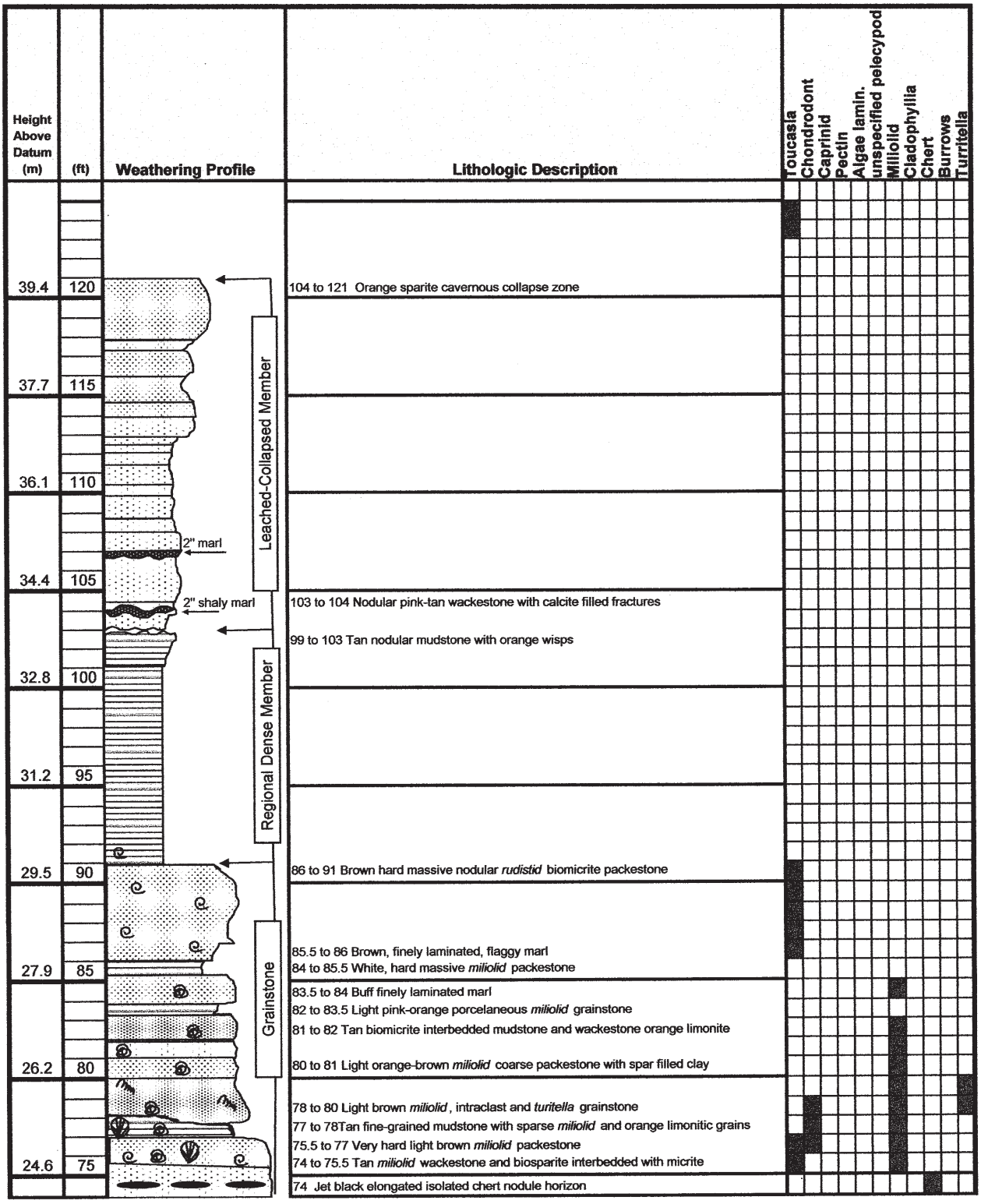

Geologist: Nico M. Hauwert

Digitized by: Neil A. Taurins
Feb., 1996

Red Bud Trail Measured Section

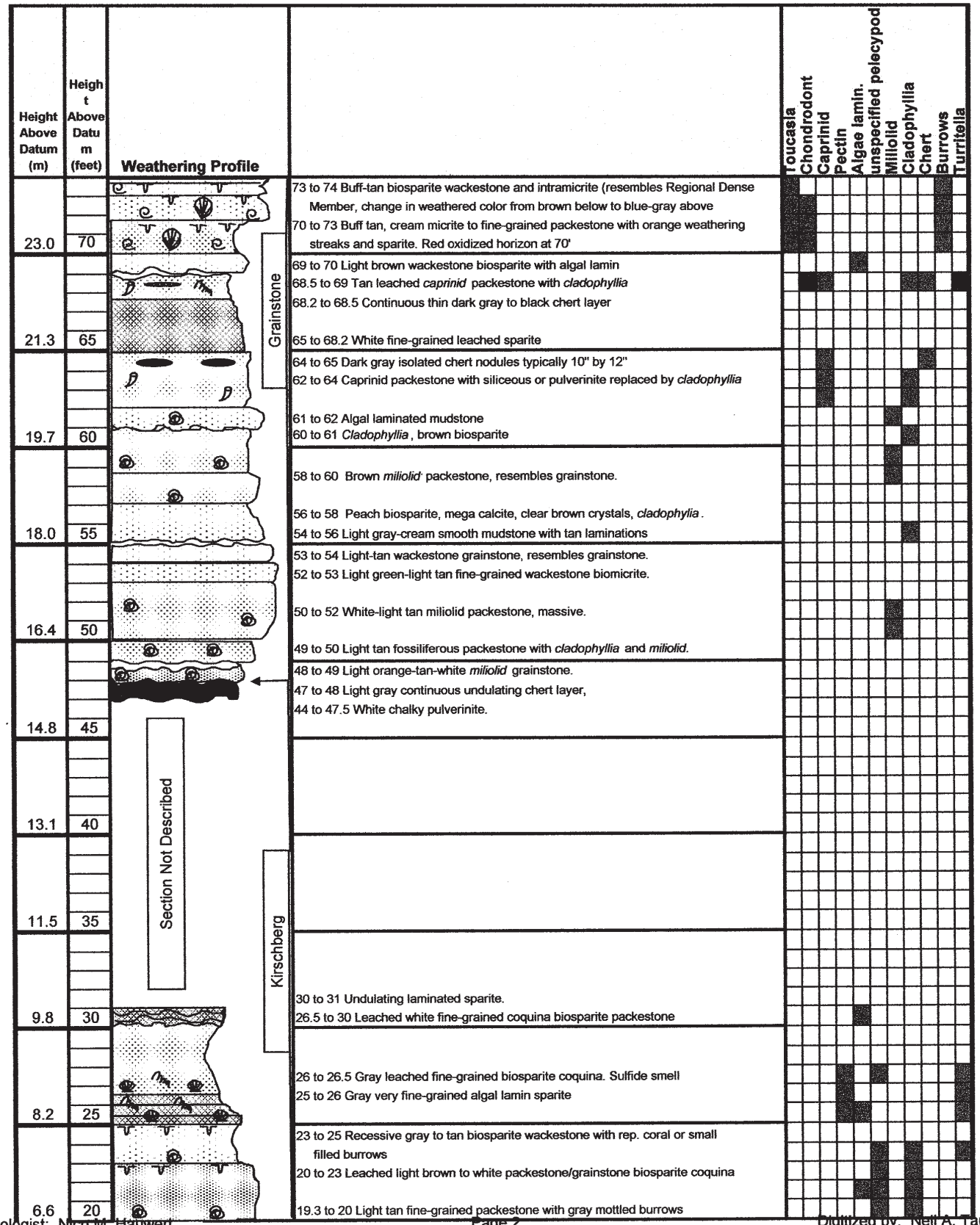

Geologist: Nico M. Hauwert

Page 2

Digitized by: Neil A. Taurins
Feb., 1996

Red Bud Trail Measured Section

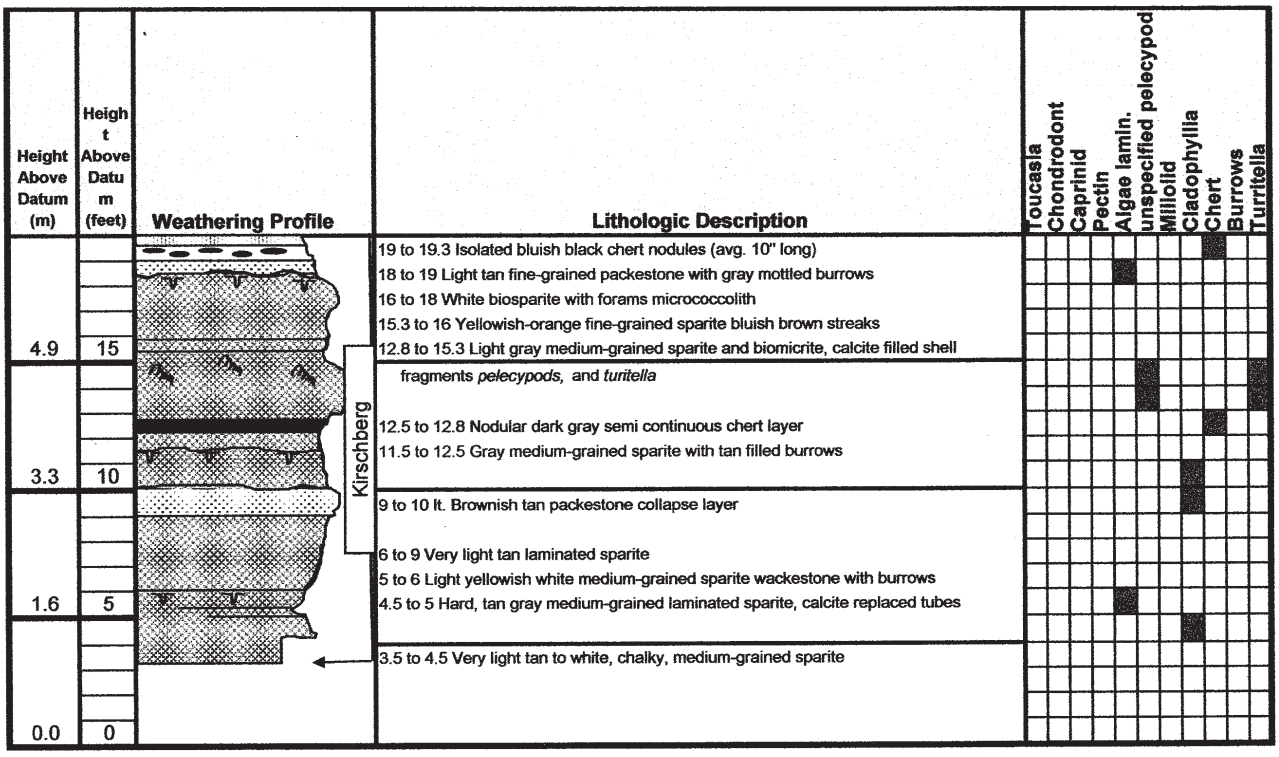

Midnight Cave Measured Section

Geologist: Nico M. Hauwert **Date:** 7/5/95

Height Above Datum (m)	Height Above Datum (feet)	Weathering Profile	Lithologic Description
0.0	0		
			0 to -2 White *Miliolid* grainstone
			-2 to -2.5 Nodular layer
-1.6	-5		-2.5 to -4 Creme to very light tan grainstone consisting of medium grained carbonate sands.
-3.3	-10		-4 to -8 White to very light tan grainstone consisting of fine-grained carbonate sand grains. Recrystallized and burrowed layer. Highly permeable.
-4.9	-15		-8 to -14 Heavily recrystallized, permeable interval.
			-14 to -18 Light tan to light brown, fine-grained carbonate sand packestone/grainstone. Honeycombed weathering.
-6.6	-20		-18 to -22 White recrystallized wackestone. Unident. shells.
			Honeycombed.
			-21.5 Possible chert concretions.
-8.2	-25		-22 to -25 Softer pulverulite, solution-collapse interval
			-25 to -26.5 Tan medium grained carbonate sand packestone/grainstone with yellow weathering bands.
-9.8	-30		-28 to -35 Light grayish-tan micrite with orange wispy
-11.5	-35		stains. "Rhythmic beds" of the Dolomitic Member.
			-35 to -37 Tan wackestone to packestone consisting of med. carbonate sand grains. *Miliolid* and *Chrondodonta*.
-13.1	-40		
			-37 to -45 V. hard tan micrite to wackestone. Conchoidal fracture. *Miliolids*. Unidentified *pelecypod* at -43.
-14.8	-45		
			-45 to -48 Yellow micrite
			-47 to -48 Tan wackestone/packestone with *Toucasia*
			-48 to -48.5 Thin marly layer. *Forams*. Black weathered stain
-16.4	-50		-48 to -50 Tan micrite weathering to yellow microcrystalline. *Toucasia*. -50 lower horizontal cave passage.

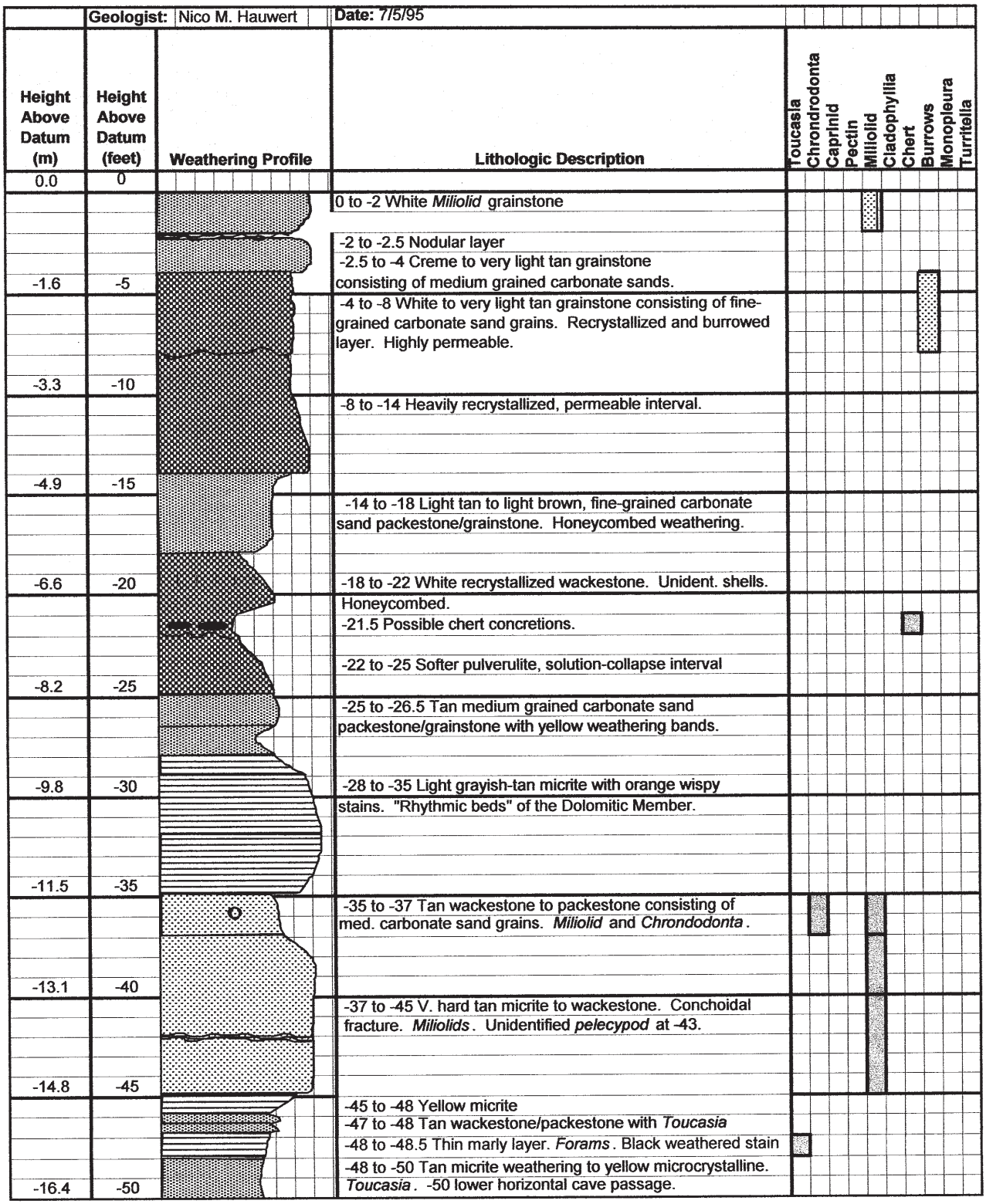

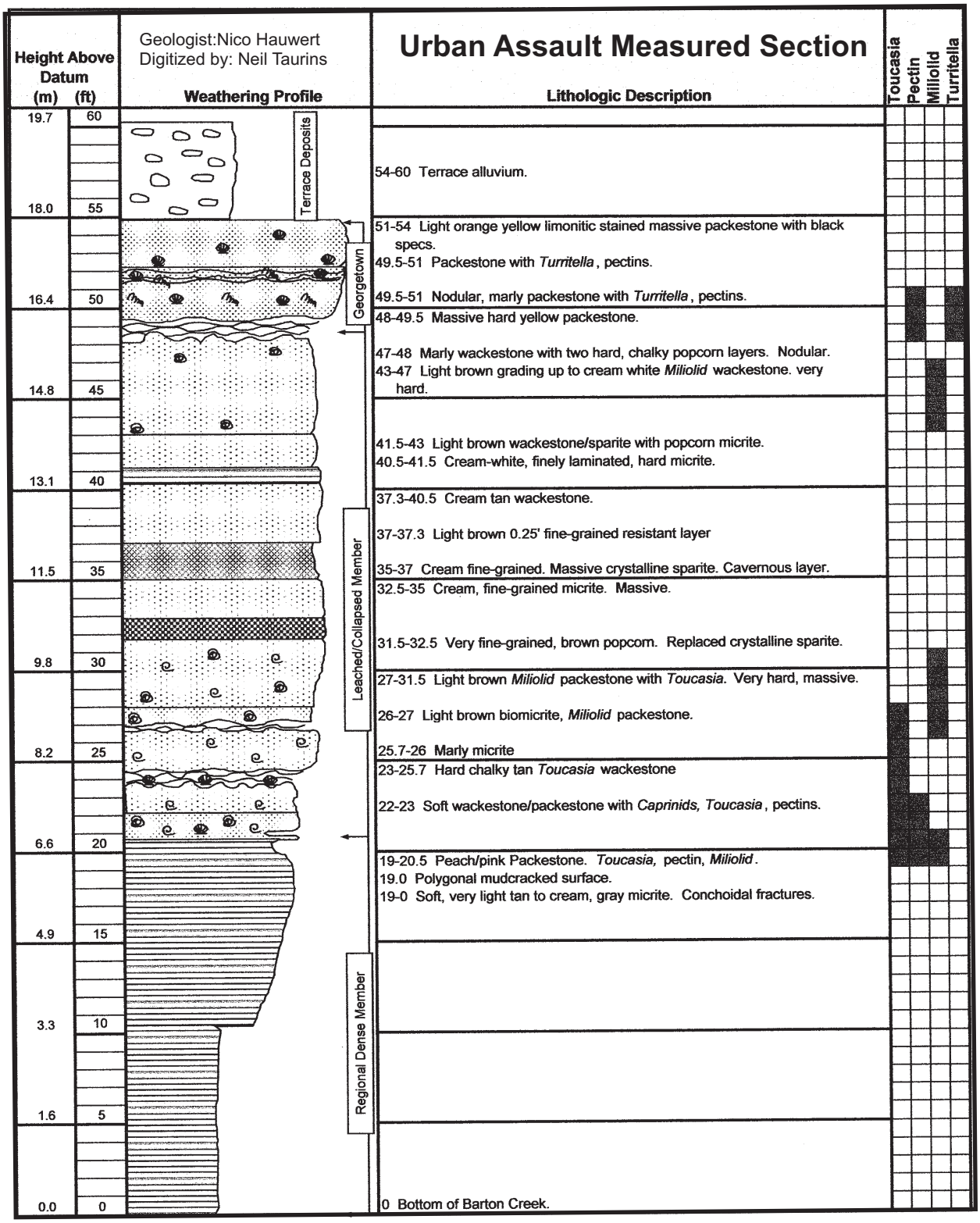
Geologist:Nico Hauwert
Digitized by: Neil Taurins
Urban Assault Measured Section
Height Above Datum
(m) (ft)
Weathering Profile
Lithologic Description
Toucasia
Pectin
Miliolid
Turritella
Terrace Deposits
Georgetown
Leached/Collapsed Member
Regional Dense Member
19.7 60
18.0 55
16.4 50
14.8 45
13.1 40
11.5 35
9.8 30
8.2 25
6.6 20
4.9 15
3.3 10
1.6 5
0.0 0
54-60 Terrace alluvium.
51-54 Light orange yellow limonitic stained massive packestone with black specs.
49.5-51 Packestone with Turritella, pectins.
49.5-51 Nodular, marly packestone with Turritella, pectins.
48-49.5 Massive hard yellow packestone.
47-48 Marly wackestone with two hard, chalky popcorn layers. Nodular.
43-47 Light brown grading up to cream white Miliolid wackestone. very hard.
41.5-43 Light brown wackestone/sparite with popcorn micrite.
40.5-41.5 Cream-white, finely laminated, hard micrite.
37.3-40.5 Cream tan wackestone.
37-37.3 Light brown 0.25' fine-grained resistant layer
35-37 Cream fine-grained. Massive crystalline sparite. Cavernous layer.
32.5-35 Cream, fine-grained micrite. Massive.
31.5-32.5 Very fine-grained, brown popcorn. Replaced crystalline sparite.
27-31.5 Light brown Miliolid packestone with Toucasia. Very hard, massive.
26-27 Light brown biomicrite, Miliolid packestone.
25.7-26 Marly micrite
23-25.7 Hard chalky tan Toucasia wackestone
22-23 Soft wackestone/packestone with Caprinids, Toucasia, pectins.
19-20.5 Peach/pink Packestone. Toucasia, pectin, Miliolid.
19.0 Polygonal mudcracked surface.
19-0 Soft, very light tan to cream, gray micrite. Conchoidal fractures.
0 Bottom of Barton Creek.
Turritella
Toucasia
Burrows
Caprinid
Texigryphaea
Pectin
Miliolid
Chondrodont
Arcostrea
Ammonite
Clam
Wackestone/Micrite
Grainstone
Sparite/Crystalline
Nodular
Packestone
Fissile/Laminated
Wavy/Laminated

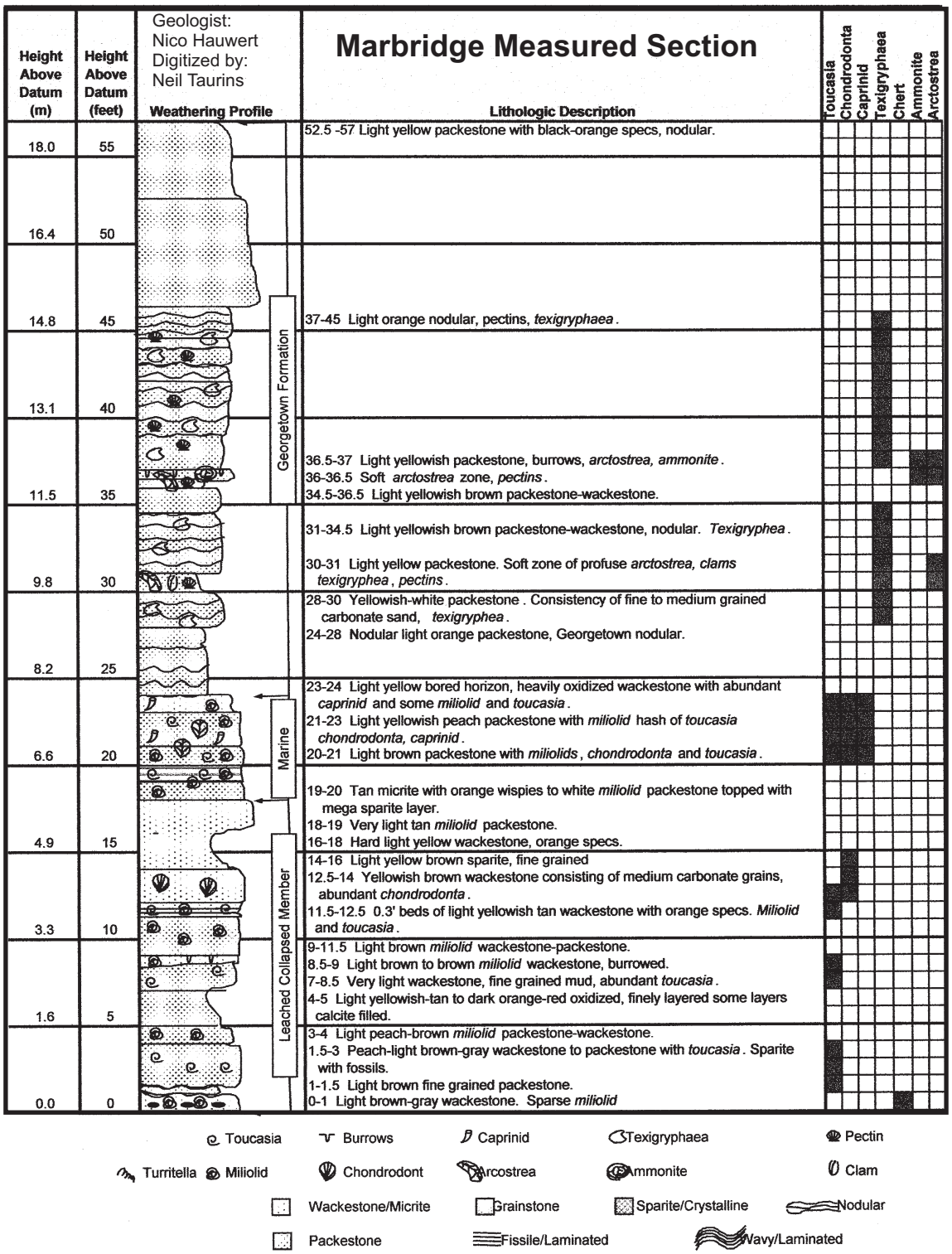
Geologist:
Nico Hauwert
Digitized by:
Neil Taurins
Marbridge Measured Section
Height Above Datum (m)
Height Above Datum (feet)
Weathering Profile
Lithologic Description
Toucasia
Chondrodonta
Caprinid
Texigryphaea
Chert
Ammonite
Arctostrea
18.0
55
52.5 -57 Light yellow packestone with black-orange specs, nodular.
16.4
50
14.8
45
37-45 Light orange nodular, pectins, texigryphaea.
13.1
40
11.5
35
36.5-37 Light yellowish packestone, burrows, arctostrea, ammonite.
36-36.5 Soft arctostrea zone, pectins.
34.5-36.5 Light yellowish brown packestone-wackestone.
9.8
30
31-34.5 Light yellowish brown packestone-wackestone, nodular. Texigryphea.
30-31 Light yellow packestone. Soft zone of profuse arctostrea, clams texigryphea, pectins.
8.2
25
28-30 Yellowish-white packestone. Consistency of fine to medium grained carbonate sand, texigryphea.
24-28 Nodular light orange packestone, Georgetown nodular.
6.6
20
23-24 Light yellow bored horizon, heavily oxidized wackestone with abundant caprinid and some miliolid and toucasia.
21-23 Light yellowish peach packestone with miliolid hash of toucasia chondrodonta, caprinid.
20-21 Light brown packestone with miliolids, chondrodonta and toucasia.
4.9
15
19-20 Tan micrite with orange wispies to white miliolid packestone topped with mega sparite layer.
18-19 Very light tan miliolid packestone.
16-18 Hard light yellow wackestone, orange specs.
3.3
10
14-16 Light yellow brown sparite, fine grained
12.5-14 Yellowish brown wackestone consisting of medium carbonate grains, abundant chondrodonta.
11.5-12.5 0.3' beds of light yellowish tan wackestone with orange specs. Miliolid and toucasia.
1.6
5
9-11.5 Light brown miliolid wackestone-packestone.
8.5-9 Light brown to brown miliolid wackestone, burrowed.
7-8.5 Very light wackestone, fine grained mud, abundant toucasia.
4-5 Light yellowish-tan to dark orange-red oxidized, finely layered some layers calcite filled.
0.0
0
3-4 Light peach-brown miliolid packestone-wackestone.
1.5-3 Peach-light brown-gray wackestone to packestone with toucasia. Sparite with fossils.
1-1.5 Light brown fine grained packestone.
0-1 Light brown-gray wackestone. Sparse miliolid
Georgetown Formation
Marine
Leached Collapsed Member
Toucasia
Burrows
Caprinid
Texigryphaea
Pectin
Turritella
Miliolid
Chondrodont
Arcostrea
Ammonite
Clam
Wackestone/Micrite
Grainstone
Sparite/Crystalline
Nodular
Packestone
Fissile/Laminated
Wavy/Laminated

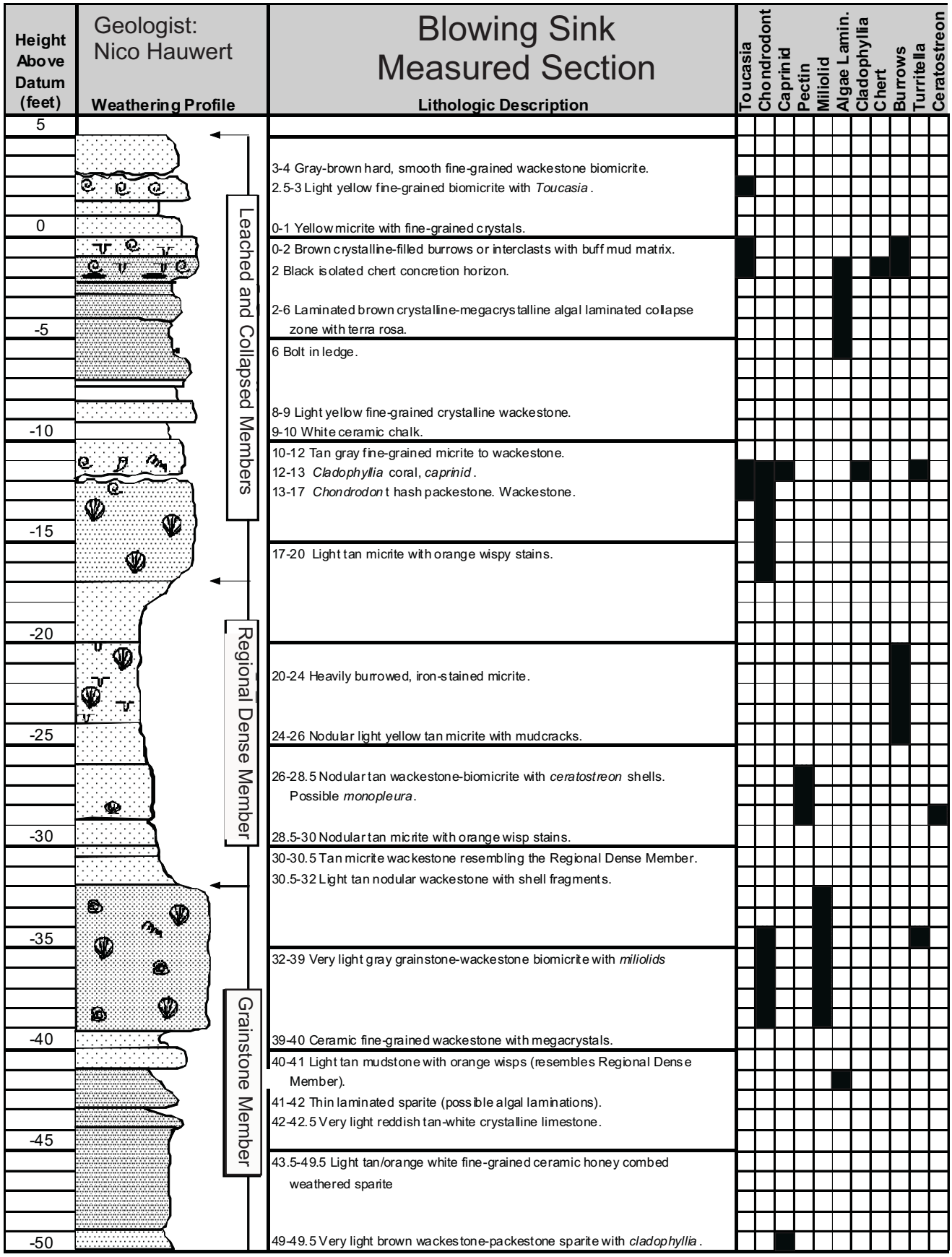
Geologist:
Nico Hauwert
Blowing Sink
Measured Section
Height Above Datum (feet)
Weathering Profile
Lithologic Description
Toucasia
Chondrodont
Caprinid
Pectin
Miliolid
Algae Lamin.
Cladophyllia
Chert
Burrows
Turritella
Ceratostreon
5
0
-5
-10
-15
-20
-25
-30
-35
-40
-45
-50
Leached and Collapsed Members
Regional Dense Member
Grainstone Member
3-4 Gray-brown hard, smooth fine-grained wackestone biomicrite.
2.5-3 Light yellow fine-grained biomicrite with Toucasia.
0-1 Yellow micrite with fine-grained crystals.
0-2 Brown crystalline-filled burrows or interclasts with buff mud matrix.
2 Black isolated chert concretion horizon.
2-6 Laminated brown crystalline-megacrystalline algal laminated collapse zone with terra rosa.
6 Bolt in ledge.
8-9 Light yellow fine-grained crystalline wackestone.
9-10 White ceramic chalk.
10-12 Tan gray fine-grained micrite to wackestone.
12-13 Cladophyllia coral, caprinid.
13-17 Chondrodont hash packestone. Wackestone.
17-20 Light tan micrite with orange wispy stains.
20-24 Heavily burrowed, iron-stained micrite.
24-26 Nodular light yellow tan micrite with mudcracks.
26-28.5 Nodular tan wackestone-biomicrite with ceratostreon shells. Possible monopleura.
28.5-30 Nodular tan micrite with orange wisp stains.
30-30.5 Tan micrite wackestone resembling the Regional Dense Member.
30.5-32 Light tan nodular wackestone with shell fragments.
32-39 Very light gray grainstone-wackestone biomicrite with miliolids
39-40 Ceramic fine-grained wackestone with megacrystals.
40-41 Light tan mudstone with orange wisps (resembles Regional Dense Member).
41-42 Thin laminated sparite (possible algal laminations).
42-42.5 Very light reddish tan-white crystalline limestone.
43.5-49.5 Light tan/orange white fine-grained ceramic honey combed weathered sparite
49-49.5 Very light brown wackestone-packestone sparite with cladophyllia.

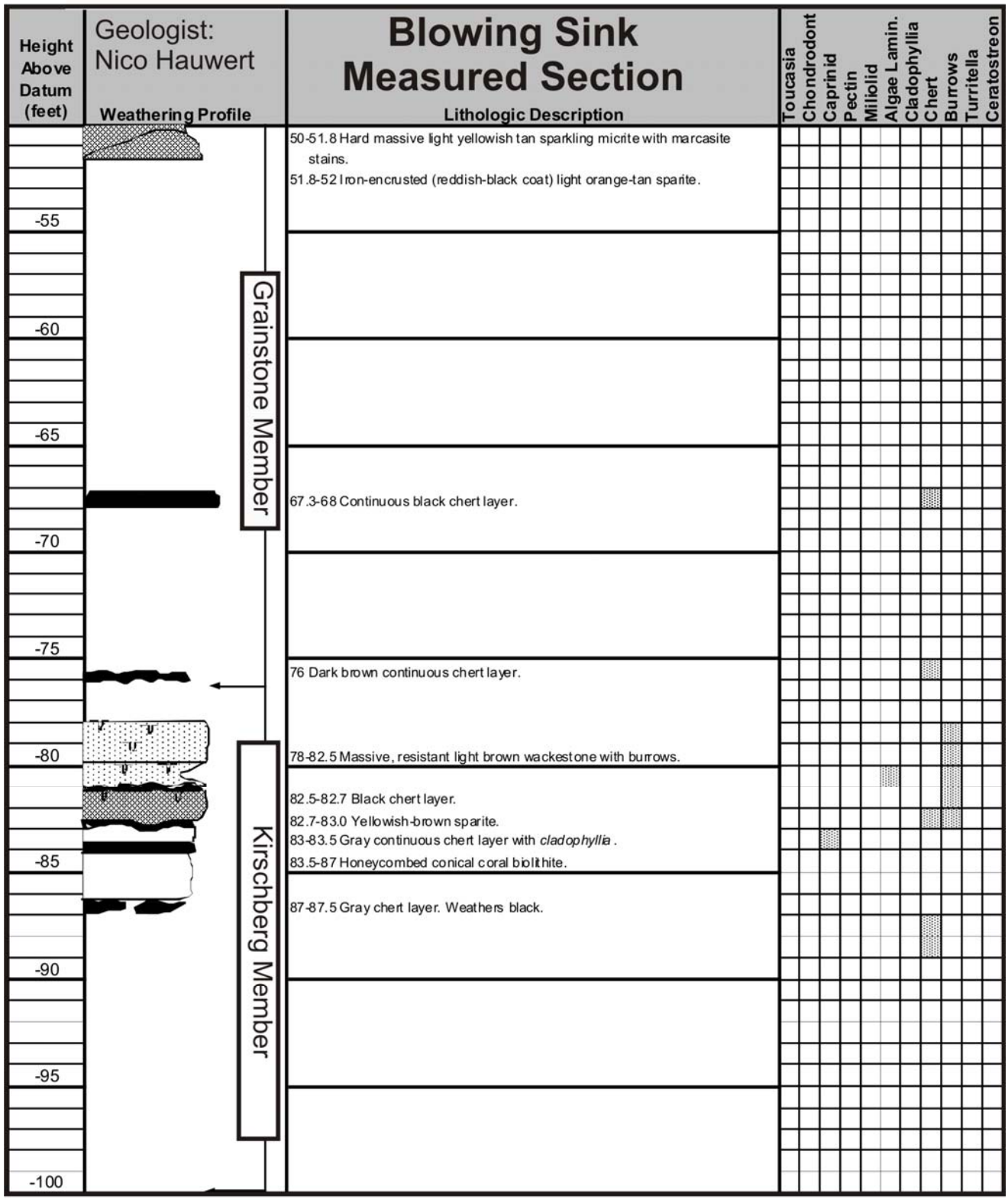
Height Above Datum (feet)
Geologist: Nico Hauwert
Weathering Profile
Blowing Sink Measured Section
Lithologic Description
Toucasia
Chondrodont
Caprinid
Pectin
Miliolid
Algae Lamin.
Cladophyllia
Chert
Burrows
Turritella
Ceratostreon
50-51.8 Hard massive light yellowish tan sparkling micrite with marcasite stains.
51.8-52 Iron-encrusted (reddish-black coat) light orange-tan sparite.
67.3-68 Continuous black chert layer.
76 Dark brown continuous chert layer.
78-82.5 Massive, resistant light brown wackestone with burrows.
82.5-82.7 Black chert layer.
82.7-83.0 Yellowish-brown sparite.
83-83.5 Gray continuous chert layer with cladophyllia.
83.5-87 Honeycombed conical coral biolithite.
87-87.5 Gray chert layer. Weathers black.
-55
-60
-65
-70
-75
-80
-85
-90
-95
-100
Grainstone Member
Kirschberg Member
Turritella
Toucasia
Burrows
Caprinid
Texigryphaea
Pectin
Miliolid
Chondrodont
Arcostrea
Ammonite
Clam
Wackestone/Micrite
Grainstone
Sparite/Crystalline
Nodular
Packestone
Fissile/Laminated
Wavy/Laminated

General Marker Beds of the Edwards Group, South Austin Area, Travis County

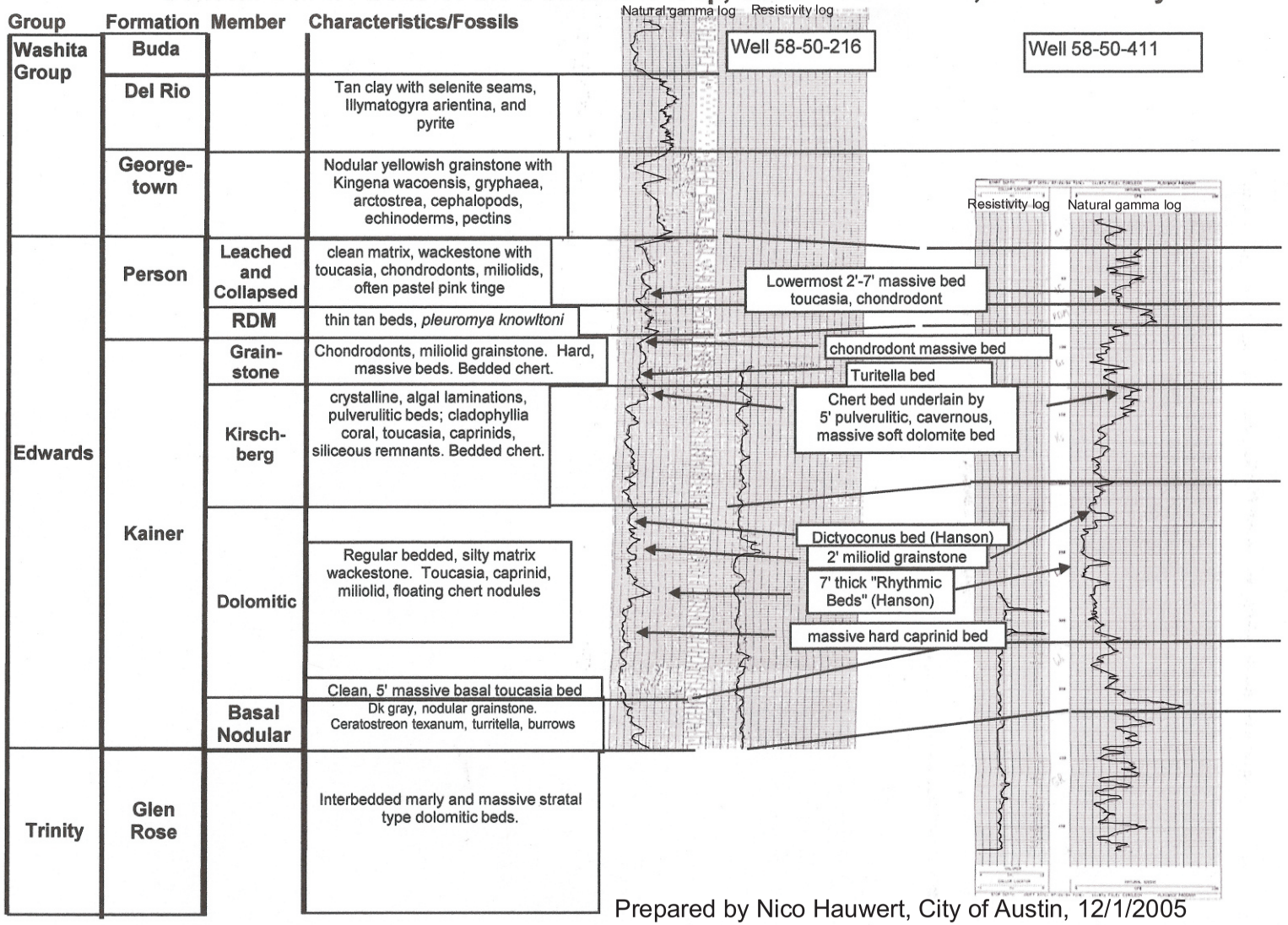

Prepared by Nico Hauwert, City of Austin, 12/1/2005

APPENDIX C

CAVE STRATIGRAPHY

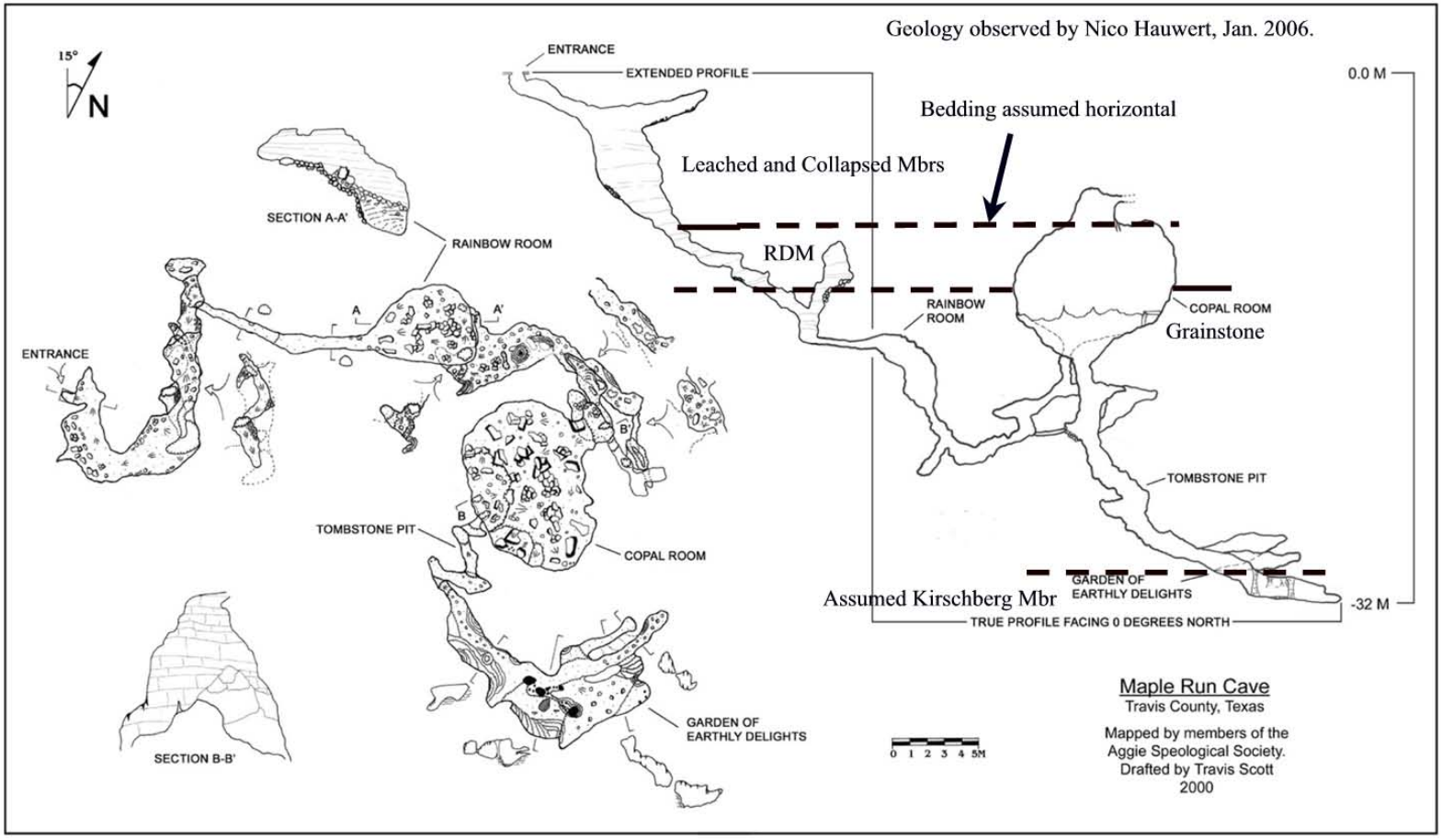
Geology observed by Nico Hauwert, Jan. 2006.
15°
N
ENTRANCE
EXTENDED PROFILE
0.0 M
Bedding assumed horizontal
Leached and Collapsed Mbrs
SECTION A-A'
RAINBOW ROOM
RDM
RAINBOW ROOM
COPAL ROOM
Grainstone
A
A'
ENTRANCE
B
B'
TOMBSTONE PIT
TOMBSTONE PIT
COPAL ROOM
GARDEN OF EARTHLY DELIGHTS
Assumed Kirschberg Mbr
GARDEN OF EARTHLY DELIGHTS
-32 M
TRUE PROFILE FACING 0 DEGREES NORTH
SECTION B-B'
0 1 2 3 4 5M
Maple Run Cave
Travis County, Texas
Mapped by members of the Aggie Speological Society.
Drafted by Travis Scott
2000

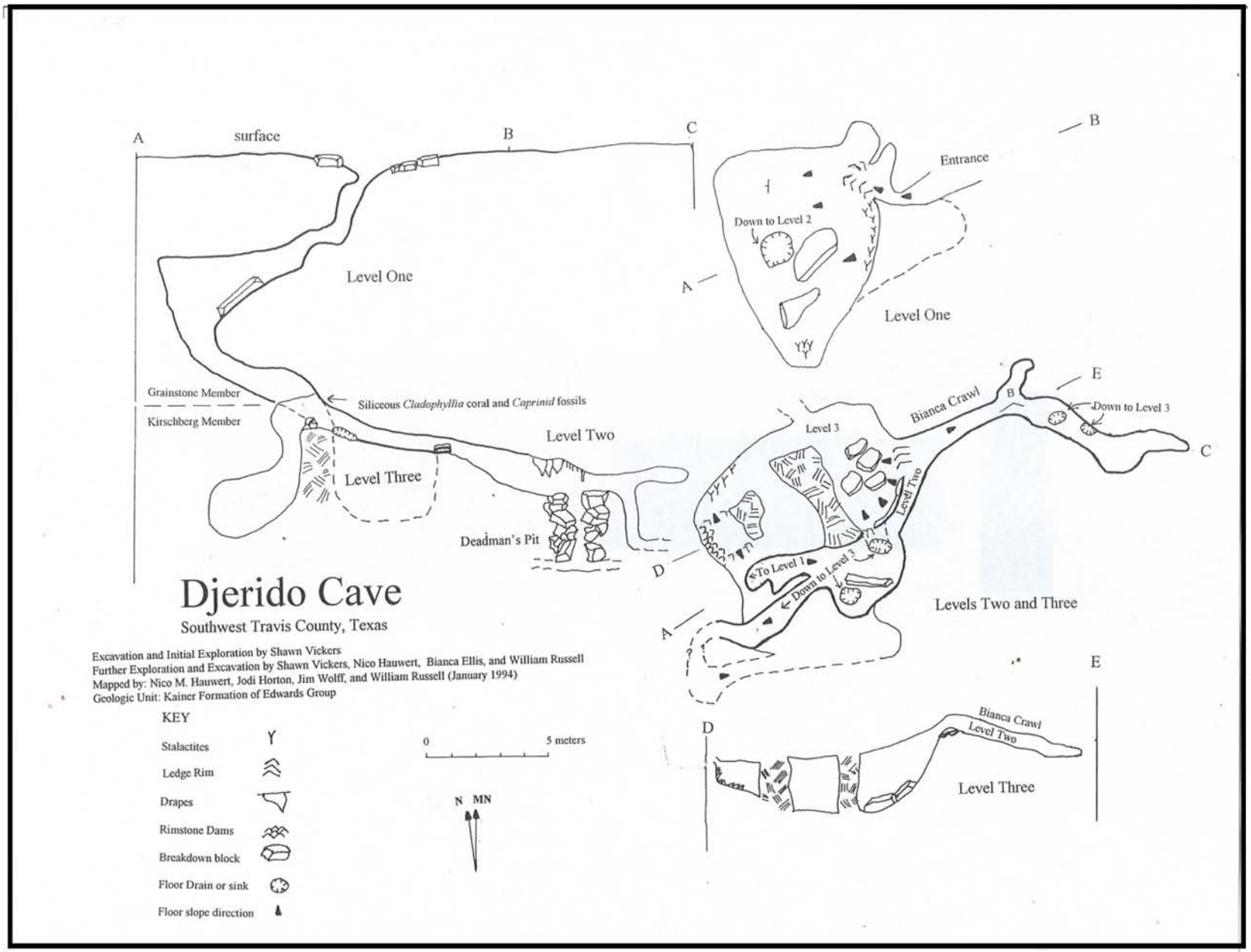
A
surface
B
C
Level One
Grainstone Member
Kirschberg Member
Siliceous *Cladophyllia* coral and *Caprinid* fossils
Level Two
Level Three
Deadman's Pit
D
Djerido Cave
Southwest Travis County, Texas
Excavation and Initial Exploration by Shawn Vickers
Further Exploration and Excavation by Shawn Vickers, Nico Hauwert, Bianca Ellis, and William Russell
Mapped by: Nico M. Hauwert, Jodi Horton, Jim Wolff, and William Russell (January 1994)
Geologic Unit: Kainer Formation of Edwards Group
KEY
Stalactites
Ledge Rim
Drapes
Rimstone Dams
Breakdown block
Floor Drain or sink
Floor slope direction
0
5 meters
N MN
B
Entrance
Down to Level 2
A
Level One
E
Bianca Crawl
B
Down to Level 3
Level 3
C
Level Two
To Level 1
Down to Level 3
A
Levels Two and Three
E
D
Bianca Crawl
Level Two
Level Three

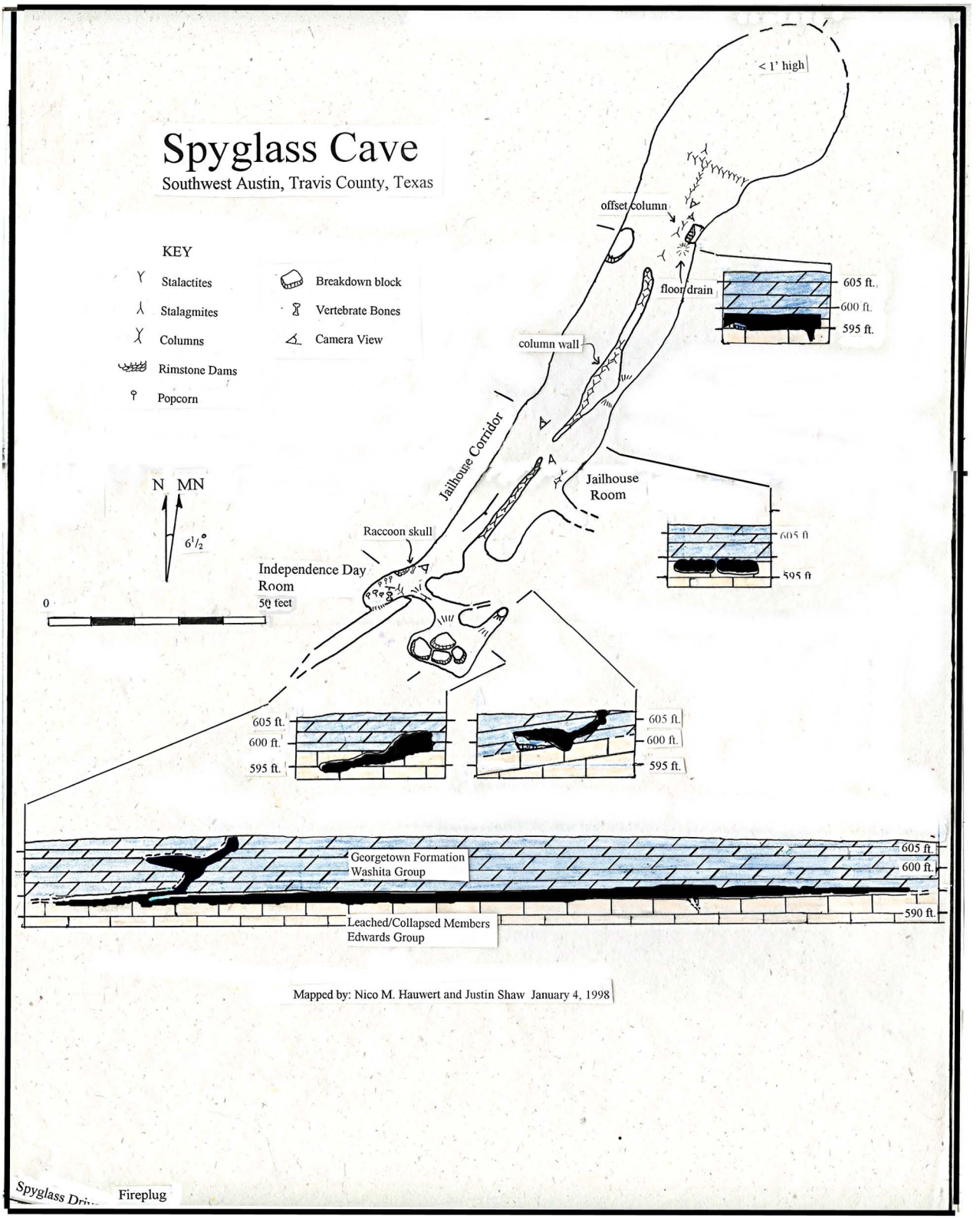
Spyglass Cave
Southwest Austin, Travis County, Texas
KEY
Stalactites
Stalagmites
Columns
Rimstone Dams
Popcorn
Breakdown block
Vertebrate Bones
Camera View
< 1' high
offset column
floor drain
605 ft.
600 ft.
595 ft.
column wall
Jailhouse Corridor
Jailhouse Room
N MN
6 1/2°
Raccoon skull
Independence Day Room
0
50 feet
605 ft.
595 ft.
Georgetown Formation
Washita Group
Leached/Collapsed Members
Edwards Group
590 ft.
Mapped by: Nico M. Hauwert and Justin Shaw January 4, 1998
Spyglass Dri...
Fireplug

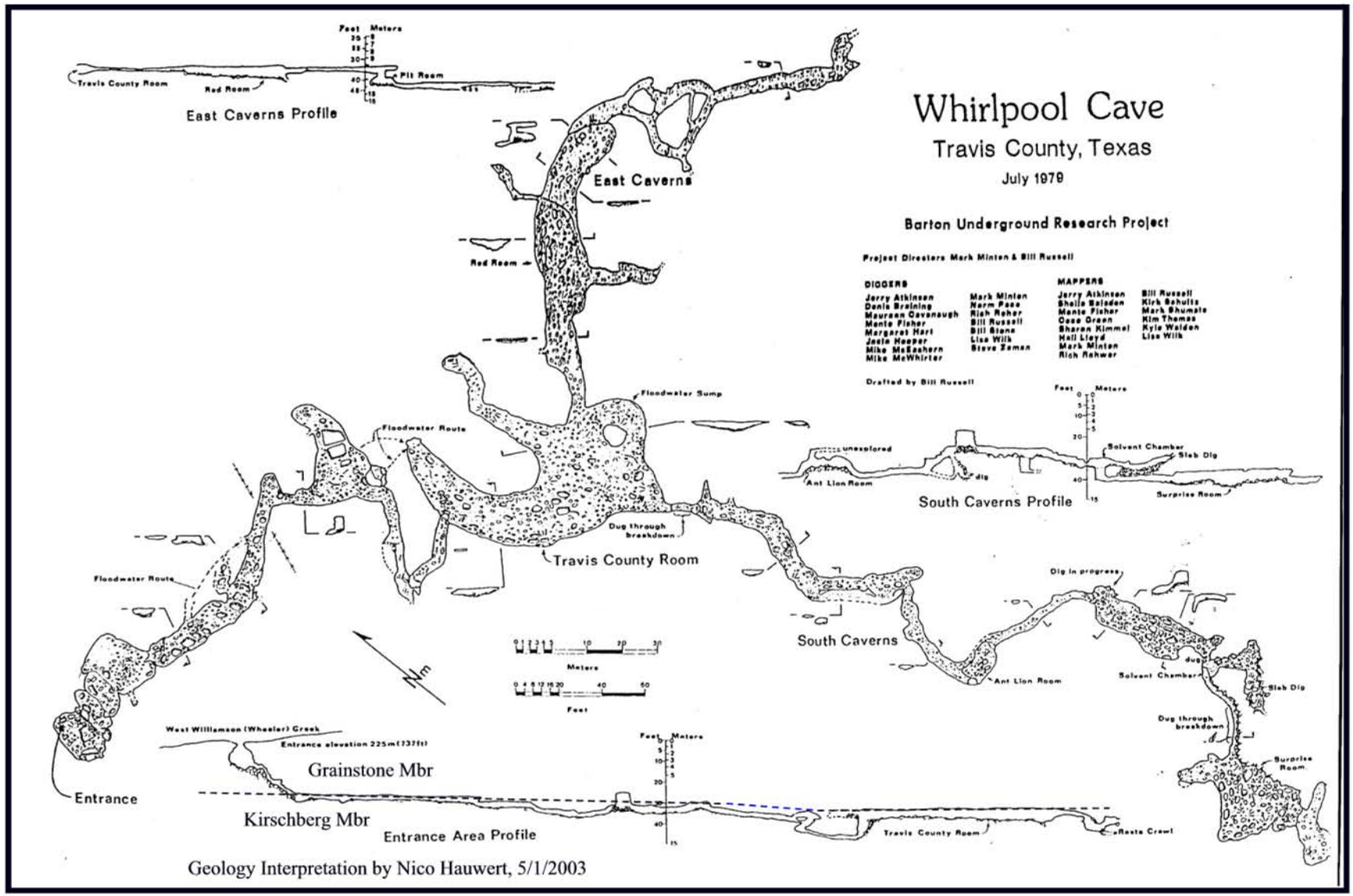
Whirlpool Cave
Travis County, Texas
July 1979
Barton Underground Research Project
Project Directors Mark Minton & Bill Russell
DIGGERS
Jerry Atkinson
Denis Breining
Maureen Cavenaugh
Monte Fisher
Margaret Hart
Josie Hooper
Mike McEachern
Mike McWhirter
Mark Minton
Norm Pace
Rich Reher
Bill Russell
Bill Stone
Lisa Wilk
Steve Zeman
MAPPERS
Jerry Atkinson
Sheila Baldon
Monte Fisher
Cece Green
Sharon Kimmel
Hall Lloyd
Mark Minton
Rich Rehwer
Bill Russell
Kirk Schultz
Mark Shumate
Kim Thomas
Kyle Walden
Lisa Wilk
Drafted by Bill Russell
East Caverns Profile
Travis County Room
Red Room
Pit Room
East Caverns
Floodwater Sump
Floodwater Route
Dug through breakdown
Travis County Room
South Caverns
South Caverns Profile
unexplored
Ant Lion Room
dig
Solvent Chamber
Slab Dig
Surprise Room
Dig in progress
Entrance
West Williamson (Wheeler) Creek
Entrance elevation 225m (737ft)
Grainstone Mbr
Kirschberg Mbr
Entrance Area Profile
Meters
Feet
Geology Interpretation by Nico Hauwert, 5/1/2003

Airman's Cave Geology

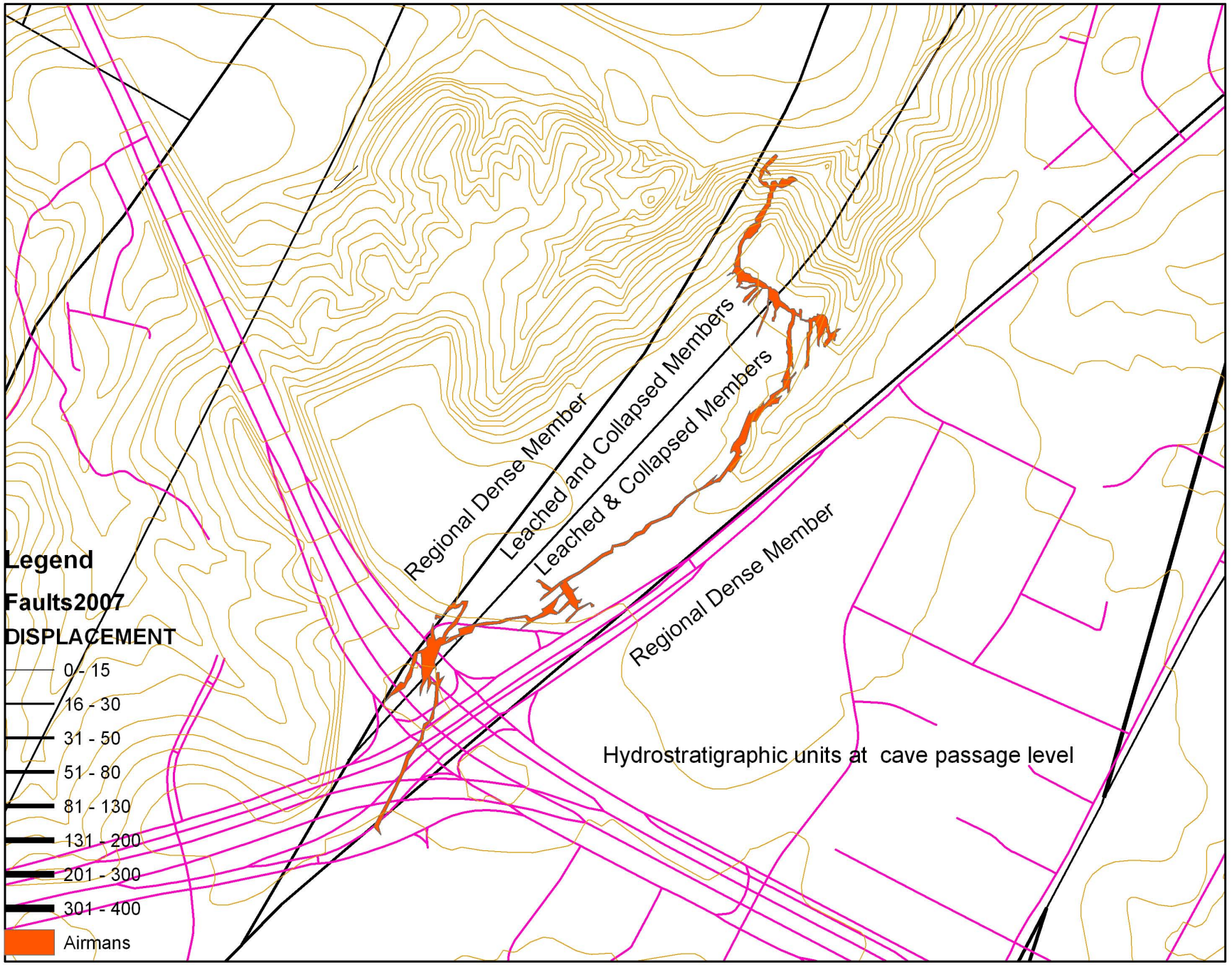

APPENDIX D

ANALYTICAL SOLUTIONS FOR AQUIFER TEST

APPENDIX D

ANALYTICAL SOLUTIONS FOR AQUIFER TESTS

A standard analytical model for pumping test data from a confined aquifer was developed by Theis (1935) for homogeneous, isotropic aquifers of infinite aerial extent and uniform thickness. The model also assumes an initially horizontal potentiometric surface with horizontal, unsteady flow where water is released instantly from storage with decline in head. The Theis solution is given by:

$$\text{Drawdown} = s = \frac{Q\,w(u)}{4\pi T}$$

where Q = pumping rate, W(u) = well function, and T= transmissivity.

Moench (1984) provided an analytical solution for groundwater flow through a double porosity system with permeable block slabs separated by open fractures lined with less-permeable fracture skins. This solution assumes a uniform thickness aquifer of infinite areal extent, with a flat potentiometric surface. It also assumes unsteady flow and that water is released instantly from storage with decline in hydraulic head. The solution for drawdown is a Laplace transformation:

$$\text{dimensionless drawdown in pumped well} = h_{wd} = \frac{2[K_0(x)+SwK_1(x)]}{P\{pW_D[K_0(x)+xS_wK_1(x)]+xK_1(x)\}}$$

$$\text{dimensionless drawdown in observation well} = h_D = \frac{2[K_0(r_Dx)}{P\{pW_D[K_0(x)+xS_wK_1(x)]+xK_1(x)\}}$$

where:

$$x = \sqrt{p+q_D}$$

$$q_D = \frac{\gamma^2 m\tanh(m)}{1+S_f m\tanh(m)}$$

$$m = \frac{\sqrt{\sigma p}}{\gamma}$$

$$\gamma = \frac{r_w \sqrt{K'/K}}{b'}$$

σ = S'_s/S_s = specific storage in blocks/specific storage in fractures

r_D = r/rw = radial distance to observation well/radius of well

storage in fracture = $S_f = \frac{K'b_s}{K_s b}$

$$W_D = \frac{\pi r_c^2}{2\pi r_w^2 S_s H}$$

$$q_D = \frac{\gamma^2 m \tanh(m)}{1+S_f m \tanh(m)}$$

Explanation of Terms

$K_1(x)$ = modified Bessel function of second kind, first order

p = Laplace Transform variable

K_0 = modified Bessel function of second kind, third order

r = radial distance from pumping well

b_s = fracture skin thickness

b = saturated thickness of the aquifer

b′ = average half thickness of the slab

Cooper-Jacob (1946) Solution

Transmissivity = T = $(\Delta s * 4\pi) / 2.3Q$

where:
Δs= drawdown (m)
Q = pumping rate (m3/min)
pi = 3.14159265

APPENDIX E.

AQUIFER TEST RESULTS

Aquifer Test Results

Well No.	Y	X	Distance to Flowpath (m)	Flowpath Rank	Saturated Thickness (m)	Transmissivity (m2/day)	T/sat th (m/day)	Storativity	System	Date	Duration (min)	RATEGPM
58-42-821	30.263060	-97.813890	656	1	141	15	0.11	0.05	Trigg-Forrister	2/2/82	90	16
58-50-860	30.153610	-97.821660	1,640	1	148	12	0.08	10^{-6} to 10^{-10}	Native Texas Nurs.	6/29/90	368	36
58-57-913	30.033890	-97.891110	3	1	148	7,500	50.80	$1x10^{-10}$	Hays High School	8/5/94	1440	347
58-57-913	30.033890	-97.891110	3	1	148	2,400	16.26	0.005	Hays High School	7/11/96	194	200
58-58-108	30.105280	-97.861950	11	1	148	67,000	453.81	$1x10^{-14}$	Leisurewoods	7/28/92	240	450
58-58-220	30.093330	-97.814450	525	1	148	5 - 87	0.59	0.059	Hunter Industries	11/8/89	435	200
58-58-410	30.066830	-97.838820	1,640	1	148	15	0.10	$5x10^{-3}$				
58-58-506	30.078330	-97.830560	108	1	148	140 - 370	2.51	$1x10^{-7}$	Goforth (A)	9/27/77	420	380
58-58-508	30.079170	-97.830990	118	1	148	250	1.69	$1x10^{-5}$	Goforth No. 4	8/18/96	605	1350
58-50-731	30.152970	-97.858700	11	2	125	300 - 1,450	11.63	--	Shady Hollow (A)	5/26/83	1440	200
58-50-731	30.152970	-97.858700	11	2	125	1,200 - 8,100	64.97	$1x10^{-12}$	Shady Hollow (B)	9/1/93	1440	200
58-50-848	30.130140	-97.821690	148	2	164	310	1.89	0.02				
58-50-850	30.125900	-97.815800	82	2	131	470 - 630	4.80	0.04	Creedmoore Well Site 2		17280	1284
58-57-305	30.099170	-97.892220	262	2	82	1,680	20.48		Dahlstrom	9/15/99	1380	
58-57-308	30.109560	-97.878370	433	2	118	87	0.74	10^{-3} to10^{-5}	Huntington Estates	9/19/96	1350	110
58-58-102	30.104590	-97.854340	98	2	148	140 - 550	3.73	0.001	Cimarron Park	9/11/96	564	600
58-58-127	30.117500	-97.873610	292	2	131	124	0.94	0.02	Hays Hills B. Church	6/1/90	211	71
58-58-404	30.070830	-97.863890	136	2	148	1,100	7.45	$3X10^{-4}$	Centex Materials (B)	8/18/93	527	860
58-58-405	30.067500	-97.863610	33	2	148	4,100	27.77	10^{-5} to 10^{-10}	Centex Materials (C)	8/25/93	540	1080

APPENDIX F.

SPECIFIC CAPACITY TEST RESULTS

Specific Capacity Tests

Well Number	System Name	Latitude	Longitude	Test Date	Duration (min)	Discharge (gpm)	Drawdown (feet)	Specific Capacity (gal/min/ft)	Specific Capacity m2/day	Transmissivity m2/day	Source
58-42-812	W.F. Guyton & Assoc.	30.265000	-97.813056	Jun-69		20	1.50	13.33	238	280.8	S
58-42-821	Trigg-Forister Bldg.	30.261111	-97.810556	Feb-82		16	10.40	1.54	28	27.3	P
58-42-8M	Allen Keller Co.	30.259167	-97.796389	Jun-79		100	60.00	1.67	30	29.7	S
58-42-8S	Espey Huston & Assoc	30.271667	-97.818889	Apr-82		150	6.00	25.00	447	553.7	D
58-42-8VW	Villita West	30.26528	-97.81528	4/2/1998	15	4.0	11.24	0.36	6.4	5.6	BSEACD
58-42-913	Park Hills BC	30.26667	-97.78222	8/27/1998	5	22	1.96	11.22	201	233.2	BSEACD
58-49-7RP	Poe	30.13912	-97.9661	5/8/1996	26	8.5	140.3	0.06	1.1	0.8	BSEACD
58-49-7VR	Robinson	30.14833	-97.98611	1/28/1999	43	13.0	0.30	43.33	775	1002.9	BSEACD
58-49-935	Manning	30.14537	-97.88725	8/17/1998	55	20	262	0.08	1.4	1.1	BSEACD
58-49-935	Manning	30.14537	-97.88725	3/1/1994	31	12.0	440	0.03	0.5	0.4	BSEACD
58-49-937	Tabor Bear	30.15801	-97.88773	4/13/2000	40	6.3	7.13	0.88	16	14.8	BSEACD
58-49-9DT	Tomlinson	30.15084	-97.87555	3/19/1997	31	9.0	5.74	1.57	28	27.8	BSEACD
58-49-9DW	Weaver	30.13556	-97.89389	10/6/1999	49	15	97.25	0.15	2.8	2.3	BSEACD
58-49-9ES	Sparks	30.13333	-97.88111	2/2/1999	30	12.0	30.70	0.39	7.0	6.2	BSEACD
58-49-9H	Charles Ranch	30.159167	-97.898333	Aug-87		287	138.0	2.08	37	37.8	D
58-49-9JF	Foley	30.12861	-97.88277	2/2/1999	19	13.1	1.00	13.10	234	275.5	BSEACD
58-49-9KM	Molenar	30.14861	-97.87611	8/4/1998	11	10.0	19.10	0.52	9.4	8.5	BSEACD
58-49-9LB	Bray	30.13611	-97.88223	11/7/1996	30	10.0	37.00	0.27	4.8	4.2	BSEACD
58-49-9WH	Holke	30.13528	-97.89584	8/6/1999	27	12.5	80.90	0.15	2.8	2.3	BSEACD
58-49-9WM	Ryder	30.13836	-97.89324	8/9/2000	31	10.0	16.50	0.61	11	10.0	BSEACD
58-50-122	White Prop	30.23839	-97.83824	8/27/1998	50	21	62.34	0.34	6.0	5.3	BSEACD
58-50-1AM	AMLI Resid. Const., Inc.	30.22833	-97.84	4/1/1999	44	4.8	33.95	0.14	2.5	2.1	BSEACD
58-50-1C1	Capital City Oil	30.23389	-97.8625	3/13/1997	35	11.5	2.50	4.60	82	89.0	BSEACD
58-50-201	Jentsch	30.21958	-97.79373	8/31/1998	36	10.0	0.58	17.24	308	370.7	BSEACD
58-50-207	Onion Crk Meadows	30.12022	-97.8207	8/27/1999	8	11.0	1.62	6.79	121	135.5	BSEACD
58-50-222	Besse	30.21722	-97.81879	3/3/1994	21	14.7	6.38	2.30	41	42.2	BSEACD
58-50-222	Besse	30.21722	-97.81879	8/25/1998	36	15	5.81	2.58	46	47.7	BSEACD
58-50-222	Besse	30.21722	-97.81879	8/4/1999	35	15	5.77	2.60	46	48.0	BSEACD
58-50-222	Besse	30.21722	-97.81879	8/7/1997	25	15	3.82	3.93	70	75.0	BSEACD
58-50-223	City of Sunset Valley	30.227500	-97.809722	Jun-90		125	49.65	2.52	45	46.4	A
58-50-224	Safeway Rental	30.23833	-97.83056	8/26/1998	40	12.0	2.20	5.45	98	107.0	BSEACD
58-50-2OW	Picard	30.22668	-97.80922	1/20/1999	29	10.0	0.29	34.48	617	783.6	BSEACD
58-50-2NB2	HE Brodie	30.23753	-97.80183	10/30/1995	30	1.2	15.70	0.08	1.4	1.1	BSEACD
58-50-402	John F. Rehm	30.17832	-97.84766	3/24/1999	24	10.0	16.68	0.60	11	9.9	BSEACD
58-50-406	Gantt, Brian	30.19674	-97.84316	9/4/1998	65	5.0	215	0.02	0.4	0.3	BSEACD
58-50-414	Lee V. Johnson	30.179722	-97.840833	Nov-86		51	18.00	2.83	51	52.7	D
58-50-416	Wetzel	30.1766	-97.86723	8/18/1998	88	10.0	5.50	1.82	33	32.7	BSEACD
58-50-4BK	Kimbro	30.17417	-97.8575	2/2/1999	36	5.0	0.64	7.81	140	157.7	BSEACD
58-50-4DG	Griffen	30.175	-97.84666	5/20/1999	35	6.3	65.15	0.10	1.7	1.4	BSEACD
58-50-704	Marbridge Found. #5	30.136667	-97.855556	Feb-68		1150	31.00	37.10	663	848.0	S
58-50-728	Mabee Village	30.13861	-97.85555	2/22/1995	20	51	0.20	255.00	4561	6800.8	BSEACD
58-50-730	McCoys	30.14	-97.83833	7/15/1998	60	5.3	2.61	2.03	36	36.8	BSEACD
58-50-731	Shady Hollow Estates	30.149444	-97.860000	May-83		210	10.00	21.00	376	458.7	P
58-50-7BM	not sure bms	30.1625	-97.87334	12/8/1999	27	11.0	16.60	0.66	12	11.0	BSEACD
58-50-7BW	Wheeless	30.13192	-97.83516	6/27/2000	23	9.0	0.41	21.95	393	481.1	BSEACD
58-50-7DM	Meredith	30.15316	-97.83937	7/9/1998	31	12.5	0.59	21.19	379	463.1	BSEACD
58-50-7DP	Pailthrop	30.13083	-97.85555	3/13/1998	25	13.6	12.53	1.09	19	18.7	BSEACD
58-50-7ME	Everitt	30.14111	-97.83806	4/14/1998	28	4.0	4.30	0.93	17	15.8	BSEACD
58-50-7SHI	Hinton	30.15222	-97.85445	6/29/1998	10	15	15.00	1.00	18	17.1	BSEACD
58-50-7SW	Wiley	30.16593	-97.86705	10/23/1996	27	10.0	100.0	0.10	1.8	1.4	BSEACD
58-50-7WC	Lancaster	30.14209	-97.85368	5/4/2000	13	10.0	0.4	25.00	447	553.7	BSEACD
58-50-805	Canterbury Trails	30.15768	-97.82887	1/22/1998	15	35	88.95	0.39	7.0	6.3	BSEACD
58-50-825	Thomas	30.13447	-97.81059	12/20/1995	25	7.5	84.47	0.09	1.6	1.3	BSEACD
58-50-825	Thomas	30.13447	-97.81059	9/4/1998	40	11.0	79.35	0.14	2.5	2.0	BSEACD
58-50-830	Slaughter Creek Acres	30.160278	-97.817778	Aug-71		45	160	0.28	5.0	4.4	S
58-50-835	Onion Creek Acres	30.145833	-97.812500	May-69		270	12.00	22.50	402	494.1	S
58-50-852	Malone	30.16167	-97.81834	8/20/1998	25	40	85.69	0.47	8.3	7.5	BSEACD
58-50-855	San Leanna	30.14624	-97.81927	8/20/1998	27	164	116.1	1.41	25	24.9	BSEACD
58-50-8KF	Francis	30.14806	-97.825	8/18/1999	51	8.0	47.77	0.17	3.0	2.5	BSEACD
58-50-8LS	Salgado	30.16556	-97.83139	3/1/2000	16	14.0	0.26	53.85	963	1268.1	BSEACD
58-50-8RG	Greene	30.13944	-97.83111	4/14/1999	22	12.0	18.65	0.64	12	10.6	BSEACD
58-57-2MS	Salinas	30.09306	-97.91917	8/10/1998	9	10.0	27.70	0.36	6.5	5.7	BSEACD
58-57-307	Dahlstrom Middle Sch.	30.099722	-97.882222	May-90		68	18.34	3.71	66	70.5	F
58-57-307	Dahlstrom M.S.	30.09986	-97.88229	8/18/1998	60	72	4.83	14.91	267	316.8	BSEACD
58-57-312	Rocket Water Supply	30.10611	-97.90334	8/31/1998	69	50	44.74	1.12	20	19.3	BSEACD
58-57-312	Rocket Water Supply	30.10611	-97.90334	8/4/1999	33	50	17.90	2.79	50	51.9	BSEACD
58-57-3AG	Aguirre	30.09222	-97.88194	12/8/1999	10	16	2.73	5.68	102	111.7	BSEACD
58-57-3AW	Wilson	30.09572	-97.87863	8/10/1999	11	10.0	0.34	29.41	526	659.9	BSEACD
58-57-3BD	Davis	30.11278	-97.88528	12/15/1999	19	20	60.55	0.33	5.9	5.2	BSEACD
58-57-3BD	Davis	30.11278	-97.88528	3/22/2000	28	10.0	4.14	2.42	43	44.4	BSEACD
58-57-3BF	Freitag	30.1076	-97.9059	9/25/1997	32	18	8.74	2.06	37	37.4	BSEACD
58-57-3BL	Larvin	30.09111	-97.88139	3/13/2000	18	9.0	0.05	180.00	3219	4668.6	BSEACD
58-57-3CA	Attal	30.11194	-97.89027	2/9/2000	41	4.5	0.34	13.24	237	278.6	BSEACD

Specific Capacity Tests

Well Number	System Name	Latitude	Longitude	Test Date	Duration (min)	Discharge (gpm)	Drawdown (feet)	Specific Capacity (gal/min/ft)	Specific Capacity m2/day	Transmis-siviy m2/day	Source
58-57-3CC	Pardinek	30.11676	-97.88226	8/9/2000	24	10.0	1.28	7.81	140	157.7	BSEACD
58-57-3CG	Gee	30.08889	-97.91389	9/30/1998	21	14.0	36.06	0.39	6.9	6.2	BSEACD
58-57-3CT	Thompson	30.11404	-97.89149	10/6/1999	14	10.0	17.66	0.57	10	9.3	BSEACD
58-57-3DB	Boone	30.11445	-97.91221	9/15/1999	16	9.0	6.92	1.30	23	22.7	BSEACD
58-57-3DK	Klingeman	30.09417	-97.88416	2/29/2000	24	9.0	4.91	1.83	33	32.9	BSEACD
58-57-3EG	Garza	30.10563	-97.8888	6/17/1998	22	22	0.19	115.79	2071	2899.1	BSEACD
58-57-3GAH	Herzog	30.12278	-97.90667	10/29/1998	25	5.0	123.4	0.04	0.7	0.5	BSEACD
58-57-3JC	Clites	30.0875	-97.91583	3/13/2000	39	13.5	9.55	1.41	25	24.9	BSEACD
58-57-3JH	Hardin	30.12222	-97.90556	6/21/2000	32	8.0	104.6	0.08	1.4	1.1	BSEACD
58-57-3JK	Krause	30.09222	-97.87917	6/16/1998	21	23	0.70	32.86	588	743.8	BSEACD
58-57-3KD	Duckworth	30.08833	-97.91444	10/7/1999	16	15	68.17	0.22	3.9	3.3	BSEACD
58-57-3KK	Strickland	30.10173	-97.89841	7/13/1998	16	14.5	24.20	0.60	11	9.8	BSEACD
58-57-3LB	Bonner	30.11944	-97.90691	4/14/1999	35	8.0	33.10	0.24	4.3	3.7	BSEACD
58-57-3LS	Strock	30.12444	-97.88	1/27/1999	19	13.0	0.19	68.42	1224	1642.5	BSEACD
58-57-3MD	Diaz	30.09805	-97.88556	8/20/1999	15	12.5	3.52	3.55	64	67.3	BSEACD
58-57-3MH	Holt	30.11333	-97.91361	2/2/2000	58	8.0	13.91	0.58	10	9.4	BSEACD
58-57-3MR	Ryden	30.11167	-97.9125	12/30/1998	26	7.3	18.80	0.39	6.9	6.2	BSEACD
58-57-3MV	Vera	30.11389	-97.87833	1/7/1999	22	11.0	0.45	24.44	437	540.4	BSEACD
58-57-3ON	Nicholas	30.08889	-97.90833	9/30/1998	24	14.0	36.00	0.39	7.0	6.2	BSEACD
58-57-3RA	Allen	30.08799	-97.91394	9/25/1997	30	13.0	0.65	20.00	358	435.1	BSEACD
58-57-3RC	Castillo	30.12444	-97.90639	1/7/1999	18	14.0	67.28	0.21	3.7	3.1	BSEACD
58-57-3RN	New	30.11111	-97.89111	6/24/1998	15	21	0.90	23.33	417	513.9	BSEACD
58-57-3RO	Rose	30.11944	-97.91	12/15/1998	48	8.5	10.48	0.81	15	13.7	BSEACD
58-57-3RS	Solitt	30.11401	-97.87897	9/14/1998	15	7.0	0.47	14.89	266	316.5	BSEACD
58-57-3RV	Quintas	30.1175	-97.90889	10/1/1999	38	11.5	52.23	0.22	3.9	3.3	BSEACD
58-57-3SM	Sonntag	30.12472	-97.90694	1/5/2000	22	10.0	98.03	0.10	1.8	1.5	BSEACD
58-57-3SW	Woelfel	30.11417	-97.91444	3/4/1996	30	10.0	83.25	0.12	2.1	1.7	BSEACD
58-57-3TD	Dickey	30.12072	-97.91077	7/11/1996	18	10.0	90.75	0.11	2.0	1.6	BSEACD
58-57-3TG	Huth/Gonzales	30.08972	-97.9125	4/14/1999	10	12.5	10.40	1.20	21	20.9	BSEACD
58-57-3TK	Thames	30.09712	-97.88792	7/12/2000	17	10.0	1.38	7.25	130	145.4	BSEACD
58-57-3WL	Lawler	30.10972	-97.91055	1/7/1999	24	10.0	21.48	0.47	8.3	7.5	BSEACD
58-57-4AR	Rickman	30.04639	-97.97472	2/12/1998	23	12.0	90.00	0.13	2.4	1.9	BSEACD
58-57-4DB	Bandy	30.05417	-97.97639	5/13/1999	19	15	75.6	0.20	3.5	3.0	BSEACD
58-57-4GH	Howard	30.04434	-97.95837	7/11/2000	31	10.0	71.29	0.14	2.5	2.1	BSEACD
58-57-4HG	Gallagher	30.04667	-97.96056	11/24/1998	22	12.0	72.07	0.17	3.0	2.5	BSEACD
58-57-4JZ	Zoehlke	30.05	-97.97778	8/16/2000	33	12.5	19.83	0.63	11	10.4	BSEACD
58-57-4MP	Kunkle	30.055	-97.96722	2/12/1998	29	10.0	56.96	0.18	3.1	2.6	BSEACD
58-57-4PA	Angel	30.05	-97.97916	7/21/1998	20	14.5	101.7	0.14	2.5	2.1	BSEACD
58-57-4PA	Angel	30.05	-97.97916	7/5/1996	11	10.0	26.88	0.37	6.7	5.9	BSEACD
58-57-4PM	Moreno	30.04645	-97.96012	11/11/1998	14	11.0	17.28	0.64	11	10.5	BSEACD
58-57-4RR	Running Rope	30.05233	-97.99524	2/3/1999	27	13.3	53.40	0.25	4.5	3.8	BSEACD
58-57-4SB	Burrier	30.04445	-97.95972	11/19/1998	28	23	0.57	40.35	722	928.6	BSEACD
58-57-4TH	Haggard	30.05	-97.97694	8/11/1997	3	5.0	150	0.03	0.6	0.4	BSEACD
58-57-506	Grote	30.045	-97.96167	8/14/1998	35	20	213.2	0.09	1.7	1.3	BSEACD
58-57-5BM	Miranda	30.04556	-97.95805	2/23/1999	28	10.0	33.32	0.30	5.4	4.7	BSEACD
58-57-5CK	Kelly	30.04445	-97.95333	2/9/1999	31	10.0	3.76	2.66	48	49.2	BSEACD
58-57-5J2	Inn Above Onion Creek	30.0495	-97.93567	7/11/2000	140	10.0	44.65	0.22	4.0	3.4	BSEACD
58-57-5JO	Inn Above Onion Creek	30.04694	-97.93806	3/9/1994	55	8.0	200	0.04	0.7	0.5	BSEACD
58-57-5TS	Schneider	30.045	-97.95695	2/9/1999	26	11.0	23.01	0.48	8.5	7.7	BSEACD
58-57-606	Barton Prop	30.04773	-97.88367	12/28/1998	17	7.5	6.51	1.15	21	19.9	BSEACD
58-57-6CS	6S1/Cliff Sorrel?	30.08139	-97.91333	3/3/1999	30	8.0	6.60	1.21	22	21.1	BSEACD
58-57-6DC	Conner	30.04322	-97.89894	3/10/1999	19	6.0	0.90	6.67	119	132.8	BSEACD
58-57-6JS	Stavlo	30.08055	-97.90556	9/30/1998	17	13.0	5.06	2.57	46	47.4	BSEACD
58-57-6KM	Matzig Cove	30.08278	-97.91028	5/25/2000	18	10.0	0.56	17.86	319	385.0	BSEACD
58-57-6KW	Weisbeck	30.08278	-97.9125	3/7/1998	44	10.0	0.10	100.00	1788	2474.6	BSEACD
58-57-6LW	Wimmer	30.08137	-97.91212	6/11/1998	18	22	14.70	1.46	26	25.8	BSEACD
58-57-6SI	Simmons	30.08139	-97.91333	6/10/1999	13	12.5	9.30	1.34	24	23.6	BSEACD
58-57-8DC	Crowell	30.04111	-97.95417	12/8/1998	33	9.0	0.05	180.00	3219	4668.6	BSEACD
58-57-8DG	Grimes	30.04028	-97.93278	4/8/1999	34	8.0	13.46	0.59	11	9.8	BSEACD
58-57-8MR	Ragland	30.04028	-97.93389	10/13/1999	15	13.5	39.02	0.35	6.2	5.4	BSEACD
58-57-8SR	Richards	30.04111	-97.94778	11/12/1998	14	11.0	0.41	26.83	480	597.6	BSEACD
58-57-910	Mt. City Oaks WSC	30.034722	-97.899167	Jul-90		184	0.25	736.00	13163	21366.1	E
58-58-102	Cimarron Park #2	30.106111	-97.854167	Apr-84		600	4.00	150.00	2683	3834.2	P
58-58-115	Estate Utilities WSC	30.123056	-97.871944	Nov-79		660	12.00	55.00	984	1297.4	S
58-58-122	Twin Oaks	30.09472	-97.84361	12/17/1993	19	6.0	2.10	2.86	51	53.2	BSEACD
58-58-123	Elizabeth Porter	30.109444	-97.841667	Feb-85		400	15.00	26.67	477	593.7	D
58-58-1A	Frank Burdette	30.123889	-97.871389	Jun-90		10.8	0.29	37.07	663	847.3	E
58-58-1AS	Sampsom	30.10583	-97.87083	4/21/1998	60	6.0	3.08	1.95	35	35.2	BSEACD
58-58-1B	Hays Hills Baptist Ch.	30.117222	-97.874444	Jun-90		71	7.00	10.14	181	209.0	P
58-58-1CD	Draper	30.08333	-97.87305	2/10/1999	16	8.0	0.71	11.27	202	234.1	BSEACD
58-58-1EE	Neptune-Wilkinson	30.084444	-97.866667	Apr-84		225	127.0	1.77	32	31.8	D
58-58-1GB	Buchanan	30.10762	-97.87096	10/7/1999	27	16	16.80	0.95	17	16.2	BSEACD
58-58-1JM	Miller	30.11444	-97.87167	3/5/1998	48	5.0	6.20	0.81	14	13.6	BSEACD
58-58-1KM	Marks	30.09347	-97.84483	9/29/1998	20	19	3.93	4.83	86	93.9	BSEACD

Specific Capacity Tests

Well Number	System Name	Latitude	Longitude	Test Date	Duration (min)	Discharge (gpm)	Drawdown (feet)	Specific Capacity (gal/min/ft)	Specific Capacity m2/day	Transmissivity m2/day	Source
58-58-1MA	Acosta	30.10028	-97.865	2/16/2000	39	12.0	0.78	15.38	275	327.8	BSEACD
58-58-1MH	Harper	30.10972	-97.87195	9/25/1997	10	18	0.28	64.29	1150	1535.5	BSEACD
58-58-1MO	Oakes	30.10695	-97.86806	10/12/1999	6	11.0	1.01	10.89	195	225.7	BSEACD
58-58-1PK	Kaskie	30.10306	-97.8725	1/11/2000	24	7.0	0.91	7.69	138	155.0	BSEACD
58-58-1PW	Wentworth	30.11315	-97.87292	2/9/2000	43	12.0	1.09	11.01	197	228.3	BSEACD
58-58-1RC	Cullen	30.10028	-97.85167	2/10/2000	23	12.5	0.90	13.89	248	293.5	BSEACD
58-58-202	Mystic Oak WSC #1	30.124444	-97.813333	unk		42	185	0.23	4.1	3.5	S
58-58-206	Rainbow Ranch	30.10222	-97.82584	5/26/1999	15	10.0	0.90	11.11	199	230.6	BSEACD
58-58-208	Onion Crk Meadows	30.11639	-97.81976	8/5/1993	7	92	54.48	1.69	30	30.1	BSEACD
58-58-219	John Rogers	30.09167	-97.8175	8/20/1998	36	12.0	48.80	0.25	4.4	3.8	BSEACD
58-58-2JS	Stafford	30.11722	-97.825	7/13/1998	7	16	6.6	2.42	43	44.5	BSEACD
58-58-2SG	Gasparotto	30.10806	-97.81805	1/7/1999	26	6.5	27.28	0.24	4.3	3.6	BSEACD
58-58-406	Texas-Lehigh Cement	30.061389	-97.855556	Aug-66		1200	53.00	22.64	405	497.5	D
58-58-412	Plum Creek No. 1	30.07667	-97.83444	9/30/1998	235	510	112.0	4.55	81	88.0	BSEACD
58-58-412	Plum Creek WSC	30.076389	-97.834167	Jun-90		470	52.60	8.94	160	182.3	E
58-58-413	City of Buda #3	30.072222	-97.834444	Mar-87		430	99.33	4.33	77	83.3	P
58-58-423	Comal Tackle	30.06781	-97.85912	7/15/1999	35	17	3.04	5.59	100	109.9	BSEACD
58-58-4BP	Pool	30.07278	-97.87361	11/16/1999	18	11.0	4.23	2.60	47	48.1	BSEACD
58-58-4DL	Lowden	30.07944	-97.86945	6/24/1998	19	15	0.65	23.08	413	507.8	BSEACD
58-58-4JP	Puckett	30.08046	-97.86948	3/7/2000	9	8.0	1.82	4.40	79	84.7	BSEACD
58-58-506	Goforth WSC	30.078333	-97.830278	Sep-77		310	65.00	4.77	85	92.5	P
58-58-508	Goforth WSC	30.078611	-97.830556	Jul-90		227	90.90	2.50	45	46.0	A

APPENDIX G.

PHOTOGRAPHS FROM RESEARCH SITES

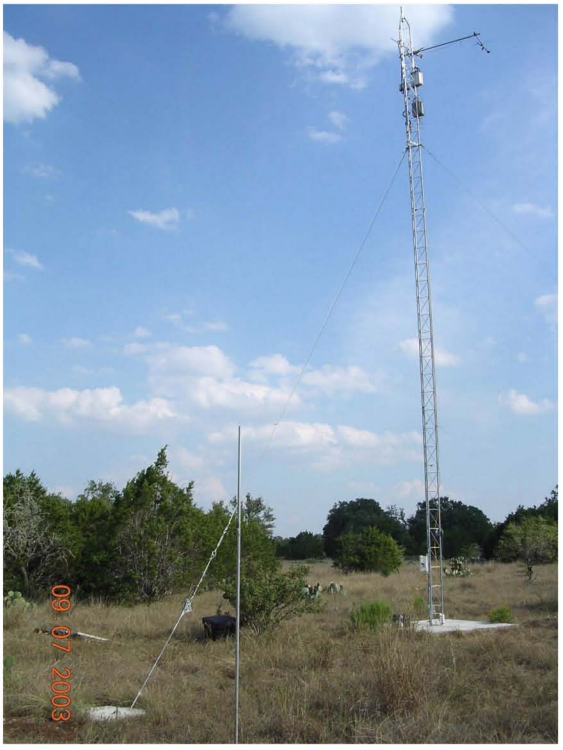

(a)

(b)

(c)

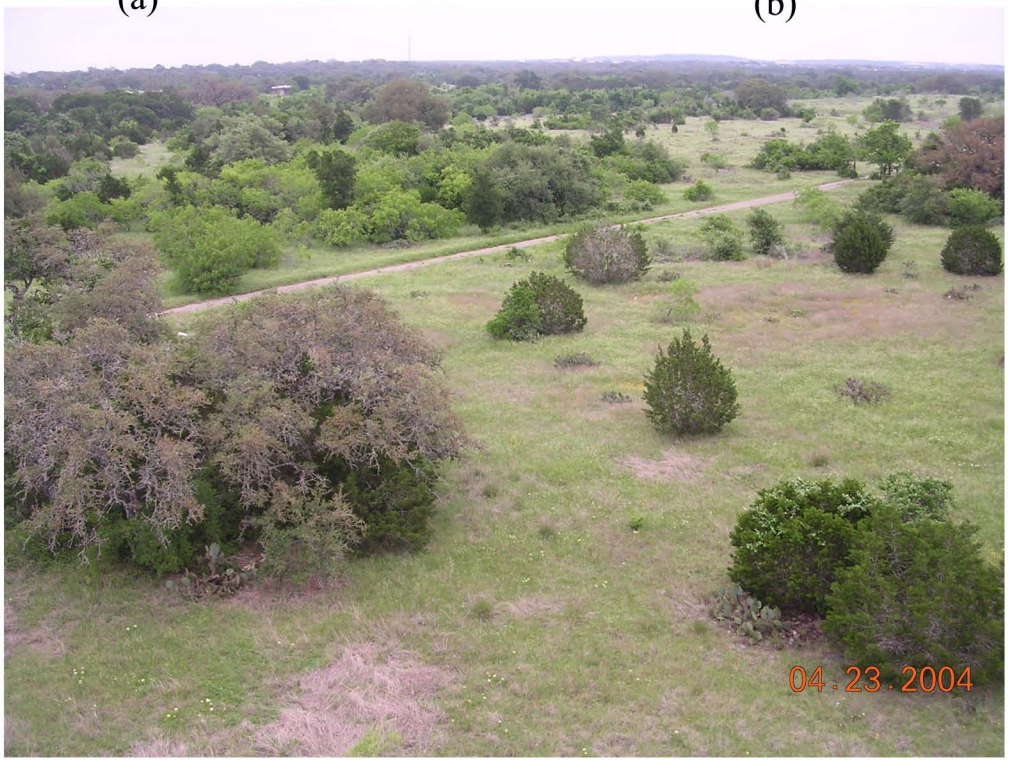

The J17 Research tract including (a) the eddy flux evapotranspiration measurement tower (ET tower), (b) a view of the J17 tract viewing northeast from the ET tower towards HQ Flat Cave (which is on the other side of the tree cluster), and (c) a view to the southwest from the ET tower

(a) photo by David A. Johns, City of Austin

(b) photo by Nico Hauwert, City of Austin

Contrast in recharge over the Kirschberg Member in Onion Creek showing (a) Crippled Crayfish Cave recharges about 0.27 m3/s during flowing creek conditions, and (b) David Johns watches a pool in Onion Creek slowly dry two weeks after the creek ceased flowing. This pool is only about 70 m upstream of Crippled Crawfish Cave.

(a)

(b)

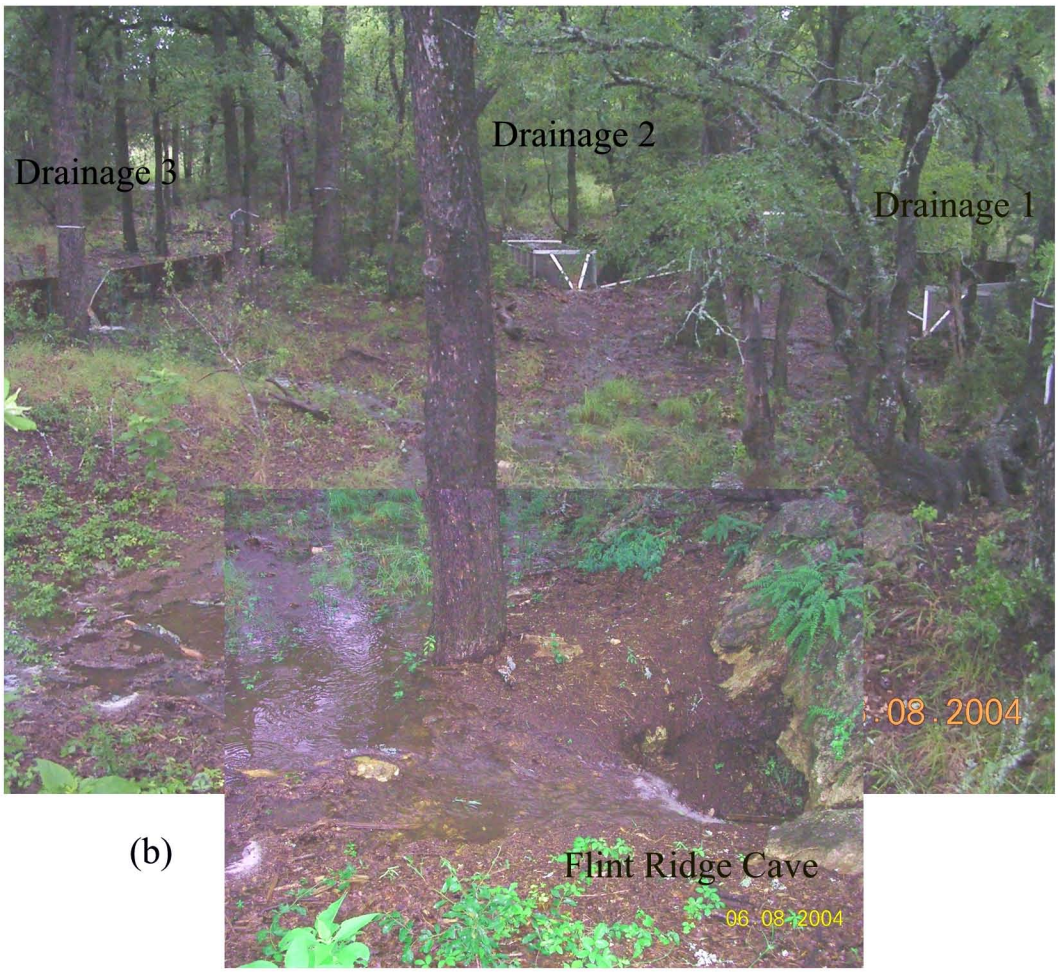

Runoff entering (a) HQ Flat Cave flume from single main approach channel and (b) Flint Ridge Cave through three primary drainages on June 8 and 9, 2004.

APPENDIX H.

LIST OF VEGETATION ON RESEARCH SITES

Juniperus ashei (ashe juniper)
Quercus fusiformis (Escarpment live oak)
Mahonia trifoliolata (agarita)
Ulmus crassifolia (cedar elm)
Diospyros texana (Texas persimmon)
Vitis mustangensis (mustang grape)
Celtis occidentalis (hackberry)
Prosopis glandulosa (mesquite)
Opuntia macrorhiza (prickly pear)
Forestiera pubescens (elbow bush)
Smilax bona-nox (greenbriar)
Toxicodendron radicans (poison ivy)
Zanthoxylum hirsutum (toothache tree)
Rhus lanceolata (flameleaf sumac)
Bothriochloa ischaemum var. songarica (King Ranch bluestem)
Bothriochloa saccharoides var. torreyana (silver bluestem)
Schizachyrium scoparium var. frequens (little bluestem)

APPENDIX I.

TRACER PROPERTIES

This section discusses the hydraulic characteristics and health properties of several fluorescent dyes introduced, including sodium fluorescein (fluorescein), rhodamine WT, eosine, sulforhodamine B, and pyranine, and evaluates factors that can affect their use within the Barton Springs Segment. Their sorptive characteristics influence how well the tracer is recovered at monitored discharge sites. Also, each tracer has different responses to factors such as sunlight, temperature, acidity, and chlorine. This type of comparison is important to help distinguish when limitations resulting from the type of tracer used will limit recoveries. The tracers selected for the study have been well tested to determine their low toxicity for drinking water sources and aquatic life.

Transport and Recovery of the Tracers

In one reported groundwater trace, two organic tracers were used simultaneously from the same location. One of the tracers, fluorescein, was detected in 18 domestic wells, but the rhodamine WT tracer was only detected in two of the 18 wells (Aley, 2002). In a separate study, Brown and Ford (1971) discovered three different breakthrough curves using rhodamine WT, fluorescein, and rhodamine B tracers from the same site in a karst area of Canada. In this 1.3 mile trace, 98% of the rhodamine WT was recovered and none of the fluorescein was detected. Furthermore, the rhodamine B took twice as long as the rhodamine WT for its initial arrival. Obviously, different properties of the tracers themselves will influence the result of any tracer test. When interpreting the results of tracer studies, it is important to understand the properties of the tracers and how they can influence the recovery and travel time measured as well as the shape of the breakthrough curve. No direct comparison of the tracers' performance within the Barton Springs Segment was conducted as part of this study. However, some information on tracer properties is available in the literature.

Sorption

Sorption includes both absorption and adsorption. *Absorption* is the assimilation of dissolved constituents of a solution (solute) inside a solid matrix. *Adsorption* is the attraction of a solute to a solid surface by weak electrical attraction or stronger chemical bonds. The amount of a solute that is adsorbed onto a solid depends on the characteristics of the solute, the nature of the solid, and the concentration of the solute (Helfferich, 1962, Mercer and Faust, 1981). As a result of adsorption, organic tracers move more slowly than water and ionic or radioactive tracers (Davis et al., 1985). *Conservative* tracers have low sorptive properties and are preferred for estimating groundwater-flow rates. Organic tracers adsorb to varying degrees on sediments and clay.

Based on experimental data of fluorescence changes with a suspended kaolinite mixture, Smart and Laidlaw (1977) found that at a 20 g/l suspended clay concentration, 51% of sulforhodamine B, 67% of rhodamine WT, 93% of fluorescein, and 95% of pyranine remained dissolved in solution. Suspended sediment not only adsorbs the organic tracers, but to a lesser degree also raises the background fluorescence and reduces the tracer fluorescence by light absorption and scattering. Suspended sediment is usually not a significant problem when sediment concentrations are less than 1,000 mg/l, the sediment is not composed of extremely fine particles or organic matter, and the suspended sediment is allowed to settle and separate prior to analysis.

Some studies show that rhodamine WT is strongly sorbed in sediment-laden water and organic sediments (Smart and Laidlaw, 1977; Aley, 2002), but otherwise appears to be relatively conservative as a tracer (Wilson, 1971; Smart and Laidlaw, 1977; Aley, 2002, Aulenbach and others, 1978; Brown and Ford, 1971). The inconsistent sorptive nature of rhodamine WT is due in part to its molecular structure. Rhodamine WT typically shows a two-peak breakthrough curve in chromatograms (Rochat, et al., 1975; Hofstraat, et al., 1991) as well as in column tests (Sabatini and Austin, 1991). This two step breakthrough curve is attributed to two isomers of rhodamine WT, one which is relatively conservative, and the other which has relatively high sorption (Shiau, Sabatini, and Harwell, 1992). Rhodamine WT breakthrough curves show spreading from this

nonequilibrium sorption. For this reason, relatively higher masses of rhodamine WT are necessary to obtain a recovery comparable to fluorescein.

The ionic tendency of the tracer and the type of aquifer medium will affect the amount of sorption that occurs. Rhodamine WT and sulforhodamine B have both cationic and anionic groups that will tend to sorb on most surfaces, although they sorb less on anionic surfaces, such as kaolinite sediment (Smart and Laidlaw, 1977) and sand or sandstone aquifers (Sabatini, 2000). Fluorescein and eosine are anionic and tend to sorb most strongly onto positively charged surfaces such as limestone (Sabatini, 2000). If significant, this factor allows fluorescein to pass with greater ease through fine-grained sediment at recharge feature entrances, but cause a reduction in fluorescein as it passes through the aquifer.

Greater losses occur in soil than in cave sediment or cave stream pebbles possibly due to greater sorption and biological decomposition (Aley, 2002). Fluorescein and rhodamine WT are most strongly sorbed onto organic materials. Sorption of the tracers within shallow, fine-grained sediment covering the opening of injection sites probably accounts for a significant loss of the tracer mass. Most of the injection sites (A, B, C, E, G, K, P, M, N, and O) were filled with an undetermined thickness of sediments near the surface that acted to reduce the recovered tracer mass. For traces F, H, J, D, I, L, M', Q, and R, the tracer was poured directly into conduit openings. Trace T was likely completely obstructed by a trash and sediment plug at the bottom of the cave and was encountered years later during a cave cleanup and exploratory excavation.

Partial or complete saturation of the sorption media (fracture skins) cause the percent recovery of the organic tracers increases significantly with larger injection tracer mass. Low injection masses of tracer are a significant cause for error in qualitative calculations of percent recovery because of arrival of tracers below the detection limit and the greater significance of possible errors in discharge estimations (Smart and Laidlaw, 1977). Consequently, percent recoveries of a small mass of tracer injected cannot be accurately used to calculate the results of a larger injection mass, and estimates of percent recovery for a larger injection mass will invariably be underestimated.

Hydrogen Ion Concentration (pH)

Smart and Laidlaw (1977) examined the effect of pH on the organic tracers. Low pH caused tracer degradation from changes in ionization and chemical structure. Each of the organic dyes discussed here have a net negative charge (anionic) at pH greater than 7, and reverse charges or become positively charged at some lower pH, depending on its general chemical group. This charge reversal appears to result in a loss of fluorescence. Rhodamine WT undergoes a decline in fluorescence at a pH less than 5. Variations in pH have little effect on the fluorescence of sulforhodamine B (a sulphonate acid group). Tracer degradation at lower pH may also result from other chemical structure changes. For example, fluorescein abruptly changes from a fluorescent quinoid structure to a colorless leuco compound below 6 pH. Pyranine experiences a sharp shift in the absorption spectrum causing an elimination of fluorescence below 6.5 pH. Even below 9.5 pH, pyranine shows a substantial decrease in fluorescence (Aley, 2002). The pH of natural waters within the Barton Springs Segment generally range from 6.8 to about 7.5 (Hauwert and Vickers, 1994), so that the effects of pH are likely only a consideration for pyranine traces.

Chlorine

Of the tracers examined in the literature, only rhodamine WT was tested for its response to chlorine (Deaner, 1973). In this test, strong declines in fluorescence were observed at high concentrations of chlorine and for high periods of exposure to chlorine. For example, when 0.01 mg/l of rhodamine WT is exposed to a 20 mg/l chlorine residual for 20 hours, a 23% reduction in the original concentration can be expected. In the Barton Springs Segment tracing study, chlorinated water was occasionally used to flush the tracer. Based on a 1 mg/l chlorine residual and 20-hour exposure duration, only about a 2% reduction in the original concentration of rhodamine WT is expected.

Salinity

Laboratory tests by Feuerstein and Selleck (1963) found fluorescein to be strongly affected by high levels of chloride up to 18,000 mg/l, and that sulforhodamine B showed

only slight degradation. Additional laboratory tests by Smart and Laidlaw (1977) found very different results of sodium chloride degradation of organic tracers. Using chloride concentrations of up to 17,800 mg/l, rhodamine WT and sulforhodamine B fluorescence declined 8% and 4%, respectively. No fluorescence degradation was measured in either fluorescein or pyranine. Within the Barton Springs Segment, chloride concentrations generally ranged from about 5 to 20 mg/l in 20 wells and springs sampled in the freshwater portion over two sampling events (Hauwert and Vickers, 1994). Chloride concentrations from one Saline-Water Zone sample location ranged from 273 mg/l to 388 mg/l over two sampling events. Old Mill Springs shows elevated levels of chloride attributed to mixing of the fresh water and Saline-Water Zones. Some minor reduction in fluorescence due to chloride is possible in tracer concentrations measured at Old Mill Springs. Trace 9d into a Saline-Water Zone well within 3 km of Barton Springs was never recovered.

Temperature

Temperature variations at the time of analysis can be significant for sulforhodamine B and rhodamine WT, but less significant for fluorescein and pyranine (Smart and Laidlaw, 1977). For the Barton Springs Segment tracing study, all analytical results were corrected for temperature by OUL.

Photodecay

Exposure to light causes fluorescent tracers to absorb light, increasing molecular vibration, and raising the energy state (Smart and Laidlaw, 1977). The higher energy state leads to greater chemical reactivity and greater decomposition through oxidation. Fluorescein, eosine, and pyranine show strong photodecay, causing nearly complete loss of a 1,000 ppb tracer concentration within 3 hours (Aley, 2002). A similar test of rhodamine WT revealed only a 17% reduction in a 1,000 ppb sample after 5 hours, but a 68% reduction in the concentration of a 100 ppb sample, and resulted in an emission wavelength shift that resembled eosine. Sulforhodamine B samples of 1,000 and 100 ppb concentration showed losses of 5% and 40%, respectively, over 5 hours of exposure.

Photodecay is not a major source for tracer degradation in the traces where the entire trace occurs underground. However, photodecay could represent a major factor for tracer degradation in traces A, A', B, E, G, and N, 9b, 10c where a portion of the tracer may have been exposed at the surface for several hours, or was only detected in a river downstream of the spring discharge point.

Detection Limits

As indicated in Table 2.1, the detection limits vary for the tracers used. The detection limit for rhodamine WT is an order of magnitude higher than that for fluorescein. Some mass of a tracer arrives at the discharge spring below the detection limit. Table AI.1 shows that the mass of tracer that can be expected to discharge at the detection limit under average flow over a 24-hour period at Barton and Cold Springs is relatively small.

In general, the tracers used in this study have been rated in order of decreasing recovery as follows: fluorescein, pyranine, eosine, rhodamine WT, and sulforhodamine B (Behrens, 1986; Aley, 2002). Pyranine, however, shows the poorest ability to adsorb on charcoal receptors and then release the tracer to an elutant for analysis. Based on about 1,000 traces reported in the literature, Aley (1997 and 2000a) found that recoveries typically ranged from 20% to 50%.

Table AI.1 Calculated tracer recoveries at their detection limits

Tracer	Total Tracer Mass Discharging over 24 hours			
	Barton Springs flow 1.4 m3/s or 53 cfs		Cold Springs Flow 0.4 m3/s or 14 cfs	
	(lbs/day)	(kg/day)	(lbs/day)	(kg/day)
Fluorescein	0.00014	0.00006	0.00004	0.00002
Rhodamine WT	0.00200	0.00091	0.00053	0.00024
Eosine	0.00143	0.00065	0.00038	0.00017
Sulforhodamine B	0.00572	0.00260	0.00151	0.00069

GLOSSARY

Aperture: smallest diameter section at the entrance of conduit or cave draining a sinkhole or planar opening between fracture or fissure sides.

Artesian area: portion of the Barton Springs Segment located east of the Edwards outcrop area and west of the Saline-Water Zone where overlying clays, limestones, and shales are present. The artesian area is generally but not necessarily under artesian groundwater conditions.

Artificial internal drainage basin: man-made permeable basins, such as quarries, where surface drainages are captured and do not flow beyond the depression.

Barton Springs Segment: a freshwater portion of the Balcones Fault Zone portion of the Edwards Aquifer between the Kyle and Driftwood area and the Colorado River that discharges from Barton Springs and to the south bank of the Colorado River. It includes the Manchaca, Sunset Valley, and Cold Springs groundwater basins and excludes the Saline-Water Zone and contributing area.

Bowl: volume of rock that has been dissolved or collapsed at the entrance of a recharge feature. It is a measure of the hydraulic connection of a recharge feature to the aquifer and the relative recharge significance of a feature. Where the bowl is roughly conical the bowl volume can be calculated as:

Bowl Volume = (average rim radius)^2*C

or more accurately

Bowl Volume = rim area * C/3

In some cases the bowl includes a vertical shaft resembling a cylinder in shape that originated as vadose shafts intercepted by surface erosion and not by surface dissolution. However where vertical shafts are attributed to surface dissolution, the following formula can be used:

Cylinder volume = 6.28 * (shaft diameter)^2 * C or 6.28 * (shaft diameter)^2 * Z

C: depth (in feet) from the extrapolated rim surface to the aperture in a sinkhole. Represents greatest depth of material removed by recent surface dissolution, but not ancient groundwater dissolution.

Catchment Area: land surface area draining to a recharge feature. Typically delineated through a combination of field measurements and observations, areas defined in the field using a Trimble XRS or similar quality GPS, and two or ten foot contour interval surface maps. Flow observations associated with recharge events and debris lines can be used to help delineate catchment areas. Catchments for creek bottom recharge features are

typically delineated by DEM elevation models in GIS or created as shapefiles from contour maps.

Collapse Sinkhole: sinkhole entrance primarily formed by collapse of a cave roof, evidenced by an underhanging entrance. These karst features generally do not divert much surface recharge, but serve as important habitat for karst species and are well-connected hydraulically to the water table. Examples of collapse sinkholes in the Barton Springs Segment are Goat and Get Down Caves (Appendix E).

Confining units: rock units overlying the Edwards Group including, in descending stratigraphic order, rocks of the Taylor Group, Austin Group, Eagle Ford Group, Buda Formation, and Del Rio Formation. The use of the term "confining units" based on mapping of surface exposures is not intended to imply that surface connections with the Edwards Aquifer necessarily are absent or that artesian conditions are present.

Contributing area: areas of the Onion Creek, Bear, Slaughter, Williamson, and Barton Creek watersheds underlain by continuous exposure of the Glen Rose Formation.

Contributing Zone: a TCEQ and City of Austin regulatory area. In regards to the Barton Springs Segment, TCEQ defines a Contributing Zone (30 TAC, § 213.22(3)) as:

> "The area or watershed where runoff from precipitation flows downgradient to the recharge zone of the Edwards Aquifer. The Contributing Zone is located upstream (upgradient) and generally north and northwest of the Recharge Zone for the following counties:
>
> (C) all areas within Hays and Travis Counties, except the area within the watersheds draining to the Colorado River above a point 1.3 miles upstream from Tom Miller Dam, Lake Austin at the confluence of Barrow Brook Cove, Segment 1403 of the Colorado River Basin."

Contributing Zone Within the Transition Zone: TCEQ regulatory area defined as:

> "The area or watershed where runoff from precipitation flows downgradient to the Recharge Zone of the Edwards Aquifer. The Contributing Zone Within the Transition Zone is located downstream (downgradient) and generally south and southeast of the Recharge Zone and includes specifically those areas where stratigraphic units not included in the Edwards Aquifer crop out at topographically higher elevations and drain to stream courses where stratigraphic units of the Edwards Aquifer crop out and are mapped as Recharge Zone" (30 TAC, § 213.22(3)).

Edwards Aquifer: the rocks consisting of the Georgetown Formation and Edwards Group south of the Colorado River or Edwards Formation and Georgetown Formation north of the Colorado River that is west or north of the Saline-Water Zone.

Edwards outcrop area: portion of the Barton Springs Segment where the Edwards Group or Georgetown Formation outcrops at the surface or below unconsolidated alluvial deposits or soils. Also included are areas of overlying or underlying rocks that are entirely contained by outcrop areas of Edwards Group or Georgetown Formation. This area was previously known as the "Hardscrabble Country" (Taylor and Schoch, 1921) and was mapped and revised by Guyton and Associates (1958), Slagle et al. (1986), and Small et al. (1995).

Fault: a shear fracture where one side of the fracture plane moved relative to the other (at least 1 m).

Fissure: planar fracture aperture enlarged by removal of materials by processes such as solution and erosion, and faults apertures with poorly matching sides.

Flow Conditions: a relative measure of recharge and groundwater storage conditions of the Barton Springs Segment based on springflow rates of Barton Springs. In this study, flow conditions are based on the combined flows of Main Barton, Eliza, and Old Mill spring outlets of Barton Springs. Low flow is considered present when these Barton Springs outlets flow less than 1.1 m^3/s (40 ft^3/s); average flow is between 1.1 m^3/s (40 ft^3/s) and 2 m^3/s (70 ft^3/s), and high flow is considered to be above 2 m^3/s (70 ft^3/s.)

Fractures: joints or faults formed nearly instantaneously from stress failure, and are not significantly modified by solution. Unless specified, fractures generally refer to extensional fractures formed by maximum stress parallel to the fracture plane and least stress (tension) perpendicular to the fracture plane. Fracture can be horizontal, vertical, or of any orientation.

Fracture Aperture: discharge through a fracture or fissure can be described by the cubic law as:

Cubic Law $Q = p_w g b^3 i / 12\mu$ $K = p_w g b^2 / 12\mu$

where:

Q – discharge (L^3/t)
p_w – fluid density (M/L^3)
g – gravitational acceleration (L/t^2)
b – aperture (L)
i – hydraulic gradient
μ - dynamic viscosity ($M/ L^2/t$)
K - hydraulic conductivity

HQ Flat: Headquarters Flat sinkhole, named and identified by the Texas Speleological Survey, is located on the J17 WQPL.

Internal drainage basins: natural catchments where at least 90% of the runoff generated area does not discharge from the basin on the surface under natural conditions.

Intervening areas: Edwards outcrop areas of the Barton Springs Segment that lie outside the floodplain of the major creeks and include tributaries to the major creeks.

Karst feature: natural openings and macropores resulting from solution of soluble rocks and associated collapse. Includes caves, sinkholes, sinking streams, swallets, solution cavities, and springs.

Major creeks: the main channels of Onion, Bear, Little Bear, Slaughter, Williamson, and Barton Creeks.

Rim: edge of local dissolution associated with a recharge feature, usually marked aerially by a sharp break in slope around the aperture. Measured by X and Y diameter (in feet) or as an area delineated by GPS unit.

Preferential flow: rapid, nonuniform and turbulent transport of solutes and water through conduits and other preferential pathways through the soil and rock (Stagnitti, 1994; Hauwert et al, 2004).

Solution Sinkhole: sinkhole formed primarily by dissolution, as evidenced by a prominent concave bowl.

Ponded internal drainage basins: internal drainage basin with a drain or aperture that is obstructed by sediment and other debris to the extent drainage is significantly inhibited.

Recharge Zone: regulatory area defined by TCEQ or City of Austin and Travis Country that generally includes the Edwards outcrop area.

TCEQ Chapter 313 defines the Recharge Zone as:

> "generally, that area where the stratigraphic units constituting the Edwards Aquifer crop out, including the outcrops of other geologic formations in proximity to the Edwards Aquifer, where caves, sinkholes, faults, fractures, or other permeable features would create a potential for recharge of surface waters into the Edwards Aquifer. The recharge zone is identified as that area designated as such on official maps located in the appropriate regional office and groundwater conservation districts" (30 TAC, § 213.3(25).

The TCEQ Chapter 213.3 (Definitions) defines the Edwards Aquifer as:

> "that portion of an arcuate belt of porous, waterbearing, predominantly carbonate rocks known as the Edwards (Balcones Fault Zone) Aquifer trending from west to east to northeast in Kinney, Uvalde, Medina, Bexar, Comal, Hays, Travis, and Williamson Counties; and composed of the Salmon Peak Limestone, McKnight

Formation, West Nueces Formation, Devil's River Limestone, Person Formation, Kainer Formation, Edwards Group, and Georgetown Formation. The permeable aquifer units generally overlie the less-permeable Glen Rose Formation to the south, overlie the less permeable Comanche Peak and Walnut Formations north of the Colorado River, and underlie the less-permeable Del Rio Clay regionally" (30 TAC, § 213.3(25).

The TCEQ Recharge Zone is mapped in:
http://www.tceq.state.tx.us/gis/metadata/edw_utm27_met.html

TCEQ: Texas Commission on Environmental Quality. The state environmental protection agency formerly known as the Texas Water Commission and Texas Natural Resources Conservation Commission.

Transition zone: regulatory area defined by TCEQ in Chapter 313 as:

"that area where geologic formations crop out in proximity to and south and southeast of the recharge zone and where faults, fractures, and other geologic features present a possible avenue for recharge of surface water to the Edwards Aquifer, including portions of the Del Rio Clay, Buda Limestone, Eagle Ford Group, Austin Chalk, Pecan Gap Chalk, and Anacacho Limestone. The transition zone is identified as that area designated as such on official maps located in the appropriate regional office and groundwater conservation districts" (30 TAC, § 213.3(34).

TSS: Texas Speleological Survey. A volunteer organization that investigates, maps, and stores data on Texas caves.

Underlying units: rock units underlying the Barton Springs Segment including the Trinity Group.

WQPL: Water-Quality Protection Lands, acquired by the City of Austin for purposes of water-quality protection for the Barton Springs Segment and authorized by a 1999 Proposition 2 bond election.

Z: depth or extent of straight-line conduit or cave that extends downward vertically or horizontally from the entrance aperture.

REFERENCES

Abbott, P.L., 1973, The Edwards Limestone in the Balcones Fault Zone, south-central Texas [Ph.D. thesis]: Austin, University of Texas, 123 p.

Abbott, P.L., 1977, Effect of Balcones Faults on groundwater movement, south central Texas: The Texas Journal of Science, v. XXIX, nos. 1 and 2, Sept. 1977.

Abbott, P.L., 1984, Geologic History of the Edwards Limestone: Influences on regional aquifer development: *in* Woodruff C.M. and Slade, R.M. ed., Hydrogeology of the Edwards Aquifer-Barton Springs Segment, Travis and Hays Counties, Texas, Austin Geological Soc. Guidebook 6, p. 47-60.

Abelin, H., Neretnieks, I., Tunbrant, S., and Moreno, L., 1985, Final report on migration in a single fracture– experimental results and evaluation, Stripa Project Report 85-03, OECD/NEA, SKB-KBS: Stockholm, 162 p.

Agneni, A., 1992, Bias in modal parameters due to aliasing in the time domain, Meccanica, v. 26, no. 4, p. 221-228

Adkins, W.S., 1932, The Mesozoic Systems in Texas, *in* Sellards, E.H., Adkins, W.S., and Plummer, F.B., eds., The Geology of Texas, v. 1, Stratigraphy: Austin, University of Texas, Bulletin 3232, p. 239-517.

Alexander, K.B., 1990, Correlation of structural lineaments and fracture traces to water-well yields in the Edwards Aquifer, Central Texas [MS Thesis]: Austin, University of Texas, 113 p.

Aley, T. J., Williams, J.H., and Massello, J.W., 1972, Groundwater contamination and sinkhole collapse induced by leaky impoundments in soluble rock terrain: Missouri Geological Survey and Water Resources Engineering Geology Series no. 5, 32 p.

Aley, T. J., 1972, Groundwater contamination from sinkhole dumps: Caves and Karst, v. 14, no. 3, p. 17-23.

Aley, T.J., 1975, A predictive hydrologic model for evaluating the effects of land use and management on the quantity and quality of water from Ozark Springs: Ozark Underground Laboratory, Springfield, MO.

Aley, Thomas J., 1997, Groundwater tracing in the epikarst: Proceedings of the 6th Multidisciplinary Conference on Sinkholes and the Engineering and Environmental Impacts of Karst, A.A. Balkema, p. 207-211.

Aley, T.J. and Field, M.S., 1993, Wellhead protection tracer study, Walkersville, Maryland: Ozark Underground Laboratory contract report for the Burgess and Commissioners of Walkersville, Maryland, 98 p. plus appendices and maps.

Aley, T.J., 2000a, Procedures and criteria for analysis of fluorescein, eosine, and rhodamine wt dyes in water or charcoal samples: Ozark Underground Laboratory, Protem, Missouri, 10 p.

Aley, T.J., 2000b, Sensitive environmental systems: karst systems: *in* Lehr, J. H., ed., Standard Handbook of Environmental Science, Health, and Technology: McGraw-Hill, Chapter 19.1, p. 19.1-19.10.

Aley, T.J., 2002, The Ozark Underground Laboratory's groundwater tracing handbook: Ozark Underground Laboratory, Protem, Missouri, 35 p.

Aley, T.J., 2007, personal communication regarding dye properties and response to sewage spill near Walkersville, Maryland: Ozark Underground Lab, Protem, Mo.

Alley, W., 1984, The Palmer Drought Severity Index: limitations and assumptions. Journal of Climate and Applied Meteorology, v. 23, p. 1100– 1109.

ASTM, 1995, Standard guide for design of ground-water monitoring systems in karst and fractured-rock aquifers: American Society of Testing and Materials, D5717-95, 17 p.

Amorocho, J., 1982, Stochastic modeling of rainfall in time and space: from statistical analysis of rainfall, in Singh, V. P., ed., Proceedings, International Symposium on Rainfall Runoff Modeling, Mississippi, 1981, Water Resources Publications, Fort Collins, Colorado, pp. 3-20.

Andrews, F.; Schertz, T., Slade, R., Jr., and Rawson, J., 1984, Effects of storm-water runoff on water quality of the Edwards Aquifer near Austin, Texas: USGS WRI 84-4124, 50 p.

Arnow, T.,1963, Groundwater geology of Bexar County, Texas, USGS WSP 1588, 36 p.

Atkinson, T. C., Smith, D.I., Lavis, J.J., and Whitaker, R.J., 1973. Experiments in tracing underground waters in limestone: Journal of Hydrology, v. 19, p. 323-349.

Atkinson, T.C., 1977, Diffuse flow and conduit flow in limestone terrain in the Mendip Hills, Somerset, U.K.: Journal of Hydrology, v. 15, p. 93-110.

Aulenbach, D.B., Bull, J.H., and Middlesworth, B.C., 1978, Use of tracers to confirm ground-water flow: Groundwater, v. 16, p. 149.

Baker, E.T., Jr., Slade, R.M., Jr., Dorsey, M.E., Ruiz, L.M., and Duffin, G.L., 1986, Geohydrology of the Edwards Aquifer in the Austin area, Texas: Texas Department of Water Resources Report 293, 215 p.

BCCP (Balcones Canyonland Conservation Preserve) Karst Subcommittee, 2007, Problems associated with public release of cave location data: 2nd Draft Version of Report prepared by BCCP Karst Subcommittee for the BCCP Scientific Advisory Committee. Nico Hauwert, chair and primary author.

Barnes, V.E., 1944, Gypsum in the Edwards Limestone of Central Texas, Austin: University of Texas Publication no. 4301, p. 35-46.

Barrett, M.E. and Charbeneau, R.J., 1996, A parsimonious model for simulation of flow and transport in a karst aquifer: The University of Texas at Austin Center for Research Technical Report 269, 149 p.

Barron, E.J., Thompson, S.L., Schneider, S.H., 1981, An ice-free Cretaceous? Results from climate model simulations: Science, v. 212, p. 501-508.

Barron, E.J., Fawcett, P.J., Peterson, W.H., Pollard, D., Thompson, S. L., 1995, A "simulation" of Mid-Cretaceous climate: Paleoceanography, v. 10, p. 953-962.

Barton, G., and Risser, D., 1991, Approach for delineating the contributing areas of a well field in a carbonate-valley aquifer: *in* Proceedings from the 3rd Conference on Hydrogeology, Ecology, Monitoring, and Management of Groundwater in Karst Terranes, U.S EPA and NGWA, p. 59-75.

BS/EACD, 1994, Guidelines for the preparation of site-specific hydrogeologic studies for well sites on the Barton Springs Segment of the Edwards Aquifer: Barton Springs/Edwards Aquifer Conservation District, 5 p.

BS/EACD, 1997, Rules and Bylaws of the BS/EACD. 56 p.

Bear J., 1993, Modeling flow and contaminant transport in fractured rocks, *in* Bear, J., ed, Flow and Contaminant Transport in Fractured Rocks, Academic Press, Inc., San Diego, p. 1-37.

Behrens, H., 1986, Water tracing chemistry: a factor determining performance and analytics of tracers: Proceedings of the 5th International Symposium on Underground Water Tracing, Institute of Geology and Mineral Exploration, Athens, Greece, p. 121-133.

Bennett, P., 2000, personal communication regarding methods of measuring discharge of Cold Springs using tracers and developing rating curve with well water-levels: UT Geological Sciences, Austin, TX.

Bennett, P., 2009, personal communication regarding the use of chloride in calculationg recharge: UT Geological Sciences, Austin, TX.

Berner, R.A., Lasaga, A.C., Garrels, R.M., 1983, The carbonate-silicate geochemical cycle and its effect on atmospheric carbon dioxide over the past 100 million years: American Journal of Science, v. 283, p. 641-683.

Beven, K. and G.H. Hornberger, G. H., 1982. Assessing the effect of spatial pattern of precipitation in modeling streamflow hydrographs: Water Resources Bulletin, v. 18, no. 5, p. 823-829.

Bevin, K., and Germann, P., 1982, Macropores and water in soils: Water Resources Research., v. 18. p. 1311-1325.

Billings, M.P., 1947, Structural Geology: New York Prentice-Hall, 473 p.

Black C.A., 1965, Methods of Soil Analysis: Part I Physical and Mineralogical Properties: Madison, Wisconsin, American Society of Agronomy, 1188 p.

Bonacci, O., 1995, Ground water behaviour in karst: example of the Ombla Spring (Croatia): Journal of Hydrology, v. 165, p. 113-134.

Bradley, M. D., 1983, The scientist and engineer in court: Washington DC, American Geophysical Union Water Resource Monograph, v. 8, 111 p.

Brown, M. C. and Derek C. Ford, 1971, Qualitative tracer methods for investigation of karst hydrology systems, with reference to the Maligne Basin area: Transactions of the Cave Research Group of Great Britain v. 13, no. 1, p. 37-51.

Brune, G., 1981, Springs of Texas: Ft. Worth Texas, Branch-Smith, Inc., 566 p.

Brune, G., and Duffin, G.L., 1983, Occurrence, availability, and quality of ground water in Travis County, Texas: Texas Department of Water Resources Report 276, 219 p.

Burdon, D.J. and Papakis, N.,1963, Handbook of karst hydrogeology with special reference to the carbonate aquifers of the Mediterranean Region: Athens, Greece, United Nations Special Fund Karst Groundwater Investigations, Institute for Geology and Subsurface Research, 276 p.

Burns and McDonnell, 1922, Report on water supply development and improvements for Austin, Texas: Unpublished consulting report, Kansas, Missouri.

Bryan, F., 1936, Evidence of recent movements along faults of the Balcones system in central Texas: Am. Assoc. of Petroleum Geologists Bulletin, v. 20, p. 1357-1371.

Calvo-Cases, A., Boix-Fayos, C., Imeson A.C., 2003, Runoff generation, sediment movement and soil water behavior on calcareous (limestone) slopes of some Mediterranean environments in southeast Spain: Geomorphology, v. 50, p. 269–291.

Caran, S.C., Housh, T., and Cherepon, A.J., 2006, Volcanic features of the Austin area, Texas: Austin Geological Society Field Trip Guidebook 026, 124 p.

Cehrs, D. and Bianchi, W.C., 1996, Are consulting and good science compatible?: Ground Water v. 34, no. 6, p. 961.

Chatwin, P.C., 1971, On interpretation of some longitudinal dispersion experiments: Journal of Fluid Mechanics, v. 48, no. 4, p. 689-702.

Chernyshev, S.N., 1983, Fissures of rocks: Moscow, Nauka, 240 p.

City of Austin, 1991, Report of the Barton Springs Task Force to the Texas Water Commission: City of Austin, Texas.

City of Austin, 1992, Diagnostic study of water quality conditions in Town Lake, Austin, Texas: City of Austin Environmental and Conservation Services Department, COA-ERM/WRE 1992-01, 35 p.

City of Austin, 1997, The Barton Creek report: City of Austin, Drainage Utility Department, Environmental Resources Management Division. Water Quality Report Series COA-ERM/1997, 335 p.

City of Austin, 2006, Environmental Criteria Manual: Chapter 30-5, Environment, Subchapter A, Water Quality, 57 p.

City of Buda, 2005, Unified Development Code: Chapter 5, 12 p.

Clement, T. J. and Sharp, J.M., Jr., 1988, Hydrochemical facies in the bad-water zone of the Edwards Aquifer, Central Texas: *in* Proceedings, Ground Water Geochemistry Conference, Dublin, Ohio, National Groundwater Association (formerly National Water Well Association, p. 127-149.

Coleman, A.M. and Balchin, W.G.V., 1959, The origin and development of surface depressions in the Mendip Hills: Proc. Geol. Assoc., v. 70, p. 291-309.

Collier Consulting, Inc., 2001, Hydrogeology report in support of a pumpage increase application, Creedmoor-Maha Water Supply Corporation: Consulting report submitted to BS/EACD. 42 p. plus appendices.

Collins, E.W., 1993, Fracture zones between overlapping en echelon fault strands: outcrop analogs within the Balcones Fault Zone, Central Texas: Gulf Coast Association of Geological Societies Transactions, v. 43, p. 77–85.

Collins, E.W., 1995, Structural framework of the Edwards Aquifer, Balcones Fault Zone, Central Texas: Gulf Coast Association of Geological Societies Transactions, v. 45, p. 135–142.

Collingwood, D.M., and Rettger, R.E., 1926, The Lytton Springs oil field, Caldwell County, Texas: Bulletin of the American Association of Petroleum Geologists, v. 10, p. 953-975.

Cooke, J.M., Stern, L.A., Banner, J.L., Mack, L.E., Stafford, T.W., Jr., Toomey, R.S, III, 2003, Precise timing and rate of massive Late Quaternary soil denudation: Geology, p. 853-856.

Cooper, H.H. and Jacob, C.E., 1946, A generalized graphical method for evaluating formation constants and summarizing well field history: Am. Geophys. Union Trans., v. 27, p. 526-534.

Cowan, B.C., Banner, J.L, Hauwert, N.M., and Musgrove, M.L., 2007, Geochemical and physical tracing of rapid response in the vadose zone of the Edwards karst aquifer: Geological Society of America Annual Meeting Paper no. 69-3.

Crompton, J.L., 2007a, Chapter 1: The Impact of Parks and Open Spaces on Property Taxes: de Brun, Constance T.F. ed., The Economic Benefits of Land Conservation, The Trust for Public Land, p. 1-12.

Crompton, J.L., 2007b, Chapter 5: Competitiveness: Parks and Open Space as Factors Shaping a Location's Success in Attracting Companies, Labor Supplies, and Retirees: de Brun, Constance T.F. ed., The Economic Benefits of Land Conservation, The Trust for Public Land, p. 48-54.

Cronin, Stewart, 1932, Disconformity between Edwards and Georgetown in Hays and Comal Counties [M.S. thesis]: Austin, Texas, University of Texas, 32 p.

Damon, H.G., 1924, Vertical displacement of the main fault of the Balcones Fault Zone at a point west of the City of Austin, Texas [M.A. thesis]: University of Texas at Austin, Texas. 33 p.

Davis, S.N. and DeWiest, R.J., 1966, Hydrogeology: New York, John Wiley & Sons, 463 p.

Davis, S., Campbell, D., Bentley, H., Flynn, T., 1985, Ground water tracers: National Ground Water Association, 200 p.

Dawdy, D.R. and Bergmann, J.M., 1969, Effect of rainfall variability on streamflow simulation: Water Resources Res., v. 5, no. 5, p. 958-966.

Deaner, D.G., 1973, Effect of chlorine on fluorescent dye: Journal of Water Pollution Contr. Fed. v. 45, no. 3, p. 507-514.

DeCook, K. J., 1957, Geology of San Marcos Quadrangle, Hays County, Texas [M.A. thesis]: University of Texas at Austin, Texas, 90 p.

DeCook, K.J., 1963, Geology and ground-water resources of Hays County, Texas: USGS Water Supply Paper 1612, 72 p.

Dekker, L.W., and Ritsema, C.J., 1994, Variation in water content and wetting patterns in Dutch water repellent peaty clay and clayey peat soils: Catena v. 28, p. 89-105.

Dekker, L.W., Ritsema, C.J., and Oostindie, K., 2001, Wetting patterns and preferential flow in soils: in Bosch, D.D. et al., ed., Preferential Flow, Water Movement and Chemical Transport in the Environment, St. Joseph, Michigan, ASAE 701P0006, p. 85-88.

De La Garza, L., Slade, R.M., 1986, Relations between areas of high transmissivity and lineaments, the Edwards Aquifer, Barton Springs Segment, Travis and Hays Counties: *in* Abbott, P.L. and Woodruff, C.M., ed, The Balcones Escarpment, Geology, Hydrology, Ecology and Social Development in Central Texas, Geological Society of America Annual Meeting, San Antonio, Texas, p. 131-144.

Delin, G.N., Healy, R.W., Landon, M.K., and Bohlke, J.K., 2000, Effects of topography and soil properties on recharge and movement of water through the unsaturated zone at two sites in an agricultural field: Journal of the American Water Resources Association, v. 36, part 6, p. 1401-1416.

Delin, G.N. and Herkelrath, W.N., 2005, Use of soil moisture probes to estimate ground water recharge at an oil spill site: Journal of American Water Resources Association, v. 41 no. 6. p. 1259-1277.

De Silva, R.P., 2004, Spatial variability of groundwater recharge - I. Is it really variable?:Journal of Spatial Hydrology v. 4, no. 1.

Dingman, S.L., 1994, Physical Hydrology: New Jersey, Prentice Hall, 575 p.

Domenico, P.A. and Schwartz, F.W., 1998, Physical and Chemical Hydrogeology, Second edition: New York, John Wiley & Sons, 506 p.

Donath, F.A., 1962, Analysis of basin-range structure, South-Central Oregon: Geological Society of America Bulletin, v. 73, p. 1-16.

Donath, F.A., 1970, Some information squeezed out of rock: American Scientist, v. 58, no. 1, p. 54-72.

Dublyanskii, V.N., Pribluda, V.D., and Kodzhaspirov, A.A., 1984, Evaluation of the karst-water balance of the southwestern upland Crimea: in Castany, G., et al., ed., Hydrogeology of Karstic Terrains, Case Histories, International Association of Hydrogeologists, v. 1, p. 18-20.

Duffield, G.M., 2000, Aqtesolv for Windows: Manual produced by HydroSolv, Inc. 164 p.

Dugas, W.A., Hicks, R.A., and Wright, P., 1998, Effect of removal of Juniperus ashei on evapotranspiration and runoff in the Seco Creek watershed: Water Resources Research v. 34, no. 6, p. 1499-1506.

Dunham, R.J., 1962, Classification of carbonate rocks according to depositional texture, in Classification of Carbonate Rocks Symposium: American Association of Petroleum Geologists Memoir 1, p. 108-121.

Eckoff, Watson, and Preator Engineering (consulting firm), 1996; revised 1997, Drinking water source protection plan for Dewitt Spring, city of Logan, Utah; prepared for the city of Logan and submitted to the Utah Department of Environmental Quality, Division of Drinking Water, Salt Lake City, Utah.

Elliott, W.R., and Veni, G., 1994, The Caves and Karst of Texas: A guidebook for the 1994 Convention of the National Speleological Society with Emphasis on the Southwestern Edwards Plateau: National Speleological Society, 342 p.

Elliott, William R.,1997, The caves of the Balcones Canyonlands Conservation Plan, Travis County, Texas, Unpublished report to Travis County, 156 p.

Ellis, P.M., 1985, Diagenesis of the lower Cretaceous Edwards Group in the Balcones Fault Zone Area, South-Central Texas [PhD thesis]: University of Texas at Austin, 326 p.

Ernst, C., Gullick, R., Nixon, K., 2007, Chapter 3: Protecting the Source, Conserving Forests to Protect Water: de Brun, Constance T.F. ed., The Economic Benefits of Land Conservation, The Trust for Public Land, p. 24-27.

Ewers, R.O., 1982, Cavern development in the dimensions of length and breadth [PhD thesis]: Ontario, Canada, McMaster University, 398 p.

Fairley, J.P., Podgorney, R.K., and Wood, T.R., 2004, Unsaturated flow through a small fracture-matrix network: Part 2 Uncertainty in Modeling Flow Process: Vadose Zone Journal v. 3, p. 101-108.

Federal Register, 1988, A portion of the Austin-area Edwards Aquifer in parts of Hays and Travis counties, Texas, sole source aquifer final determination: FRL-3392-5, vol. 53, no. 109, p. 20897.

Federal Register, 1997, Endangered and Threatened Wildlife and Plants; Final Rule to List the Barton Springs Salamander as Endangered: 50 CFR Part 17, v. 62, no. 83, p. 23377-23392.

Ferguson, B., 1994, Stormwater Infiltration: Boca Raton, Florida, Lewis Publishers, p. 12.

Fetter, C.W., 1992, Contaminant hydrogeology: New York, McMillan Publishing Co., 458 p.

Feuerstein, D.L, and Selleck, R.E., 1963, Fluorescent tracers for dispersion measurements: Journal of Sanitary Engineering Division, American Society of Civil Engineers, v. 89, p. 1-21.

Field, M., 2002a,The QTRACER2 program for tracer-breakthrough curve analysis for tracer tests in karstic aquifers and other hydrologic systems: Washington, D.C., U.S. Environmental Protection Agency, Publication EPA/600/R-02/001, 179 p.

Field, M., 2002b, A lexicon of cave and karst terminology with special reference to environmental karst hydrology: Washington, D.C., U.S. Environmental Protection Agency, Publication EPA/600/R-02/003, 214 p.

Fieseler, R.G., 1998, Implementation of best management practices to reduce nonpoint source loadings to Onion Creek recharge features: Barton Springs/Edwards Aquifer Conservation District report.

Flawn, P.T., Goldstein, A., Jr., King, P.B., and Weaver, C.E., 1961, The Ouachita System: The University of Texas at Austin, Bureau of Economic Geology, Publication no. 6120, 401 p.

Flores, R., 1990, Test well drilling investigation to delineate the downdip limits of usable-quality groundwater in the Edwards Aquifer in the Austin Region, Texas: Texas Water Development Board Report no. 325, 70 p.

Flury, M., Fluhler, H., Jury, W.A. and Leuenberger, J., 1994, Susceptibility of soils to preferential flow of water: A field study: Water Resource Resources, v. 30, p. 1945–1954.

Ford, D., 1964, Origin of closed depressions in the central Mendip Hills, Somerset, England: 20th Intl. Geographers Congress Abstracts of Papers, London, p. 105-106.

Ford, D.C. and Ewers, R.O., 1978, The development of limestone cave systems in the dimensions of length and depth: Canadian Journal of Earth Science, v. 15, p. 1783-1798.

Ford, D.C. and Williams, P., 1992, Karst Geomorphology and Hydrology, Second Edition: Chapman and Hall Publishers, 600 p.

Ford, D.C., 1999, Perspectives in karst hydrogeology and cavern genesis: Karst Modeling, Karst Waters Institute Special Publication no. 5, p. 17-29.

Ford, R., 2000, Hydrogeologic study of proposition 2 watershed preserves Bear Creek area, Hays and Travis Counties, Texas: consulting report prepared for the COA Water & Wastewater Utility by HBC Engineering, Inc., 15 p. plus appendices.

Freeman, J., Madsen, R., Hart, K., 2008, Statistical Analysis of Drinking Water Treatment Plant Costs, Source Water Quality, and Land Cover Characteristics: The Trust for Public Land, 30 p.

Fu, L., Milliken, K.L., and Sharp Jr., J.M., 1993, Porosity and permeability variations in fractured and liesegang-banded Breathirr sandstones (middle Pennsylvanian), eastern Kentucky: diagenetic controls and implications for modeling dual-porosity systems: Journal of Hydrology, v. 154, p. 351-381.

Garcia-Fresca, B., 2004, Urban effects on groundwater recharge in Austin, Texas [M.S. thesis]: University of Texas at Austin, 173 p.

Garcia-Fresca, B., and Sharp, J.M. Jr., 2005, Hydrogeologic consideration of urban development: urban induced recharge: in Ehlen, J., et al., Humans as Geologic Agents, GSA Review in Engineering, v. XVI, p. 123-136.

Garner, B.D., 2005, Geochemical evolution of groundwater in the Barton Springs Segment of the Edwards Aquifer [MS thesis]: University of Texas at Austin, 317 p.

Garner, B.D. and Mahler, B., 2007, Relation of specific conductance in groundwater to intersection of flow paths by wells, and associated major ion and nitrate geochemistry, Barton Springs Segment of the Edwards Aquifer, Austin, Texas, 1978-2003: USGS Scientific Investigations Report 2007-5002, 39 p.

Gary, M.O. and Sharp J.M., 2006, Volcanic karstification of Sistema Zacatón, Mexico: *in* Harmon, R.S., and Wicks, C., eds., Perspectives on karst geomorphology, hydrology, and geochemistry-A tribute volume to Derek C. Ford and William B. White: Geological Society of America Special Paper 404, p. 79-89, doi 10.1130/2006.2404(08).

Garza, S., 1962, Recharge, discharge, and changes in ground-water storage in the Edwards and associated limestones, San Antonio area, Texas - a progress report on studies, 1955-59: Texas Board of Water Engineers Bulletin 6201, 51 p.

Gelhar, L.W., Welty, C., and Rehfeldt, K. R., 1992, A critical review of data on field-scale dispersion in aquifers: Water Resources Res. v. 28, no. 7, p. 1955-1974.

Gee, G. W., Zhang, Z. F., Tyler, S. W., Albright, W. H., and Singleton, M. J., 2005, Chloride Mass Balance Cautions in Predicting Increased Recharge Rates: Vadose Zone Journal, v. 4, no. 1, p. 72-78.

Ginsberg, M., and Palmer, A., 2002, Delineation of source-water protection areas in karst aquifers of the Ridge and Valley and Appalachian Plateaus physiographic provinces, rules of thumb for estimating the capture zones of springs and wells: EPA report 816-R-02-015, 41 p.

Gomez-Hernandez, J.J., 2006, Complexity: Groundwater, v. 44, no. 6, p.782-785.

Grego, C.R., Vieira S.R., Antonio, A.M., Della Rosa S.C., 2006, Geostatistical analysis for soil moisture content under the no tillage cropping system: Sci. Agric. (Piracicaba, Braz.), v. 63, no. 4, p. 341-350.

Green, R., 1984, Shady Hollow Sink Demise: The Texas Caver, v. 29. no. 6, p. 8.

Grimshaw, T.W., 1976, Environmental geology of urban and urbanizing areas, a case study from the San Marcos Area, Texas [Ph.D. thesis]: University of Texas at Austin, 244 p.

Gunn, J., 1983, Point recharge of limestone aquifers-A model from New Zealand karst: Journal of Hydrology, v. 61, p. 19-29.

Gunn, J., 2007, Contributory area definition for groundwater source protection and hazard mitigation in carbonate aquifers: *in* Parise, M. and Gunn, J., eds., Natural and Anthropogenic Hazards in Karst Areas: Recognition, Analysis, and Mitigation, London, Geological Society, Special Publication no. 279, p. 97-109.

Guyton W.F. and Associates, 1964, Report on Barton Springs and associated ground-water conditions with particular reference to possible effects of a proposed sewer line in Barton Creek area, Austin, Texas.

Halihan, T., Mace, R.E., and Sharp, J.M. Jr., 2000, Flow in the San Antonio segment of the Edwards Aquifer: matrix, fractures, or conduits: *in* Sasowsky, I.D. and Wicks, C.W. ed., Groundwater Flow and Contaminant Transport in Carbonate Aquifers, Rotterdam: Balkema, p. 129-146.

Ham, J.M. and Heilman, J.L., 2003, Experimental test of density and energy balance corrections on carbon dioxide flux as measured using open-path Eddy Covariance: Agronomy Journal, v. 95, p. 1393-1403.

Hamlin, M.J., 1983, The significance of rainfall in the study of hydrogeological processes at basin scale: Journal of Hydrology, v. 65, p. 73-94.

Hanson, John A., 1995, Composite measured section of the Edwards Group in the Barton Springs Segment: in Hauwert, N.M. and Hanson, J.A., ed., A Look at the Hydrostratigraphic Members of the Edwards Aquifer in Travis and Hays Counties, Texas, Austin Geological Society Guidebook.

Hantush, M., 1966a, Wells in homogeneous anisotropic aquifers: Water Resources Research, v. 2, no. 2, p. 273-279.

Hantush, M., 1966b, A method for analyzing a drawdown test in anisotropic aquifers: Water Resources Research, v. 2, no. 2, p. 281-285.

Harmel, R.D., Cooper, R.J., Slade, R.M., Haney, R.L., and Arnold. J.G., 2006, Cumulative uncertainty in measured streamflow and water quality data for small watersheds: Transactions of ASABE v. 49, no. 3, p. 689-701.

Harrison, A.D., 1996, Recharge mechanisms of swelling clays and shales, Central Texas [M.S. thesis]: Baylor Univ., Waco, 187 p.

Hauwert, N.M., 1991, The Bowling Green Fault Zone in Wood and Southern Lucas Counties, Ohio [M.S. thesis]: Ohio, University of Toledo, 96 p.

Hauwert, N.M. and Vickers, S., 1994, Barton Springs/Edwards Aquifer hydrogeology and groundwater quality: Report by the Barton Springs/Edwards Aquifer Conservation District for the Texas Water Development Board, 36 p. and figures. Accompanying addendum released by Nico M. Hauwert, BS/EACD, January 1996.

Hauwert, N.M., and Rauschuber, D.G., 1994, Antioch Cave: hydrogeology and proposed recharge enhancement: from Edwards Aquifer: The Barton Springs and San Marcos Springs Area, American Institute of Hydrologists 1994 Annual Conference Field Guide Book.

Hauwert, N.M., 1995, Localization of sediment and trace metals along a karst conduit flow route in the Barton Springs Segment of the Edwards Aquifer: Hauwert N.M. et al., ed, A Look at the Hydrostratigraphic Members of the Edwards Aquifer in Travis and Hays counties, Texas, Austin Geological Society, Austin, Texas, p. 39-51.

Hauwert, N.M., and Russell, W., 1996, Influence of geologic structure and stratigraphy on the development of Airman's Cave, southwest Austin, Texas: Geological Society of America 1996 Karst Hydrogeology Session.

Hauwert, N.M., 1997, Barton Springs Edwards Aquifer yield analysis (low flow conditions): Alternative Regional Water Supply Plan, Barton Springs/Edwards Aquifer Conservation District, Chapter III, p. 1-22.

Hauwert, N.M., Hanson, J., and Small, T., 1997, Geologic map of the Barton Springs Segment of the Edwards Aquifer: Map revision distributed by the Barton Springs/Edwards Aquifer Conservation District, Scale 1:28,000.

Hauwert, N.M. and Warton, M., 1997, Initial groundwater tracing study of Buttercup Creek area, Cedar Park, south Williamson County, Texas: Mike Warton & Associates, Cedar Park, Texas. 15 p + appendices.

Hauwert, N.M., Johns, D.A., and Aley, T.J., 1998, Preliminary Report on Groundwater Tracing Studies within the Barton Creek and Williamson Creek Watersheds, Barton Springs Edwards Aquifer, report by the Barton Springs/Edwards Aquifer Conservation District and City of Austin Watershed Protection Department, 57 p.

Hauwert, N.M., Hanson, J., and Small, T., 2003, Geologic Map of the Barton Springs Segment of the Edwards Aquifer. Map revision distributed by the Barton Springs/Edwards Aquifer Conservation District, Scale 1:28,000.

Hauwert, N.M., Johns, D.A., Sansom, J.W. Jr., and Aley, T.J., 2004a. Groundwater tracing study of the Barton Springs Segment of the Edwards Aquifer, southern Travis and northern Hays Counties, Texas: Barton Springs/Edwards Aquifer Conservation District and COA Watershed Protection Department, 112 p plus appendices.

Hauwert, N.M., Johns, D., Hunt, B., Beery, J., Smith, B, and Sharp, J.M., 2004b, Flow systems of the Edwards Aquifer Barton Springs Segment interpreted from tracing and associated field studies: from Edwards Water Resources In Central Texas, Retrospective And Prospective Symposium Proceedings, San Antonio, Hosted by the South Texas Geological Society and Austin Geological Society, 18 p.

Hauwert, N.M., Litvak, M.E., and Sharp, J.M., 2005, Characterization and water balance of internal drainage sinkholes: in Beck, B. ed., Geotechnical Special Publication No. 144, Sinkholes and the Engineering and Environmental Impacts of Karst, Proceedings of the Ninth Multidisciplinary Conference, p. 188-200.

Helfferich, F., 1962, Ion Exchange: McGraw-Hill, New York, 640 p.

Helmke, M.F., Simkins, W.W., and Horton, R., 2005, Fracture-controlled nitrate and atrazine transport in four Iowa till units: Journal of Environmental Quality, v. 34, p. 227-236.

Hendrickx, J. M. H. and Walker, G., 1997, Recharge from precipitation, Chapter 2: in Simmers, I. (ed.), Recharge of phreatic aquifers in (semi)-arid areas, Balkema, Rotterdam, The Netherlands.

Hess, J.W., Jr., and W.B. White, 1974, Hydrograph analysis of carbonate aquifers: Institute of Land and Water Resources, The Pennsylvania State University Res. Publication no. 83, 63 p.

Hill, D.E., and Parlange, J.Y., 1972, Wetting front instability in layered soils: Soil Science Society of America Proc., v. 36, p. 697-702.

Hill, R.T., 1892. On the occurrence of artesian and other underground waters in Texas, New Mexico, and Indian territory: together with the geology and geography of those regions: U.S. Geological Survey Report. 166 p.

Hill, R.T., and Vaughan, T.W., 1898, Geology of the Edwards Plateau and Rio Grande Plain adjacent to Austin and San Antonio, Texas, with reference to the occurrence of underground waters: USGS 18th Annual Report, Part 2, p. 193-321.

Hill, R.T., 1901, Geography and geology of the Black and Grand Prairies, Texas: USGS 21st Annual Report, part 7.

Hillel, D., 1998, Environmental Soil Physics: San Diego, Academic Press, 771 p.

Hinsby, K., McKay, L.D., Jorgensen, P., Lenczewski, M., Gerba, C.P., 1996, Fracture aperture measurements and migration of solutes, viruses, and immiscible creosote in a column of clay-rich till: Ground Water, v. 34, no. 6, p. 1065-1075.

Hofstratt, J.W., Steendijk, M., Vriezekolk, G., Schreurs, W., Broer, G.J.A.A., Wijnstok, N., 1991, Determination of rhodamine wt In surface water by solid-phase extraction and HPLC with fluorescence detection: Water Resources Research, v. 25, p. 883.

Hodgson, R.A., 1961, Classification of structures on joint surfaces: American Journal of Science., v. 259, p. 453-502.

Horton, R.E., 1940, An approach toward a physical interpretation of infiltration-capacity: Soil Sci. Soc. Am. Proc., v. 5, p. 399-417.

Hough, VanNess, 1960, Photogeologic techniques applied to mapping of rock joints: West Virginia Geol. and Econ. Surv. Report of Investigations, v. 19, 21 p.

Housh, T., 2006, Detailed stop descriptions: Stop 2 - St. Elmo Road railroad cut and Stop 3 - Williamson Creek, Austin: Caran, S.C., Housh, T., and Cherepon, A.J., Volcanic Features of the Austin Area, Texas, Austin Geological Society Field Trip Guidebook 026, p. 40-53.

Hovorka, S.D., Ruppel, S.C., Dutton, A.R., and Yeh, J., 1993, Edwards Aquifer Storage Assessment, Kinney County to Hays County, Texas: Bureau of Economic Geology report to Edwards Underground Water District, 101 p.

Hovorka, S.D., Mace, R.E., Collins, E.W., 1995, Regional distribution of permeability in the Edwards Aquifer: Bureau of Economic Geology report to Edwards Aquifer Authority (formerly Edwards Underground Water District), Austin, Texas, 128 p.

Hovorka, S.D., Mace, R.E., Collins, E.W., 1998, Permeability structure of the Edwards Aquifer, South Texas: Implications for aquifer management: Bureau of Economic Geology Report of Investigation no. 250, Austin, Texas, 55 p.

Huang, Y. and Wilcox, B.P., 2005, How karst features affect recharge? Implication for estimating recharge to the Edwards Aquifer: in Beck, B., ed., Geotechnical Special Publication No. 144, Sinkholes and the Engineering and Environmental Impacts of Karst, Proceedings of the Ninth Multidisciplinary Conference, , Sept. 24-28, 2005, San Antonio, Texas. p. 200-206.

Hubbert, M.K., 1940, The theory of ground-water motion: Journal of Geology, v. 48, p. 785-944.

Hunt, B.B., Smith, B.A., Campbell, S., Beery, J., Hauwert, N., Johns, D., 2004, Dye tracing recharge features under high-flow conditions, Onion Creek, Barton Springs Segment of the Edwards Aquifer, Hays County, Texas: BSEACD report, also presented as appendix G in Hauwert, et al., 2004a. 16 p.

Huntley, D., Nommensen, R., and Steffey, D., 1992, The use of specific capacity to assess transmissivity in fractured-rock aquifers: Ground Water. v. 30, no. 3. p. 396-402.

Huntoon, P.W., 1981, Fault controlled ground-water circulation under the Colorado River, Marble Canyon, Arizona: Ground Water, v. 19. no. 1, p. 20-27.

Huntoon, P.W., 1992. Concepts pertaining to hydrodynamic controls on karstic permeability in carbonate terranes: Handout from Practical Karst Hydrogeology with Emphasis on Ground Water Monitoring course, National Groundwater Association, Cave City, Kentucky, Nov. 30-Dec. 4, 1992.

Huntoon, P.W., 1995, Is It Appropriate to Apply Porous Media Groundwater Circulation Models to Karstic Aquifers? .: *in* El-Kadi, M., ed., Assessment of Models for

Groundwater Resource Analysis and Management, Boca Raton, Florida, Lewis Publishers, p. 339-358.

Hushey, W.L. and Crawford, P.B., 1967, Performance of Petroleum Reservoirs Containing Vertical Fractures in the Matrix: Society of Petroleum Engineers Journal, v. 19, no. 6, p. 221.

Jakucs, L., 1977, Morphogenetics of Karst Regions: Variants of Karst Evolution, New York, John Wiley & Sons, 284 p.

Jarvis, N.J., Leeds-Harrison P.B. and Dosser, J.M., 1987, The use of tension infiltrometers to assess routes and rates of infiltration in a clay soil: European Journal of Soil Science, v. 38, issue 4, p. 633.

Jennings, J.N., 1975, Doline morphology as a morphogenetic tool: New England examples: New Zealand Geog., v. 31, p. 6-28.

Jennings, J.N., 1985, Karst Geomorphology: Oxford, Basil Blackwell, 293 p.

Johns, D.A., 1994, Groundwater quality in the Bull Creek Basin, Austin, Texas, in Johns, D.A. and Woodruff, C.M., Jr., ed., Edwards Aquifer-water quality and land development in the Austin area, Texas, Austin Geological Society Guidebook no. 15, p. 18-36.

Johns, D.A. and Pope, S.R., 1998, Urban impacts on the chemistry of shallow groundwater: Barton Creek watershed, Austin, Texas: Gulf Coast Association of Geological Societies Transactions, v. XLVIII, p. 129-138.

Johns, D., 2006, Effects of low spring discharge on water-quality at Barton, Eliza, and Old Mill springs, Austin Texas: City of Austin short report, 15 p.

Jones, W.K., 1976, Dye tracer tests in karst areas: National Speleological Society Bulletin, v. 46, p. 3-9.

Jones, W.K., 1999, Pump tests of wells at the National Training Center near Shepardstown, West Virginia: Proceeding from Karst Modeling conference, Karst Waters Institute Special Publication no. 5, p. 259-261.

Jones, I.C., Banner, J.L., Humphrey, J.D., 2000, Estimating recharge in a tropical karst aquifer: Water Resources Res., v. 36, no. 5, p. 1289–1299.

Jones, I.C., 2002, Geochemical evolution of groundwater in the Pleistocene limestone aquifer of Barbados [PhD thesis]: University of Texas at Austin, 273 p.

Kabir, J., 1987, Underground drainage of urban runoff from natural depressions: Engineering Hydrology, Proceedings from 1st American Society of Civil Engineers, p. 359-363.

Karrenberg, H. and Weyer, K.U., 1970, Beiziehungen zwischen geologischen Verhaultnissen und Trockwetterabfluss in kleinen Einzugsgebieten des Rheinischen Schiefergebirges: Z. Deutsch. Geol. Ges., Sonderh. Hydrogeol. Hydrogeochem., p. 27-41.

Kastning, E.H., Jr., 1986, Cavern development in the New Braunfels area, central Texas, in Abbott, P.L., and Woodruff, C.M., Jr., ed., The Balcones Escarpment, Geology, Hydrology, Ecology and Social Development in Central Texas: Geological Society of America, p. 91-100.

Kastning, K.M. and Kastning, E.H., 2003, Site characterization of sinkholes based on resolution of mapping: in Geotechnical Special Publication no. 122, Sinkholes and the Engineering and Environmental Impacts of Karst, Proceedings of the Ninth Multidisciplinary Conference, p. 72-81.

Katzer, F., 1909, Karst und Karsthydrographie. Zur Kunde der Balkanhalbinsel: Kajon, Sarajevo, 94 p.

Kelly, B.P., and Pomes, M.L., 1998, Preferential flow and transport of nitrate and bromide in claypan soil: Groundwater, v. 36. no. 3, p. 484-494.

Kemmerly, P.R., 1976, Definitive doline characteristics in the Clarksville quadrangle, Tennessee: Bull. Geol. Soc. Amer., v. 87. p. 42-46.

Kehew, A.E., 2001, Applied Chemical Hydrogeology, Prentice Hill, Upper Saddle River, New Jersey, P. 275-277.

Kilpatrick, F.A., and Schneider, V.R, 1983, Use of flumes in measuring discharge: Techniques of Water-Resources Invest. of the USGS, Book 3, Chapter A14. 46 p.

Kilpatrick, F.A., and Cobb, E.D., 1985, Measurement of discharge using tracers: Techniques of Water-Resources Investigations of the USGS, Book 3, Chapter A16, p. 52.

Kimball, B.A., and Jackson, R.D, 1979, Modification of the aerial environment of crops: Soil Heat Flux, ASAE Monograph No. 2, American Society of Agricultural Engineers, p. 211–229.

Kiraly, L., 2002, Karstification and groundwater flow: *in* Gabrovsek, F. ed., Evolution of Karst: From Prekarst to Cessation, Postojna-Ljubljana, p. 155–190.

Klemt, W.B, Knowles, T.R., Elder, G.R., and Sieh, T.W., 1979, Ground-water resources and model application for the Edwards (Balcones Fault Zone) Aquifer in the San Antonio Region, Texas: Texas Dept. of Water Resources Report 239, 88 p.

Klimchouk, A., 2000a, The formation of epikarst and its role in vadose speleogenesis: *in* Klimchouk A., Ford D. C., Palmer A. N. and Dreybrodt W. eds., Speleogenesis: Evolution of karst aquifers, Huntsville, National Speleological Society, p. 91-99

Klimchouk, A. 2000b, Speleogenesis under deap-seated and confined settings, *in*: Klimchouk A., Ford D. C., Palmer A. N. and Dreybrodt W. eds., Speleogenesis: Evolution of karst aquifers, Huntsville, National Speleological Society, p. 244-260.

Klimchouk, A., 2004, Toward defining, delimiting and classifying epikarst: Its origin, process and variants of geomorphic evolution: *in* Jones, W.K., et al., ed., D.C., Karst Water Institute special publication, v. 9, p. 23-35.

Kolb, R.A., 1981, Geology of the Signal Hill Quadrangle, Hays and Travis counties, Texas [M.S. thesis]: University of Texas at Austin, 80 p.

Kresic, N., 1997, Quantitative Solutions in Hydrogeology and Groundwater Modeling: NY, Lewis Publishers, 460 p.

Krothe, N.C., and Bergeron, M.P., 1981, The relationship between fracture traces and joints in a Tertiary basin, southwest Montana: Groundwater, v. 19, no. 2, p. 136-143.

Kruseman, G.P., and deRidder, N.A., 1990, Analysis and evaluation of pumping test data: Wagening, the Netherlands, International Institute for Land Reclamation and Improvement publication, no. 47, 376 p.

Kuhn, T.S., The structure of scientific revolutions, 3rd ed.: Univ. of Chicago Press, Chicago and London, 212 p.

Kulander, B.R., Barton, C.C. and Dean, S. L., 1979, The application of fractography to core and outcrop fracture investigations: Report prepared for US DOE, 174 p.

Kung, K.J.S, Kladivko, E.J., Gish, T.J., Steenhuis, T.S., Bubenzer, G. and Helling, C.S., 2000, Quantifying preferential flow by breakthrough of sequentially applied tracers: silt loam soil: Soil Science Society America Journal, v. 64, p.1296-1304.

Kuniansky, E.L., Fahlquist, L., and Ardis A.F., 2001, Travel times along selected flow paths of the Edwards Aquifer, Central Texas: in Kuniansky, E.L., ed., 2001, U.S. Geological Survey Karst Interest Group Proceedings, Water-Resources Investigations Report 01-4011, p. 69-77

Lamarck. J.B., 1806, Mémoires sur les fossiles des environs de Paris (suite 6): Annales du Muséum d'Histoire Naturelle, v. 7, p. 53-430.

Land, L.F., and Dorsey, M.E., 1988, Reassessment of the Georgetown Limestone as a hydrologic unit of the Edwards Aquifer, Georgetown area, Texas: USGSWater-Resources Investigations Report no. 88-4190, 49 p.

Land, L.S., and Prezbindowski, D.R., 1985, Chemical constraints and origins of four groups of Gulf Coast reservoir fluids: discussion: American Association of Petroleum Geologists Bulletin, v. 69, p. 119-121.

Larkin, T.J. and Bomar, G.W., 1983, Climatic Atlas of Texas: Texas Department of Water Resources, Report LP-192, 151 p.

Lattman, L.H., 1958, Techniques of mapping geologic fracture traces and lineaments on aerial photographs: Photogrammetric Engineering, v. 24, p. 568-576.

Lattman, L.H. and Matzke, R.H., 1961. Geological significance of fracture traces: Photogrammetric Engineering, v. 27, no. 5, p. 635-638.

Lattman, L.H., and Nickelson, R.P., 1958, Photogeologic feature trace mapping in the Appalachian Plateau: American Assoc. of Petroleum Geologists Bulletin, v. 42, p. 2238-2245.

Lavalle, P., 1968, Karst morphology in south central Kentucky: Geographer Annual, v. 50, p. 94-108.

Lerner, S. and Poole W., 1999, The economic benefits of parks and open space: Trust for Public Land, 48 p.

Lexchin, J., Bero, L.A., Djulbegovic, B., and Clark, O., 2003, Pharmaceutical industry sponsorship and research outcome and quality, systematic review: British Medical Journal, no. 356, p. 1167-1170. http://repositories.cdlib.org/postprints/791.

Li, X.Y., Contreras, S., Solé-Benet, A., 2008, Unsaturated hydraulic conductivity in limestone dolines, Influence of vegetation and rock fragments: Geoderma, v. 145, p. 288–294.

Lindley, A., 2005, The hydrologic function of the soil and bedrock system at upland sinkholes in the Edwards Aquifer Recharge Zone of South-Central Texas: In Beck, B., ed., Geotechnical Special Publication No. 144, Sinkholes and the Engineering and Environmental Impacts of Karst, Proceedings of the Ninth Multidisciplinary Conference, p. 224-229.

Litvak, M.E., Miller, S., Wofsy, S.C., and Goulden, M., 2003, Effect of stand age on whole ecosystem CO2 exchange: Journal of Geophysical Research, v. 108, no.

D3, p. 6-1 – 6-11, 8225, doi:10.1029/2001JD000854, 2003. Special Section: Comparison of Carbon Exchange between Boreal Black Spruce Forests and the Atmosphere for a Wildfire Age Sequence (FIRE-EXB).

Lowe, D. J., 2000, Role of stratigraphic elements in speleogenesis: the speleinception concept: *in* Klimchouk A., Ford D. C., Palmer A. N. and Dreybrodt W. eds., Speleogenesis, Evolution of karst aquifers. Huntsville, National Speleological Society, p. 65-76.

Lundquist, J.J., 2000, Foraminiferal biostratigraphy and paleoceanographic analysis of he Eagle Ford, Austin, and Lower Taylor Groups (Middle Cenomanian through Lower Campanian) of Central Texas [PhD dissertation]: University of Texas, Austin, 545 p.

Lynch, F.L., Mahler, B.J., and Hauwert, N.M., 2004, Provenance of suspended sediment discharged from a karst aquifer determined by clay mineralogy: *in* Sasowsky, I.D., and Mylroie, J., ed., Studies of cave sediments: Physical and chemical records of paleoclimate, New York, New York, Kluwer Academic Plenum Publishers, p. 83-91.

Lynch, L., 2007, Chapter 2: Economic Benefits of Farmland Preservation: de Brun, Constance T.F. ed., The Economic Benefits of Land Conservation, The Trust for Public Land, p. 13-23.

Mace, R.E., 1997, Determination of transmissivity from specific capacity tests in a karst aquifer: Groundwater, vol. 35, no. 5 p. 738-742.

Mace R.E. and Hovorka S.D., 2000a, Estimating porosity and permeability in a karstic aquifer using core plugs, well tests, and outcrop measurements: *in* Sasowsky I.D. et al., ed., Groundwater flow and contaminant transport in carbonate aquifers, Balkema, Rotterdam, p. 93–111

Mace, R., Chowdhury, A.H., Anaya, R., and Way, S.C., 2000b Groundwater availability of the Trinity Aquifer, Hill Country Area, Texas: numerical simulations through 2050, TWDB report no. 353, 117 p.

Maclay R.W., and Rettman, P.L., 1972, Hydrologic investigation of the Edwards and Associated limestones in the San Antonio area: project report 1970-1971 EUWD, 24 p.

Maclay R.W. and Small T.A., 1984, Carbonate geology and hydrology of the Edwards Aquifer in the San Antonio area, Texas: U.S. Geological Survey Open-File Report 83-537, 72 p.

Mahler, B.J., 1997, Mobile sediments in a karst aquifer [Ph.D. Thesis]: University of Texas at Austin, 171 p.

Mahler, B.J. and Lynch, F.L., 1999, Muddy waters: temporal variation in sediment discharging from a karst spring: Journal of Hydrology, v. 214, p. 165-178.

Mahler, B.J., Garner, B.D., Musgrove, M.L., Guilfoyle A.L., and Rao, M.V., 2006, Recent (2003-05) water quality of Barton Springs, Austin, Texas, with emphasis on factors affecting variability: USGS SIR 2006-5299, 13 p.

Mahler, B. and Massei, N., 2007, Anthropogenic contaminants as tracers in an urbanizing karst aquifer: Journal of Contaminant Hydrology, v. 91, Issue 1-2, p. 81-106.

Mandel, S., 1966, A conceptual model of karstic erosion by groundwater: Bulletin of American Institute of Hydrologists: v. 11, no. 4, p. 61-73.

Martel, E.A., 1910, La the´orie de ‘‘Grundwasser’’ et les eaux souterraines du karst: Ge´ographie, v. 21, p. 126–130.

Marrett, R., 1996, Agregate properties of fracture populations: Journal of Structural Geology, v. 18, p. 169-178.

Marrett, R., Ortega, O.J., and Kelsey, C.M.,1999, Extent of power-law scaling for natural fractures in rock, Geology v. 27, p. 799-802.

Massei, N., Mahler, B.J., Bakalowicz, M,, Fournier, M., and Dupont, J.P., 2007, Quantitative interpretation of specific conductance frequency distributions in karst: Groundwater, v. 45, no. 3, 288–293.

Maxey, G.B., 1964, Hydrogeology: in Chow,V.T. ed., Handbook of Applied Hydrology, New York, McGraw-Hill Book Company, Section 4-I, Part I, p. 1-38.

Mayer, J.R. and Sharp, J.M., 1995, The role of fractures in regional groundwater flow: in Rossmanith, H.P. ed., Mechanics of Jointed and faulted Rock, Balkema, Rotterdam, p. 375-381.

McReynolds, J.C., 1958, Structural geology of southwest Austin area, Travis County, Texas [M.A. thesis]: University of Texas at Austin, Texas, 43p.

Meehan, R.L., 1984, The Atom and the Fault: Cambridge, Mass, MIT Press, 161 p.

Meinzer, O.E., 1923, The Occurrence of groundwater in the United States with a discussion of principles: USGS Water-Supply Paper 489, 321 p.

Mercer, J.W. and Faust, C.R., 1981, Ground-Water Modeling: National Water Well Association, 60 pp.

Mial, C.E. and Mial, A.D., 2002, The EXXON factor: The roles of corporate and academic science in the emergence and legitimation of a new global model of sequence stratigraphy: The Sociological Quarterly, v. 43 no. 2 p. 307.

Mikels, J.K., 2001, Hydrogeologic report in support of a pumpage volume amendment application: City of Buda, Hays County, Texas: GEOS Consulting report for the City of Buda, Texas, 9 p. plus figures and appendices.

Milanović, P.T.,1981, Karst Hydrogeology: Littleton, Colorado, Water Resources Publications, 434 p.

Milulla, C., Einsiedl, F., Schlumprecht, C., and Wohnlich, S., 1997, Sorption of uranine and eosine on an aquifer material containing high organic carbon: in Kranjc, A. ed., Tracer Hydrology-1997, Rotterdam, Netherlands:Balkema, 77-84.

Moench, A.F., 1984, Double-porosity models for fissured groundwater reservoir with fracture skin: Water Resources Research, v. 20, no. 7, p. 831-846.

Moller, P., Weise, S.M., Tesmer, M., Dulski, P., Pekdeger, A., Bayer, U., Magri, F., 2007, Salinization of groundwater in the North German Basin: results from conjoint investigation of major, trace element and multi-isotope distribution: International Journal of Earth Science, DOI 10.1007/s00531-007-0211-1, 16 p.

Monteith, J.L., and Unsworth, M.H., 1990, Principles of Environmental Physics, 2nd ed., Butterworth-Heinemann , Elsevier, 291 p.

Moon, C.G., 1942, A study of the igneous rocks of Travis County, Texas [M.S. thesis]: University of Texas at Austin, 61 p.

Moore, C.H., 1961, Stratigraphy of the Walnut Formation, south-central Texas: Journal of Science, v. 13, no. 1, p. 17-40.

Moore, C.H., 1964, Stratigraphy of the Fredericksburg Division, south-central Texas: Austin, University of Texas, Bureau of Economic Geology Report of Investigations no. 52, 37 p.

Moreno, L., Neretnieks, I., and Klockars, C.E., 1983, Evaluation of some tracer tests in the granitic rock at Finnsjon, KBS TR, p. 83-38.

Morris, R., 2007, The Blue Death: NY, Harper Collins, 310 p.

Mulkay, M., 1979a, Science and Sociology of Knowledge: London, Allen and Unwin, Ltd.

Mulkay, M., 1979b, Knowledge and utility, implications for the sociology of knowledge: Social Studies of Science, v. 9, no. 1, European Issue, p. 63-80.

Mull, D.S., Liebermann, T.D., Smoot, J.L., and Woosley, L.H., Jr., 1988, Application of dye-tracing techniques for determining solute-transport characteristics of ground water in karst terranes: United States Environmental Protection Agency Region 4, Atlanta, Georgia, publication EPA 904/6-88-001, 103 p.

Muller, D.A. and Price, R.D., 1979, Groundwater availability in Texas, estimates and projections through 2030: Texas Department of Water Resources, Rep. 238, 77 p.

Musgrove, M.L., Banner, J.L., Mack, L.E., Combs, D.M., James, E.W., Cheng, H., Edwards, R.L., 2001, Geochronology of late Pleistocene to Holocene speleothems from central Texas: implications for regional paleoclimate.: GSA Bulletin, v. 113, no. 12, p. 1532-1543.

National Atmospheric Deposition Program (NADP), 2009, Rainfall water-quality data and isopleths maps: http://nadp.sws.uiuc.edu.

National Research Council, 2001, Conceptual Models of Flow and Transport in the Fractured Vadose Zone: Washington DC, National Academy Press, 374 p.

Neretnieks, I., 1993, Solute transport in fractured rock-applications to radionuclide waste repositories: *in* Bear, J, et al., ed., Flow and Contaminant Transport in Fractured Rock, San Diego, Academic Press, Inc., p. 39-127.

Neuzill, C.E., and Tracy, J.V., 1981, Flow through fractures: Water Resources Research, v. 17 no. 1, p. 191-199.

Newton, J.G., 1984, Review of induced sinkhole development: *in* Beck, B. ed., Sinkholes: Their Geology, Engineering and Environmental Impact, Proceedings of the First Multidisciplinary Conference on Sinkholes, p. 3-9.

Nicks, A.D., 1982, Space-time quantification of rainfall inputs for hydrological transport models: Journal of Hydrology, v. 59, p. 249-260.

Nowak, D.J., Wang, J., Endreny, T., 2007, Chapter 4: Environmental and Economic Benefits of Preserving Forests within Urban Areas: Air and Water Quality: *in* de Brun, Constance T.F. ed., The Economic Benefits of Land Conservation, The Trust for Public Land, p. 28-47.

Ockerman, D., 2002, Simulation of runoff and recharge and estimation of constituent loads in runoff, Edwards Aquifer Recharge Zone (outcrop) and catchment area, Bexar County, Texas: USGS WRI 02-4241, 31 p.

Oetting, G.C., 1995, Evolution of fresh and saline groundwaters in the Edwards Aquifer, Central Texas, geochemical and isotopic constraints on processes of fluid-rock interaction and fluid mixing [M.A. thesis]: University of Texas at Austin, 203 p.

Oetting, G.C., Banner, J.L., and Sharp, J.M., 1996, Regional controls on the geochemical evolution of saline groundwaters in the Edwards Aquifer, central Texas: Journal of Hydrology, v. 181, p. 251-283.

Ogden, A.E., Quick, R.A., Rothermel, S.R., and Lunsford, D.L., 1986, Hydrogeological and hydrochemical investigation of the Edwards Aquifer in the San Marcos area, Hays County, Texas: San Marcos, TX, Edwards Aquifer Research and Data Center R1-86, 364 p.

Paillet, F.L., Hess, A.E., Cheng, C.H., Hardin, E., 1987, Characterization of fracture permeability with high-resolution vertical flow measurements during borehole pumping: Ground Water, v. 25, no. 1, p. 28-40.

Paillet, F.L., 1988, Characterization of fracture flow systems using geophysical log estimates of in-situ permeability and other hydraulic data: *in* Ram Arora, ed., Symposium Proceedings of International Conference on Fluid Flow in Fractured Rocks, Hydrogeology Program, Georgia State University, p. 312-327.

Palmer, A.N., 1975, Origin of maze caves: Nat'l Speolological Soc. Bull., v. 37, p. 56-76.

Palmer, A.N., 1986, Prediction of contaminant paths in karst aquifers: NGWA Proceedings of the Environmental Problems in Karst Terranes and their Solutions Conference, p. 32-53.

Palmer, A.N., 1991, Origin and morphology of limestone caves: Geological Society of America Bulletin, v. 103, p. 1-21.

Palmer, A.N., 1999, Anisotropy in carbonate aquifers: Proceeding from Karst Modeling conference, Karst Waters Institute Special Publication no. 5, p. 223-227.

Palmer, A.N., 2003**,** Speleogenesis in carbonate rocks. / Speleogenesis and Evolution of Karst Aquifers 1 (1), www.speleogenesis.info, 11 p., re-published from: Gabrovsek, F. (Ed.), 2002. Evolution of karst: from prekarst to cessation. Postojna-Ljubljana: Zalozba ZRC. p. 43-60.

Panno, S.V., Hackley, K.C., Hwang, H.H., Greenberg, S., Krapac, I.G., Landsberger, S., and O'Kelly, D.J., 2002, Source identification of sodium and chloride contamination in natural waters: Preliminary results: in Proceedings of the 12th Annual Conference of the Illinois Groundwater Consortium, 23 p. www.siu.edu/orda/igc/index.html.

Parise, M. and Gunn, J., 2007, Natural and anthropogenic hazards in karst areas: an introduction: *in* Parise, M. and Gunn, J., eds., Natural and Anthropogenic Hazards in Karst Areas, Recognition, Analysis, and Mitigation, London, Geological Society, Special Publication no. 279, p. 1-3.

Parten, S.M., 1991, Evaluation of wastewater collection and treatment alternatives for the City of Rollingwood [MS Thesis]: University of Texas at Austin, 257 p.

Petersen, J.F., 2005, San Antonio, an environmental crossroads on the Texas spring line: *in* Miller, C. ed., On the Border, Ft. Worth, Texas, Trinity University Press, p. 17-37.

Pimentel, D., Harvey, C., Resosudarmo, P., Sinclair, K., Kurz, D., McNair, M., Crist, S., Shipritz , L., Fitton, L., Saffouri, R., and Blair, R., 1995, Environmental and economic costs of soil erosion and conservation benefits: Science v. 267, p. 1117-1123.

Powers, J.G. and Shevenell, L., 2000, Transmissivity estimates from well hydrographs in karst and fractured aquifers: Groundwater v. 38, no. 3, p. 361-369.

Proctor, C.V. Jr., Brown, T.E., McGowen, J.H., Waechter, N.B., and Barnes, V.E., 1981, Austin Sheet: Francis Luther Whitney Memorial Edition: Austin, Texas, Bureau of Economic Geology, map sheet, originally printed 1974; revised 1981; reprinted 2002.

Quinlan, J.F., 1978, Types of karst, with emphasis on cover beds in their classification and development [Ph.D. thesis]: University of Texas at Austin, 325 p.

Quinlan, J.F. and J.A. Ray, 1981, Groundwater basins in the Mammoth Cave region, Kentucky: occasional publication no. 1, Friends of the Karst, Mammoth Cave. Map sheet.

Quinlan, J.F., 1989, Groundwater monitoring in karst terranes: recommended protocols & implicit assumptions: EPA/600/X-89 /050, 79 p.

Quinlan, J.F., 1990, Special problems of groundwater monitoring in karst terranes: Ground Water and Vadose Zone Monitoring: in Nielsen, D.M. and Johnson, A.I. Ed., American Society for Testing and Materials STP 1053, p. 275-304.

Quisenberry, V.L., and R.E. Phillips, 1976, Percolation of surface-applied water in the field: Soil Science Society of America Journal, v. 40, p. 484-489.

Razack, M. and Huntley, D., 1991, Assessing transmissivity from specific capacity in a large and heterogeneous alluvial aquifer: Groundwater, v. 29, no. 6, p. 856-861.

Reddell, J.R. and Russell, W.H.., 1961, The Caves of Travis County: Texas Speleological Survey, 31 p.

Reeves, R.D., 1976, Chemical and bacteriological quality of water at selected sites in the San Antonio area, Texas August 1968-January 1975: San Antonio, Texas, Texas Water Quality Board, Field Operations Division, Report IMS-45, in cooperation

with the USGS, Edwards Underground Water District and Texas Water Development Board, 122 p.

Renken, R.A., Cunningham, K.J., Zygnerski, M.R., Wacker, M.A., Shapiro, A.M., Harvey, R.W., Metge, D.W., Osborn, C.L., and Ryan, J.N., 2005, Assessing the vunerability of a municipal well field to contamination in a karst aquifer: Environmental and Engineering Geoscience, v. XI, no. 4, p. 319-331.

Rightmire, C.T., Pearson, F.J., Back, W. Rye, R.O, and Hanshaw, B.B, 1974, Distribution of sulphur isotopes of sulphates in groundwaters from the principal artesian aquifer of Florida and the Edwards Aquifer of Texas, United States of America: Isotope Techniques in Groundwater Hydrology 1974 Vol II. International Atomic Energy Agency, Vienna, p. 191-207.

Robins, N.S., 1993, Reconnaissance survey to determine the optimum groundwater potential of the Island of Jersey: *in* Banks S. and Banks, D. eds., Hydrogeology of Hard Rocks Published by NGU (Norway Geological Survey), N-7491 Trondheim, Norway, p. 327-337.

Robinson, N.I., Sharp, J.M., and Kreisel, I., 1998, Contaminant transport in sets of parallel finite fractures with fracture skins: Journal of Contaminant Hydrology, v. 31. p. 83-109.

Rochat, J., Alary, J., Molinari, J., and Charriere, R., 1975, Separations Physicochimiques De Colorants Xantheniques Utilises Comme Traceurs En Hydrologie: Journal of Hydrology, v. 26, p. 277-293.

Rodda, P. U., Garner, L. E., and Dawe, G. L., 1970, Austin West, Travis County, Texas: The University of Texas at Austin Bureau of Economic Geology, Geologic Quadrangle Map 38, 11 p.

Roemer, F., 1849a, Texas with particular reference to German immigration and the physical appearance of the country: translated from German by Oswald Mueller and published in 1935 by Standard Printing Company, San Antonio Texas, 308 p.

Roemer, F. 1849b. Texas Mit besonderer Rucksicht auf deutsche Auswanderung and die physischen Verhaltnisse des Landes nach eigener Beobachtung geschildert. Adoph Marcus, Bonn, 464 p., 1 map.

Roglic, J., 1972, Historical reviews of morphological concepts, from Karst: *in* Herak, M., and Stringfield, V.T. ed., Important Karst Regions of the Northern Hemisphere, New York, Elsevier Publishing Co., p.1-17.

Romm, E.S., 1966, Flow Characteristics of Fractured Rocks: Nedra, Moscow, 283 p.

Rose, P.R., 1972, Edwards Group, surface and subsurface, central Texas: The University of Texas Bureau of Economic Geology Report of Investigations 74, 198 p.

Rovey, C. W., 1994, assessing flow systems in carbonate aquifers using scale effects in hydraulic conductivity: Environmental Geology, v. 24, p. 244-253.

Russell, W.B., 1993, Buttercreek Creek Karst: Austin, TX, University Speleological Society, 76 p.

Russell, W.B., 1996, Environmental Evaluation of Blowing Sink Cave, A report prepared for the City of Austin Power and Light Department: Capital Caver no. 3, Texas Cave Management Association, p. 3-17.

Russell, W.B., and Jenkins, J., 2002, Preliminary report on the caves and karst features of the J17 Tract, Travis County, Texas: Austin, TX, Texas Cave Management Association, 23 p.

Russell, W.B., 2004, Travis County caves for Oak Hill Quadrangle: Texas Speleological Survey.

Russell, W.B., 2007, Stratigraphic distribution of cave volume in the Edwards Limestone, southern Travis County, Texas: Austin Geological Society Bull., v. 3, p 37-41.

Sabatini, D.A., and T.A. Austin, 1991, Characteristics of rhodamine WT and fluorescein as adsorbing groundwater tracers: Groundwater, v. 29, no. 3, p. 341-349.

Sabatini, D.A., 2000, Sorption and interparticle diffusion of fluorescent dyes with consolidated aquifer media: Groundwater, v. 38, no. 5, p. 651-656.

Sanders, M., 2007, Personal communication from plant surveys on WQPL sites: Biologist City of Austin Wildlands Conservation.

Sansom, J., 1997, Personal communication of igneous deposits observed on Queenswood Drive in South Austin.

Sansom, J.W. and Lundelius, E., 2005, Inner Space Cave: Discovery and geological and paleontological investigations: *in* Mace, R. ed., v.1, Austin Geological Society Bulletin, p. 53-69. http://www.austingeosoc.org/docs/bulletin-600com-post.pdf

Savin, S.M., 1977, The history of the Earth's surface temperature during the past 100 million years: Annual Review of Earth and Planetary sciences, v. 5, p. 319-355.

Sawicki, L., 1909, Ein Beitrag zum geographischen Zyklus im Karst: Geographische Zeitschrijt, v. 15, p. 185-204.

Sayre, A.N., and Bennett, R.R., 1942, Recharge, movement, and discharge in the Edwards Limestone reservoir, Texas: American Geophysical Union Transactions, v. 23, p. 19-27.

Scanlon, B., Langford, R., and Goldsmith, R.,1999, Relationship between geomorphic settings and unsaturated flow in an arid setting:Water Resources Research, v. 35, no. 4, p. 983-999.

Scanlon, B.R., 2000, Uncertainties in estimating water fluxes and residence times using environmental tracers in an arid unsaturated zone: Water Resources Research, v. 36, no. 2, p. 395-409.

Scanlon, B.R., Healy, R.W., and Cook, P.G., 2002, Choosing appropriate techniques for quantifying groundwater recharge: Hydrogeology Journal, v. 10, p. 18-39.

Scanlon, B.R., Mace, R.E., Barrett, M.E., and Smith, B., 2003, Can we simulate regional groundwater flow in a karst system using equivalent porous media models? Case study, Barton Springs Edwards Aquifer, USA: Journal of Hydrology, v. 276, p. 137-158

Schindel, G.M., Quinlan, J.F., Davies, G., Ray, J.A., 1986, Guidelines for Wellhead and Springhead Protection Area Delineation in Carbonate Rocks: EPA 904-B-97-003, 28 p. + appendices and plate.

Schindel, G.M., Quinlan, J.F., Davies, G., and Ray, J., 1996, Guidelines for wellhead and springhead protection area delineation in carbonate rocks: EPA 904-B-97-003, 28 p.

Schindel, G.M., 2006, personal communication on results of ongoing tracer studies: Edwards Aquifer Authority, San Antonio, Texas.

Sellards, E.H., Adkins, W.S., Plummer, F.B., 1933, The geology of Texas, v. 1, Stratigraphy: University of Texas Bulletin no. 3232, p. 239–518.

Sellards, E.H. and Baker, C.L., 1934, The structural and economic geology of Texas: University of Texas Bulletin, no. 3401, 814 p.

Senger, R.K., 1983, Hydrogeology of Barton Springs, Austin, Texas [M.S. Thesis]: University of Texas, Austin, Texas, 120 p.

Senger, R.K. and Kreitler, C.W., 1984, Hydrogeology of the Edwards Aquifer, Austin Area, Central Texas: The University of Texas at Austin Bureau of Economic Geology Report of Investigations no. 141, 35 p.

Shade, B.L., Alexander, E.C. and Alexander, S.C., 2001, The sandstone karst of Pine County, Minnesota: GSA Annual Meeting Paper No. 29-0.

Shade, B.L. and Krejca, J.K., 2007, Karst sensitivity map for Hays County: Zara Environmental LLC report to Loomis Associates, 25 p.

Shah, S.M.S, O'Connell, P.E. and Hosking, J.R.M., 1996, Modeling the effects of spatial variability in rainfall on catchment response: Journal of Hydrology, v. 175, p. 89-111.

Sharma, M.L. and Hughes, M.W., 1985, Groundwater recharge estimation using chloride, deuterium and oxygen-18 profiles in the deep coastal sands of Western Australia. Journal of Hydrology, v. 81, p. 93-109.

Sharp. J. M., 1990, Stratigraphic, Geomorphic, and Structural Controls of the Edwards Aquifer, Texas: in Simpson. E.S., and Sharp, J.M., ed., Selected Papers on Hydrogeology: Heise, Hannover, Germany, International Association of Hydrogeologists, v. 1, p. 67-82.

Sharp, J.M.,1993, Fractured aquifers/reservoirs, approaches, problems, and opportunities: *in* Banks, D., and Banks, S., ed., Hydrogeology of Hard Rocks, Memoires of the 24th Congress, International Association of Hydrogeologists: v. 24, p. 23-38.

Sharp, J.M., Robinson, N.I., Smyth-Boulton, R.C., and Milliken, K.L., 1995, Fracture skin effects in groundwater transport: *in* Rossmanith, H.P. ed., Mechanics of Jointed and Faulted Rock, A.A. Balkeme, Rotterdam, p. 449-454.

Sharp, J.M., and Banner, J.L., 1997, The Edwards Aquifer, a resource in conflict: GSA Today, v. 7, p. 1-9.

Sharp, J.M.,1999, A glossary of hydrogeological terms: Department of Geological Sciences, The University of Texas, Austin, Texas, 35p.

Sharp, J.M., Halihan, T., Uliana, M.M., Tsoflias, G.P., Landrum, M.T., and Marrett, R., 2000, Predicting fractured rock hydrogeological parameters from field and laboratory data: *in* Sililo, O., et al., ed., Groundwater: Past Achievements and Future Challenges Proceedings of the 30th Congress, International Association of Hydrogeologists, Cape Town, South Africa, p. 319-324.

Sharp, J.M., Hansen, C.N., Krothe J., 2001, Effects of urbanization on hydrogeological systems: The physical effects of utility trenches: *in* Seiler, K.P. and Woolrich, S., eds, New approaches characterizing groundwater flow, supplemental volume, Proceedings of 31st Congress International Association of Hydrogeologists, 5p.

Shaw, E.M., 1994, Hydrology in Practice (3nd ed.), London, UK., Taylor & Francis, 569 p.

Sheeba, T.M., Debajyoti, P, and Murray, K.E., 2005, Oxygen and hydrogen isotopic evolution of groundwater in the Edwards and Trinity Aquifer system, south-central Texas: GSA annual meeting, Salt Lake City, Paper 91-15.

Sheng, F., Wang, K., Zhang, R., Liu, H., 2009, Characterizing soil preferential flow using iodine–starch staining experiments and the active region model: Journal of Hydrology, v. 367, p. 115–124.

Sherer. P.M., 2006, The Benefits of Parks, Why America Needs More City Parks and Open Space: Trust for Public Land.

Shiau, B., Sabatini, D.A., and Harwell, J.H., 1992, Sorption of rhodamine WT as affected by molecular properties: *in* Hotzl H. and Werner, A. ed., Tracer Hydrology, Balkema, Rotterdam, p. 57-64.

Shiau, B.J., D.A. Sabatini, and Harwell, J.H., 1993, Influence of rhodamine WT properties on sorption and transport in subsurface media: Groundwater v. 31, no. 6, p. 913-920.

Shumard, B.F., 1860, Observations upon the Cretaceous strata of Texas: St. Louis, Transactions of the Academy of Science, v. 1, p. 582-590

Slade, R., Ruiz, L. and Slagle, D., 1985, Simulation of the flow system of Barton Springs and associated Edwards Aquifer in the Austin Area, Texas: U.S. Geological Survey Water-Resources Investigations Report 85-4299, 49 p.

Slade, R., Dorsey, M., and Stewart, S., 1986, Hydrology and water quality of the Edwards Aquifer associated with Barton Springs in the Austin Area, Texas: USGS Water-Resources Investigations Report no. 86-4036, 117 p.

Slade, R. M., 2004, General methods, information, and sources for collecting and analyzing water-resources data: CD-ROM. Copyright 2004 Raymond M. Slade.

Slade, R., 2005, personal communication on suggestions for groundwater tracing to establish recharge contribution of Barton Creek and development of long-term discharge record for Barton Springs: Retired former USGS hydrologist, Austin, TX.

Slade, R., 2008, personal communication on Barton Springs flow record: Retired former USGS hydrologist, Austin, TX.

Slagle, D., Ardis, A., and Slade, R., 1986, Recharge Zone of the Edwards Aquifer hydrologically associated with Barton Springs in the Austin area, Texas: USGS WRI report 86-4062, Single sheet map.

Small, T.A., Hanson, J.A., and Hauwert, N.M., 1996, Geologic framework and hydrogeologic characteristics of the Edwards Aquifer outcrop (Barton Springs Segment), northeastern Hays and southwestern Travis Counties, Texas: U.S. Geological Survey Water Resources Investigations 96-4306, 15 p. Prepared in cooperation with the BS/EACD and TWDB.

Smart, P.L. and Laidlaw, I.M.S., 1977, An evaluation of some fluorescent dyes for water testing: Water Resources Research, v. 13, no. 1, p.15-33.

Smart P.L. and Hobbs, S. L., 1986, Characterization of carbonate aquifers: a conceptual base: NGWA Proceedings of the Environmental Problems in Karst Terranes and their Solutions Conference, p. 1-14.

Smart, C.C., 1988, Artificial tracer techniques for the determination of the structure of conduit aquifers: Groundwater, v. 26, p. 445-453.

Smith, B.A., Morris, B., Hunt, B., Helmcamp, S., Johns, D., Hauwert, N., 2001, Water quality and flow loss study of the Barton Springs Segment of the Edwards Aquifer: EPA-funded 319h grant report by the Barton Springs/Edwards Aquifer Conservation District and City of Austin, submitted to the Texas Commission on Environmental Quality (formerly TNRCC) 85 p. + figures and appendix.

Smith, B.A. and Hunt, B.B., 2002, Petition for the adoption of rules: changes to the recharge zone map boundary within the Barton Springs Segment of the Edwards Aquifer, Travis and Hays Counties, Texas: Report by the BS/EACD to TCEQ, 9 p.

Smith, B.A. and Hunt, B.B., 2004, Evaluation of sustainable yield of the Barton Springs Segment of the Edwards Aquifer, Hays and Travis Counties, Central Texas: BSEACD Report, 55 p.

Smith, B.A., Hunt, B.B. and Schindel, G.M., 2005, Groundwater flow in the Edwards Aquifer, comparison of groundwater modeling and dye trace results: *in* Beck, B. ed., Geotechnical Special Publication No. 144, Sinkholes and the Engineering and Environmental Impacts of Karst, Proceedings of the Ninth Multidisciplinary Conference, p. 131-141.

Smith, B.A., Hunt, B.B., Beery, J., 2006, Summary of 2005 groundwater dye tracing, Barton Springs Segment of the Edwards Aquifer, Hays and Travis Counties, Central Texas: BS/EACD Report of Investigations 05012006, 31 p.

Smith, B.A., 2006, personal communication of modeled aquifer volumes: BS/EACD, Austin, TX.

Smith, B.A., Hunt, B.B., Holland, W.F., Schindel, G.M., 2007, Variability of hydraulic relationships between the Edwards and Trinity Aquifers of the Balcones Fault

Zone of Central Texas: NGWA 2007 Groundwater Summit Program & Abstract Book.

Smith, R.M., 1978, Geology of the Buda-Kyle area, Hays County, Texas [M.A. Thesis]: University of Texas at Austin, 153 p.

Smyth, R.C. and Sharp, J.M., 2006, The hydrology of tuffs, in Heiken, G., ed., Tuffs-their properties, uses, hydrology, and resources: Geological Society of America Special paper 408, p. 91-111, doi: 10.1130/2006.2408(4.1).

Spangler, L.A., 2002, Use of dye tracing to determine conduit flow paths within source-protection areas of a karst spring and wells in the Bear River Range, Northern Utah: in Kuniansky, E. Ed., USGS WRI-02-4172 Karst Interest Group Proceedings, p. 75-80.

Snyder, F., 1985, Geologic map of the Oakhill quadrangle: City of Austin 7.5 min. map.

State of Utah, Department of Environmental Quality, Division of Drinking Water, 1995, Drinking water source protection rule, R309-113, 17 p.

Stein, W.G., 1995, Hays County ground-water divide: *in* Hauwert, N.M. and Hanson, J.A., ed, A Look at the Hydrostratigraphic Members of the Edwards Aquifer in Travis and Hays Counties, Texas: Austin Geological Society Guidebook, p. 23-34.

St. Clair, A. E., 1979, Quality of water in the Edwards Aquifer, central Travis County, Texas [MA Thesis]: University of Texas at Austin, 97 p.

Stricklin, F.L., Smith, C.I., and Lozo, F. E., 1971, Stratigraphy of lower Cretaceous Trinity deposits of central Texas: Bureau of Economic Geology ROI 71, 63 p.

Strong, W.M., 1957, Structural geology of the Pilot Knob area, Travis County, Texas [M.S. thesis]: University of Texas at Austin, Texas, 71 p.

Sukhija, B.S., Reddy, D.V., Nagabhushanam, P., Hussain, S., Giri, V.Y., and Patil, D.J., 1996, Environmental and injected tracers methodology to estimate direct precipitation recharge to a confined aquifer: Journal of Hydrology, v. 177, p. 77-97.

Taucer, P.I., Munster, C.L., Wilcox, B.P., Shade, B., Dasgupta, S., Owens, M.K., and Mohanty, B., 2005, Large plot tracing of subsurface flow in the Edwards Aquifer epikarst: *in* Beck, B. ed., Geotechnical Special Publication no. 144, Sinkholes and the Engineering and Environmental Impacts of Karst, Proceedings of the Ninth Multidisciplinary Conference, p. 207-216.

Taylor, T.U. and Schoch, E.P., 1922, Supplemental report Austin city water survey: details of subterranean water reservoirs, chemical compositions of water, etc.: Report to the City of Austin, 21 p.

Teledyne ISCO, 1999, 3230 Flow Meter Installation and Operation Guide.

Texas Commission on Environmental Quality, 2005, Background and summary of the factual basis for the proposed rules, Chapter 213 - Edwards Aquifer, Rule Log No. 2003-029-213-WT, p. 3-5.

Texas Dept. of Transportation (TxDot, formerly Texas Dept. of Highways and Public Trans.), 1989, Final Environmental Impact Statement, Austin Outer Parkway State Highway 45, Segment 3, Travis and Hays Counties, Texas.

Texas Memorial Museum, 2008, website: http://www.utexas.edu/tmm/exhibits/mosasaur/index.html

Theis, C.V., 1935, The relation between the lowering of the piezometric surface and the rate and duration of a well using groundwater storage: Am. Geophysical Union Trans., v. 16, p. 519-524.

Thrailkill, J., 1968, Chemical and hydrologic factors in the excavation of limestone caves, Geological Society of America Bull. v. 79, p. 19-46.

Thrailkill, J., 1985, Flow in a limestone aquifer as determined from water tracing and water levels in wells: Journal of Hydrology, v. 78, p. 123-136.

Thornthwaite, C.W. and Mather, J.R., 1955, The Water Balance: Centerton, New Jersey, 1955 Publications in Climatology, v. VIII, no. 1.

Toomey, R.S., Blum, M.D., and Valastro, S., 1993, Global and Planetary Change, v. 7 n. 4, p. 299-320.

Toran, L., Herman, E.K., White, W.B., 2007, Comparison of flowpaths to a well and spring in a karst aquifer: Groundwater, v. 45, no. 3, p. 281–287.

Trainer, F.W., 1967, Measurement of the abundance of fracture traces on aerial photographs: USGS Professional Paper 575-C, p. 184-188.

Troester, J.W., White, E.L., White, W.B., 1984, A comparison of sinkhole depth frequency distributions in temperate and tropic karst regions: *in* Beck, B. ed., Sinkholes, Their Geology, Engineering and Environmental Impact Proceedings of the First Multidisciplinary Conference on Sinkholes and the Engineering and Environmental Impacts of Karst, p. 65-73.

Tsang, Y.W. and Witherspoon, P.A., 1981, Hydromechanical behavior of a deformable rock fracture subject to normal stress: Journal Geophysical Research, v. 86, no. B10, p. 9287-9298.

Twine, T.E., Kustas, W.P., Norman, J.M, Cook, D.R., Houser, P.R., Meyers, T.P., Prueger, J.H., Starks, P.J., Wesely, M.L., 2000, Correcting eddy-covariance flux underestimates over a grassland: Agricultural and Forest Meteorology, v. 103, p. 279-3000.

Underground Resource Management (URM), 1983. Hydrogeologic evaluation of the Shady Hollow Estates subdivision: Consulting report for Pence-Lewis Development, Austin, Texas, 38 p. plus appendices.

Vacher, H.L., Ayers, J.F., 1980, Hydrology of small oceanic islands: utility of an estimate of recharge inferred from the chloride concentration of the freshwater lens: Journal of Hydrology, v. 45, p. 21–37.

Vengosh, A. and Keren, R., 1996, Chemical modifications of groundwater contaminated by recharge of treated sewage effluent: Journal of Contaminant Hydrology, v. 23, p. 347-360.

Veni, G., 1992, Geologic controls on cave development and the distribution of cave fauna in the Austin, Texas, region: Report prepared for U.S. Fish and Wildlife, 77 p.

Veni, G., 1997, Geomorphology, hydrogeology, geochemistry, and evolution of the karstic lower Glen Rose Aquifer, south-central Texas: Pennsylvania State University, Texas Speleological Survey, Texas Speleological Monographs, no. 1, 409 p.

Veni, G., 1999, A geomorphological strategy for conducting environmental impact assessments in karst areas: Geomorphology, v. 31, p. 151-180.

Veni, G., 2000, Hydrogeologic assessment of Flint Ridge Cave, Travis County, Texas: Consulting report submitted to the COA, 55 p.

Vickers, J., 1996, Hydrogeologic report for Cimarron Park well no. 2: Unpublished report submitted by the WellSpec Company to the BS/EACD, 33 p.

Vig, N.J. and Kraft, M.E., 1984, Environmental policy in the 1980's, Reagan's New Agenda: Washington D.C., Congressional Quarterly Press, 377 p.

Vogt, E.Z. and Hyman, R., 1979, Water Witching U.S.A., 2nd Ed.: Chicago, University of Chicago Press, 260 p.

Walsh, J.B. and Brace, W.F., 1973, Mechanics of rock deformation: in Rock Mechanics Symposium, American Society of Mechanical Engineers, United Eng. Center, NY., p.1-24.

Washburn, J., 2003, Science's worst enemy: corporate funding: Discover op/ed October 1, 2003. http://discovermagazine.com/2007/oct/sciences-worst-enemy-private-funding.

Washburn, J., 2005, University, Inc., The Corporate Corruption of American Higher Education: New America Foundation, New America Books/Basic Books, 256 p.

Werchan, L.E., Lowther, A.C., and Ramsey, R.N., 1974, Soil survey of Travis County: U.S. Department of Agriculture, Soil Conservation Service and the Texas Agriculture Experiment Station, 123 p.

Wesson, R.L., Helly, E.J., Lajoie, K.R. and Wentworth, C.M., 1975, Faults and future earthquakes: in Studies for Seismic Zonation of the San Franciso Bay Region, USGS Professional Paper 941-A, p. A5-A30.

Weyer, K.U., 1971, Ermittlung der Grundwassermengen in den Festgesteinen der Mittelgebirge aus Messungen des Trockenwetterabflusses [Ph.D. Thesis]: Bonn, Germany, 142 p.

Weyer, K.U., 1972, Conceptual models for evaluation of the subterranean water cycle in Paleozoic highlands: International Geological Congress 24th Session, Section 11 Hydrogeology, Montreal, Canada, p. 107-117.

White, D.E., 1965, Saline waters in sedimentary rocks: *in* Young, P. and Galley J.E. ed., Fluids in the subsurface environment, Am. Assoc. Pet. Geol. Mem., v. 4, p. 342–365.

White, W.B., 1977, Conceptual models for carbonate aquifers: revisited: *in* Diliamarter, R.R., and Csallany, S.C., ed., Hydrologic Problems in Karst Regions, Western Kentucky University, Bowling Green, Kentucky, p. 176-187.

White, E.L. and White, W.B., 1979, Quantitative morphology of landforms in carbonate rock basins in the Appalachian Highlands: Geological Society of America Bulletin, Part I, v. 90, p. 385-396.

White, W.B., 1988, Geomorphology and Hydrology of Karst Terrains: Oxford University Press, New York, 464 p.

White, W.B., 1999a. Karst Hydrology: Recent Developments and Open Questions: *in* Beck, B., et al., ed., Proceedings of the 7th Multidisciplinary Conference on Sinkholes, p. 3-21.

White, W.B., 1999b, Conceptual Models for Karstic Aquifers: *in* Palmer, A.N., et al., ed., Karst Modeling, Karst Waters Institute Special Publication 5, p. 11-16.

White, W.B., 2000, Development of speleogenic ideas in the 20th Century: The Modern Period, 1957 to the present: in Klimchouk A., et al., ed., Speleogenesis.Evolution of karst aquifers, Huntsville, National Speleological Society, p. 39-43.

White W.B. and White E.L.**,** 2006**,** Size scales for closed depression landforms: the place of tiankengs: Speleogenesis and Evolution of karst aquifers online scientific journal, v. 4, no. 1, http://www.speleogenesis.info.

White, W.B., 2007, A brief history of karst hydrogeology: contributions of the NSS. Journal of Cave and Karst Studies, v. 69, no. 1, p. 13–26.

Wilcox, R.E., Harding, T.P., and Seely, D.R., 1973, Basic wrench tectonics: American Association of Petroleum Geologists Bulletin, v. 57, p. 74-76.

Williams, P.W., 1972, Morphometric analysis of polygonal karst in New Guinea: GSA Bulletin, v. 83, p. 761-796.

Wilson, J. F., 1971, Fluorometric Procedures For Dye Tracing: USGS Techniques of Water Resources Investigations, v. 3, 31 p.

Wilson, C.B., Valdes, J.B., and Rodriguez-Iturbe, I., 1979, On the influence of the spatial distribution of rainfall on storm runoff: Water Resources Res., v. 15, p. 321-328.

Windhager, S., 2007, Personal communication of botany of the Wildflower Center and adjacent J17tract: Lady Bird Wildflower Center, Austin, Texas.

Witherspoon, P.A., Wang, J.S.Y., Iwai, K., and Gale, J.E., 1980, Validity of the cubic law for fluid flow in a deformable rock fracture: Water Res. Research, v. 16, no. 6, p.1016-1024.

Woodruff, C.M. Jr., 1977, Stream piracy near the Balcones Fault Zone, central Texas: Journal of Geology, v. 85, p. 483-490.

Woodruff, C.M. Jr., 1984a, Water budget analysis for the area contributing recharge to the Edwards Aquifer, Barton Springs Segment: in C. Woodruff and R. Slade, ed., Hydrogeology of the Edwards Aquifer-Barton Springs Segment, Travis and Hays Counties, Texas, Austin Geological Society Guidebook 6, p. 36-42.

Woodruff, C.M. Jr., 1984b, Stream piracy—possible controls on recharge/discharge geometry: Edwards Aquifer, Barton Springs Segment: in Woodruff C.M. and Slade, R.M. ed., Hydrogeology of the Edwards Aquifer-Barton Springs Segment, Travis and Hays Counties, Texas, Austin Geological Soc. Guidebook 6, p. 36-42.

Woodruff, C.M., 1985, Structural features of the Austin Chalk, from, Young K. and Woodruff, C.M, ed, Austin Chalk in its Type Area-Stratigraphy and Structure, Austin Geological Society Guidebook 7. P. 53-62.

Woodruff, C.M., and Foley, D., 1985, Thermal regimes of the Balcones/Ouachita trend, central Texas: Gulf Coast Associated Geological Societies Transactions, v. 35, p. 287-292.

Woodruff, C.M., Jr., 2001, Letter estimating recharge to Kentucky Sink on Brodie Springs tract: submitted by Niemann & Niemann, LLP to City of Austin, 2 p.

Worthington, S., 1999, A comprehensive strategy for understanding flow in carbonate aquifers: Karst Modeling, Karst Waters Institute Special Publication 5, p. 30-37.

Worthington, S., 2003, Numerical simulation of the aquifer at Mammoth Cave: Abstract from Proceedings from the International Conference on Karst Hydrogeology and Ecosystems, p. 10-11.

Young, K. and Marks, E., 1952, Zonation of upper Cretaceous Austin Chalk and Burditt Marl, Williamson County, Texas: American Association of Petroleum Geologists Bulletin v. 36, no. 3, p. 477-488.

Young, K., Barker, D.S., and Jonas, E.C., 1975, Stratigraphy of the Austin Chalk in the vicinity of Pilot Knob: Austin, Texas, Geological Society of America, South-Central Section, 9th Annual Meeting Field Trip Guidebook, 28 p.

Young, K., 1977, Guidebook to the Geology of Travis County: The University of Texas at Austin, Student Geology Society, Austin, 179 p.

Young, K., 1982, Cretaceous volcanism in the Austin area, Texas: Austin Geological Society Guidebook 4.

Young, K., 1986, The Pleistocene terra rossa of central Texas: in Abbott, P.L., and Woodruff, C.M., Jr., ed., The Balcones Escarpment-Geology, Hydrology, Ecology and Social Development in Central Texas: Geological Society of America.

Zahm, C.K., 1998, Use of outcrop fracture measurements to estimate regional groundwater flow, Barton Springs Segment of the Edwards Aquifer [M.S. thesis]: Austin, University of Texas, 153 p.

Zimmerman, M.D., Bennett, P.C., Sharp, J.M., Jr., and Choi, W.J., 2002, Experimental determination of sorption in fractured flow systems: Journal of Contaminant Hydrology, v. 58, no. i. 1-2, p. 51-77.

VITA

Nico Mark Hauwert attended grade school through high school in Houston, Texas, before attending the University of Texas, completing a Bachelor of Science in Geological Sciences in 1984. Nico found Austin fascinating with its clean cool waters, cliffs, and caves and became an avid cave explorer, hoping one day to research them for a career. At that time, Nico found geologists with bachelor's degrees were in high demand in fast food restaurants but unfortunately not much in cave science at that time. He found employment in most any odd job one could think of including cook, bartender, carpenter, roofer, painter, dishwasher, landscaper, office clerk, interpreter, electronics salesman, canvasser, janitor, lab assistant, and well logger. During a vagabond period, he independently studied natural systems as he backpacked, caved, and traveled throughout Peru for six months in 1985 and two months across Europe in 1986, assisted in several cave expeditions in Mexico, and worked as a park ranger in Crater Lake National Park in Oregon. In 1987, Nico moved to Toledo, Ohio where he completed a master's degree in geology at the University of Toledo in 1991. While in Ohio, he studied karst phenomena in their Ordovician and Silurian dolomites, getting into mischief very quickly by discovering a 7-mile-wide karstic fault zone and cave streams underneath the glacial till that trended towards a nearby proposed low-level nuclear waste site. In Ohio, Nico served as teaching assistant, conducted assessments of materials for asbestos in analytical labs, served as driller assistant, and interned with the Ohio Environmental Protection Agency NPDES program. Nico returned to Texas in 1990, working as hydrogeologist for Hall Southwest Corporation until 1993 and then as senior hydrogeologist/Assessment Program manager for the Barton Springs/Edwards Aquifer Conservation District. He has served as president and vice president of the Austin Geological Society. In 2000, he

entered the Ph.D. program at the University of Texas and continued work as hydrogeologist/senior environmental scientist for the City of Austin Watershed Protection and Development Review.

Permanent address: 2401 Bahama, Austin, Texas 78733

This dissertation was typed by Nico M. Hauwert.